ANTHROPOGENIC ^{14}C IN THE NATURAL (AQUATIC) ENVIRONMENT

FIONA H. BEGG, B.Sc.(Hons).

Thesis presented for the degree of Doctor of Philosophy

University of Glasgow

Scottish Universities Research and Reactor Centre,
East Kilbride.

November 1992.

TABLE OF CONTENTS

LIST OF FIGURES

LIST OF TABLES

ACKNOWLEDGEMENTS

I would like to thank all my supervisors for their individual contributions during the period of this research: Dr. Marian Scott for her unfailing enthusiasm and encouragement, Drs. Gordon Cook and Martin McCartney for their constructive discussions and suggestions, and finally, Professor Murdoch Baxter for his guidance and constructive criticism at the start of the project.

I am indebted to a number of people at S.U.R.R.C. - Phil and Bob for their tuition and advice in the ^{14}C lab., Alison and Julie in the Isotope Geology Unit for analysis of the $\delta^{13}C$ samples, Joe and Paul for their advice on γ-ray spectroscopy and also Doug Harkness for his straight talking.

In addition to the help received by personnel at S.U.R.R.C., I am also grateful for the co-operation of the staff at MAFF (Fisheries Lab., Lowestoft) especially Alan Young, Dave Allington and Peter Kershaw who assisted in sample collection onboard ship and to the Natural Environment Research Council for the funding for the project.

Finally, I would like to thank my family and Phil for their constant support and encouragement throughout the years that this has taken to complete.

DECLARATION

Preliminary reports of some of the data forming Chapter 3 have already been published in either peer-reviewed proceedings or journals (Begg *et al.*, 1991; Begg *et al.*, 1992).

All sample analysis carried out during this study, with the exception of the final stages of the AMS measurements and the counting of the KCFC/ASG cartridges used in the extraction of caesium from the water column, was undertaken by the candidate at S.U.R.R.C..

ABSTRACT

Increasing global awareness of the radiological significance of ^{14}C releases from the nuclear and radiochemical industries has resulted in a number of studies within the last decade investigating the atmospheric releases and their effect on the terrestrial biosphere. However, liquid discharges also occur, with preliminary studies indicating enriched ^{14}C specific activities present in fish and shellfish harvested in the vicinity of discharge locations.

The basis of this study was to determine the behaviour and environmental distribution of anthropogenically produced ^{14}C released to the aquatic environment from the nuclear fuel reprocessing plant at Sellafield, owned by British Nuclear Fuels and the radiochemical plants in Cardiff and Buckinghamshire owned by Amersham International plc. Most sampling was undertaken in the Irish Sea with smaller scale studies being carried out in the Bristol Channel and the Grand Union Canal.

Within the study area, from Earnse Point 40 km south of Sellafield, northwards to the Clyde Sea area, preliminary studies on intertidal biota samples *ie.* mussels, winkles and seaweed indicated enriched ^{14}C specific activities in all the samples relative to the current ambient level of 115.4 pM. The highest activities were observed in the immediate vicinity of the discharge location; mussels with a measured activity of 787 pM, winkles of 613 pM and seaweed of 415 pM. The ^{14}C specific activity observed at most sites appeared to be organism dependent with mussels>winkles>seaweed. This is the result of differences in the uptake mechanisms of the organisms and indicates that the dissolved inorganic carbon and the particulate material within the water column are enriched in ^{14}C. However, on analysis of the biogeochemical fractions of the water column, enriched ^{14}C activities were observed only in the DIC fraction which could explain those activities found in the seaweed but not those in the mussels and winkles. Enriched ^{14}C activities were found in the phytoplankton, indicating that there is a source of enriched organic particulate material within the water column as a result of photosynthetic uptake of enriched DIC, however this will be a seasonal effect. Nevertheless, this enrichment is still not high enough to support the activities observed in the mussels and winkles, although, this was only a single sample and may not be a true reflection of the activities present. A similar anomaly is present in the activities found in bottom-dwelling fish and the sediments on which they feed; the fish

are more highly enriched than the organic fraction of the sediments. These discrepancies may point to higher discharges having occurred in the past and/or to areas within the Irish Sea which are of a more enriched nature and were not investigated during this study.

Prior to 1985, the discharges of ^{14}C from Sellafield were not monitored and hence are merely best estimates. A temporal study of Nori (*Porphyra umbilicalis*) samples collected within the period 1967 - 1988 were analysed in an attempt to confirm these estimates. To ensure that Nori did reflect past discharges, ^{137}Cs and ^{241}Am were also analysed. The agreement observed between the ^{137}Cs and ^{241}Am discharges and measured activities was excellent, indicating that Nori did reflect Sellafield discharges. However, a similar agreement was not obtained for ^{14}C, suggesting that either the estimated discharges are incorrect or that due to biological activity, Nori does not reflect ^{14}C discharges in the same way that it does for ^{137}Cs and ^{241}Am.

The geographical distribution of Sellafield-derived ^{14}C in the DIC was determined by extensive sampling within the Irish Sea and Scottish coastal water areas. ^{137}Cs, a known conservative radioactive tracer of water movement, was also analysed at the sites to allow comparison with the chemical behaviour of ^{14}C. The results indicate that the behaviour of ^{14}C in seawater, like that of ^{137}Cs, is largely conservative. There was, however, a slight increase in the $^{14}C/^{137}Cs$ ratio with increasing distance from Sellafield. This may be a reflection of biological uptake of carbon or the desorption of ^{137}Cs from the sediments. A more complex treatment of the data was carried out using a compartmental model, based on the hydrography of the study area, which was initially developed from ^{137}Cs data. The agreement between the predicted and observed values indicates that the ^{14}C distribution (as DIC) is being determined by water movement and the local current system *ie.* ^{14}C in the DIC is behaving in a relatively conservative manner in the water column.

Similar observations were made in the Bristol Channel as a result of discharges from the radiochemical plant owned by Amersham International plc *ie.* intertidal biota and organic sediments were enriched, and the DIC of the water column was also enriched with decreasing activities observed with increasing distance from the point of release. However, at this site, the POC and DOC were also enriched in ^{14}C, indicating that the discharges are in a different chemical form from those at Sellafield. Given the nature of the work undertaken at Amersham, it would appear feasible for the discharges to be in both the dissolved inorganic and the organic (particulate and dissolved) forms, with those from

Sellafield being in the dissolved inorganic form only.

Enrichments were not found at the final site, *ie.* the Grand Union Canal, Buckinghamshire, except in one fish sample, although discharges are thought to occur, indicating that perhaps the time of sampling was unfavourable.

To complete this work, a brief study of the global implications of aqueous releases was undertaken by using globally averaged mathematical models of the carbon cycle. These indicated that for every 10% of the total ^{14}C discharges from the nuclear industry that were released to the surface oceans as opposed to the atmosphere, the increase in the specific activity of the oceans was only half the subsequent decrease in the atmospheric ^{14}C specific activities, due to the greater mass of carbon present for dilution. Therefore, increasing discharges to the surface oceans would result in a decrease in the atmospheric ^{14}C specific activity and, hence, the radiological dose received by the global population.

CHAPTER 1

INTRODUCTION

1.1 INTRODUCTION

Annually, a number of radionuclides are routinely discharged, under authorisation, from the nuclear and radiochemical/pharmaceutical industries within the U.K. to both the atmosphere and coastal waters. One of these radionuclides, ^{14}C, may be radiologically significant on a global scale due to its' long half-life (5730±40 years; Godwin, 1962) and mobility in the environment. However, most studies on ^{14}C releases have concentrated on those to the atmosphere, their subsequent environmental distribution and the radiological implications to local and global populations (Hayes and MacMurdo, 1977; Kabat, 1979; McCartney *et al.*, 1986; McCartney, 1987; Joshi *et al.*, 1987; Levin *et al.*, 1988; McCartney *et al.*, 1988a,b). Little work has been carried out on those discharges to the aquatic environment, due mainly to the ^{14}C discharge pathway being considered to be predominantly gaseous in nature.

Within the United Kingdom there are several sites known to discharge both gaseous and aqueous ^{14}C. This study was undertaken to determine the effects of discharging ^{14}C *via* low-level liquid effluent into coastal waters, such as the Eastern Irish Sea and the Bristol Channel from the nuclear fuel reprocessing plant at Sellafield, Cumbria and the radiochemical plant owned by Amersham International plc at Cardiff, respectively. During this work, studies have been carried out to determine the chemical form of these discharges and how they are dispersed both geographically and within the biogeochemical phases of carbon present in the water column. Marine organisms living in the vicinity of such releases will potentially be exposed to enriched material in their diets which they may transfer to local consumers when harvested. A wide selection of marine biota were studied, in part to help with determining the chemical form and dispersal pathways already discussed but also to estimate the radiological effects of these aqueous discharges.

In addition to the information obtained on the local scale from such studies, nuclear fuel cycle-derived aqueous ^{14}C is a potentially valuable tracer for studies of the global marine carbon cycle. Certain processes within the marine carbon cycle are poorly understood, *eg.*

the transfer, and rates of transfer, between the various biogeochemical fractions and the origin and quantity of dissolved organic carbon present. Known sources of ^{14}C to marine systems may provide an ideal opportunity to determine such quantities permitting the incorporation of these into global carbon cycles models to improve their representation of such a complex system.

1.2 NATURAL ^{14}C PRODUCTION AND DECAY

^{14}C is the only naturally occurring radioactive isotope of carbon and is present in very small quantities compared to the stable isotopes ^{12}C and ^{13}C, (^{12}C = 98.9%, ^{13}C = 1.1%, ^{14}C = 1 atom per 10^{12} stable atoms). Production, which was first postulated by Libby (1946), occurs in the upper atmosphere due to the collision of cosmic-ray-produced neutrons with naturally present ^{14}N nuclei *ie.*

$$^{14}_{7}N + ^{1}_{0}n \rightarrow ^{14}_{6}C + ^{1}_{1}p \qquad (1.1)$$

The rate of this production has been derived from the natural ^{14}C inventory to be 1.0×10^{15} Bq yr^{-1} (United Nations, 1977) which is in good agreement with the figure of 1.4×10^{15} Bq yr^{-1} previously reported by Light *et al.* (1973), calculated from cosmic ray flux estimates. Once produced, this ^{14}C undergoes oxidation to $^{14}CO_2$ and as such is incorporated into the global carbon cycle by the same processes as $^{12}CO_2$ and $^{13}CO_2$.
Decay of ^{14}C nuclei occurs by the release of a beta particle to form the stable nucleus ^{14}N with the energy produced shared between the beta particle and an antineutrino *ie.*

$$^{14}_{6}C \rightarrow ^{14}_{7}N + ^{0}_{-1}\beta + \bar{\upsilon} \qquad (1.2)$$

The maximum energy associated with the beta particle is 156 keV with an average energy of 45 keV. The half-life of ^{14}C is 5730±40 years (Godwin, 1962) which corresponds to a mean life of 8267 years.

1.3 THE GLOBAL CARBON CYCLE

As with the other essential elements required for life *eg.* nitrogen and oxygen, the movement of carbon throughout the environment can be described schematically in a global cycle. This in essence shows all the carbon-containing pools and how they are linked to one another so that they maintain a steady state *ie.* the total amount of carbon remains the same in any one pool where transfer in is matched by transfer out. Over the years, the complexity of the conceptual models has increased as knowledge concerning the different processes in the various reservoirs has increased. The development and applications of some of these models will be discussed in Chapter 4. However, it is useful to provide, at this point, a general description of the global carbon cycle and its four major reservoirs (Fig 1.1) before considering the chemistry of carbon in the oceans in more detail.

1.3.1 The Atmosphere

McEwan and Phillips (1975) proposed that the atmosphere consisted of five regions divided primarily on the basis of temperature - the troposphere, stratosphere, mesosphere, thermosphere and the exosphere. Almost all the carbon present in the atmosphere is contained in the lowest two regions which are the troposphere and the stratosphere (84% and 16% of the carbon, respectively) (Baxter and Walton, 1970), hence, these are the regions of interest in carbon cycle modelling. The lower of these two is the troposphere which contains three quarters of the atmosphere by weight, and nearly all the moisture, with the dry and cloudless stratosphere above it.

A great deal of research has been undertaken on the mixing processes occurring within and between the troposphere and stratosphere (Lal and Rama, 1966; Nydal, 1967, 1968; Young and Fairhall, 1968; Walton *et al.*, 1970), and the important points can be summarised as follows:-

1) mixing processes in the troposphere are due to eddy diffusion and convection whereas in the stratosphere the former is the only mechanism of importance.

2) mixing processes in the stratosphere are slower than those in the troposphere as most of the movement is due to horizontal diffusion.

Figure 1.1: A simple representation of the global carbon cycle.

3) interhemispheric mixing of the tropospheric carbon occurs in approximately one year whereas that for the stratosphere takes 5 years.

4) the exchange of carbon from the stratosphere to the troposhere takes 2-4 years.

Overall, these exchange rates are considered to be rapid, hence, in modelling studies the atmosphere is considered to be a single well-mixed carbon reservoir.

Prior to the Industrial Revolution, the atmosphere was thought to contain 5.9×10^{17} g of carbon as CO_2 (280 ppm) (Neftel *et al.*, 1985; Friedli *et al.*, 1986) but by 1980 this figure had risen to 7.2×10^{17} g (338 ppm) (Keeling *et al.*, 1982) due both to the combustion of fossil fuels and global deforestation. The present rate of increase is thought to be approximately 1.5 ppm per year (Siegenthaler, 1990). Observed fluctuations in this rate are considered to be associated with El Nino/Southern Oscillation (ENSO) events, in which, increased amounts of CO_2 are absorbed into the tropical Pacific as surface water temperatures rise and upwelling of nutrient-rich deep waters ceases (Siegenthaler, 1990). In relation to CO_2, other carbon-containing gases in the atmosphere are present in small quantities and account for only 4×10^{15} g of carbon (CH_4 = 1.5 ppm; CO = 0.5 ppm).

Due to exchanges with other reservoirs, namely the terrestrial biosphere and the hydrosphere, the residence time of carbon in the atmosphere is fairly short, at about 4 years (Nydal, 1967, 1968; Young and Fairhall, 1968; Walton *et al.*, 1970; Gammon *et al.*, 1985).

1.3.2 The Terrestrial Biosphere

The terrestrial biosphere is generally considered as two distinct but connected compartments - the terrestrial biota, representing both the living and standing dead material, and the humus component, defined as dead material which has fallen or is incorporated into the soil. The terrestrial biota pool contains approximately 5.6×10^{17} g of carbon (Siegenthaler, 1989) compared to the $1.5\text{-}2.0 \times 10^{18}$ g present in the humus (Bolin *et al.*, 1981; Olson *et al.*, 1985; Siegenthaler, 1989; Schlesinger, 1990). The inventory of carbon in the terrestrial biota has decreased over the years with the historic terrestrial biomass containing $7.0\text{-}11.0 \times 10^{17}$ g of carbon compared to the levels thought to be present today of $4.2\text{-}6.6 \times 10^{17}$ g of carbon (Olson 1974,1985; Matthews, 1983; Solomon *et al.*, 1985; Siegenthaler, 1989). Uncertainties in the peat content of soils is the principal contributor to the size range reported for the humus component.

The exchange of carbon between the terrestrial biosphere and the atmosphere is governed by photosynthesis and respiration. Firstly, photosynthesis by plants removes CO_2 from the atmosphere, converts it to carbohydrates which may then be stored and used as an energy supply, when required, for metabolic processes. During respiration, CO_2 is released back to the atmosphere through the leaves or into the soil by the roots. The amount of carbon released during respiration does not equal the amount taken up by photosynthesis as 4.5-6.2x10^{16} g of carbon $year^{-1}$ (Solomon *et al.*, 1985) is incorporated into the plant as structural material during growth. This carbon is then available to heterotrophic organisms such as animals which directly consume the plants, or soil microbes which gradually decompose the plant litter releasing CO_2 *via* respiration. This implies that the net annual exchange of carbon between the atmosphere and the terrestrial biosphere is 4.5-6.2x10^{16} g of carbon which is approximately 50% of the carbon taken up during photosynthesis.
The residence time of carbon within the terrestrial biosphere is complicated by the wide range of materials present in the reservoir. In general, plant leaves, litter and other rapidly exchanging organic materials, which constitute about 20% of the carbon, have a short residence time of 1-2 years. The remaining 80% of the terrestrial biota is thought to have a residence time of <100 years (Houghton *et al.*, 1985; Olson *et al.*, 1985). For the humus component, the residence times are considerably longer at 100-1000 years (Houghton *et al.*, 1985; Olson *et al.*, 1985).

1.3.3 The Hydrosphere

The hydrosphere encompasses all water bodies, not only the saline oceans and coastal waters but also the freshwater, polar ice caps, lakes and rivers. As oceans cover ≥70% of the surface of the earth, they constitute the major part of the hydrosphere and are considered to be the most influential in exchanging carbon. Overall, the oceans contain approximately 3.84x10^{19} g of carbon, of which only 1.0x10^{18} g is organic in nature, with by far the greatest proportion being inorganic. Within the organic phase, 3x10^{15} g is present as particulate material (including the marine biomass) with the remainder considered as dissolved organic carbon.
The chemistry of the carbon cycle within the marine system will be discussed more fully in Section 1.7, hence, at this stage it is sufficient only to indicate the relative fluxes and

the overall effect on the global carbon cycle.

The hydrosphere can be thought to exchange with the atmosphere and the lithosphere. The gross annual exchange between the atmosphere and surface oceans is $1.0\text{-}1.1 \times 10^{17}$ g of carbon (Bolin *et al.*, 1979) and is driven by small differences in the partial pressure of CO_2 (pCO_2) in both reservoirs. Transfer is assumed to be by molecular diffusion through the thin film at the very surface of the oceans. This transfer is controlled by factors such as temperature, surface film thickness, wind conditions and oceanographic processes *eg.* turbulent mixing. Exchange between the hydrosphere and the lithosphere is extremely small and is often discounted in models. However, the top 10 cm of sediment is thought to be fairly well-mixed and reactive, hence, is often included in the oceanic reservoir (Solomon *et al.*, 1985). An estimated 4×10^{15} g of carbon (Baes *et al.*, 1976) is considered to be in these mobile deposits, in the form of calcium carbonate.

The retention time of carbon in the surface oceans is considered to lie in the range of 5-8 years (Craig, 1957b; Bolin *et al.*, 1981; Baes *et al.*, 1985) whereas that for the deep ocean is 500-1000 years (Craig, 1957b; Bolin *et al.*, 1981; Baes *et al.*, 1985).

1.3.4 The Lithosphere

When considering the global carbon cycle, the reservoir containing the most carbon actually takes least part in short term cycling. The lithosphere contains 6.5×10^{22} g of carbon, of which 75% is present in an inorganic form, with the remainder being organic in nature (Kempe, 1979). Calcite and aragonite (forms of calcium carbonate) are the main forms of the inorganic fraction of the lithosphere. Less than 1% of the organic lithospheric carbon is present in the form of fossil fuels.

Lithospheric carbon exchanges with the hydrosphere at the ocean - sediment boundary. Transport to the sediments occurs due to the gravitational sinking (sedimentation) of organic particles or precipitation of dissolved inorganic carbonates. Diagenetic dissolution of the carbonates returns carbon from the sediments to the water column. These fluxes tend to be very small (Olson *et al.*, 1985), hence, the residence time of sedimentary carbon tends to be in the order of 10^8 years.

1.3.5 The Distribution of ^{14}C in the Global Carbon Cycle

Due to the cycling of carbon in nature, ^{14}C produced in the stratosphere is eventually

incorporated into the other carbon-containing reservoirs. The distribution of both the stable and radioactive isotopes is determined by the same exchange processes, but, due to isotopic fractionation and ageing, differences in the specific activities of ^{14}C in the reservoirs do occur.

Only small changes in the ^{14}C:^{12}C ratio are induced due to isotopic fractionation on transfer of carbon from one reservoir to another. This effect is due to slight differences in the thermodynamic properties of the isotopes (Craig, 1953) and can be calculated from $^{13}C/^{12}C$ measurements. More important is radioactive decay of ^{14}C, coupled with the residence time of carbon within each reservoir. This effectively means that the longer ^{14}C stays in a reservoir, the more chance there is for radioactive decay to occur and the lower the ^{14}C specific activity will be. In addition, the specific activity of any exchanging reservoirs will influence the resultant specific activity. Prior to large injections of ^{14}C from anthropogenic sources, the highest specific activity (226 Bq kg^{-1} C) was found in the atmosphere (Karlen *et al.*, 1964), where ^{14}C is produced and subject to rapid exchange with other reservoirs (*ie.* a short residence time). The terrestrial biota has a similar specific activity to the atmosphere due to its fairly rapid equilibrium. Due to the longer residence time of carbon in the humus component, the specific activity found here is less than that seen in the terrestrial biota (215 Bq kg^{-1} C). Within the hydrosphere, the specific activity decreases with increased depth of sampling. In the surface waters which are well-mixed, the ^{14}C specific activity is similar to that found in the humus component of the terrestrial biosphere (215 Bq kg^{-1} C), while the value attributed to the deep ocean is 190 Bq kg^{-1} C. As the exchange of carbon to the lithosphere is so slow, it is assumed that this reservoir contains no ^{14}C. These figures are shown in Figure 1.1 which details the general global carbon cycle and the exchanges between reservoirs.

1.4 NATURAL VARIATIONS IN ^{14}C PRODUCTION

Investigation of the constancy of ^{14}C production by de Vries in 1958 showed that the atmospheric ^{14}C concentration had risen by approximately 2% in the years around 1700 A.D. and this was subsequently known as the "de Vries effect". Further work by Willis *et al.* (1960) partially confirmed this by the documentation of similar variations.

This research led to a study to reconstruct the past fluctuations in atmospheric ^{14}C

concentration (Suess, 1970a). Suess's work used samples of known-age tree rings, spanning the last 8000 years, as indicators of the atmospheric ^{14}C concentration in the years of their growth. These samples were taken from the Bristlecone pine chronology constructed by the Laboratory of Tree-Ring Research, Arizona (Ferguson, 1968, 1969, 1970, 1972). The ^{14}C record was extended back to 10,000 years B.P. (*ie.* 10,000 years before 1950) using the annual clay deposition layers (varves) in the Lake of the Clouds, Minnesota (Stuiver, 1970). A further varve chronology from Sweden (de Geer, 1940) was used by Tauber (1970) to determine the ^{14}C concentrations back to 12,500 years B.P. A series of papers published in a special calibration issue of the journal Radiocarbon (Stuiver and Pearson, 1986; Pearson and Stuiver, 1986; Stuiver and Becker, 1986; Pearson *et al.*, 1986; Vogel *et al.*, 1986; de Jong *et al.*, 1986; Linick *et al.*, 1986; Kromer *et al.*, 1986; Becker and Kromer, 1986; Stuiver *et al.*, 1986a,b) brought together all the chronologies (both fixed and floating), to produce a ^{14}C record back to 13,300 B.P.. Figure 1.2 illustrates the changes in atmospheric ^{14}C specific activity, expressed as per mil deviation from the natural level ($\Delta^{14}C$), in the last eight millennia (Stuiver *et al.*, 1986a). More recent work by Bard and co-workers is attempting to calibrate ^{14}C ages with the $^{230}Th/^{234}U$ ages found in Barbados corals to extend the record of ^{14}C variations back to 30,000 years (Bard *et al.*, 1990). The results obtained show good agreement with the tree-ring and Lake of Clouds varve calibrations, although not with the Swedish varve data for the period 8000 - 11,000 years B.P.. This is thought to be due to missing varves in the Swedish chronology (Stuiver *et al.*, 1986a).

Regardless of these discrepancies, two major trends are apparent from the results. The first of these is a long-term decrease in ^{14}C concentration (approximately 10%) between 6000 and 2500 years B.P. with a second short-term fluctuation of 1-2% over a period of centuries, superimposed upon it.

Many theories have been put forward to explain these observed variations, including changes in oceanic ventilation and associated climatic changes (Siegenthaler *et al.*, 1980; Keir, 1983; Prentice and Fung, 1990; Adams *et al.*, 1990), changes in the flux of cosmic rays, changes in solar activity and variations in shielding by the earth's magnetosphere. The long-term large scale variation is thought to be due to changes in the cosmic ray flux incident on the earth's atmosphere. This in turn is due to changes in the earth's magnetic field (Bucha, 1970; Bruns *et al.*, 1983). As the earth's magnetic dipole moment increases,

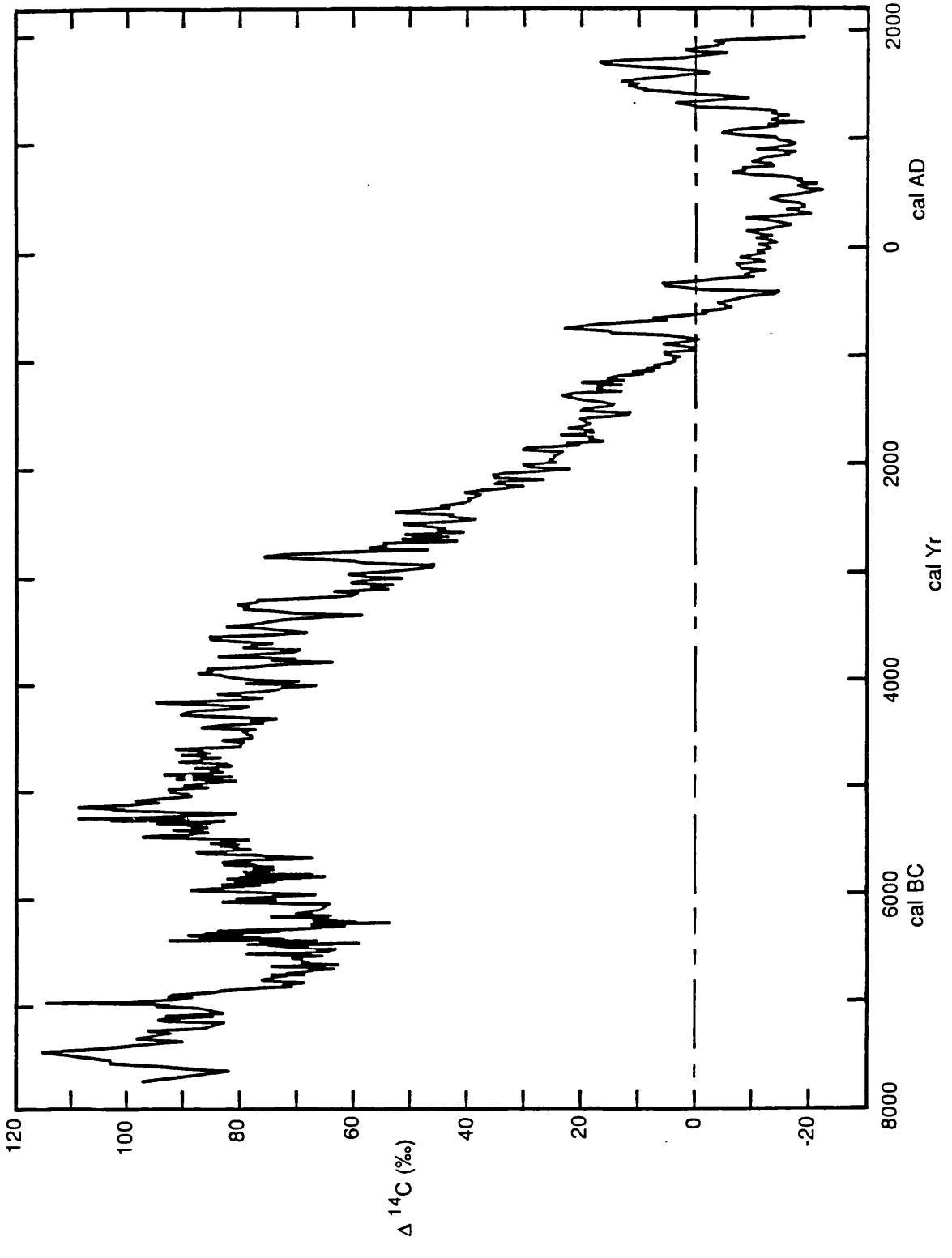

Figure 1.2: Atmospheric $\Delta^{14}C$ in the last eight millennia.

the deflection of cosmic rays increases, hence, the ^{14}C production rate decreases (Elsasser *et al.*, 1956). The earth's magnetic field has fluctuated in an almost sinusoidal manner with a time period of 8000 years (Bucha and Neustupny, 1967). Mazaud *et al.* (1991) reported the influence of geomagnetic field intensity changes on atmospheric ^{14}C content and concluded that this may be the major source of millennial variations in the abundance of atmospheric ^{14}C during the past 50,000 years.

The presence of short term variations were independently reported in the late 1970s, early 1980s (de Jong *et al.*, 1979; Bruns *et al.*, 1980; Stuiver, 1982) and are thought to be due to changes in the solar sunspot activity (Stuiver, 1961; Suess, 1970b; Baxter and Walton, 1971). Periods of high solar activity result in decreased cosmic ray incidence on the earth and hence a reduced ^{14}C production rate. The periodicity of this high activity has been a topic of much discussion with 11 - 400 year cycles being reported (Suess, 1970b; Houtermans, 1971; Baxter and Farmer, 1973; Damon *et al.*, 1973).

1.5 ANTHROPOGENIC VARIATIONS IN ^{14}C PRODUCTION

As mentioned in the introductory section, the ratio of ^{14}C:^{12}C present in the carbon cycle has been perturbed not only by natural variations but also by the influence of man. Overall, three main processes have been directly responsible for variations in the specific activity. These will be discussed individually in the following sections.

1.5.1 Suess Effect

The Industrial Revolution brought about a large increase in the quantity of fossil fuels (coal, oil, gas and lignite) combusted to produce energy. In the production of this energy ^{14}C-free CO_2 is released to the atmosphere, hence, increasing the ^{12}C:^{14}C ratio. This reduction in the atmospheric specific activity was first noted by Suess (1953, 1955) and is generally known as the "Suess Effect".

A record of the levels of CO_2 emissions from fossil fuel combustion and cement production (CO_2 is released from decomposition of limestone in cement manufacture) was published by Rotty and Masters (1985) and is presented in Figure 1.3. The fossil fuel data are taken from the UN Series - World Energy Supplies and are based on fuel production, as opposed to fuel consumption figures. The data show an almost constant annual increase

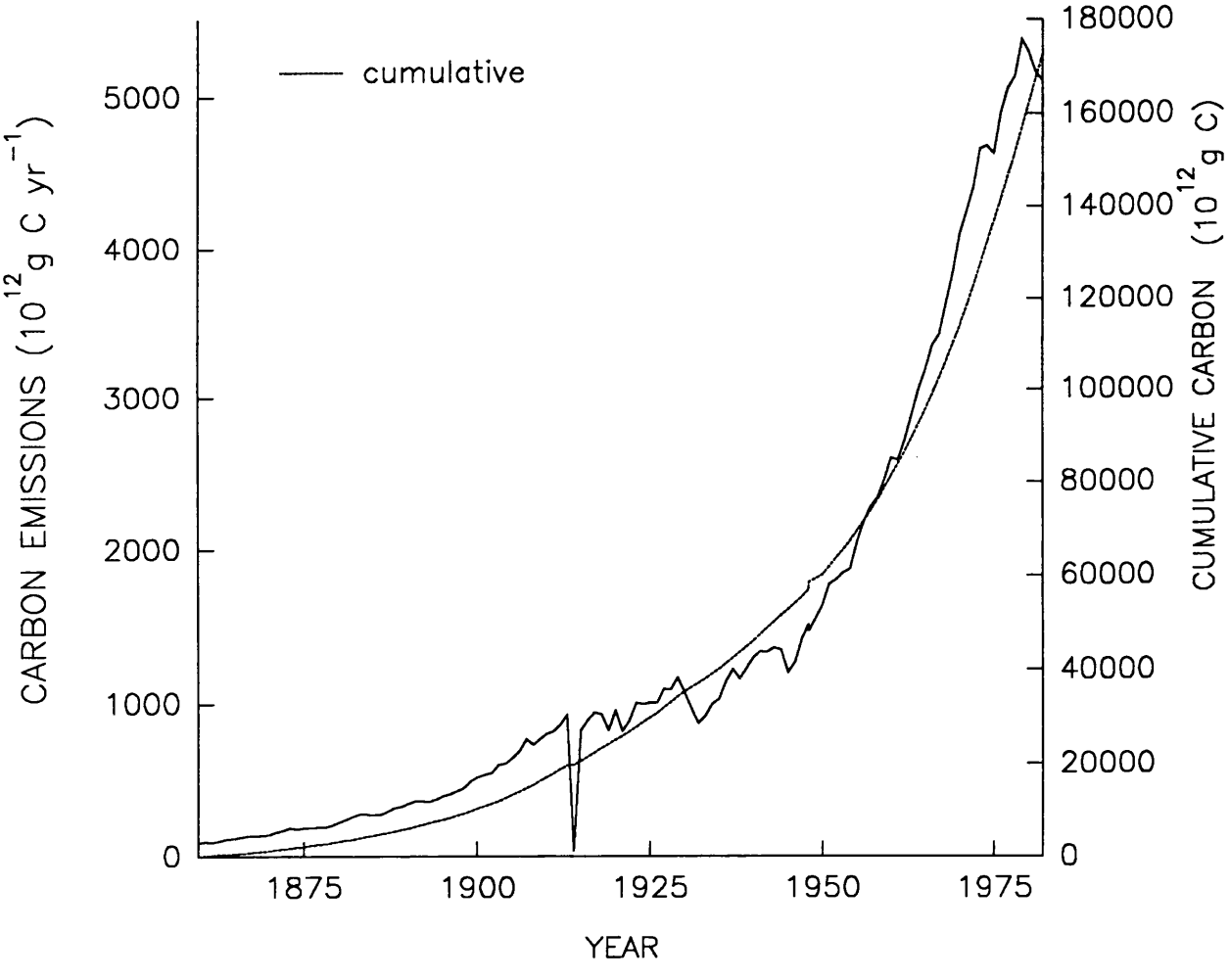

Figure 1.3: CO_2 emissions from fossil fuel combustion and cement manufacture.

of 4.3% in globally emitted CO_2 for over 100 years, except during the periods of the World Wars and the 1930's depression. The reduction in the rate of increase apparent in 1973 can be attributed to the OPEC price rise and hence the reduction in the production of oil.

In addition to these figures for CO_2 emissions, data on the ^{14}C atmospheric specific activity for the northern hemisphere in the period 1860 - 1950 can be deduced from tree-ring data (Damon *et al.*, 1973; Stuiver and Quay, 1981). These are presented in Figure 1.4. It is evident from measured ^{14}C specific activities that the increase in CO_2 emissions resulted in an increase in the ^{12}C:^{14}C ratio between 1860 and 1950 AD. The extent of this decline in ^{14}C specific activity by 1950 was approximately 2% and 3% in the southern and northern hemispheres respectively (Suess, 1955; Fergusson, 1958; Houtermans *et al.*, 1967). This discrepancy between the two hemispheres is a direct result of the mixing time between the two, the enhanced use of fossil fuels in the northern hemisphere and the higher atmosphere to ocean flux in the southern hemisphere (Young and Fairhall, 1968). Stuiver and Quay (1981) confirmed that this decrease in atmospheric ^{14}C specific activity was the result of increased CO_2 emissions, with only a small percentage (0.3%) due to natural variations.

Overall, CO_2 emissions have been steadily increasing since 1950, as observed in the CO_2 concentration data collected at Mauna Loa (Keeling *et al.*, 1982) and other monitoring stations, but the effect of fossil fuel CO_2 on the atmospheric ^{14}C specific activity has been lost since the start of large scale nuclear weapons tests in 1945 and the resultant injections of ^{14}C into the atmosphere.

1.5.2 Nuclear Weapons Testing

The testing of nuclear weapons began in New Mexico in 1945 and has taken place periodically since that time. The most significant periods of testing were 1954 - 1958 and 1961 - 1962 when many large yield explosions were carried out (Carter and Moghissi, 1977).

^{14}C is produced in nuclear explosions *via* neutron activation of atmospheric nitrogen ($^{14}N(n,p)^{14}C$) with the estimated production to 1980 being 2.2-3.5x10^{17} Bq (Lassey *et al.*, 1988; Taylor *et al.*, 1990). This equates to an average production rate of 4.0 x 10^{14} Bq $Mton^{-1}$, but obviously this is dependent on the type of nuclear device exploded and whether

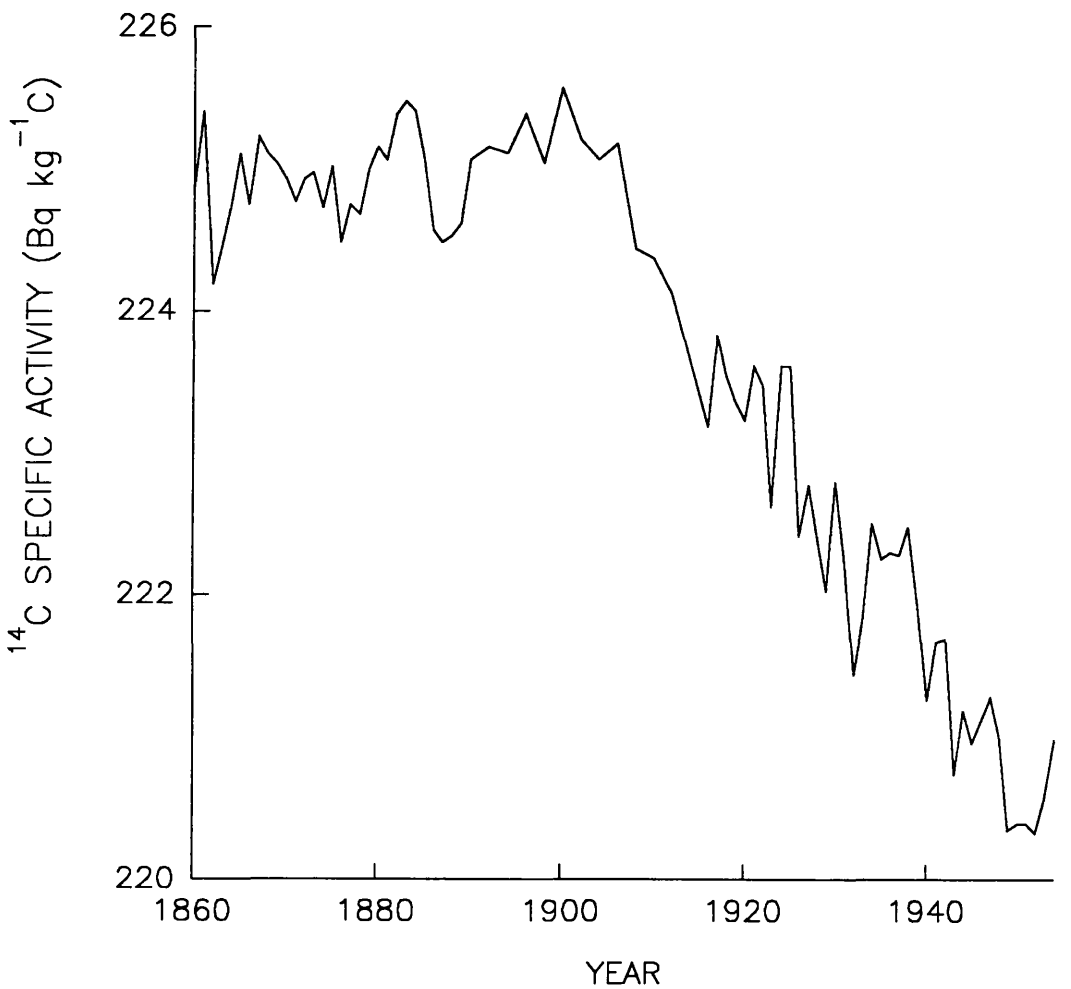

Figure 1.4: The atmospheric ^{14}C specific activity of the northern hemisphere (1860-1954).

the explosion occurs in the atmosphere or at the earth's surface. In the case of ground tests, only ~50% of the amount of ^{14}C associated with atmospheric tests is produced, due to the capture of the neutrons by soil or water. Figure 1.5 shows the estimated annual and cumulative ^{14}C productions for the period 1945 to 1980 which was the year of the last reported atmospheric nuclear explosion (Cambray *et al.*, 1985).

Due to nuclear weapons test inputs of ^{14}C into the atmosphere, the specific activity increased dramatically until 1963-64 when it reached double the initial value (Fig 1.6). The data used to obtain Figure 1.6 are based on ground level measurements of the ^{14}C in atmospheric CO_2 at mid and high latitudes of both the southern and northern hemispheres. These measurements were carried out by a number of workers (Broecker and Walton, 1959; Munnich, 1963; Ostlund and Engstrand, 1963; Olsson and Karlen, 1965; Sternberg and Olsson, 1967; Nydal, 1968; Vogel and Lerman, 1969; Olsson and Klasson, 1970; Vogel, 1970; Walton *et al.*, 1970; Baxter and Walton, 1971; Vogel and Marais, 1971; Baxter and Stenhouse, 1976; Tans, 1978; Nydal *et al.*, 1979; Nydal and Lovseth, 1983; Segl *et al.*, 1983; McCartney, 1987) with measurements prior to 1977 being collated and reported collectively (Tans, 1981).

On the whole, the majority of the nuclear weapons tests occurred in the northern hemisphere which is reflected in the higher observed ^{14}C specific activities. This also illustrates the finite mixing time between the two hemispheres with the results from lower latitudes showing intermediate values (Nydal, 1968; Young and Fairhall, 1968). The maximum value was obtained in 1963-64, almost two years after the maximum production period, indicating that the injection of ^{14}C was into the stratosphere and that a lag period prior to equilibrium with the troposphere occurred. Since this period of maximum specific activity, the atmospheric ^{14}C content has been decreasing due to exchange with the biosphere and oceans. The rate of this decrease is thought to be ~6.1% $year^{-1}$ (Lassey *et al.*, 1988) with the present day specific activity considered to be 265 $Bqkg^{-1}C$.

1.5.3 Nuclear Fuel Cycle

1942 saw the occurrence of the first man-made nuclear chain reaction which was self-sustaining and since then the nuclear industry has grown considerably. Although both the U.K. and the U.S.A. had prototype stations (*ie.* Calder Hall and Shippingport, respectively) under operation by the end of the 1950s the real nuclear era began with the introduction

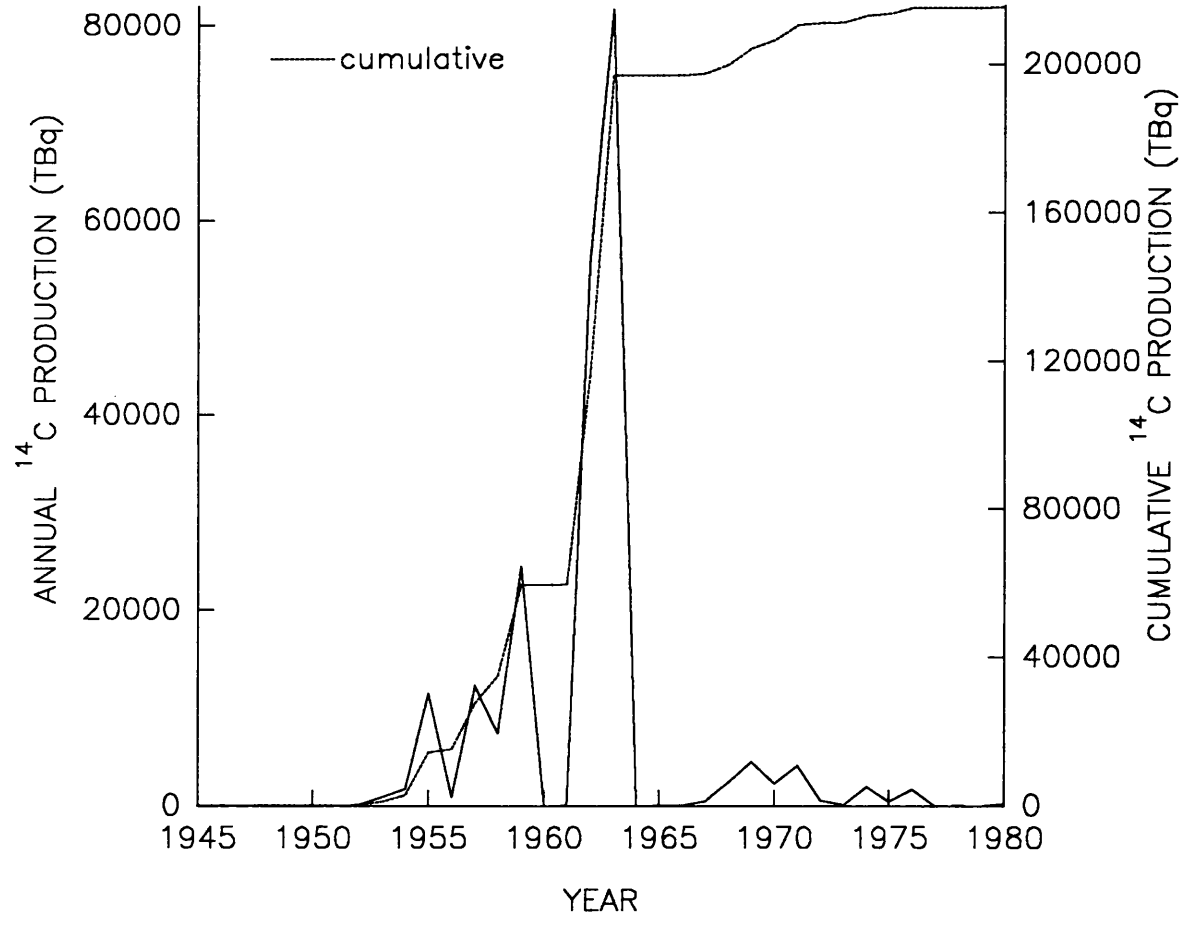

Figure 1.5: The estimated annual and cumulative ^{14}C production from nuclear weapons tests (1945-1980).

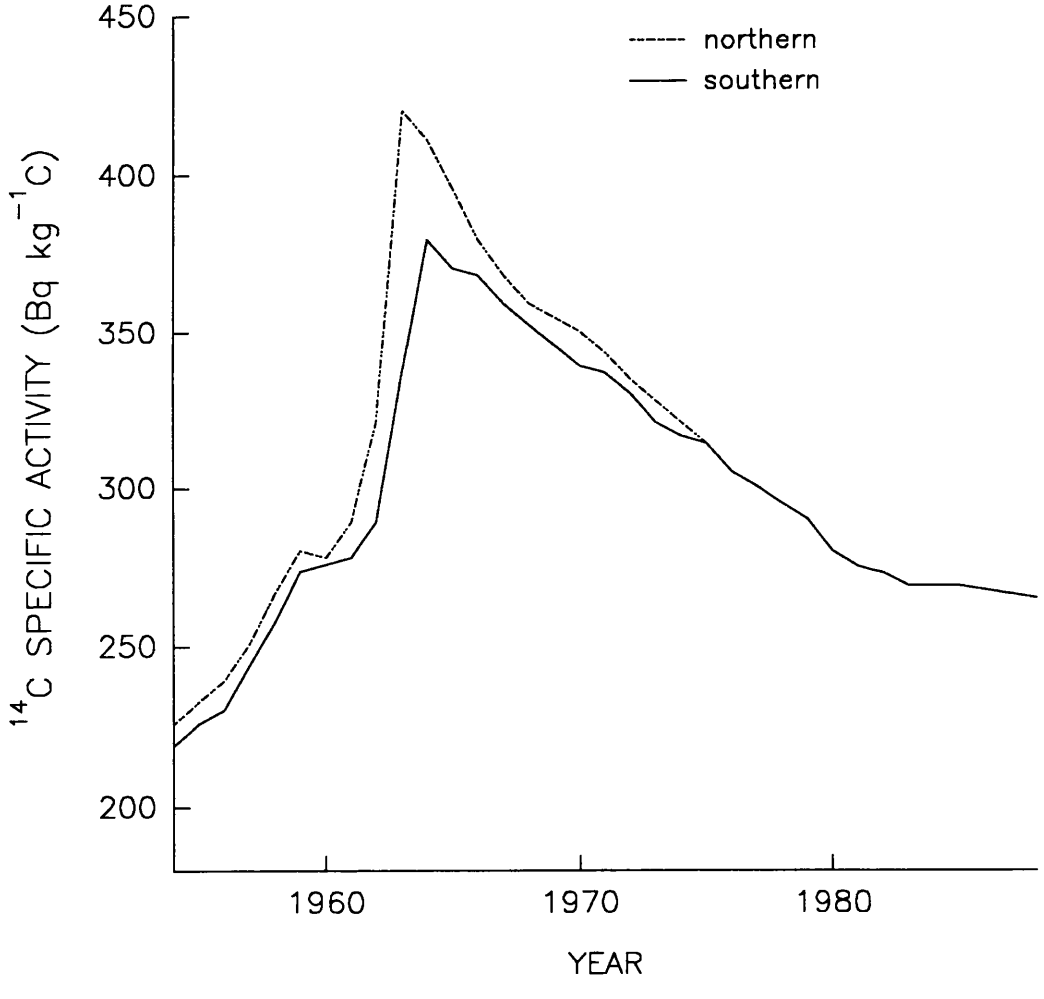

Figure 1.6: The ^{14}C specific activity in the northern and southern hemispheres (1954-1990).

of the Magnox reactors in 1962 (U.K.) and Oyster Creek power station in 1969 (U.S.A.). By the end of 1991 there were 421 reactor units in operation in 24 countries, supplying ~20% of the worlds electricity requirements, with a further 76 reactors in 17 countries under construction (IAEA, 1991a). Added to this, there are 323 research reactors in operation in 52 countries (IAEA, 1991a). ^{14}C is produced as an activation product in nuclear reactors and is released during normal operations, at decommissioning and during fuel reprocessing.

1.5.3.1 Reactor components

Since the inception of the nuclear power industry, a number of reactor designs have been developed, but, on the whole, thermal reactors are constructed from the same basic components (see Fig 1.7). These consist of:-

1. the fuel (U or UO_2) which undergoes fission and is surrounded by cladding of zircalloy or stainless steel.
2. control rods (boron or cadmium) which absorb neutrons to control the rate of reaction.
3. the moderator (graphite, H_2O or D_2O) to slow down fast neutrons to thermal neutrons without absorbing them, in order to increase the probability of another fission reaction.
4. the coolant (H_2O or CO_2) which removes the heat from the reactor core so that it can generate the steam to drive the electrical generators.

The most common designs of thermal reactor in operation worldwide include Boiling Water Reactors (BWR), Pressurised Water Reactors (PWR), Heavy Water Reactors (HWR), Gas-cooled Reactors such as Magnox reactors, Advanced Gas-cooled Reactors (AGR) and High Temperature Gas-cooled Reactors (HTGR). Although these have the same basic design features as shown in Figure 1.7, each have their own individual characteristics (see Table 1.1).

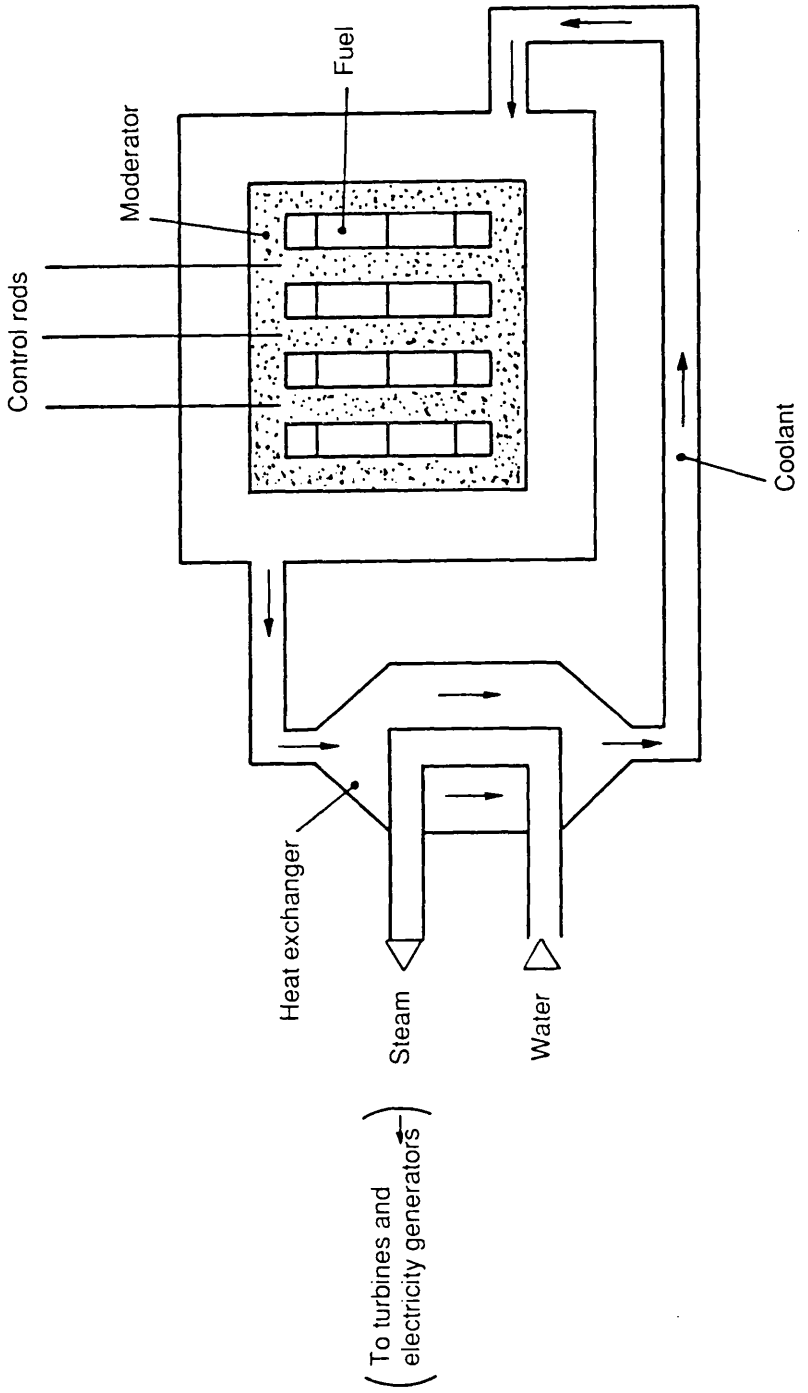

Figure 1.7: A schematic diagram of a thermal nuclear reactor.

	BWR	PWR	HWR	GAS COOLED	AGR	HTGR
FUEL	enrich. UO_2 pellet	enrich. UO_2 pellet	UO_2 pellet	U rod	enrich. UO_2 hollow pellet	UO_2 UO_2-ThO_2 coated particle
CLADDING	zircalloy	zircalloy	zircalloy	magnox	stainless steel	fuel embedded in
MODERATOR	H_2O	H_2O	D_2O	graphite	graphite	graphite matrix
COOLANT	H_2O	H_2O	D_2O	CO_2	CO_2	He gas

Table 1.1: Specifications of nuclear reactor designs.

1.5.3.2 The nuclear fuel cycle

The nuclear fuel cycle begins with the mining of uranium-containing ores which contain typically <0.5% U_3O_8. These have to undergo extensive separation/purification procedures before being passed either to a ^{235}U-enrichment plant or to a fabrication plant. Oxide fuel enriched in ^{235}U is required for BWR, PWR and AGR reactors. The fabrication plant ensures that the individual specifications of each reactor design are taken into account in the production of fuel elements. Once the fuel has been used in the reactor - the life span of fuel rods depends on the type of reactor - the fuel elements undergo reprocessing. Reprocessing is the "separation of fissile and fertile nuclear materials from fission products and other impurities in the fuel which has been irradiated in and discharged from a nuclear reactor" (Allardice *et al.*, 1983). This results in the production of pure compounds of the fissile and fertile materials which can then be re-used. In addition, a mixture of fission products and impurities in solid, liquid or gaseous phases are produced, these have to be disposed of safely.

In the U.K., reprocessing facilities are available at Sellafield in Cumbria for fuel from Magnox, AGR and LWR reactors, and at Dounreay in Caithness for fuel from Fast Reactors.

Of all the stages in the nuclear fuel cycle, those which contribute most to ^{14}C releases to

the environment are the actual running of the reactor and the reprocessing of the spent fuel. Sometime in the future, a considerable amount of ^{14}C may be released when nuclear plants undergo decommissioning.

1.5.3.3 ^{14}C production in nuclear reactors

^{14}C is produced in nuclear reactors as an activation product due to a number of reactions, occurring not only in the fuel but also in the cladding, coolant, moderator and the structural materials. A summary of the likely reactions is shown in Figure 1.8.

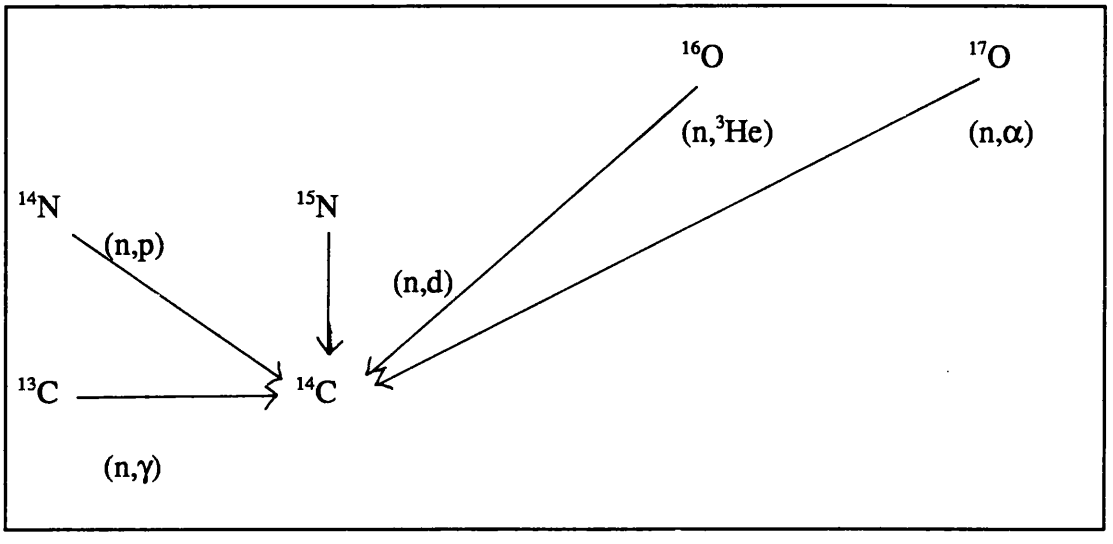

Figure 1.8: ^{14}C production pathways in a nuclear reactor.

The amount of ^{14}C produced in the reactor is dependent upon a number of factors within the reactor itself *eg.* the neutron flux, the neutron capture cross section of the target atom at a particular neutron energy, the amount of target atom present in the different reactor components and the abundance of the target isotopes in the target elements.

In thermal reactors there is a 20,000:1 ratio in favour of the reaction $^{14}N(n,p)^{14}C$ as opposed to the reaction involving the heavy isotope of oxygen ($^{17}O(n,\alpha)^{14}C$) due to the differences in fractional isotopic abundance and thermal cross section. The important characteristics of each isotope of interest are detailed in Table 1.2.

REACTION	ISOTOPIC ABUNDANCE	NEUTRON CAPTURE CROSS SECTION (barns)	
		THERMAL	FAST
$^{13}C(n,\gamma)^{14}C$	1.108	$1.0x10^{-3}$	$5.0x10^{-7}$
$^{14}N(n,p)^{14}C$	99.635	1.8	$1.3x10^{-2}$
$^{15}N(n,d)^{14}C$	0.365	small	$1.0x10^{-3}$
$^{16}O(n,^{3}He)^{14}C$	99.759	small	$3.0x10^{-8}$
$^{17}O(n,\alpha)^{14}C$	0.037	0.235	$1.2x10^{-4}$

Table 1.2: Target isotope characteristics.

^{14}C can also be produced in the reactor core due to the ternary fission of ^{235}U and ^{239}Pu but the amount produced is relatively small and is in the order of 1.7 and 1.8 atoms per 10^6 fissions, respectively (Hayes and MacMurdo, 1977).

Because each design of nuclear reactor has its own characteristics, the amount of ^{14}C produced in each will be different. The majority of the work carried out in determining the likely production rate of ^{14}C in nuclear reactors has been theoretical although some direct measurements have been made. These studies were carried out in the late 1970s and early 1980s by a number of workers (Kelly *et al.*, 1975; Magno *et al.*, 1975; Fowler *et al.*, 1976; Hayes and MacMurdo, 1977; United Nations, 1977; Davis, 1979; Kabat, 1979; Bonka, 1980; Beninson and Gonzalez, 1981; United Nations, 1982; Bush *et al.*, 1983; Martin, 1986). McCartney (1987) summarised these findings and calculated averages for each popular reactor design. Further work has since been undertaken and the revised figures (McCartney, pers. comm. 1992) are detailed in Table 1.3.

REACTOR DESIGN	^{14}C PRODUCTION RATE (TBq(GW(e)year)$^{-1}$)				
	Coolant	Moderator	Fuel	Structural Material (incl. Fuel Cladding)	Total
PWR		0.4	0.6	1.4	2.4
BWR		0.5	0.6	2.3	3.4
HWR*		20	1.1	1.9	23.0
GRAPHITE MODERATED**	0.3	8.0	2.2	1.8	12.3
LMFBR	-	-	0.2	0.6	0.8

Table 1.3: ^{14}C Production in the constituent components of nuclear reactors.

* some older HWR reactors use N_2 as an annulus gas hence increasing their potential ^{14}C production. The figures reported assume an equal mix of reactors using N_2 and CO_2 annulus gases as adopted by NCRP (1985).

** MAGNOX, AGR and HTGR reactors are included in this classification.

In reactors such as PWRs, BWRs and HWRs, ^{14}C is produced from both ^{14}N and ^{17}O present in the components. The $^{14}N(n,p)^{14}C$ reaction occurs in the fuel and its associated cladding and in the structural material of the reactor core, whereas, the $^{17}O(n,\alpha)^{14}C$ reaction occurs in the fuel, the coolant and the moderator. ^{14}N is present in the construction materials as an impurity and the amount of ^{14}C produced from this source is dependent upon the level of ^{14}N present. Most studies on likely production rates have assumed a nitrogen concentration of 1-5 ppm in the coolant and 10-25 ppm in the fuel and graphite moderators. The calculated ^{14}C production rates for PWRs and BWRs are similar but those for HWRs are greater due to the increased mass of moderator.

For the Magnox gas-cooled reactors, ^{14}C is produced by three reactions. ^{13}C present in the moderator and coolant interacts with neutrons to produce ^{14}C ($^{13}C(n,\gamma)^{14}C$) as does ^{17}O in the coolant and ^{14}N present as an impurity in the moderator, the coolant, the fuel and its associated cladding. In these reactors the moderator is the major source of ^{14}C. AGR systems are very similar to the Magnox reactors in their production of ^{14}C although the levels produced are considerably less.

The higher operating temperatures of the HTGR systems requires the use of enriched uranium-carbide-coated fuel particles embedded in a graphite matrix acting as the moderator. ^{14}C production occurs in the fuel, moderator and coolant *via* the $^{13}C(n,\gamma)^{14}C$ and $^{14}N(n,p)^{14}C$ reactions.

Although at present, the nuclear industry is dependent on thermal reactors such as those discussed, future developments may involve Liquid Metal Fast Breeder Reactors (LMFBR) where the fuels are mixed uranium and plutonium oxides, the core is cooled with liquid sodium and there is no moderator. ^{14}C production in these reactors is mainly from ^{17}O in the fuel and ^{14}N in the fuel and its associated cladding. Overall, LMFBR systems produce less ^{14}C due to the decrease in the neutron capture cross-section of the target isotopes with the increase in neutron energy. Fusion reactors may also feature in the future of the nuclear power industry. Very little is known of the likely ^{14}C production rates in this type of reactor but work by Scheele and Burger (1976) calculated that ^{14}C production from ^{13}C, ^{17}O and ^{14}N in a 5,000 MW(th) toroidal fusion reactor could be as high as 0.3 TBq/day if stainless steel was used in the structural components.

The fate of ^{14}C produced within nuclear reactors is dependent on the position of production. Any ^{14}C produced within the structural materials is likely to remain there until decommissioning while that produced in the fuel or fuel cladding will be transferred to the reprocessing plant where it may be released to the environment or retained as solid waste. ^{14}C produced in the coolant or moderator may be released to the atmosphere at the reactor site if it is not retained by ion-exchange resins used in the clean-up of the coolant. These ion-exchange resins are then disposed of to low-level waste burial sites where eventually ^{14}C may leak back to the atmosphere or into the groundwater.

The chemical form of ^{14}C released to the environment is dependent on the reactor type. For PWRs the releases to the atmosphere are usually in the form of simple hydrocarbons *eg.* CH_4, C_2H_6 whereas for BWRs 95% of the releases are as $^{14}CO_2$, 2.5% as ^{14}CO and the remaining 2.5% as simple hydrocarbons (Kunz *et al.*, 1975) with <1% being released in the liquid effluent (Fowler *et al.*, 1976). In HWR systems, most of the coolant and moderator derived ^{14}C is released to the atmosphere (Beninson and Gonzalez, 1981) with 50% in the reduced form ($^{14}CD_4$, deuterium from heavy water, D_2O, instead of the more usual $^{14}CH_4$ if H_2O present) and 50% in the oxidised $^{14}CO_2$ form (Beninson, 1984). Due to corrosion of the graphite moderator in Magnox reactors, some of the ^{14}C produced can

leak into the coolant system, leading to increased releases of $^{14}CO_2$ to the atmosphere (Bush *et al.*, 1983). This problem also arises in AGR systems. In addition, the graphite sleeves of the moderator can be reprocessed, hence, ^{14}C will be released at the reprocessing plant. The moderator of HTGR systems must be removed prior to reprocessing of the fuel, hence, any ^{14}C present will be oxidised and released at the reprocessing plant whereas coolant-derived ^{14}C will be released at the reactor site itself. In LMFBR systems, the ^{14}C is either released to the environment at the reprocessing plant or is retained as solid waste. The fate of ^{14}C produced in fusion reactors is similar to that of LMFBR reactors. Table 1.4 summarises the form and location of ^{14}C releases to the environment from each reactor design.

REACTOR TYPE	**^{14}C PRODUCTION TBq(GW(e)year)$^{-1}$**	**GASEOUS WASTE TBq(GW(e)year)$^{-1}$**		**SOLID WASTE TBq(GW(e)year)$^{-1}$**
		Reactor	**Reproc. Plant**	
PWR	2.4	0.4	0.6	1.4
BWR	3.4	0.5	0.6	2.3
HWR	23.0	13.1	1.1	8.8
GRAPHITE MODERATED	12.3	0.3	2.2	9.8
LMFBR	0.8	-	0.2	0.6

Table 1.4: ^{14}C form and location of release in the various reactor designs.

From 1989 figures for the % power generated by each reactor design, an annual production rate of 4.6 TBq GW(e) has been calculated (McCartney, pers. comm., 1992). Assuming that all the fuel is reprocessed and that all the ^{14}C in the fuel is released to the atmosphere, the ^{14}C release rate in the gaseous form is 1.8 TBq (GW(e)year)$^{-1}$. The remainder of the ^{14}C constitutes the solid waste (2.8 TBq(GW(e)year)$^{-1}$) and includes that produced in the fuel cladding, structural material, graphite moderator and 50% of that produced in the moderator of HWRs (which is retained in resins).

If these figures are then applied to the most recent installed capacity data (IAEA, 1991a), a potential ^{14}C production rate of ~1470 TBq year^{-1} is obtained with ~590 TBq year^{-1} (40%) of that being released to the atmosphere and the remainder retained as solid waste. Assuming that gaseous discharges occurring at the reprocessing plants are 25% of the total gaseous wastes then ~148 TBq of ^{14}C will be released per year during reprocessing.

So far, only atmospheric releases have been discussed, but liquid discharges also occur from reprocessing plants as have been noted at Sellafield (Section 1.8.1). Taking values calculated from Sellafield discharge data, liquid discharges of ^{14}C appear to account for 20-45% of the total ^{14}C released. This would give an annual global release of 30-67 TBq of ^{14}C to the marine environment.

The potential ^{14}C production from the nuclear fuel cycle is similar in magnitude to that from natural production although actual releases to the atmosphere are likely to be only ~50% of this. In addition, total ^{14}C released to the environment from the nuclear fuel cycle up to 1985 is only ~1% of that produced by the nuclear weapons tests of the 1950's and 60's (Lassey *et al.*, 1988).

1.5.4 Other Sources

1.5.4.1 Chernobyl

The incident at the Chernobyl nuclear plant in the Ukraine in April 1986 has been well documented. The quantity of ^{14}C released has not been reported but an approximate value of 5 TBq has been calculated (UN, 1988). An input of this magnitude would not be expected to cause a significant increase in atmospheric ^{14}C levels on a global scale although Kuc (1987) observed a local increase of ~9% in the atmospheric specific activity over Krakow in a three week period following the accident.

1.5.4.2 Research reactors

There are 323 research reactors in operation worldwide (IAEA, 1991a) but the total power capacity is no greater than that of one large nuclear power station. Within these reactors the release rate of ^{14}C will be highly variable and dependent on the exposure of air to the neutron flux. Overall, the global significance of ^{14}C from research reactors is considered to be negligible at <1% of that from the civil power industry (McCartney, pers. comm., 1992).

1.5.4.3 Pharmaceutical and radiochemical industries

Present production of ^{14}C from the pharmaceutical and radiochemical industries is assumed to be ~50 TBq yr^{-1} of which 40% is released to the atmosphere. The remaining 60% is incorporated into solid waste and buried at shallow landfill sites where it may leak back into the atmosphere at ~0.06% yr^{-1} (Baxter, pers. comm., 1989). These atmospheric releases result in an approximate 5% increase above that from civil power reactor operations. No data are available on liquid releases to the marine environment.

1.6 RADIOLOGICAL IMPLICATIONS OF ^{14}C RELEASES

Although not the major concern of this study, the radiological implications of anthropogenic releases of ^{14}C must be considered. Human exposure to ^{14}C can occur by three means, *ie.* external irradiation from ^{14}C in the atmosphere, internal irradiation after inhalation of atmospheric ^{14}C and internal irradiation after ingestion of ^{14}C in food.

As ^{14}C is a weak β-emitter only the irradiation to the skin needs to be considered for external irradiation. The radiation dose to man from external irradiation by ^{14}C can be calculated directly from the atmospheric ^{14}C specific activity (McCartney, 1987) by the equation:-

$$H_s^{ext}(t) = (3.9 \times 10^{-12})\ A(t) \qquad (1.3)$$

where $H_s^{ext}(t)$ is the dose equivalent in Sieverts per year (Sv yr^{-1}) and A(t) is the atmospheric ^{14}C specific activity in year t (in Bq $kg^{-1}C$). The constant in this equation is based on a carbon concentration in the atmosphere of 340 ppm (volume) and a dose equivalent rate in skin from external irradiation by ^{14}C of 2.16×10^{-8} Sv $yr^{-1}(Bq\ m^{-3})^{-1}$ (CEC, 1979).

Internal irradiation may be due either to inhalation or ingestion of ^{14}C. For Reference Man, as defined by the ICRP (1975), ingestion intake is ~0.3 kg C day^{-1} with nearly complete absorption, whereas inhalation is ~3×10^{-3} kg C day^{-1} with only 1% retained in the body. The body has a total carbon content of 16 kg which, in conjunction with the daily intake rate, gives a mean residence time of carbon in the body of 53 days. However, the residence time of carbon in the various components will vary considerably from this

average value. Stenhouse and Baxter (1977) obtained values of 5-7 years for carbon in the major organs and carbon incorporated into bone will have an even longer residence time. Once in the body, this carbon forms the structural base of all organic matter, including DNA and RNA which are genetically significant, and participates in all biological and biochemical processes. This incorporation into genetic material may increase the radiological significance of ^{14}C due to the transmutation effect. However, to date, it appears that the major contributor to the radiological significance of ^{14}C is the absorbed energy from ionisation processes occurring in the tissues.

The radiation dose to man from inhalation of atmospheric ^{14}C and ingestion of ^{14}C in food can be directly calculated from the ^{14}C specific activity in the atmosphere and food (Wirth, 1982; McCartney, 1987), *ie.*

$$H_x^{inh}(t) = (7 \times 10^{-12})\ A(t) \qquad (1.4)$$

$$H_x^{ing}(t) = (6.3 \times 10^{-8})\ A_f(t) \qquad (1.5)$$

where A(t) is the atmospheric ^{14}C specific activity in year t and $A_f(t)$ is the ^{14}C specific activity in food, respectively. If the ^{14}C release is in the $^{14}CO_2$ form, $A_f(t)$ is assumed to equal A(t) hence the radiation dose to man from all three exposure pathways is directly proportional to the atmospheric ^{14}C specific activity. The pathway of most importance to man is internal irradiation due to the ingestion of ^{14}C in food, with the other two routes being insignificant in comparison.

The use of a complex 25-box model with estimated future energy use scenarios (McCartney *et al.*, 1986; McCartney, 1987; McCartney *et al.*, 1988a,b) has indicated that the contribution of reactor-derived ^{14}C to the individual dose rate increases steadily into the future, reaching 1.8 $\mu Sv\ yr^{-1}$ in 2050 A.D.. This is approximately 12% of the total individual effective dose equivalent rate from ^{14}C of 15 $\mu Sv\ yr^{-1}$ calculated for that year. In the longer term, the collective effective dose equivalent commitment is estimated to be 141 $manSv\ (GW(e)yr)^{-1}$ indicating that ^{14}C could generate one of the largest contributions to the total dose to man from nuclear power production.

In this study the radiological significance to the population in the immediate vicinity of anthropogenic ^{14}C releases will be considered with regard to their consumption of locally caught shellfish. These calculated doses will then be considered in relation to the limits

recommended by ICRP.

1.7 THE CHEMISTRY OF CARBON IN THE OCEANS

Prior to discussion of the carbon chemistry in the world's oceans it may be appropriate to introduce some of the more general and influential geophysical processes which play a role in the observed distribution pattern of global oceanic ^{14}C.

1.7.1 Oceanic Chemical and Physical Processes

1.7.1.1 Sources of inputs

Under natural conditions the chemical make-up of the oceans is determined and maintained by the concentrations of the individual elements entering and leaving the system. Inputs into the oceans can be in the dissolved, particulate or gaseous phase and may originate from a number of sources as shown in Table 1.5.

SOURCE	DISSOLVED MATERIAL ($g\ yr^{-1}$)	PARTICULATE MATERIAL ($g\ yr^{-1}$)
Rivers	$39x10^{14}$	$183x10^{14}$
Subsurface Waters	$4.7x10^{14}$	$4.8x10^{14}$
Ice	$<7x10^{14}$	$20x10^{14}$
Marine Erosion	-	$2.5x10^{14}$
Atmospheric Supply	$2.5x10^{14}$	$6x10^{14}$
Volcanicity	-	$1.5x10^{14}$

Table 1.5: Input fluxes and origins to the oceans (from Raiswell *et al.*, 1991).

These indicate that dissolved material is transported to the oceans mainly from rivers, groundwater and atmospheric precipitation and that >95% of the particulate flux originates from rivers and glaciers. While the flux of particulate material greatly outweighs that of dissolved material, the particulate matter contribution from rivers is mainly weathered

aluminosilicates which may participate in ion exchange reactions but are generally considered to be inert in seawater (Raiswell *et al.*, 1991). Rivers are estimated to provide $0.4x10^{15}$ g of inorganic carbon (Baes *et al.*, 1985) and $0.2\text{-}1.0x10^{15}$ g of organic carbon (Richey *et al.*, 1980; Schlesinger and Melack, 1981; Meybeck, 1982) per year to the oceans. Assuming a total global flux from rivers of $3.74x10^{16}$ litres (Chester, 1990) with mean dissolved and particulate organic carbon contents of 5.75 and 2.0 mg l^{-1} respectively (Ertel *et al.*, 1986; Chester, 1990) a total organic carbon input of $0.29x10^{15}$ g is obtained. This is at the lower end of the quoted range but gives an indication of the carbon fluxes in each phase.

Atmospheric inputs are the result of both natural and anthropogenic processes, *eg.* wind erosion of the earth's surface, volcanic eruptions and cosmogenic production of both stable and radioactive nuclides, however, the physical and chemical composition varies in both time and geographical area. Inputs to the oceans have increased as a result of mans' activities, *eg.* fossil fuel burning, mining and processing of ores, waste incineration, chemical production and the use of agricultural chemicals (Chester, 1990). The transfer of inorganic carbon between the atmosphere and surface oceans is dependent on the partial pressure of CO_2 in each of the reservoirs, hence, transfer rates between the two will be variable. As with riverine inputs, organic atmospheric inputs can be subdivided into two phases - particulate and gaseous carbon. The atmospheric burden of organic carbon in the particulate phase has been estimated at $1\text{-}5x10^{12}$ g and that in the gaseous phase as $\sim 50x10^{12}$ g (Duce, 1978). The flux of carbon from the atmosphere to the ocean's surface has been calculated to be $2.2\text{-}10x10^{14}$ g yr^{-1} (Williams, 1975; Duce and Duursma, 1977) by wet deposition and $\sim 6x10^{12}$ g yr^{-1} (Duce and Duursma, 1977) by dry deposition. The estimated reverse flux is $\sim 14x10^{12}$ g yr^{-1} (Duce, 1978) indicating that surface oceans act as a sink for atmospheric organic carbon.

1.7.1.2 Circulation

Essentially, the oceans are considered to comprise of two distinct layers - the thin, less dense, warm surface layer (~2% of the total volume) which is well-mixed and is warmed by solar energy down to depths of 20 - 200 metres (average 75 m) and a thicker, colder, denser deep layer which accounts for 80% of the total volume. Between these two layers there is an area where a rapid decline in temperature occurs (the thermocline) accompanied by a region where there is a rapid increase in density (the pycnocline). The thermocline

and pycnocline are well developed in all regions except at high latitudes where they are less well defined or are absent altogether. The thermocline region accounts for 18% of the total volume and may extend down as far as 1000 metres where it forms a barrier to the mixing of surface and deep waters (Solomon *et al.*, 1985; Chester, 1990; Gross, 1990).

The currents in the surface layers are driven by the wind and tend to be mainly horizontal with very little vertical movement. One of the main features of surface circulation is a series of large anticyclonic gyres with boundary currents on their landward side which occur in sub-tropical and high pressure regions (see Fig 1.9). The depth of the surface layer is greatest in the areas 15-50° north and south of the equator *ie.* the temperate regions, and shallower in the equatorial and polar regions.

In comparison, the circulation of the deep ocean water is driven by gravity, which is the result of the density difference between water masses, and it is a much slower process than the surface water circulation. It involves both vertical and horizontal movement as the water moves down the water column until it reaches a level where the density is equal to its own and then it starts to move horizontally. This results in stratification of deep waters with the differing densities forming isopycnal surfaces down the water column (Baes *et al.*, 1985; Chester, 1990; Gross, 1990).

Deep waters undertake a "grand tour" from their source points in either the North Atlantic or the Antarctic. The North Atlantic waters have a low surface temperature and high salinity which causes them to sink to form the North Atlantic Deep Water (NADW) whereas the Antarctic waters, which originate in the Weddell Sea, are colder and dense and sink to form the Antarctic Bottom Water (ABW). The NADW flows down through the Atlantic where it is underlain by the southern ABW. This water then leaves the Atlantic/Antarctic region and flows into the Indian Ocean where it circulates before travelling up through the Southern Pacific into the Northern Pacific (see Fig 1.10). The deep water of the Northern Pacific is the oldest water in the world and hence forms a sink for all the deep waters. This deep water circulation pattern was proposed by Stommel (1958).

For any mixing of surface and deep water to occur, the thermocline/pycnocline region must be breached and this is most likely in areas of high latitude where it is not as well defined or may be absent altogether. This allows deep water to "outcrop" in the polar regions and hence recycle deep water to the surface. This recycling is required to bring important

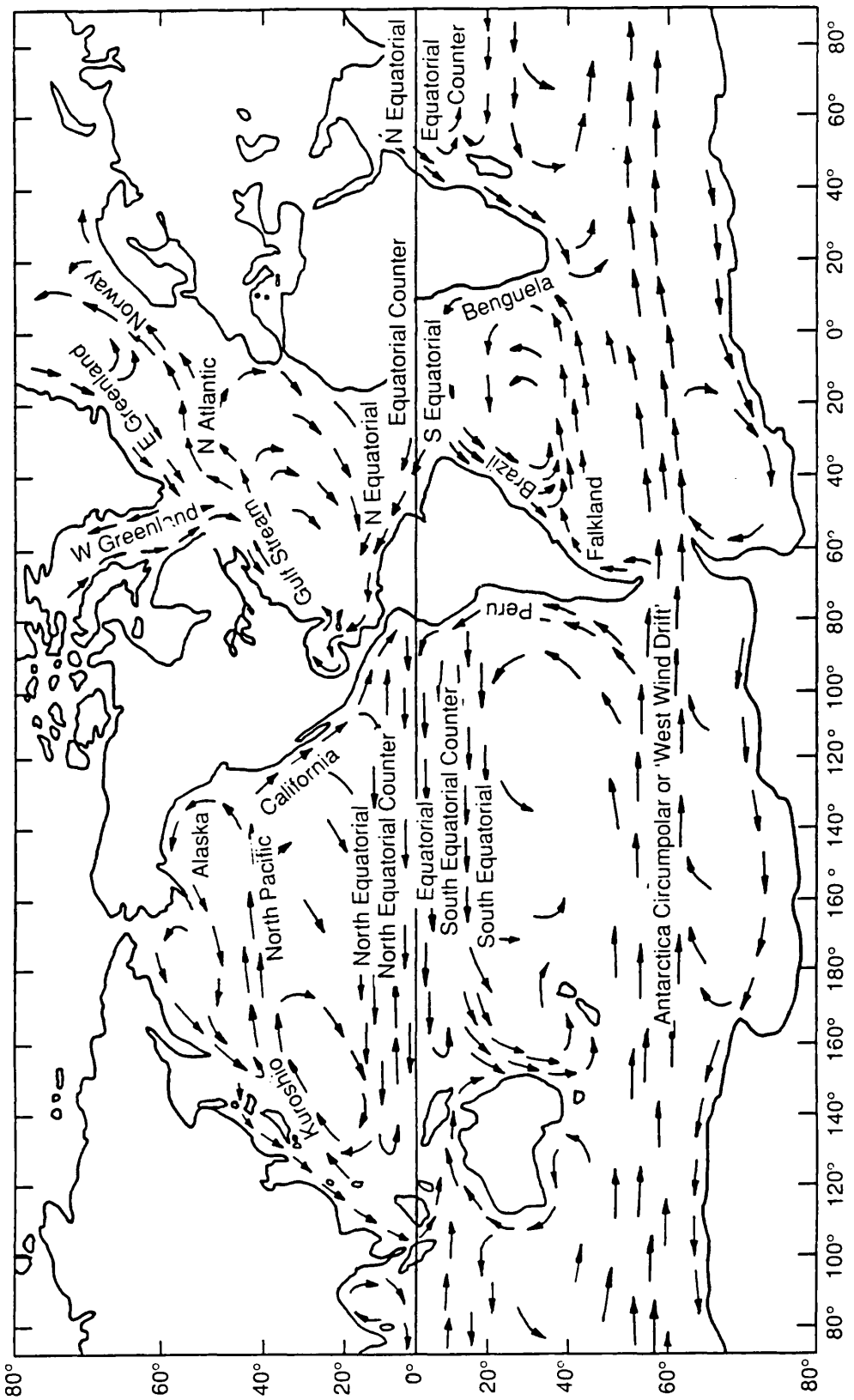

Figure 1.9: The surface water currents of the worlds' oceans.

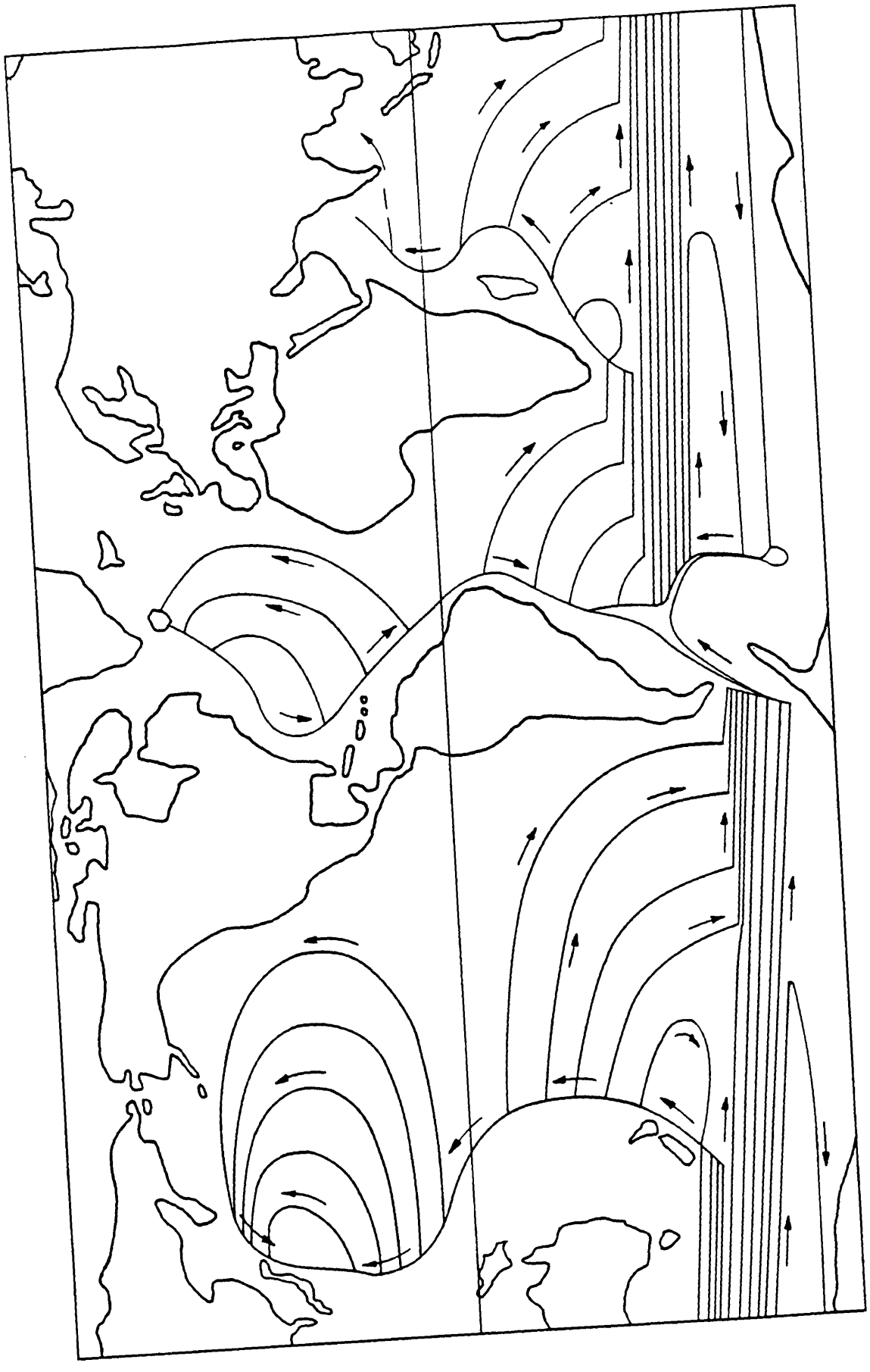

Figure 1.10: The deep water currents of the worlds' oceans.

nutrients to the surface so that they can be utilised by the marine biomass. Nutrients are also recycled to the surface in sub-tropical coastal regions where the wind drives water offshore and water from 200 - 400 m depth replaces the surface water to conserve the initial volume. Upwelling may also occur in the mid-ocean areas where diverging currents or erosion of the thermocline, due to turbulence, allows deep water to reach the surface.

1.7.1.3 Removal processes

The main route of removal for material in the water column is due to the gravitational sinking of organic particles in conjunction with the precipitation of inorganic material in a ratio of 4:1 (Li *et al.*, 1969). Organic matter, composed mainly of dead organisms and organic aggregates, undergoes oxidative destruction as it sinks from the surface. Of this organic matter ~95% is recycled in the surface ocean with the remaining ~5% continuing to sink as large organic aggregates into deep waters where they may capture fine particulate material suspended in the water column in a series of aggregation-disaggregation reactions. These aggregation-disaggregation reactions continue down the water column ensuring the removal of elements to the sediments by scavenging-type reactions. Once these aggregates reach the sediment surface they undergo further oxidative destruction to drive the processes involved in early diagenesis (Chester, 1990).

Carbonate material (calcite and aragonite) produced by foraminifera, coccolithophorids and pteropods in the surface oceans will also settle down the water column on the death of these organisms, hence, providing a supply of inorganic carbon and calcium to deeper waters. On descent through the water column, these carbonates are subject to dissolution as the solubility increases with pressure (and so depth) and decreasing temperature, hence, the formation of carbonate sediments is determined by the topography of the sea floor. There is a depth at which the supply of carbonate is equal to the carbonate undergoing dissolution; this is termed the carbonate compensation depth (CCD). This depth is different for the two types of carbonate and for each of the major oceans. Aragonite is more soluble than calcite, hence the CCD appears at 3 km in the western tropical North Atlantic, 1-2 km in the western tropical Pacific and at a few hundred metres in the tropical North Pacific (Berger, 1976) as opposed to 4.5-5 km in the Atlantic, 5 km in the tropical Indian Ocean and 3-5 km in the Pacific for calcite.

1.7.2 Carbon Chemistry

Within the marine system, the carbon cycle can be subdivided on the basis of chemical form into inorganic and organic carbon compounds.

1.7.2.1 The inorganic carbon cycle

In the oceans, only a small amount of the total carbon is in the form of dissolved carbon dioxide (<1%) but this is the main form of uptake from the atmosphere. The rate of CO_2 uptake by the oceans is dependent upon marine conditions such as temperature, salinity and the partial pressure of CO_2 as well as the prevailing wind speed. The main sources of information for the calculations of CO_2 uptake have been a series of surveys which were undertaken in the 1970's and 80's such as Geochemical Ocean Sections Study (GEOSECS), Vertical Transport and Exchange (VERTEX) and Transient Tracers in the Oceans (TTO). These provided a baseline study for future chemical changes and also investigated large scale oceanic transport and mixing processes by using ^{14}C and ^{3}H as tracers. Various workers have interpreted the GEOSECS data using a variety of methods to calculate the flux of CO_2 from the atmosphere to the mixed surface layer of the oceans. The results obtained are summarised in Table 1.6 and show reasonable agreement. An average value of 20-23 mole m^{-2} yr^{-1} was obtained for the period 1962-1972 based on bomb-^{14}C. Estimates of the pre-industrial flux, when ^{14}C concentrations were lower, range from 17.5-20 mole m^{-2} yr^{-1} based on the flux being proportional to the partial pressure of CO_2. However, regional variability does occur due to the stronger winds at high latitudes and larger CO_2 exchange flux in high southern latitudes.

AUTHOR	REGION	CO_2 INVASION RATE (mole yr^{-1} m^2)
Munnich and Roether (1967)*	Atlantic	25
Stuiver (1980)°	Western Atlantic	27.0
	Eastern Atlantic	18.7
Quay and Stuiver (1980)°	Atlantic	21
	Pacific	25
Broecker *et al.* (1985)°	Atlantic	22.3
	Pacific	19.4
	Indian	19.2

Table 1.6: Atmosphere-surface ocean CO_2 invasion rates.

* North Atlantic Survey

° GEOSECS

CO_2 is produced in the terrestrial biosphere and released to the atmosphere during respiration of plants, forest clearing, agricultural practices and the combustion of fossil fuels. Although the level of CO_2 in the oceans is relatively small, the overall amount of inorganic carbon present in the marine system is 50-60 times the amount that is present in the atmosphere (Siegenthaler, 1989; Chester, 1990). Due to atmosphere-ocean transfer of CO_2, the oceans act as a sink for excess atmospheric CO_2 and play an important role in regulating planetary CO_2.

Atmospheric CO_2 entering the surface layer is utilised by marine phytoplankton during photosynthesis ($CO_2 + H_2O \rightarrow (CH_2O)_n + O_2$) and in the formation of the carbonate shells of marine organisms. This results in a depletion of CO_2 at the surface but an increase towards the bottom of the euphotic zone due to regeneration of CO_2 from the oxidation of organic matter. Levels in the deep water tend to be fairly constant.

As CO_2 is reactive in seawater, a series of equilibria are set up which act as a buffer mechanism in the oceans and, hence, control the pH. The reactions which occur are:-

1. atmosphere - surface water

$$CO_{2\ (gas)} \leftrightarrow CO_{2\ (dissolved)} \quad (1.6)$$

2. hydration of the dissolved CO_2

$$CO_2 + H_2O \leftrightarrow H_2CO_3 \text{ (carbonic acid)} \quad (1.7)$$

3. rapid dissociation

$$H_2CO_3 \leftrightarrow H^+ + HCO_3^- \text{ (bicarbonate ion)} \quad (1.8)$$

and

$$HCO_3^- \leftrightarrow H^+ CO_3^{2-} \text{ (carbonate ion)} \quad (1.9)$$

These reactions are temperature and pressure dependent and the relative proportions of each species are set by maintaining a steady pH. The pH range which is normally associated with seawater is 7.5-8.4 and within this range ≥ 99% of the dissolved CO_2 is present as carbonate (CO_3^{2-}) and bicarbonate (HCO_3^-) ions. Within the time periods of 100-1000 years, it is these reactions which regulate the pH of the system but on geological timescales, pH is controlled by chemical equilibria between the water and the minerals which constitute the marine sediment.

The carbonate system within the oceans is closely linked to the alkalinity which is due to the dissolution of basic minerals. The alkalinity is essentially a measure of the buffering capacity of natural waters and is therefore equivalent to the charges of all the weak ions in solution and can be measured titrimetrically. It has been found that although the amounts of individual ions may differ both in time and distribution, the proportions of the ions present are fairly constant. The ions which influence the buffering capacity of the oceans include Cl^-, SO_4^{2-}, Na^+ and Ca^{2+}, but, in calculations of alkalinity, borate, bicarbonate and carbonate are the ions of major importance *ie*.

$$\text{Alkalinity} = [HCO_3^-] + 2[CO_3^{2-}] + [B(OH)_4^-] + [OH^-] - [H^+] \quad (1.10)$$

On the death of marine organisms, their carbonate shells descend in the water column where they will undergo dissolution (see Section 1.7.1.3). This downward movement of $CaCO_3$ and its subsequent dissolution ensures a supply of inorganic carbon to the surface waters in the course of natural circulation and cycling patterns within the oceans.

1.7.2.2 The organic carbon cycle

In the marine system, there are assumed to be three different forms of organic matter present - the particulate (POM or POC), the dissolved (DOM or DOC) and the volatile phases (VOM or VOC). In most studies, the volatile phase is disregarded because it forms such a small part of the overall carbon reservoir. The working definition of POM is "that fraction which is retained by a 0.45 μm filter", with the dissolved phase that which passes through the filter. In reality, the DOM will contain some colloidal material which the filter fails to retain but this is unavoidable.

(a) Particulate Organic Carbon (POC)

The absolute amount of carbon present in the organic form is small in comparison to that in the inorganic form but it is a very important part of the marine carbon cycle. Allochthonous organic matter originates from river run-off and atmospheric deposition (see Section 1.7.1.1) but the greatest source of organic carbon is *in situ* production due to photosynthesis by phytoplankton in the surface layers (autochthonous organic matter). The phytoplankton remove CO_2 from the water column and use it to produce organic matter during photosynthesis *ie.*

$$CO_2 + H_2O \leftrightarrow (CH_2O)_n + O_2 \qquad (1.11)$$

Due to this ability to fix their own carbon for metabolic purposes, the phytoplankton are known as "primary producers". The rate at which primary production takes place is controlled by a combination of variables such as light, temperature, the growth rate of the organisms and also the supply of nutrients available to the growing population. Nienhuis (1981) proposed that of these, the main restraint on primary production was the supply of nutrients which relies on the upwelling of deep water to the surface euphotic layer. Globally, there are areas of high and low primary production known as eutrophic and oligotrophic regions, respectively. Eutrophic regions are usually in coastal zones and areas of upwelling where nutrient-rich deep waters enter the biologically depleted surface layer. The areas where primary production is highest are the western coastal shelf regions off West Africa, Namibia, Peru, the Western U.S.A., Australia, India and Southeast Asia. This is in addition to the open ocean areas where upwelling, due to diverging currents, increases the supply of nutrients, *eg.* the equatorial Pacific and Antarctica.

Low productivity regions (*ie.* oligotrophic) are found where very little mixing of surface and deep water occurs. This may be due to a permanent thermocline such as those found in the central oceanic gyres of the regions 10° to 40° north and south of the Equator.
The measure of primary production rates has traditionally been carried out using ^{14}C tracer techniques but more recent work indicates that this underestimates the likely rates. Williams and Druffel (1987) calculated rates of 4-15x10^{16} g yr^{-1} which were considerably greater than previously reported values of 1.5-1.8x10^{16} g yr^{-1} (Williams, 1975) and 4x10^{16} g yr^{-1} (de Vooys, 1979). Approximately 80% of this primary production occurs in the open ocean with the remaining 20% in the coastal regions (Martin *et al.*, 1987).
So far, only the living portion of the particulate organic material has been discussed but this accounts for <1% of the total carbon present in the organic fraction. POC itself, at most, accounts for 3% of the total organic carbon, with the remainder in the dissolved phase. The non-living component of the POC consists mainly of dead organisms, faecal material and debris, organic aggregates and various complex organic particles. The formation of this fraction is thought to be due to five main reactions in the open oceans (Cauwet, 1981; Fellows *et al.*, 1981):-

1. direct detritus formation *ie.* faecal pellets and parts of organisms,
2. bacterial clustering,
3. aggregation of organic molecules due to bubbling in the surface layers,
4. flocculation/adsorption of DOC onto mineral particles, and
5. packaging of soluble organic material into POC by bacteria and other micro-organisms.

The elemental composition of marine POM has been fairly well studied and it seems to mirror that found in the water column. Unfortunately, it is not known whether the biomass dictates the composition of nutrients in the water column or whether the biomass takes up the elements in a ratio set by the nutrients in solution. Redfield (1934,1938) found that C, N and P were present in a ratio of 106:16:1 in the organic matter of phytoplankton and zooplankton as well as that present in the water column. He also found that 138 moles of oxygen are required to produce 106 atoms of carbon, 16 atoms of nitrogen and 1 atom of phosphorus when marine organic matter undergoes oxidation. More recent work has studied the levels of C, N and P present in POM and as a result, ratios of 122±18:16:1 (Takahasi *et al.*, 1985) and 126:15.7:1:23.5:23.0 for C_{org}:N:P:Si:C_{inorg} (Watson and Whitfield, 1985) have been obtained for the thermocline regions of the Atlantic and Indian

oceans and in the material leaving the euphotic zone, respectively.

Marine organisms on the whole are made up of common organic building blocks such as amino acids, proteins, carbohydrates, lipids and pigments. Degens and Mopper (1976) found that the amino acid composition of proteins was consistent between species of phytoplankton with glycine, alanine, glutamic acid and aspartic acid being the most common. These are excreted into the water column by both phytoplankton and zooplankton. In contrast, the carbohydrate composition was found to vary considerably between species (Degens and Mopper, 1976) with the general order of abundance following the order galactose > glucose > mannose > ribose > xylose > fucose > rhamnose > arabinose. Differences occur between phytoplankton and zooplankton in their lipid compositions. In phytoplankton, the most abundant form of lipids are triglycerides which do not only store energy but act as buoyancy controls and thermal/mechanical insulators. In zooplankton, fatty alcohols and long chain fatty acids make up the wax esters which are the main form of lipids. The most important pigments present are the photosynthetic pigments - chlorophyll a,b,c, and d and some carotenoids - with the maximum level found near the bottom of the euphotic zone.

The flux of POM from the surface layer to the deep ocean is dominated by the settling of fairly large particles ($\geq$ 200 μm) such as faecal pellets. The more common small particles play an insignificant part in the overall downward movement (Suess, 1980). Although vertical transport of POM is thought to be predominantly downwards, Smith *et al.* (1989) proposed that significant upward fluxes did occur in the North Pacific (up to 66.7% of the downward flux) and this was mainly due to lipid-rich transparent spheres (possibly eggs) and marine larvae which were more buoyant than the detrital particles and faecal pellets which constitute the downward-moving particles.

(b) Dissolved Organic Carbon (DOC)

The dissolved phase of organic matter formed *in situ* in the marine environment is considered to come from three main processes - exudation by phytoplankton, excretion by zooplankton and also the breakdown of detritus by microbial activity (Williams and Druffel, 1988). The estimated amount of DOC released into the system in this manner is approximately 10% of the carbon fixed during photosynthesis *ie.* 3.6×10^{15} g yr^{-1}.

Terrestrially-derived DOC from river run-off has also been studied in the marine environment with the general consensus being that <10% of the oceanic DOC pool

originated on land and has been transported to the sea in river water (Williams and Gordon, 1970; Eadie *et al.*, 1978; Meyers-Schulte and Hedges, 1986; Williams and Druffel, 1987). These measurements were carried out using a variety of methods - Meyers-Schulte and Hedges looked at the levels of lignin, a phenolic polymer produced by higher plants on land, with the assumption that any found was terrestrially derived, while other workers used both radiocarbon signals and $\delta^{13}C$ values. $\delta^{13}C$ values for terrestrially derived organic matter differ considerably from those of marine organic material produced *in situ* (-26 to -32‰ and -20 to -22‰ respectively) (Williams and Gordon, 1970; Hedges *et al.*, 1986; Williams and Druffel, 1987; Meyers-Schulte and Hedges, 1986). Mantoura and Woodward (1983) disagree with the above findings on the source of oceanic DOC. They have shown that riverine DOC behaves conservatively in estuaries resulting in as much as 50% of the marine DOC being derived from terrestrial sources.

Over the years, a great number of attempts have been made to ascertain the level of DOC present within the marine environment. To do this, a variety of methods have been developed - the difficulties lay in the size of samples required to obtain suitable levels of carbon and the refractory nature of part of the DOC which is resistant to chemical oxidation. Early work in 1934 by Krogh using dichromate oxidation resulted in a concentration of 2.28-2.4 mg C l^{-1} for the North Atlantic although Duursma (1961,1965) found a concentration considerably less than this of 0.3-1.2 mg C l^{-1} using the same technique. Dry combustion methods (Skopintsev *et al.*, 1966,1968; Starikova & Yablokova, 1974; Gordon & Sutcliffe, 1973; Mackinnon, 1978) gave values in the range 0.7-2.5 mg C l^{-1}, again for the Atlantic. Using persulphate oxidation techniques Menzel & Rhyther (1968) and Sharp (1973) obtained similar values to Duursma in the range 0.3-1.3 mg C l^{-1}. Sharp (1973) also compared his results to those obtained using wet combustion methods and found reasonable agreement between them, indicating that similar components of the DOC were being oxidised during the different methods.

In the Pacific, similar concentrations of DOC have been measured again using oxidation techniques. Plunkett and Rakestraw (1955) measured 0.6-2.7 mg C l^{-1} using dichromate oxidation whereas persulphate reactions (Holm-Hansen *et al.*, 1966; Ogura, 1970) gave values of 0.4-0.9 and 0.7-1.68 mg C l^{-1}. Work carried out in the 1980s by Miyaki *et al.* (1985) using wet combustion techniques gave a wider range of 0.8-3.8 mg C l^{-1} and Williams and Druffel (1987) have quoted an average of 1.04 mg C l^{-1} for the Northern

Pacific.

These results indicate that the measured DOC concentrations depend on the type of oxidation process which is undertaken. It has been noted that these methods are unable to oxidise the most refractory material. Sugimura and Suzuki (1988) have developed a high temperature catalytic oxidation system which to date has measured DOC concentrations 2.5 times greater than levels measured previously. The results of this method have still to be reproduced and confirmed.

Such studies have been involved in quantifying the mass of carbon in the dissolved organic phase, whereas more detailed studies on the components, *eg.* carbohydrates, proteins, amino acids *etc.*, of this fraction have been reported as a percentage of the total organic matter. Given the variability in the carbon content of these different components, the discussion which follows will refer to the dissolved organic matter as opposed to dissolved organic carbon.

Part of the DOM (20%) is made up of common building blocks *ie.* lipids, carbohydrates, amino acids, urea and pigments and this is known as the labile fraction because these molecules can be easily utilised by the oceanic biomass. The remainder of the DOM present has not been characterised but is thought to be resistant to chemical and biological attack and hence may spend a considerable time in the water column before being taken up by the sediments or other carbon pools.

The lipids and hydrocarbons present in the DOM have been studied extensively - the major components which have been isolated are the n-alkanes (C_{16}-C_{32}), pristane, phytane and fatty acid esters. Free fatty acids which are present *eg.* palmitic, oleic, myristic and stearic acids make up 1-3% of the total DOM present in seawater. Higher concentrations of lipids occur just above the pycnocline where the rapid increase in density stops further downward movement of the less dense lipids. Hydrocarbons are present in all marine organisms although they usually account for <1% of the total lipid content - they are usually present in concentrations of less than 50 $\mu g\ l^{-1}$.

Carbohydrate concentrations in the DOM of the oceans have been measured at 0.27 mg l^{-1} at the surface, increasing to 0.75 mg l^{-1} at a depth of 75 metres. A further increase was registered at depths of 350 -1000 m followed by a decrease below 2000 m (Walsh and Douglass, 1966). The composition of carbohydrates found - laminaribiose, laminatriose, glycosylglycerols, sucrose and raffinose - was also found in phytoplankton, thus it appears

that free carbohydrates in the water column may come from exudations by the biomass. Dissolved free amino acids and dissolved combined amino acids were studied by Lee and Bada (1977) who found that the levels of free amino acids were much lower than those for the combined amino acids, especially in the euphotic layer where heterotrophic activity would be greatest.

The refractory phase of the DOM in the oceans has for many years posed problems to the oceanographer and the marine chemist as it is extremely difficult to isolate and characterise. One group of organic compounds which have been isolated from sea water include humic substances which are thought to account for 40-80% of the DOC and are in the form of humic and fulvic acids. Initially, this refractory material was given the name "Gelbstoff" because of the yellow colour that it gives seawater plus the similarities to the organic acids formed in soils. More recently it has emerged that the majority of marine organic acids are formed *in situ* and hence have their own characteristic chemical makeup. The only resemblance between marine and terrestrial organic acids is the ability to complex metals and similarities in their redox functions.

The levels of these organic acids found in both coastal regions - where they are enhanced by terrestrially derived organic acids - and in the open oceans of the Gulf of Mexico indicated that fulvic acids make up 90% of the natural organic acids in both environments with 150-250 $\mu g\ l^{-1}$ and 400-800 $\mu g\ l^{-1}$ in the open oceans and coastal regions respectively (Harvey and Boran, 1985). These results substantiate earlier work carried out in the Sargasso Sea and more recent work carried out in the equatorial Pacific (Meyers-Schulte and Hedges, 1986).

The chemical structures of fulvic and humic acids have been studied using both chemical and spectral techniques, and the conclusion reached was that these substances are formed by a series of non-random reactions involving naturally occurring unsaturated lipids which are released into the water column by the oceanic biomass. Harvey *et al.* (1983) proposed that these naturally occurring unsaturated fatty acids underwent crosslinking due to free radical reactions in the surface waters where they are accelerated by light and catalysed by the presence of transition metals. At some stage during this crosslinking, the molecule becomes soluble in water and assumes the properties associated with fulvic acid. Also, in the course of these reactions, a small proportion of substituted cyclohexane rings are formed and this is thought to be the mechanism which leads to the aromaticity found in

humic acids. The degree of crosslinkage which occurs dictates the flexibility of the molecule - fulvic acids have less crosslinking and hence are quite flexible and soluble at all pHs whereas humic acids have a more rigid structure which will become insoluble at low pHs.

In the marine system, humic substances play an important role in the biology and chemistry of toxic metals by metal-organic association which decreases the metal mobility and inhibits biological uptake as well as taking part in redox reactions.

1.7.3 Radiocarbon Distribution Within the Oceans

Many measurements of ^{14}C concentration in the oceans have been made but mostly since the introduction of anthropogenic ^{14}C from nuclear weapons tests. Some pre-bomb ^{14}C measurements were made (see Broecker, 1963 for summary), but on the whole they have had to be calculated by inference. This has been complicated by the dilution due to the Suess effect.

In most oceanographic studies, ^{14}C concentrations are reported as *per mil* deviation from the standard NBS oxalic acid after fractionation has been taken into account, ($\Delta^{14}C$) (as recommended by Broecker and Olson (1961) and Stuiver and Polach, (1977)) *ie.*

$$\Delta^{14}C = (R_N/R_{St} - 1) \times 1000 \text{ ‰} \qquad (1.12)$$

where $R_N = \delta^{13}C$ normalised activity of the sample at the time of collection and R_{St} = the absolute international standard activity. This is related to the notation used throughout this work by:-

$$\%Mod \pm \sigma\%Mod = (100 + \Delta^{14}C/10) \pm \sigma\Delta^{14}C/10 \qquad (1.13)$$

Pre-industrial ^{14}C concentrations are thought on average to have been -50‰ and -160‰ for warm surface and deep waters respectively. In areas of deep water outcropping, the levels found in surface waters tend to be lower than the assumed average; $\Delta^{14}C$ levels for the polar regions are -70‰ and -100 to -120‰ for the north and south respectively.

Several systematic surveys of the ^{14}C concentration in the oceans have been carried out during the last 20 years. The Geochemical Ocean Section Survey (GEOSECS) was the

largest of these and it began in 1972 with a survey of the Atlantic ocean. This was followed by two subsequent surveys carried out in 1973-74 and 1977-78 of the Pacific and Indian oceans respectively. In addition to GEOSECS, NORPAX in 1979 produced a detailed survey of a section of the North Pacific and TTO (Transient Tracers in the Ocean) surveyed areas of the Atlantic Ocean during the period 1981-83 as a follow up to GEOSECS.

In the GEOSECS surveys, the aim was to determine baseline chemical conditions as well as to investigate large scale oceanic transport and mixing processes. The information collected during GEOSECS was interpreted by a number of workers to help deduce 1) upwelling rates and fluxes in the equatorial Atlantic to account for ^{14}C depletion in the DIC of the water column (Broecker *et al.*, 1978; Wunsch, 1984), 2) mechanisms and rates of vertical mixing in the Atlantic and Pacific thermoclines (Quay and Stuiver, 1980), 3) Atlantic circulation patterns (Stuiver, 1980), 4) replacement times for the abyssal waters of the Pacific, Atlantic and Indian Oceans respectively (Stuiver *et al.*, 1983) and 5) general features of oceanic circulation and transfer of atmospheric CO_2 (Broecker *et al.*, 1985). One common feature of all depth profiles analysed was the inclusion of bomb-derived ^{14}C (Stuiver *et al.*, 1981) producing a peak at or near the surface of $\geq$ 100‰.

The NORPAX survey of 1979 studied the upper 1000m of a north-south transect from Hawaii to Tahiti in the equatorial Pacific. Variations in $\Delta^{14}C$ and nutrient profiles occurred with latitude which helped in the deduction of equatorial upwelling rates and advective fluxes (Quay *et al.*, 1983).

Anthropogenic geochemical tracers, such as tritium and radiocarbon from nuclear weapons tests, were the main points of interest in the TTO program in the Atlantic as a sequel to the GEOSECS survey. The surveys of the North Atlantic and tropical Atlantic regions were undertaken in 1981 and 1983 respectively.

The data accumulated from these surveys have helped to identify, in conjunction with other tracers such as salinity, temperature, ^{3}H, total CO_2 *etc.*, the circulation patterns detailed in Section 1.7.1.2.

Specifically, the ^{14}C results have shown that North Atlantic water appears younger than the Antarctic, the Northern Indian and the Northern Pacific, thus supporting the circulation pattern detailed in Section 1.7.1.2.

In the Pacific, where the only source of water is from the Circumpolar current, the deep

waters have been found to have $\Delta^{14}C$ concentrations which are not horizontally homogeneous in either a north-south or east-west direction. There is a deep tongue of water with relatively high $\Delta^{14}C$ values suggesting that the northward flow of this new bottom water is compensated for by a flow southwards at intermediate depth. Deep water in the west is also found to have higher $\Delta^{14}C$ values due to the northward western boundary current and cyclonic bottom water circulation (Ostlund and Stuiver, 1980).

The Atlantic does not show such a clear cut picture. There are two sources of bottom water - one from the north (NADW) which is considered to have a pre-industrial $\Delta^{14}C$ of -70‰ (Broecker, 1979) and another from the south which is a mix of Weddell Sea Bottom water with a $\Delta^{14}C$ of -148‰ to -154‰ (Weiss *et al.*, 1979; Broecker and Peng, 1982) and deep circumpolar water. This water from the south is assumed to have a pre-industrial $\Delta^{14}C$ of -160‰ when it enters the abyssal western Atlantic at 30°S. Within the western Atlantic, the NADW forms a tongue of high $\Delta^{14}C$ water at depths of 1.5-4 km but the north-south trend and vertical variation, which are apparent, are reflections of the existence and mixing of different water types as opposed to the ageing of water bodies. As the western basin feeds the eastern basin in the Atlantic, it is not surprising that deep water in the eastern basin appears older than that in the western basin.

Within the Indian Ocean, the $\Delta^{14}C$ values are relatively low with Stuiver and Ostlund (1980) finding them almost uniform between 2000-3500 m at 0-30°S in the western basin. Between 40 and 50°S, a downward tongue of higher $\Delta^{14}C$ values appear at intermediate depth indicating some downwelling.

The surface and thermocline waters have reflected changes in atmospheric specific activities over the years. Pre-industrial values for natural $\Delta^{14}C$ are thought to be -50‰±10‰ in the temperate regions (10° - 40° north and south), -60‰ in the tropical regions (10°S to 10°N) and -70‰ and -100 to -120‰ for the north and south polar regions respectively. The influence of natural and anthropogenic perturbations have been widely studied even outwith programmes such as GEOSECS. Druffel and Suess (1983) attributed a 6 to 12‰ decrease in $\Delta^{14}C$ in corals to the Suess effect as of 1952 while other studies found evidence of localised upwelling in low $\Delta^{14}C$ values for corals (Nozaki *et al.*, 1978; Druffel, 1981) and off the west coast of Africa (Nydal *et al.*, 1980).

By 1957, any depletion due to the Suess effect in surface waters was overshadowed by the incorporation of bomb-^{14}C. The $\Delta^{14}C$ values increased rapidly until 1968 when they

levelled out or began to decline slowly. In the period 1971-1974, $\Delta^{14}C$ values in excess of +100‰ were found in the temperate regions although values in the circumpolar regions remained negative. Weiss *et al.* (1979) found values which ranged from -77 to -116‰ in the Weddell Sea in 1973 while Linick (1978) found values of -90‰ in the region 62-70°S. The constant concentrations found in the period 1968-1975 indicate that the influx from the atmosphere was being matched by downward transport. Surface water $\Delta^{14}C$ values have been detailed in a number of papers, for the Pacific (Bien *et al.*, 1960,1965; Rafter, 1968; Linick, 1978,1980), in relation to the atmosphere (Nydal, 1968; Nydal *et al.*, 1980,1984; Nydal and Lovseth, 1983) and from corals (Druffel and Linick, 1978; Nozaki *et al.*, 1978; Druffel, 1981; Druffel and Suess, 1983) while Tans (1981) computed the average surface $\Delta^{14}C$ values up to 1974 from bomb-^{14}C data. Stuiver (1980) indicated that the water column inventories of bomb-^{14}C are dependent on latitude as a direct consequence of circulation rather than as differences in the rate of CO_2 uptake. This, in conjunction with the prevailing winds, causing divergence and upwelling of relatively cool and dense water at the equator, results in tropical regions having lower inventories than temperate regions. Overall, the distribution of bomb-^{14}C in the DIC closely resembles the density structure, demonstrating that transport mainly occurs along isopycnal surfaces.

From all these studies, it is apparent that bomb-^{14}C has been an ideal tracer for transport processes in the thermocline while natural ^{14}C levels are more suited to studying the longer term processes of deep water circulation.

The above discussion has focused on ^{14}C measurements made in the DIC phase of the world's oceans as this is the fraction which has been most widely studied. Limited analyses have been carried out on the remaining fractions, with the organic fractions receiving most attention (Williams *et al.*, 1969; Williams *et al.*, 1978; Williams and Druffel, 1987; Druffel and Williams, 1990).

Williams and Druffel (1987) found correlation between the shapes of the down column profiles of DIC and DOC indicating that similar processes control the ^{14}C distribution in both reservoirs and that bomb-^{14}C has penetrated to a depth of 900 m, again in both reservoirs. The $\Delta^{14}C$ values obtained for the DOC fraction of surface and deep waters (-150‰ and -540‰, respectively) give ^{14}C apparent ages of 1310 yr B.P. and 6240 yr B.P. for the central north Pacific which is approximately twice the 3400 yr B.P. age obtained in the north-east Pacific by Williams *et al.* (1969). Relative to the DIC values, the DOC

results were depleted by ~300‰, suggesting that recycling of DOC in the oceans is on a longer timescale than that of DIC.

In a study on the POC fraction in the water column, Druffel and Williams (1990) identified two pools of particulate organic material - a suspended pool and a sinking pool. The sinking pool represented larger particles with ^{14}C specific activities similar to those found in organisms in surface waters whereas the suspended pool consisted of smaller particles with depleted ^{14}C contents. The mechanism which is thought to bring about this lowering of the $\Delta^{14}C$ is the incorporation of DOC *via* heterotrophic uptake by free-living bacteria in the water column. The differences found between the sinking and suspended pools are thought to be due to reworking within the suspended pool which results in depletion of labile constituents. If the sinking particulate material retains its ^{14}C signal until it reaches the sea floor, a similar enrichment would be found in the surface sediments. Williams *et al.* (1978) found evidence of rapid mixing and/or utilisation of POC in the mixed layer of surface sediment in the north central and north eastern Pacific ocean. The observed increase in ^{14}C specific activity below the mixed layer is thought to be due to burial of surface sediment by burrowing organisms rather than diffusion of DOC into the sedimentary column. The bioturbation mechanism was further corroborated by $^{239+240}Pu$ analyses which showed penetration down to 12-14 cm.

It would now appear that the usefulness of bomb-^{14}C for carbon cycling studies is limited, hence, one feasible alternative for future studies of carbon behaviour at least in local marine environments will be the release of ^{14}C from nuclear facilities into coastal waters.

1.8 ^{14}C PRODUCTION IN THE U.K.

Many nuclear establishments within the U.K. have the authority to discharge liquid radioactive waste into coastal waters (see Fig 1.11). Previous work on atmospheric discharges of ^{14}C (McCartney *et al.*, 1986,1988a,b) indicated that the major producer of ^{14}C in the U.K. is the nuclear fuel reprocessing plant at Sellafield in Cumbria. The radiochemical plants owned by Amersham International plc, situated at Cardiff and Amersham, also have the potential for significant ^{14}C releases.

Throughout this study, the major emphasis has been on the Eastern Irish Sea and the influence of Sellafield-derived discharges. However, the Amersham plants have also been

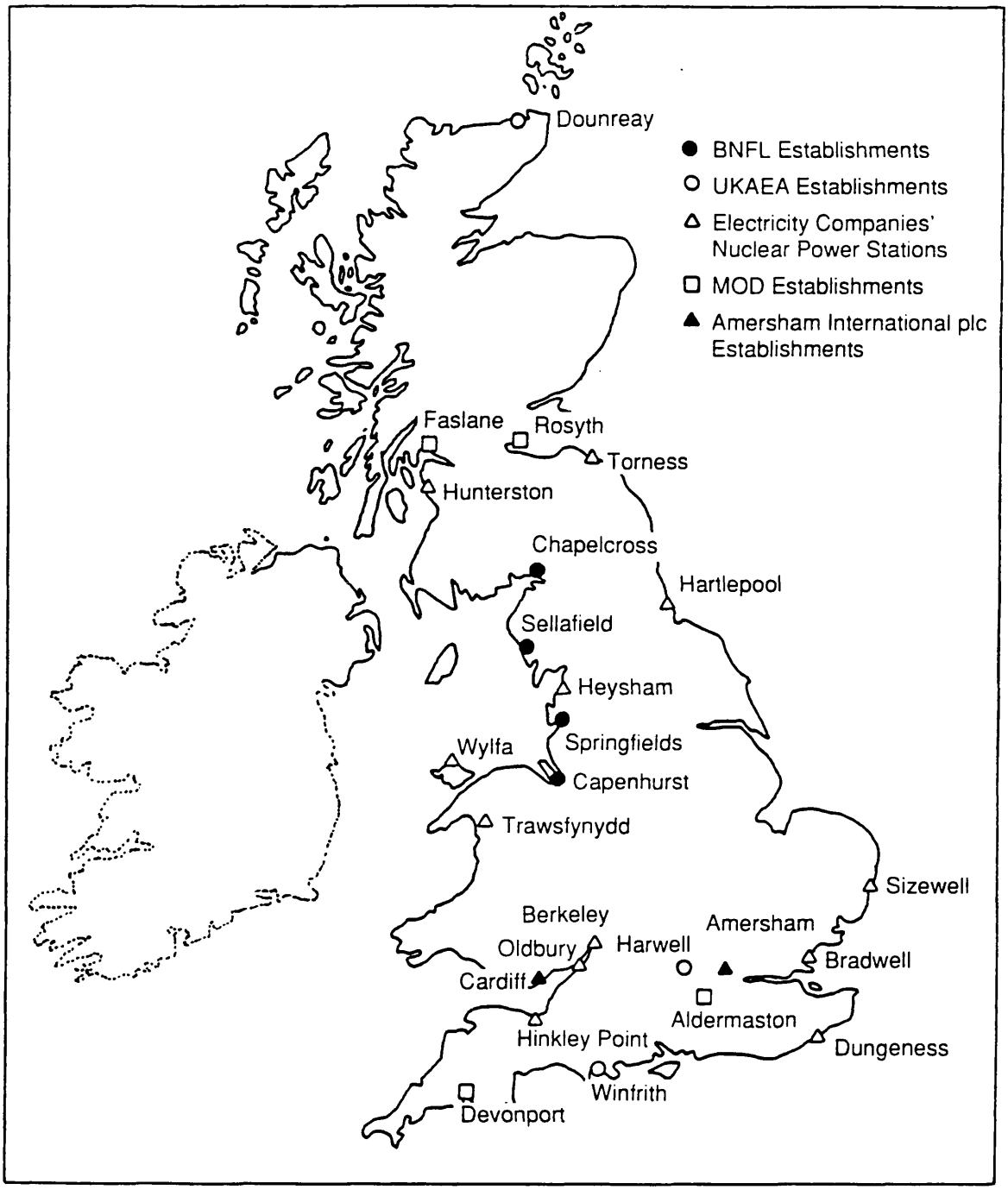

Figure 1.11: Sites in the U.K. where low-level radioactive liquid discharges occur.

studied to determine any similarities or differences in the behaviour of ^{14}C between sites. Each of these sites will be discussed individually, with details of known procedures and relevant discharge data, in the following sections.

1.8.1 Sellafield

The Sellafield plant came into operation in 1952 (although it was known as Windscale until 1981). The site incorporates facilities for the storage and decanning of fuel elements, the nuclear fuel reprocessing plant and the Calder Hall nuclear power station which houses four Magnox-type reactors. Of these facilities, it is the reprocessing of irradiated fuel which is the main source of anthropogenic ^{14}C in the area. The nuclear fuel reprocessing plant was initially constructed to separate plutonium and uranium from bulk spent nuclear fuel so that it could be used in military-based weapons programmes. Following this, the plant recovered unused fissile and fertile material from spent fuel in an attempt to conserve future fuel resources. Within the last 30 years, Sellafield has primarily reprocessed uranium from the spent fuel of Magnox reactors and more recently the uranium oxides from AGR and Light Water reactors (BWRs and PWRs). The throughput of AGR and LWR spent fuel will increase dramatically when THORP (Thermal Oxide Reprocessing Plant) comes on line later this year.

Spent fuel is transported to Sellafield mainly from within the U.K. although some does come from abroad (*eg.* Japan). Once on site, the fuel is stored underwater in large cooling ponds before the cladding is removed and the fuel dissolved in nitric acid to recover its constituent components. During these processes high, intermediate and low level wastes are produced in both liquid and solid form. For high and intermediate solid wastes, the general method of treatment is to concentrate and contain whereas that for low-level liquid waste is to dilute and disperse. Low-level solid wastes are disposed of at Drigg where large trenches are filled with waste and then covered with a waterproof covering before landscaping is carried out. Intermediate waste is encapsulated in cement inside steel drums and stored at present on site although an underground repository is under consideration for long term disposal. High-level wastes consist of the material separated from the uranium and plutonium during reprocessing and constitute 3% volume of the total reprocessing products. At present, this is stored on site in double walled stainless steel tanks but a vitrification plant has been constructed to incorporate waste into a glass matrix. These will

be stored on site for ~50 years prior to safe disposal in an underground repository.

From 1985 onwards, when the Site Ion Exchange Effluent Plant (SIXEP) and the Salt Evaporator came on-line, the discharges of radionuclides in low-level liquid waste have been considerably reduced *eg.* ^{134}Cs and ^{137}Cs. Further reductions in these discharges (especially of Pu and Am) are expected to occur when the Enhanced Actinide Removal Plant (EARP) comes into operation later this year. However, due to the increased throughput of THORP and the processing of previously accumulated intermediate waste through EARP, the levels of some radionuclides will be increased *eg.* ^{3}H, ^{99}Tc, leading to an increase in the total beta activity discharged (BNFL, 1991) which may include ^{14}C.

The low-level liquid wastes are collected from three major process streams on site. The most important of these is from the storage pond water of the Magnox decanning plant which is contaminated with radionuclides from the fuel elements. Water from these ponds is changed continuously and is passed through SIXEP which contains a series of sand filters and clinoptilolite ion exchangers to remove particulate activity and ions such as Cs^{+} and Sr^{2+} from the aqueous phase. Low-level liquid waste also arises from the storage ponds for oxide fuel in THORP but this is discharged directly to the sea. The sea tanks, which are used to store effluent from a number of processes until its composition is determined prior to discharge, are the final source of low-level liquid waste on the Sellafield site.

These liquid wastes are discharged to the Eastern Irish Sea *via* a 2.1 km long pipeline. The composition and total activity of these effluents will be dependent on the period of operation and the reprocessing programme of the plant, in addition to routine maintenance work and the efficiency of the treatment plants. As an indication of the composition of the effluent from Sellafield, Table 1.7 details the low-level liquid discharge data for some of the major radionuclides related to 1990 when the reprocessing plant was only operational for nine months (BNFL, 1991).

NUCLIDE	DISCHARGES (TBq)	AUTHORISED LIMIT (TBq)
^{3}H	1699	3500
^{14}C	2.0	4
^{60}Co	0.17	8
^{90}Sr	4.2	35
^{99}Tc	3.8	10
^{106}Ru	16.5	170
^{129}I	0.11	0.4
^{134}Cs	1.15	10
^{137}Cs	23.5	110
^{144}Ce	2.0	22
$^{239,240}Pu$	1.14	7
^{241}Pu	31.6	170
^{241}Am	0.75	3
TOTAL α	2.16	16
TOTAL β	70.9	500

Table 1.7: Radionuclides released from Sellafield in liquid effluent during 1990.

^{14}C is mainly released *via* low-level wastes, with the majority of this being to the atmosphere as $^{14}CO_2$ during acid dissolution of the fuel elements in acid. The discharges of ^{14}C were not routinely monitored until 1st January 1985, hence, discharge data prior to that time are only best estimate values and assume 10% of the total is discharged *via* the pipeline. Table 1.8 details the values reported since 1985 illustrating that discharges to the sea in fact constitute 20-45% of the total ^{14}C released.

YEAR	DISCHARGE TO SEA (TBq)	DISCHARGE TO AIR (TBq)
1985	1.3	7
1986	2.6	5.4
1987	2.1	9.5
1988	3.0	3.6
1989	2.0	4.2
1990	2.0	4.1

Table 1.8: Reported ^{14}C releases from Sellafield in liquid and gaseous forms.

1.8.2 Amersham International plc, Cardiff

The plant owned by Amersham International plc at Cardiff is employed in the production of labelled compounds, mainly for use in biomedical research and diagnostic kits used in medicine for the *in vitro* testing of clinical samples. Liquid radioactive discharges from this site are authorised and regulated by the Welsh Office. These are released through a sewer into Cardiff Bay and the Severn Estuary. ^{14}C is the main radionuclide of radiological significance which is discharged and the discharge record back to the early 1980s is detailed in Table 1.9.

YEAR	DISCHARGE (TBq)
1981	0.93
1982	1.1
1983	1.0
1984	1.1
1985	1.1
1986	1.26
1987	1.22
1988	1.16
1989	1.53

Table 1.9: Reported ^{14}C releases from Amersham International plc, Cardiff in liquid effluent.

The data show that the levels released are slightly less than those attributed to Sellafield and that throughout the past decade they have been fairly constant.

1.8.3 Amersham International plc, Buckinghamshire

This plant is the parent establishment of the company and is concerned with producing radioactive materials for use in medicine, research and industry. The discharges of liquid radioactive waste are made under authorisation to the Maple Cross sewage works where releases enter the Grand Union Canal and the River Colne, in the Thames catchment area. ^{3}H is the only nuclide for which discharge data are available, with the annual discharges of radioactive releases reported only as total activity.

1.9 AIMS OF THE PROJECT

During his work on atmospheric ^{14}C discharges from the nuclear fuel cycle, McCartney

(1987) observed enhanced levels of ^{14}C in seaweed collected from the Cumbrian coastline. This was indicative of the incorporation of Sellafield-derived ^{14}C from low-level liquid waste, into the marine food-chain and perhaps into the local human population *via* the consumption of locally caught fish and shellfish. While one of the initial aims of the project was to determine the radiological significance of these discharges to both local and global populations, this was overshadowed by the use of the ^{14}C signal from nuclear establishments as a biogeochemical tracer to determine the behaviour and fate of carbon in a coastal environment.

Due to the lack of published data on ^{14}C concentrations in the aquatic environment, initial work involved the collection and analysis of an extensive suite of both coastal biota and seawater (for dissolved inorganic carbon (DIC)) samples to determine:-

1) the spatial and temporal distribution of ^{14}C in various aquatic environments

2) the differential behaviour of anthropogenic ^{14}C discharged from various sources

3) differential uptake patterns between organisms, and finally

4) the radiological implications of the discharges to the population living in the vicinity of the discharges.

Having determined both the spatial and temporal distributions of this anthropogenic ^{14}C, the final consideration was to study it's distribution within the biogeochemical phases of the marine system. Information obtained from these studies would assist in determining the rate of transfer between the reservoirs and hence allow the development of mathematical models which could then be applied to other studies *eg.* the effect on the marine system of increased uptake of atmospheric CO_2.

CHAPTER 2

EXPERIMENTAL METHODS

2.1 INTRODUCTION

Because ^{14}C is a weak beta emitting radionuclide (E_{max} = 156 keV) and present at very low concentrations in nature (1 ^{14}C atom per 10^{12} stable carbon atoms), its analysis requires the use of sophisticated physical and chemical techniques. The detection system used to determine ^{14}C activities must consequently have a low background count rate, high efficiency for detecting ^{14}C beta emissions and good long term electronic stability.

Initial work by Libby *et al.* (1949) and Anderson and Libby (1951) required samples as solid elemental carbon, produced from CO_2 reduction with magnesium turnings and coated onto the walls of a screen wall counter. The detection efficiency of this system, however, only reached 6% due to self-absorption of the beta particles. To a large extent, the introduction of gas proportional and liquid scintillation techniques (Kulp, 1954) overcame self-absorption problems and as a result, became the methods most widely used and improved upon. In addition, advancements in mass spectrometry to include acceleration of sample atoms to energies >1 MeV has resulted in a third, non-radiometric, technique for measuring ^{14}C - Accelerator Mass Spectrometry (AMS).

Radiometric techniques, *ie.* gas proportional and liquid scintillation counting, rely on detecting beta particles released during radioactive decay *ie.* 13.56 decays per minute from 1 g of modern carbon (where modern carbon is the ^{14}C activity of 1890 wood), and generally require 2-10 g of carbon per sample to approach 1% precision within 1-2 days of counting time. With the introduction of low level detection systems, the sample size in the best systems has been reduced to 80 mg and 10 mg for liquid scintillation and gas proportional counters respectively although longer counting periods are required (Gupta and Polach, 1985). Accelerator mass spectrometry (AMS) measures the number of ^{14}C atoms present, rather than just those undergoing radioactive decay, hence, milligram quantities of sample carbon can be counted to 1% precision within a two hour counting period.

Gas proportional counting is carried out in a gas-filled hollow tube where the outer wall

acts as the cathode and a thin wire stretched along the central axis acts as the anode when a positive voltage is applied to the latter. Particles produced during radioactive decay, such as beta emissions, interact with the neutral gas molecules present in the detector causing ionisation and the formation of ion pairs. These ion pairs in turn interact with more gas molecules producing secondary ionisation events and more electrons which are attracted to the anode and recorded. The signal at the anode is proportional to the energy associated with the initial beta decay event, providing the voltage is correctly set. By looking only at the energy region of interest, the background count rate of the system for ^{14}C can be reduced. This, in conjunction with passive shielding, anti-coincidence circuitry/active shielding and on-going improvements in component design have produced a system with high efficiency, low background and long-term electronic stability. Gases which are used most frequently for radiocarbon dating include methane (Burke and Meinschein, 1955), acetylene (Barker, 1953; Suess, 1954) and carbon dioxide (de Vries and Barendsen, 1953). The development of very small counters with improved active shielding and, hence, very low background count rates has given researchers the potential to date smaller and older samples to greater precision (Otlet *et al.*, 1983; Gupta and Polach, 1985).

Liquid scintillation techniques, although initially reported in 1953 by Hayes *et al.*, did not become widely used until the 1970s. In this technique, a sample is normally dissolved in an aromatic solvent capable of absorbing and re-emitting the energy produced during a radioactive decay event. The excitation of the solvent molecule permits energy to be passed to other solvent molecules and also to solute molecules (scintillants or fluors) which are present. Excited scintillant molecules emit photons of light to return to their ground state and these photons can be detected by photomultiplier tubes (PMTs). The PMT signal is amplified, and, following analogue to digital conversion can be recorded using a multi-channel analyser (or scaler in older instruments). The intensity of light produced is proportional to the initial energy of the radioactive decay, allowing limited separation of individual isotopes with differing energy spectra. In natural radiocarbon measurements, the sample carbon (which has been synthesised to benzene) provides the solvent in which the scintillant molecules are dissolved. Benzene was first considered as a counting medium in the early 1960s (Tamers, 1960; Starik *et al.*, 1961) as it contains 92% carbon, has excellent scintillation properties, is chemically stable and its entire carbon content can

be synthesised from sample carbon. It is now almost exclusively used in radiocarbon analysis by liquid scintillation counting.

AMS is a technique developed largely within the last decade, in which a tandem electrostatic accelerator is coupled to a mass spectrometric system to measure isotopes present at the ultra-trace level *eg.* ^{10}Be, ^{14}C, ^{26}Al or ^{36}Cl. Mass spectrometry can detect ions of a particular mass, although, detection levels are of the order of 10^{-9}. This sensitivity is not high enough to detect ^{14}C atoms because of the presence of other elements and molecules of almost identical mass, *eg.* ^{14}N or ^{13}CH. This problem is overcome by accelerating the ions, in a system known as a tandem accelerator, which lowers the detection limit to 1 part in 10^{15} (Hedges and Gowlett, 1986). The tandem accelerator is so called as there are two stages of acceleration: one towards a central positive terminal and the other away from it. This is achieved because the carbon ions are made to change polarity, from negative to positive, by a "stripper" of gas or metal foil at this central point. A schematic diagram of a tandem electrostatic accelerator system is shown in Figure 2.1.

On addition to the system, carbon in the samples is ionised to give negatively charged carbon ions. This is achieved by bombarding the sample with a sputter source of Cs^+ ions. The negatively charged carbon ions so produced are then accelerated to the positive terminal of the accelerator by a voltage difference of 2 million volts (2 MV). N^- ions do not reach this positive terminal because they are unstable, therefore, removing one of the major interferences. The stripper removes four electrons from the carbon ions to give C^{3+} ions and eliminates molecules of mass 14 because none can exist with a triple positive charge. After further acceleration, this time, away from the positive electrode, magnets are used to focus and direct the ion beam, in addition to sorting the ions by mass. If ions of a similar charge and velocity, but different mass, are subjected to a magnetic field perpendicular to their direction of travel, only ions of like mass would pass through a slit at a given radius of curvature downstream from the magnet. This allows the magnet to "filter out" all charged particles except those of atomic mass 14, although, some ions will pass through the slit as they do not all have identical charge and velocity. By placing a magnet before and after acceleration of the ions, interfering ions are reduced by a factor of 10^{13} (Hedges and Gowlett, 1986) and this is increased to 10^{16} by the inclusion of a velocity filter. The C^{3+} ions with atomic mass 14 are deflected less in the magnetic field

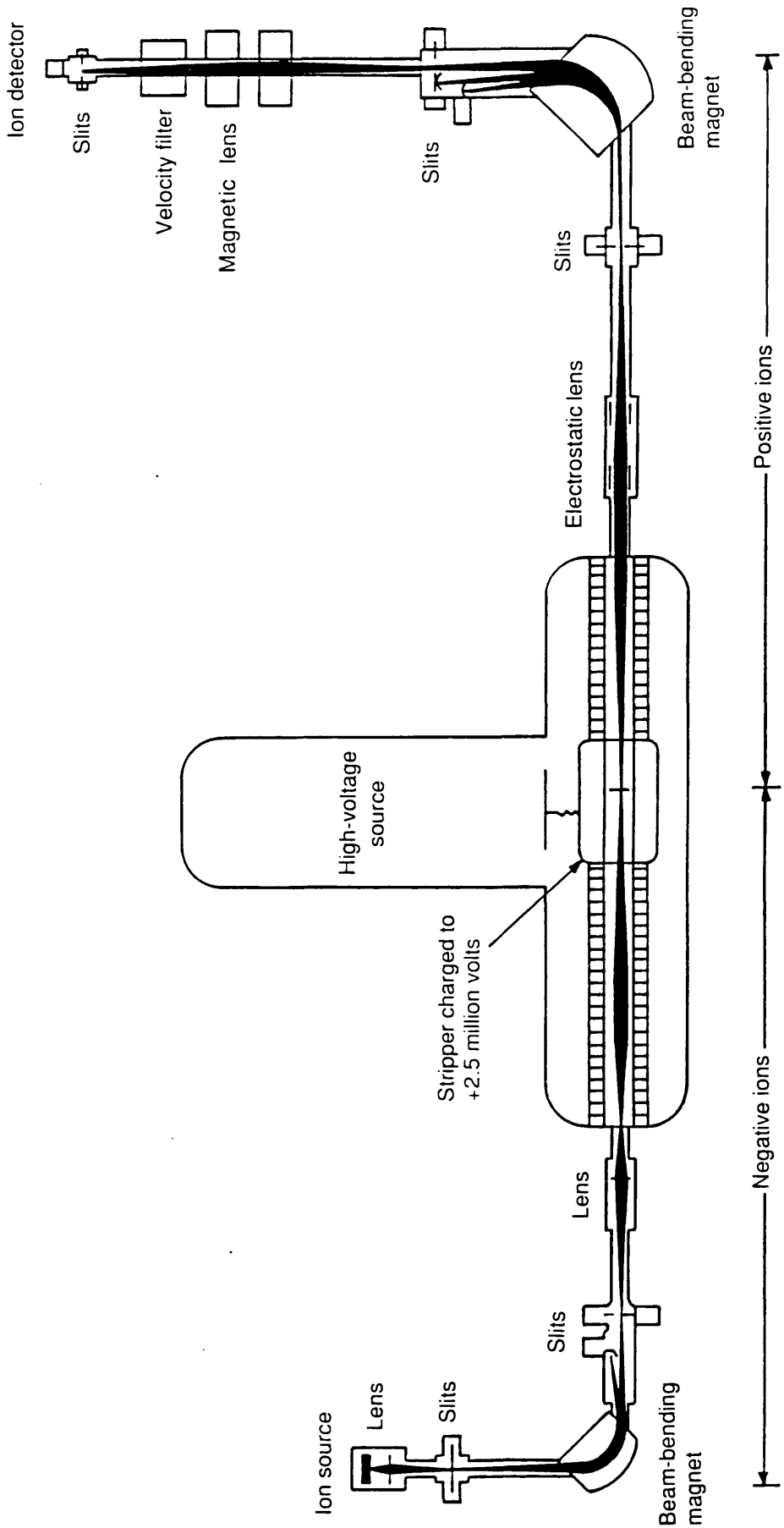

Figure 2.1: Schematic representation of an Accelerator Mass Spectrometer.

than the lighter C^{3+} ions of mass 12 or 13, hence, they can be isolated and then counted by an energy detector. The detector distinguishes ions of like mass and velocity, but different nuclear charge, by the rate at which they lose energy on collision with molecules of gas. This system is very sensitive, with the ability to detect ^{14}C ions constituting <1% of the incoming ion beam. ^{12}C and ^{13}C ions are also collected to provide an isotopic ratio and allow the calculation of any fractionation which may have occurred.

Sample sizes which could not possibly be measured using conventional radiometric techniques (0.2 - 2 mg carbon) can be analysed with a precision of 1% Modern in a counting period of ≤ 1 hour in the best systems. The number of laboratories employing AMS is limited, due both to the capital cost involved and the fact that the technique is still relatively new with its potential just being realised within the last few years.

For all but a small number of samples (35 analysed by AMS) the chosen technique in this study was liquid scintillation counting which has been the preferred radiometric technique in the laboratory for a number of years. Liquid scintillation will be discussed in greater detail in Section 2.4.

2.2 SAMPLE PREPARATION

Throughout the period of this study a wide range of sample types have been analysed. Although the range of sample types has been extensive there are five basic stages in the radiometric analysis of ^{14}C :-

1. pretreatment of samples, either to remove extraneous carbon-containing particles from the outer surfaces or to actually isolate a particular fraction of interest.
2. conversion of the sample carbon to carbon dioxide (CO_2).
3. conversion of CO_2 to acetylene (C_2H_2) *via* lithium carbide.
4. synthesis of benzene (C_6H_6) from C_2H_2 by catalytic cyclotrimerisation using a chromium based catalyst on a silica-alumina support.
5. liquid scintillation counting to measure the specific activity of the ^{14}C in the sample benzene.

Each of these stages will now be dealt with individually in greater detail.

2.2.1 Pretreatment

2.2.1.1 Intertidal biota samples

The flesh from mussel and winkle samples is separated from the shell material, rinsed in distilled water and then dried to a constant weight at 60°C. The shell material from these samples is then dried and retained, with selected samples being chosen for analysis.

The seaweed collected in conjunction with the mollusc samples was given a warm acid (0.5M HCl) rinse to remove any inorganic carbon adhering to the outer surfaces before being rinsed in distilled water and dried to constant weight at 60°C.

Nori (*Porphyra umbilicalis*) samples collected by the Ministry of Agriculture, Fisheries and Food (MAFF), as part of their monitoring programme, had already been dried and ground, hence, no pretreatment was required prior to ^{14}C analysis, although γ-ray spectrometry was carried out to determine the levels of other Sellafield-derived radionuclides present.

2.2.1.2 Fish

On receipt from MAFF, the fish - plaice and dab fillets - are kept frozen until required for analysis. When required, the samples are defrosted and cooked in a microwave oven. This cooking step allows the flesh to be flaked away from the skin, increasing the ease of handling, prior to drying to a constant weight at 60°C.

The fish collected in the Grand Union Canal are also frozen prior to analysis but in this case the whole fish, not just the edible flesh, is chopped into small pieces, dried and analysed.

2.2.1.3 Phytoplankton

MAFF preserve phytoplankton samples in formalin which has to be removed prior to analysis. To ensure as near as possible complete removal of the formalin, the phytoplankton are soaked in distilled water over a period of several days, with numerous changes of water, prior to wet oxidation.

2.2.1.4 Intertidal and bottom sediments

On their return to the laboratory, the intertidal sediments (0 - 0.5 cm surface scrapes) are slurried with distilled water and filtered using GFA glass fibre filters to remove excess salts. These are then rinsed with distilled water and dried to a constant weight. Once dry, the sediments are then sieved through 2 mm and 63 μm mesh sieves to enable some degree of particle size analysis to be carried out.

The bottom sediments, taken by Kaston corer in December 1989 during the MAFF cruise

CH62B/89, are subsampled using a plastic tube (diam. ~8 cm) to 25 cm depth and divided into 5 cm sections. Those sediments collected in 1991 during cruise CIR2/91 were also collected by a Kaston corer with only the top 2 cm being taken for analysis. All sediment samples are dried prior to analysis, although particle size analysis was not carried out on those samples collected during the CH62B/89 cruise.

2.2.1.5 Biogeochemical fractions of surface seawater

For the purpose of this study, the carbon present in the surface waters of the U.K. coastal area is considered to consist of four biogeochemical fractions - the dissolved inorganic (DIC), the dissolved organic (DOC), the particulate inorganic (PIC) and the particulate organic carbon (POC) fractions. Of these, the DIC has been the most frequently sampled and analysed as the other three fractions are all present in such small quantities that ^{14}C analysis must be carried out using the AMS technique. The average DIC concentration found in surface waters is 24 - 30 mg C l^{-1} (Lassey *et al.*, 1988; Chester, 1990) and due to the ease of extraction and isolation can be analysed by conventional radiometric techniques when 200 l of surface seawater are used. The DOC fraction has been widely studied, although, until the work of Sugimura and Suzuki (1988), who quote values as high as 3.6 mg C l^{-1} for surface waters, DOC was generally considered to be within the range 0.8 - 1.5 mg C l^{-1} (Mantoura and Woodward, 1983). The POC fraction is thought to constitute only 1 - 10% of the total organic carbon in the marine system, Druffel and Williams (1990) quote an average of 1.2 µg C l^{-1} in the deep sea which is slightly lower than the range quoted by Copin-Montegut and Copin-Montegut (1973) of between 2 - 100 µg C l^{-1} for surface waters and for waters down to 6500 m depth. Very little data are available in the literature for the concentration of carbon in the particulate inorganic fraction.

(a) DIC.

To obtain sufficient material from the DIC fraction for conventional radiometric analysis, approximately 200 l of surface seawater is collected into previously acid-washed barrels *via* a Jabsco pump. The water is then filtered through precombusted glass fibre filters (Whatman GFA), acidified and purged with CO_2-free nitrogen. The resultant CO_2 is bubbled through 4M NaOH (carbonate-free) for a period of 8 hours in a closed system. Prior to sample collection, it must be ensured that the NaOH used to trap out the DIC is carbonate free. This procedure is carried out under nitrogen to avoid absorption of

atmospheric CO_2 and involves the addition of 60 g of $BaCl_2$ (dissolved in 200 ml of distilled H_2O) to 5 l of 4M NaOH. The resultant $BaCO_3$ is filtered off using Whatman GFA glass fibre filters - the filtrate then has 200 g of Na_2SO_4 (dissolved in 200 ml of distilled water) added to it and N_2 bubbled through the solution for 30 minutes to ensure complete mixing. This bottle is then sealed and the precipitate (of $BaSO_4$) allowed to settle for 48 hours prior to the carbonate-free 4M NaOH being siphoned off, using N_2, into the bottles which connect directly onto the CO_2-stripping rig used at sea (Fig 2.2). As a check on the efficiency of this clean-up stage, three simple tests are carried out on an aliquot of the prepared carbonate-free NaOH; barium is added and production of a precipitate indicates the presence of excess SO^{2-}_4 and the addition of adequate Na_2SO_4 to remove excess barium; carbonate and sulphate are also added and in both cases if no further precipitate is observed, this indicates that all the excess barium has been removed in the clean-up stages.

(b) DOC

The concentration of DOC found in surface waters is dependent on the location of the sampling site (coastal *vs.* open ocean, oligotrophic *vs.* eutrophic regions) while the method of oxidation used in the analysis is known to influence these measurements. Over the years a number of oxidation techniques have been used and a wide range of concentration values obtained as discussed in Section 1.7.2.2(b).

The DOC samples in this study were oxidised using chromic acid/excess potassium dichromate as detailed in Section 2.2.2.1(d). To obtain sufficient DOC for ^{14}C analysis, relatively large volumes of water (25 l) have to be collected. In this study, the pre-concentration of DOC from the surface water is carried out using macroporous nonionic XAD resins and 25 l water samples. These resins have been extensively used for the extraction of trace amounts of organic compounds from natural and waste waters (Leenheer, 1981), ground waters and also seawater (Stuermer and Harvey, 1977). From the selection of resins available for the extraction of organic material, three were chosen for use in this study - XAD-2, XAD-4 and XAD-8.

These are used to extract humic, hydrophilic and fulvic acids respectively although some degree of overlap does occur between them. Both XAD-2 (85-90 Å) and XAD-8 (50 Å) are styrene-divinyl benzene co-polymers, hydrophobic in character, whereas XAD-4 is a methyl methacrylate polymer with a pore diameter of 250 Å and is less hydrophobic. At

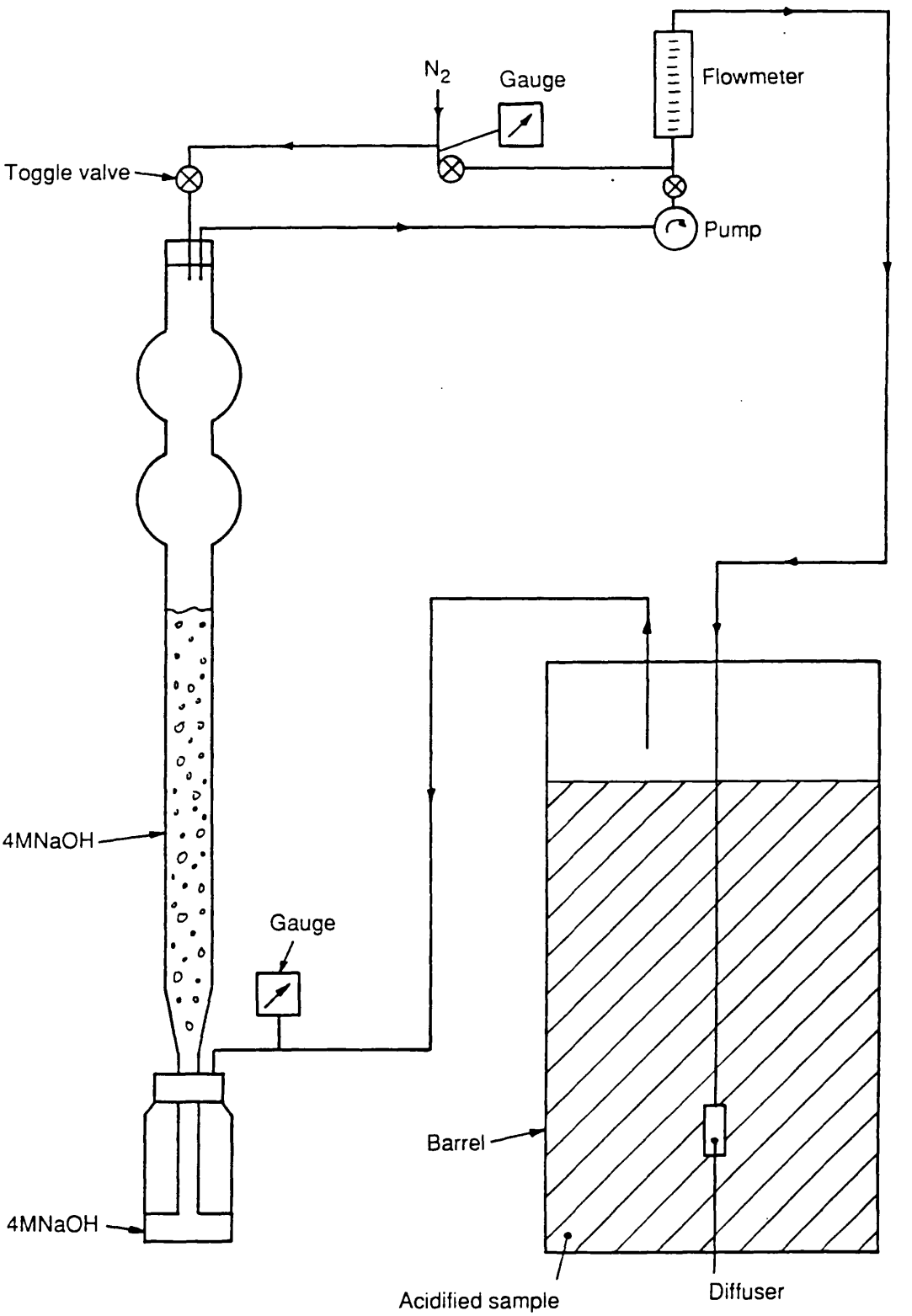

Figure 2.2: CO_2-stripping rig used at sea.

low pH, weak acids such as the organic acids present in seawater, are protonated and readily adsorb onto the resins. These can be eluted by an increase in the pH which ionises the acids and favours desorption from the resin.

Prior to sample application to these resins, a rigorous clean-up stage is carried out on all three resin types according to the method of Thurman *et al.* (1978). This technique removes any organic components such as unpolymerised monomer units, preventing organic "bleed" into the sample. Firstly, the resins are slurried in methanol to remove the fine particulate material which may block the column and restrict the flow rate. This is followed by a series of Soxhlet extractions using methanol, acetonitrile, diethyl ether and finally methanol again, for 24 hour periods. The resins are then stored in methanol until they are required.

50 cm^3 columns are packed using pre-combusted quartz wool above and below the bed of resin and washed with 2 l of distilled water to remove the methanol. This is followed by further washes with 500 ml of 0.1M NaOH and 500 ml of 0.1M HCl and a final litre wash of distilled water prior to sample application.

25 l of filtered seawater are then passed through a sequence of columns - XAD-4 at natural pH; the effluent is collected, acidified to pH2 with conc. HCl and passed through a column of XAD-2 and finally a column of XAD-8 at a rate not exceeding 15 bed volumes per hour. Once all the sample has passed through each column, the columns are washed with 500 ml of 0.1M HCl and 500 ml of distilled water to remove any organic material not adsorbed onto the resin, prior to elution with methanol (for XAD-4) or 0.1M NaOH (for XAD-2 and XAD-8). The eluent is then evaporated virtually to dryness on a hot plate and the DOC resuspended using 50% H_2SO_4, in preparation for the conversion of sample carbon to CO_2 using the wet oxidation method detailed in Section 2.2.2.1(d).

(c) PIC and POC

The pretreatment carried out on these samples is minimal and consists of washing the filters with approximately 2 l of distilled water to remove any free Cl^- ions present as these may present problems during the wet oxidation stage used later in the analyses of the POC. Prior to oxidation of the POC, the PIC must first be removed by hydrolysing with 50% H_3PO_4.

2.2.1.6 River weed

This is treated in the same manner as the seaweed *ie.* a warm acid wash (0.5M HCl)

followed by a distilled water rinse and drying to a constant weight.

2.2.1.7 Grass

The grass samples are examined for rootlets, and soil contamination, which are removed prior to an acid wash (0.5M HCl), a distilled water rinse and placement in an oven at 60°C until dry. Once dry, the samples are then chopped into lengths of approximately 1-2 cm to improve the ease of handling prior to combustion.

2.2.2 Conversion of sample carbon to CO_2

2.2.2.1 Generation of CO_2

Three methods of converting sample carbon to CO_2 have been employed during this study, but, apart from those samples being analysed by AMS, all CO_2 samples were collected in the same apparatus and dealt with in the same manner during further processing.

The three methods which have been used are:-

i) combustion of the dried sample in an oxygen-rich atmosphere - for organic samples with a high carbon content (*ie.* in a combustion bomb).

ii) hydrolysis using acids of varying strengths - for inorganic carbon samples such as dissolved inorganic carbon from seawater (8M HCl), sedimentary inorganic carbon (2M HCl), shell carbonates (4M HCl) and particulate inorganic carbon from the water column (50% H_3PO_4).

iii) wet oxidation using chromic acid and excess potassium dichromate - for samples containing low levels of organic carbon such as sediments and particulates removed from the water column.

(a) Combustion

This technique, developed by Barker *et al.* (1969), is widely used and is most useful for dried samples with a high carbon content such as the biota samples (mussels, winkles, seaweed, grass, river weed and fish) of interest in this study. The weight of sample to be combusted is determined by the weight of benzene required and the carbon content of the initial sample. Generally 10-20 g of sample are combusted to yield approximately 10 l of CO_2 and ultimately 4.5 g of benzene which is the chosen geometry for counting (see Section 2.5.1).

Combustion of the samples is carried out in a stainless steel crucible within a thick walled stainless steel reaction vessel (Fig 2.3) capable of withstanding high pressures. The

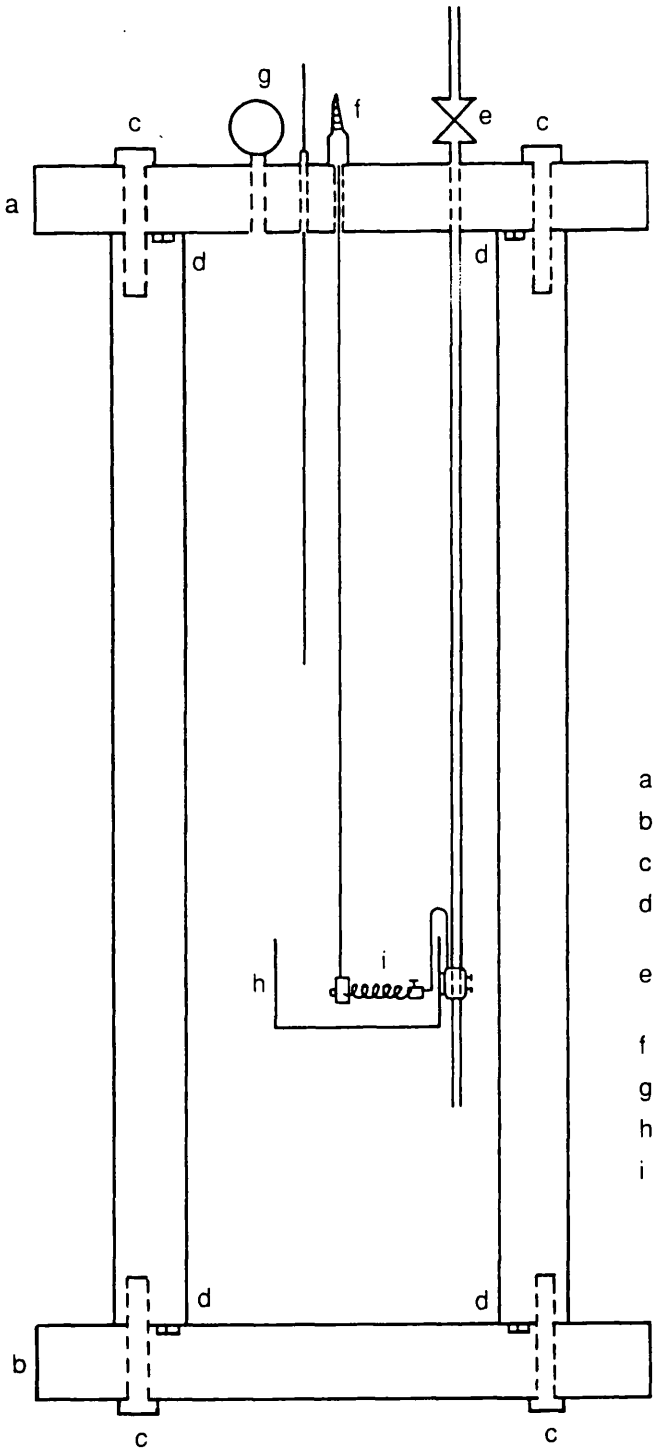

a Top flange
b Basal flange
c High tensile bolts
d 'O'-ring track and neoprene 'O'-ring
e O_2 inlet/CO_2 outlet valve and earth electrode
f Spark plug on live electrode
g Pressure gauge
h Sample crucible
i Ignition wire

Figure 2.3: Combustion vessel.

crucible is fixed to the O_2 inlet/CO_2 outlet pipe, well above the open end, to prevent scattering of the sample on addition of O_2. A coiled resistance wire is stretched across the crucible and connected to an ignition terminal. Prior to the sample being placed in the crucible, the wire fuse is tested to ensure that it glows when an electrical current is passed through it. This also ensures the removal of any grease and dust attached to the wire which may contaminate the sample. A small amount of water is placed in the bottom of the reaction vessel to trap out soluble gases (mainly oxides of sulphur and nitrogen) produced during the combustion. The sample is placed around the fuse and the lid of the reaction vessel screwed down tightly with 12 high tensile bolts. The vessel is then attached to the glass vacuum line *via* flexible steel tubing and evacuated using a rotary pump, prior to filling with CO_2-free O_2. Once the reaction vessel is filled with oxygen, a transformer is connected to the ignition terminal and the sample is combusted as the electrical current passes through the wire. Sample combustion is instantaneous and this is monitored by a sharp rise in the temperature at the base of the filling valve. The CO_2 is allowed to cool before the reaction vessel is evacuated by bleeding the CO_2 into the glass vacuum line *via* a needle valve which controls the rate of flow.

(b) Hydrolysis

This system set-up (Fig 2.4) allows the addition of acid to an inorganic carbon sample, and the collection of the resultant CO_2, at a controlled rate. Within the scope of this work, varying strengths of acid are used depending on the type of sample to be hydrolysed - 8M HCl for the DIC samples, 2M HCl for the inorganic sediments, 4M HCl for shell material and 50% H_3PO_4 for the PIC removed from the water column. The strength of acid used is determined by two factors - the ease with which the sample will undergo hydrolysis and the volume of sample to be hydrolysed. Weaker acid is used for those samples which will readily undergo hydrolysis *eg.* the inorganic sediments, whereas, stronger acid is required where the size of the reaction vessel and sample restricts the volume of acid that can be used *eg.* the DIC and PIC samples. With the exception of PIC, the sample is placed in a 2 l reaction bulb and the lid sealed using silicon grease and secured with a wire collar. This lid has a ground glass port into which a y-shaped glass extension with a splash bulb is fitted. This y-shaped extension allows the reservoir of acid and the outlet pipe (to the vacuum line) to be attached, with the splash bulb ensuring that the minimal amount of solution is taken into the line on evacuation of the reaction bulb. For solid samples such

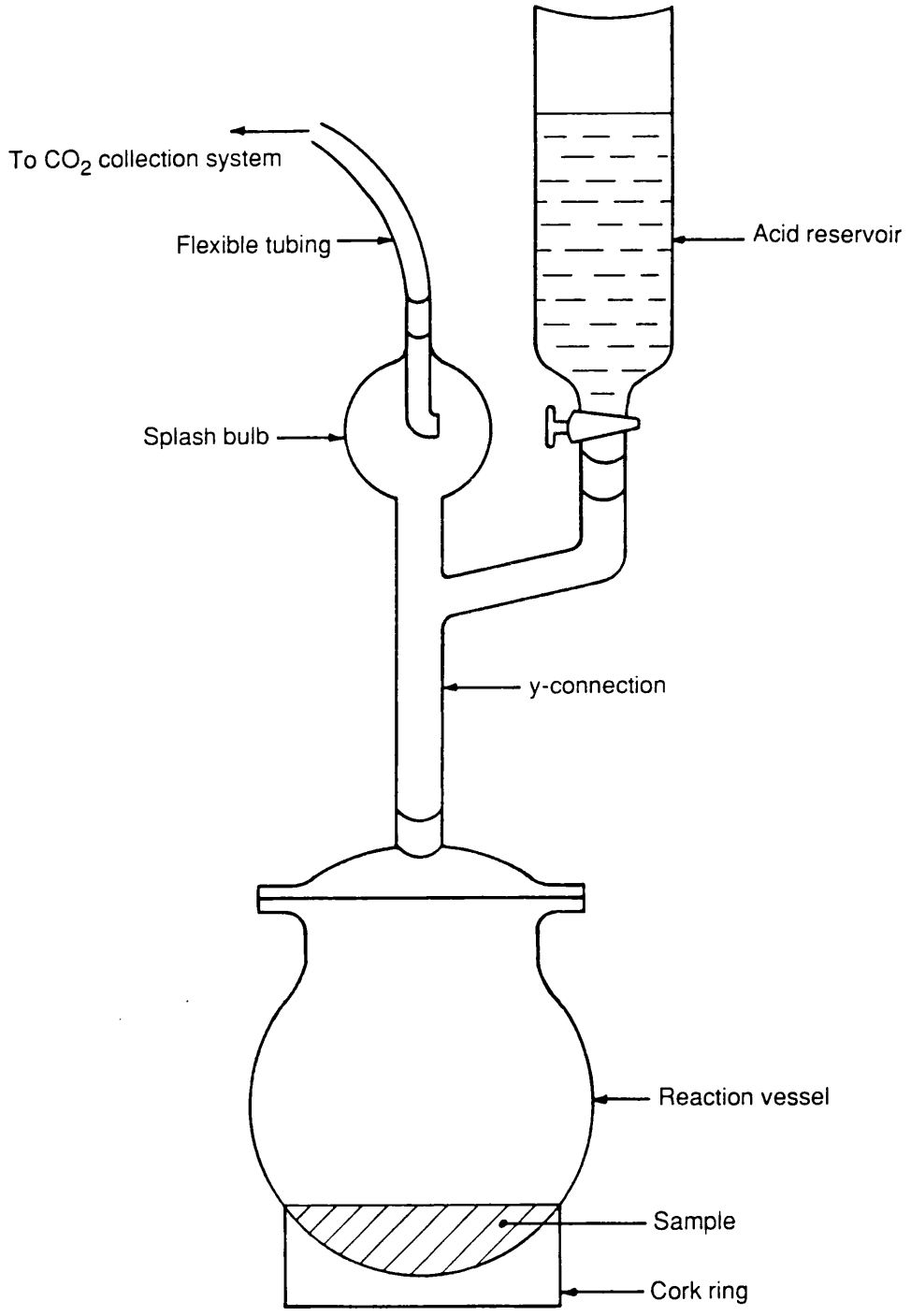

Figure 2.4: Hydrolysis reaction system.

as sediments, the sample is added immediately before setting up the apparatus. For liquid samples, such as the DIC which arrived at the laboratory as 4M NaOH containing sodium carbonate, the preferred method is to construct the hydrolysis equipment, test for leaks and then add the sample quickly through the acid reservoir. Once the set-up is complete, connected to the line, the sample added and the apparatus evacuated using a rotary pump, CO_2 is generated by the controlled addition of acid, with the CO_2 being gradually bled into the vacuum line and collected.

(c) Wet Oxidation

The use of this method is limited to samples of very low organic carbon content which will not readily combust as described in Section 2.2.2.1(a) *eg.* sediments, bones.

The apparatus for this must be set up in a fume hood and comprises a 2 l reaction bulb connected to a chromic acid reservoir and placed in a heating mantle, a secondary reaction vessel (500 ml) containing chromic acid, a 1 l vessel containing distilled water acting as a gas clean-up and cooling stage and a nitrogen supply to flush the CO_2 out of the reaction vessel (see Fig 2.5). The sample is placed in the reaction vessel with excess potassium dichromate and the system is set up, connected to the glass vacuum line *via* plastic tubing and flushed with N_2. The wet oxidation reaction is started by the addition of chromic acid from the reservoir with the heating mantle set at minimum heat. The CO_2 is continuously flushed out of the system into the collection traps *via* the secondary reaction vessel of chromic acid and the water vessel; the latter removes some NO_2 and SO_2 gases and cools the CO_2. Once all the chromic acid has been added (~500 ml), the heating mantle is set to full power and the reaction allowed to continue for a further hour with the sample mixture boiling.

(d) Generation of CO_2 for AMS analysis

Samples to be analysed by AMS are converted to CO_2 on a "micro" glass vacuum line designed specifically to deal with extremely small samples. The conversion to CO_2 is carried out in a reaction vessel which consists of two limbs (Fig 2.6) - one into which the sample is placed and the other where either the acid for hydrolysis (50% H_3PO_4) or wet oxidation (chromic acid plus excess potassium dichromate) is placed.

For conversion of the PIC, the filters containing the particulate material are torn up after pretreatment and placed into the main limb of the reaction vessel. Approximately 40 ml of H_3PO_4 are added into the side limb using a funnel with flexible tubing attached before

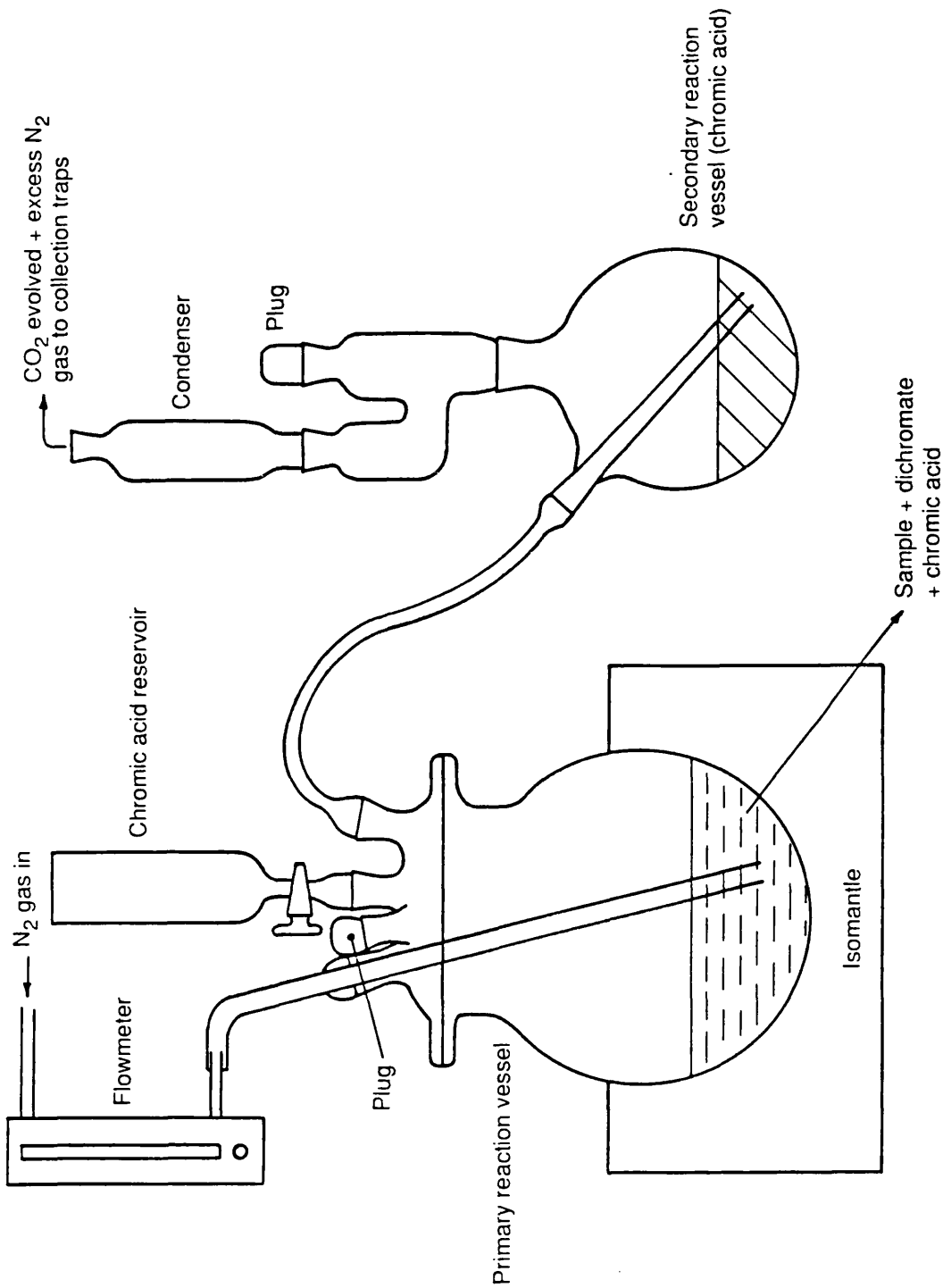

Figure 2.5: System for wet oxidation reactions.

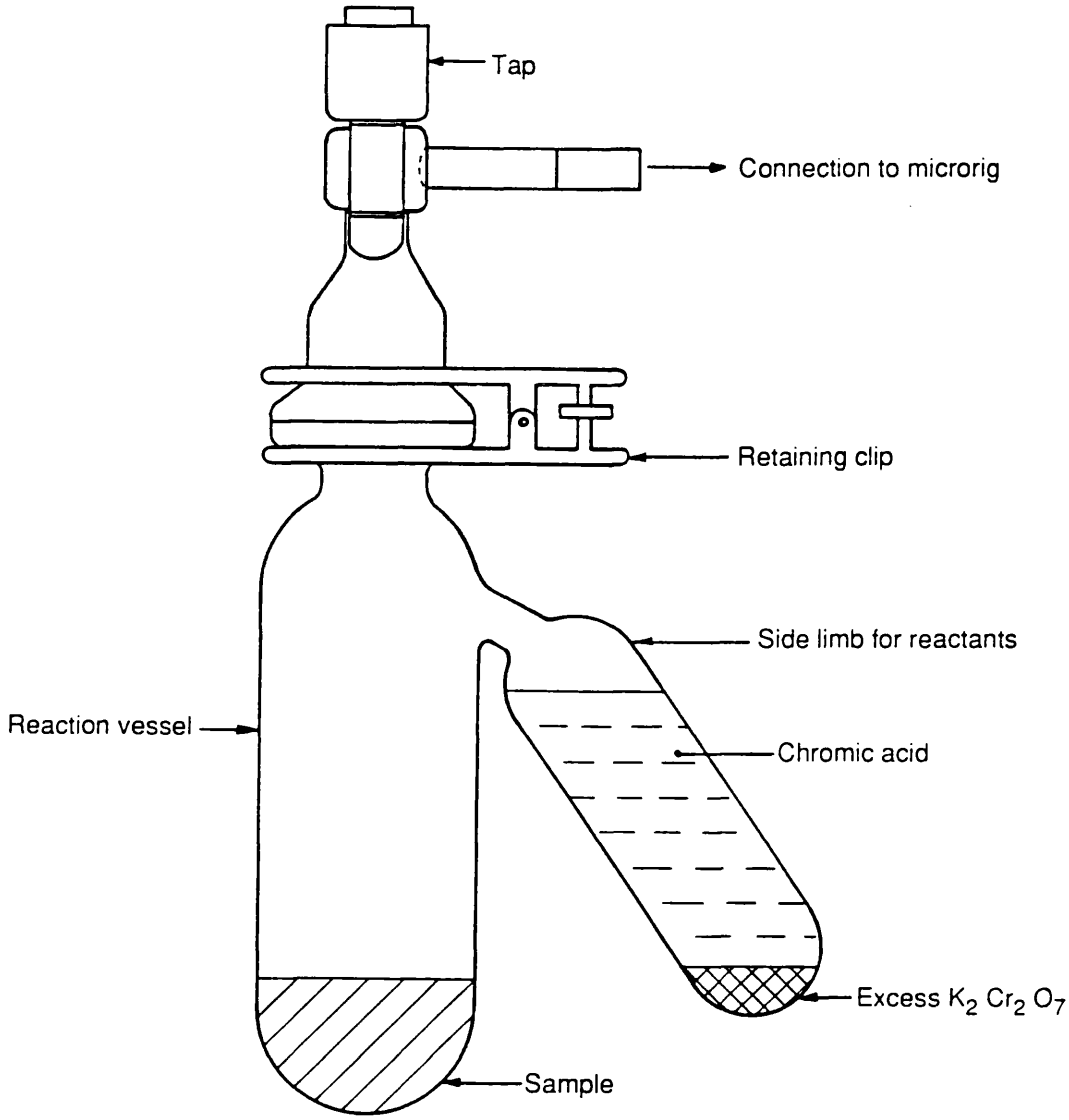

Figure 2.6: Wet oxidation reaction vessel for AMS samples.

the top is then replaced and the complete system connected to the "micro-rig" and evacuated to better than 10^{-2} torr using a mercury diffusion pump. When sufficient vacuum is attained, the reaction vessel is sealed, removed from the line and the acid added to the sample by tilting the reaction vessel. The hydrolysis is encouraged by placing the reaction vessel in an oven for 24 hours at ~80°C before collecting the CO_2 in a liquid nitrogen-cooled finger (see Section 2.2.2.2(a)).

Once the CO_2 has been removed from the vessel, the remaining material (POC) is filtered and washed with distilled water (~1.5 l) before undergoing wet oxidation to again generate CO_2. The wet oxidation of the POC and DOC are carried out in the same apparatus used for the hydrolysis of the PIC. For these reactions, chromic acid and excess potassium dichromate are added to the side limb before the reaction vessel is evacuated, isolated and the reaction initiated. The stage of the reaction can be monitored by a colour change in the reagents (orange → green as Cr(VI) → Cr(III)) and is encouraged by heating the reaction vessel in an oven for 24 hours at ~80°C. The resultant CO_2 is then removed from the reaction vessel and sealed in a glass tube prior to analysis by AMS (see Section 2.2.2.2 (a)).

2.2.2.2 CO_2 collection and storage

Depending on the method used to generate the CO_2, the collection is either carried out after all the CO_2 has been generated (combustion), periodically during the reaction as the pressure builds up in the reaction vessel (hydrolysis) or continuously throughout the whole carbon conversion procedure (wet oxidation). Despite the differences in the evacuation techniques for the various CO_2-generation methods, the collection system used to trap out the gas is essentially the same. The vacuum line consists of two traps which have industrial methylated spirits (IMS) and crushed solid CO_2 placed around them in vacuum flasks to reduce the temperature to -80°C (T1 and T2). This traps out any water vapour in the sample gas while a further series of three spiral traps (or three straight traps for wet oxidations - to prevent blockages occurring due to liquid nitrogen formation) (T3,T4 and T5), cooled to a temperature of -196°C using liquid nitrogen, trap out the sample CO_2 (Fig 2.7). During wet oxidations, the line is open to atmosphere *via* a soda lime trap (to clean up the gases being vented to the atmosphere) as a constant flow of nitrogen is used to flush the CO_2 through the system. In the other two techniques, the line is pumped down *via* the low vacuum manifold (attached to a rotary pump) and then closed off to the

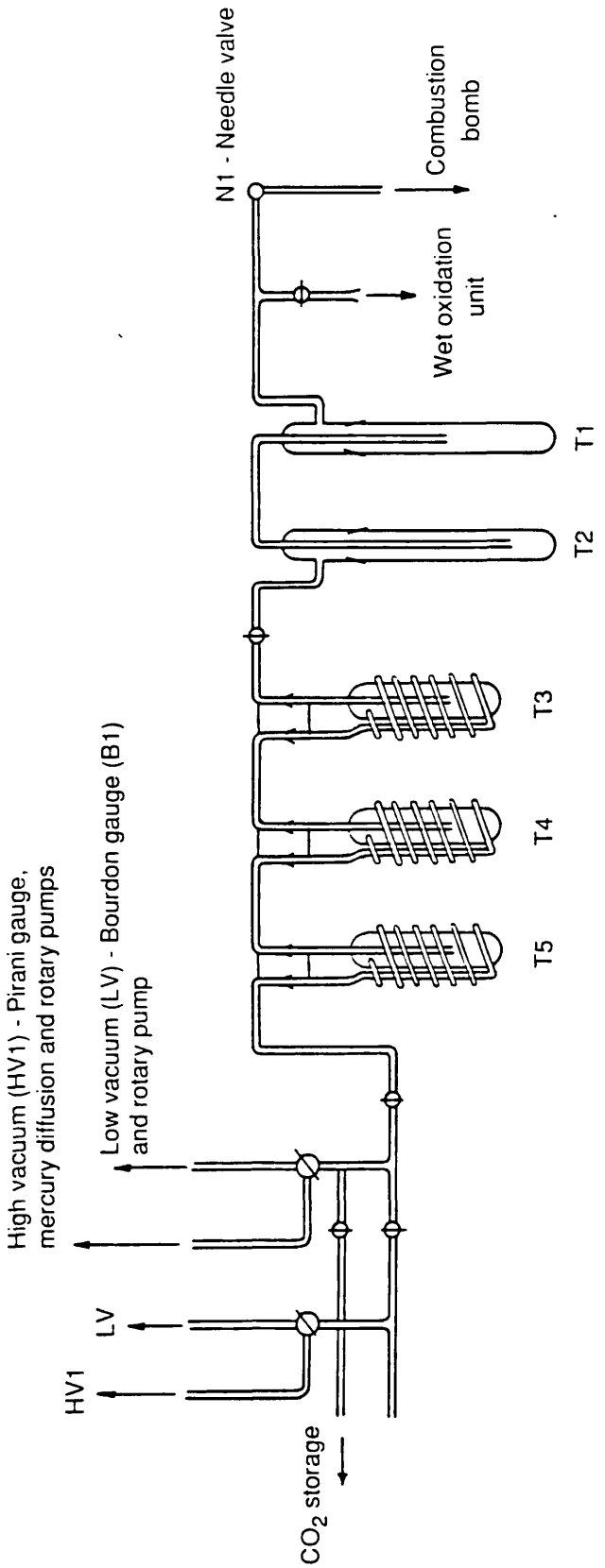

Figure 2.7: CO_2 collection and storage system.

atmosphere. CO_2 generated by combustion is pumped through the system at a pressure of 25-50 mbar (on the Bourdon gauge, B1) which reflects the excess oxygen being pumped away. At this pressure, the CO_2 is quantitatively frozen down in the spiral traps. During hydrolysis, the rate of reaction is monitored by a single-limb manometer and the pressure released by bleeding CO_2 into the collection system. This process is generally carried out without using the low vacuum manifold pump but if a pressure registers on the gauge at the spiral traps the pump can be used to remove any gas which is not freezing down. Once all the CO_2 has been collected in the spiral traps, the water traps are isolated from the pump and the sample CO_2 pumped *via* the low vacuum manifold. The IMS/CO_2 slush trap from the second water trap is then placed around the third spiral trap and a liquid nitrogen trap placed on the collection finger. The sample CO_2 is then allowed to sublime at room temperature and is then re-trapped in the liquid nitrogen-cooled finger with the IMS/CO_2 slush trap removing any last remaining traces of water. When the complete sample is in the collection finger it is pumped *via* the high vacuum manifold, which is connected to a water-cooled mercury diffusion pump backed by a rotary pump, until the vacuum is better than 10^{-2} torr (on a Pirani gauge). The sample is then transferred to storage bulbs which have the capacity to store up to 20 litres of CO_2 (although normally only 10 litres are used) and which have previously been pumped using the high vacuum manifold to better than 10^{-2} torr to eliminate memory effects. The sample is stored overnight in the bulbs and then processed further the following day.

(a) AMS samples

All the samples analysed by AMS were sent to the Oxford Radiocarbon Accelerator Unit as CO_2 in small 2 ml flame-sealed ampoules. The collection of the CO_2 was carried out on the "micro-rig" which comprises four ports for attaching reaction vessels, two spiral traps, a calibrated finger with a digital gauge read-out, a Pirani gauge and a water-cooled mercury diffusion pump backed by a rotary pump (Fig 2.8).

To collect the CO_2 from the hydrolysis/wet oxidation apparatus the reaction vessels are connected to one of the ports *via* cone and socket joints and the vacuum line pumped to better than 10^{-2} torr. A slush trap (IMS/solid CO_2) is placed around the nearest spiral trap and liquid nitrogen placed around the other to collect the CO_2, ensuring that the calibrated finger is isolated. The reaction vessel is then opened and the CO_2 allowed to pass into the second spiral trap. Once all the sample has been frozen down, the reaction vessel is

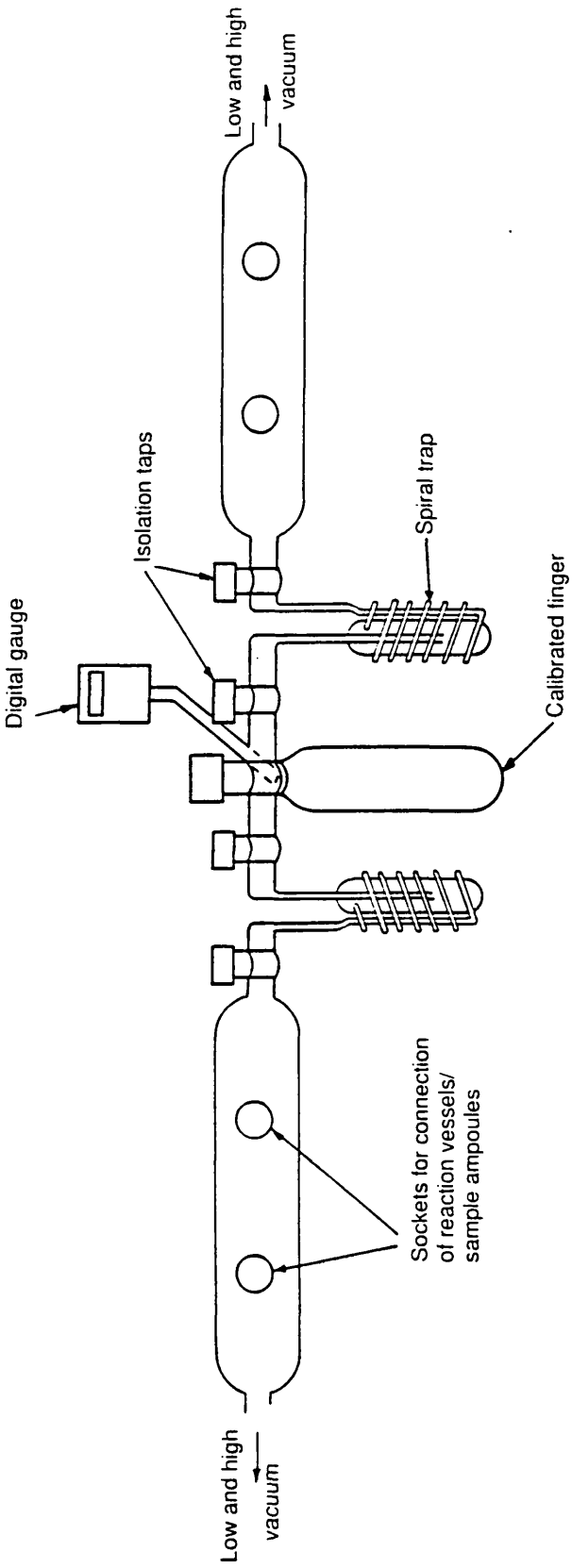

Figure 2.8: "Micro-rig" used in preparation of AMS samples.

isolated and the IMS/CO_2 trap placed on the second spiral while the calibrated finger is cooled to -196°C with liquid nitrogen and opened to allow the sample to freeze down again. It is then pumped to better than 10^{-2} torr with the mercury diffusion pump. When this vacuum has been attained, the calibrated finger is isolated, the liquid nitrogen removed and the sample allowed to sublime. The reading on the gauge defines the amount of sample obtained from the reaction.

The calibrated finger on the "micro-rig" has a volume of 22.4 ml whereas the standard ampoules required by the AMS laboratory hold ~2 ml of gas. Transfer of the CO_2 to suitable ampoules requires a subsample to be collected by bleeding 100 gauge units (1000 is equivalent to a volume of 22.4 ml) into an isolated section of the vacuum line from which it can be frozen down into the ampoule which is then flame sealed.

2.2.3 Conversion of CO_2 to Acetylene

Barker (1953) developed earlier work by Arrol and Glascock (1947) to produce a viable two stage method of converting carbon dioxide to acetylene *via* an intermediary of lithium carbide. Both reactions are carried out in a stainless steel reaction vessel which is connected to the glass vacuum line (Fig 2.9) and is designed in two parts to allow rapid isolation from the atmosphere, preventing oxidation of the lithium, in addition to easy cleaning between samples. The lower part is where the reaction occurs, with the upper part being water cooled to prevent evaporation of the molten lithium. The second (or top) half of the reaction vessel has the gas inlet/outlet valve, pressure gauge, water inlet valve and a quartz glass viewport which allows monitoring of the reaction. Two burners connected to a gas supply are used to heat the vessel.

2.2.3.1 Lithium carbide formation

The chemical equation for this reaction is:-

$$2CO_2 + 10Li \rightarrow Li_2C_2 + 4Li_2O \qquad (2.1)$$

Lithium metal is added to the reaction vessel *via* the viewport (2.5 g per litre CO_2), the pot is sealed, connected to the low vacuum manifold and evacuated. Once the cooling jacket water has been turned on, the burners are lit and the reaction vessel heated until the lithium is molten and produces a shiny mirror surface. The pump can then be turned to

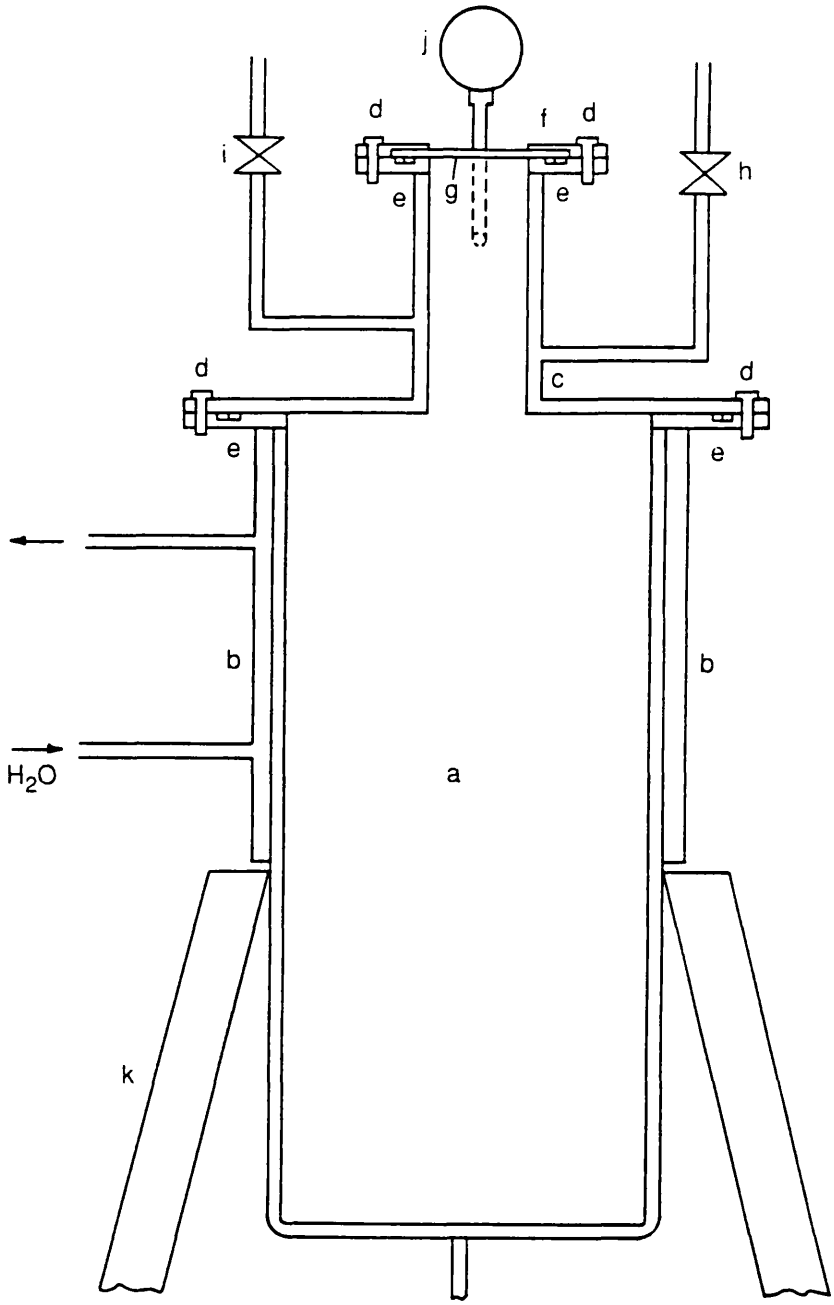

a Reaction chamber
b Cooling jacket
c Top flange
d High tensile bolts
e 'O'-ring track
f Viewport flange
g Quartz viewport
h Gas inlet/outlet
i Water inlet valve
j Bourdon gauge
k Tripod stand

Figure 2.9: Lithium reaction vessel.

the high vacuum manifold and the vessel pumped until the vacuum approaches 10^{-2} torr. Prior to CO_2 addition, a small sample is taken for mass spectrometric analysis and then the remaining sample is slowly added to the reaction vessel through the gas inlet valve, ensuring that the internal pressure does not exceed 300 torr as this reduces the acetylene yield. On addition of the sample, the lithium metal discolours and becomes black as the carbide is formed and the exothermic nature of the reaction results in a rise in temperature to ~800°C. The final part of the CO_2 sample has to be frozen down into the collection finger with liquid nitrogen and forced onto the lithium to ensure conversion of the complete CO_2 sample.

Throughout this process, some carbon may be lost due to the following side reactions,

$$4Li + 2CO_2 \rightarrow Li_2CO_3 + C + Li_2O \qquad (2.2)$$

$$Li_2O + CO_2 \leftrightarrow Li_2CO_3 \qquad (2.3)$$

but at temperatures above 600°C, Li_2CO_3 decomposes significantly due to the reversible nature of the reaction. At temperatures above 900°C this reconverted CO_2 forms Li_2C_2 by reaction (2.1) and the elemental carbon formed in equation (2.2) undergoes $2C + 2Li \rightarrow Li_2C_2$ to again form lithium carbide (Gupta and Polach, 1985).

When all the CO_2 has been adsorbed onto the lithium, the reaction vessel is isolated from the vacuum line and heated for a further 45 minutes after which time the burners are switched off and the vessel connected to the acetylene collection system and pumped through the low vacuum manifold until cooled to room temperature (usually 1-2 hours).

2.2.3.2 Hydrolysis of lithium carbide to form acetylene

Once the carbide has cooled, the second stage of the acetylene production can be carried out. The chemical equation for this reaction is:-

$$Li_2C_2 + 2H_2O \rightarrow C_2H_2 + 2LiOH \qquad (2.4)$$

The apparatus used to form and collect the acetylene is detailed in Figure 2.10. As before, for the CO_2 collection, the acetylene collection system has three spiral traps (T2, T3 and T4), but only one water trap (T1). The system is connected to a low vacuum manifold with a rotary pump, and a high vacuum manifold with an air-cooled oil diffusion pump

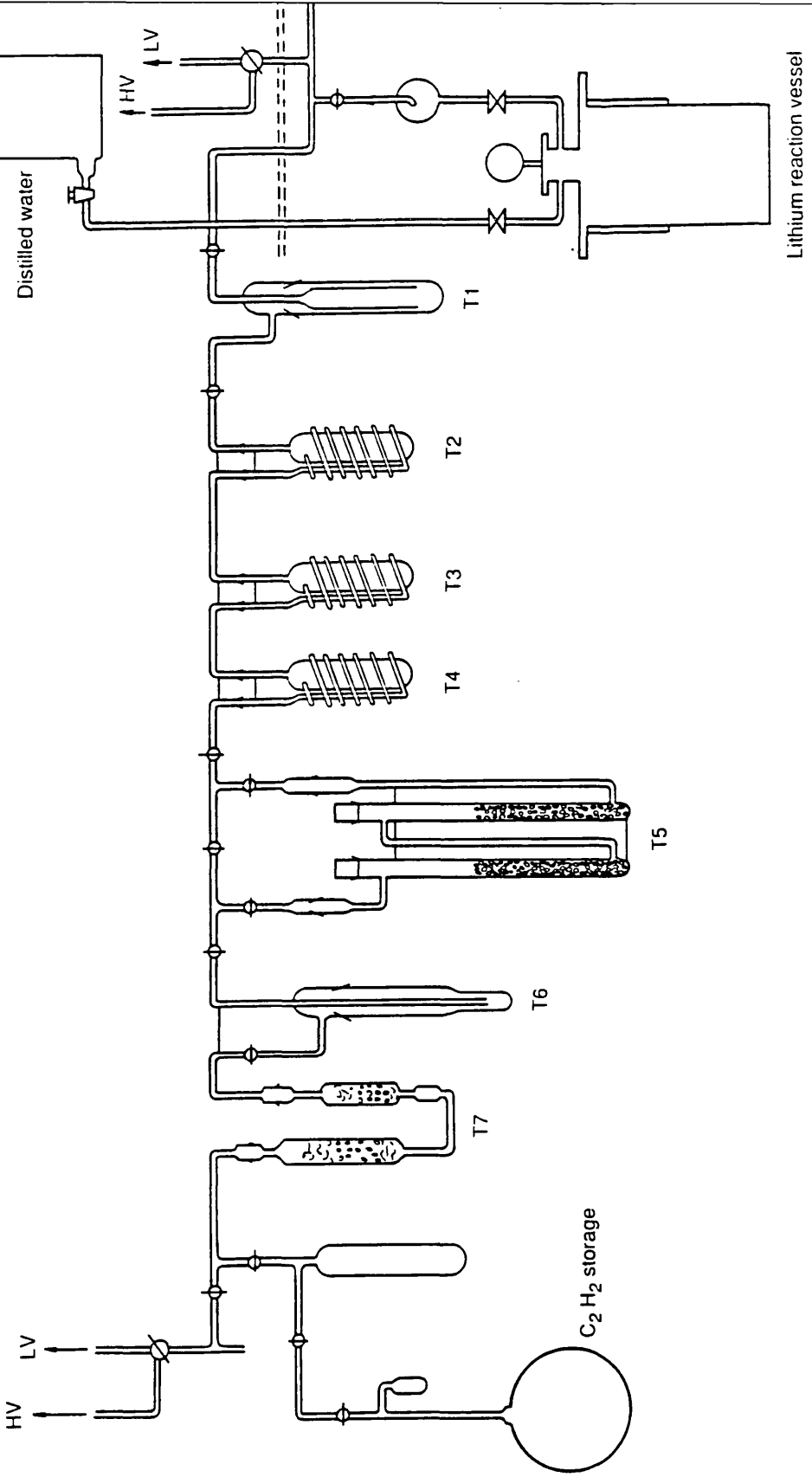

Figure 2.10: Acetylene preparation and collection system.

backed by a rotary pump (a mercury pump may cause the formation of explosive acetylides). Acetylene is produced from lithium carbide by the controlled addition of distilled water. The pressure in the reaction vessel is allowed to build up to ~700 torr before being released, passing through the IMS/CO_2 slush trap into the three liquid nitrogen-cooled traps at a rate ≤25 mbar (the reading on the gauge is due to hydrogen produced in the reaction being pumped away) until the internal pressure is ~300 torr. This process is repeated until no increase in pressure occurs on the addition of water. The residual pressure in the reaction vessel is released until the mixture begins to "boil". The reaction vessel and water trap are then isolated from the sample which is pumped *via* the low vacuum manifold and then isolated.

2.2.3.3 Acetylene purification and storage

The acetylene is subjected to a rigorous clean-up before it is converted to benzene (Fig 2.10). Once the sample has been pumped by the low vacuum manifold, the IMS/CO_2 slush trap is placed on the third spiral trap and the sample allowed to sublime at room temperature. The sample is collected in a liquid nitrogen-cooled finger, after it has passed through a scrubbing column of orthophosphoric acid (H_3PO_4) and glass beads (T5), another IMS/CO_2 water trap (T6) and finally a column containing phosphorus pentoxide (P_2O_5) - coated glass beads (T7). The H_3PO_4 column removes any ammonia present in the sample whereas the P_2O_5 column removes any final traces of moisture. When all the acetylene has frozen down in the collection finger, it is pumped *via* the high vacuum manifold until better than 10^{-2} torr. The storage bulbs for acetylene have a 6 and 12 litre capacity and are pumped to better than 10^{-2} torr to remove memory effects before the samples are stored prior to benzene synthesis.

2.2.4 Benzene synthesis

The final step in sample processing is the conversion of acetylene to benzene which involves a cyclotrimerisation reaction *ie.*

$$3C_2H_2 \rightarrow C_6H_6 \qquad (2.5)$$

In the early 1960's, this reaction was carried out by pyrolysis of acetylene at 650°C (Tamers, 1960) and by using diborane activated catalysts (Noakes *et al.*, 1963). Post-1965,

however, most radiocarbon laboratories employing liquid scintillation techniques have used transition metal activated silica-alumina catalysts (Noakes *et al.*, 1965; Tamers, 1965; Pietig and Scharpenseel, 1966) and in this study a chromium activated silica-alumina pelletised catalyst is used.

The benzene synthesis section of the glass vacuum line is detailed in Figure 2.11 and consists of a removable catalyst tube surrounded by a furnace, a thermocouple, a removable cold finger for benzene collection, a Bourdon gauge and connections to both the acetylene storage system and the low and high vacuum manifolds *via* greaseless stopcocks to prevent grease from contaminating the sample benzene. The catalyst tube is filled with new catalyst for every synthesis to reduce the risk of carry-over from previous samples, although theoretically the chromium (III) and (IV) can be reactivated back to the (VI) form (by heating in air to 450°C).

Once the catalyst tube is filled and connected to the line it is pumped *via* the low vacuum manifold while the surrounding furnace heats the catalyst to 350°C, ensuring the removal of any moisture and gases present. This temperature is maintained for 30 minutes before the furnace is turned off and the catalyst allowed to cool while being pumped by the high vacuum manifold to 10^{-2} torr. Acetylene is introduced to the catalyst when the temperature reaches 120°C and due to the exothermic nature of the reaction, the catalyst temperature increases. Further aliquots of acetylene are introduced until the temperature approaches 160°C and when the temperature ceases to rise, the benzene is transferred into the liquid nitrogen-cooled finger thus freeing active sites on the catalyst. When the catalyst has cooled to 120°C, more acetylene is added and this process is repeated until the complete acetylene sample is converted to benzene. To ensure that all the acetylene is converted to benzene, the final traces of acetylene are frozen down in the collection finger, the catalyst isolated and the benzene finger heated. Any acetylene in the benzene sample is then trapped in the Bourdon gauge from which it is allowed to slowly transfer onto the cooling catalyst in a reduced volume. When all the acetylene is on the catalyst, the furnace is heated to 160°C and the benzene which is produced is allowed to pass over into the collection finger. The sample in the collection finger is then removed from the vacuum line, capped and stored in a refrigerator for a minimum of three weeks to allow any radon present to decay.

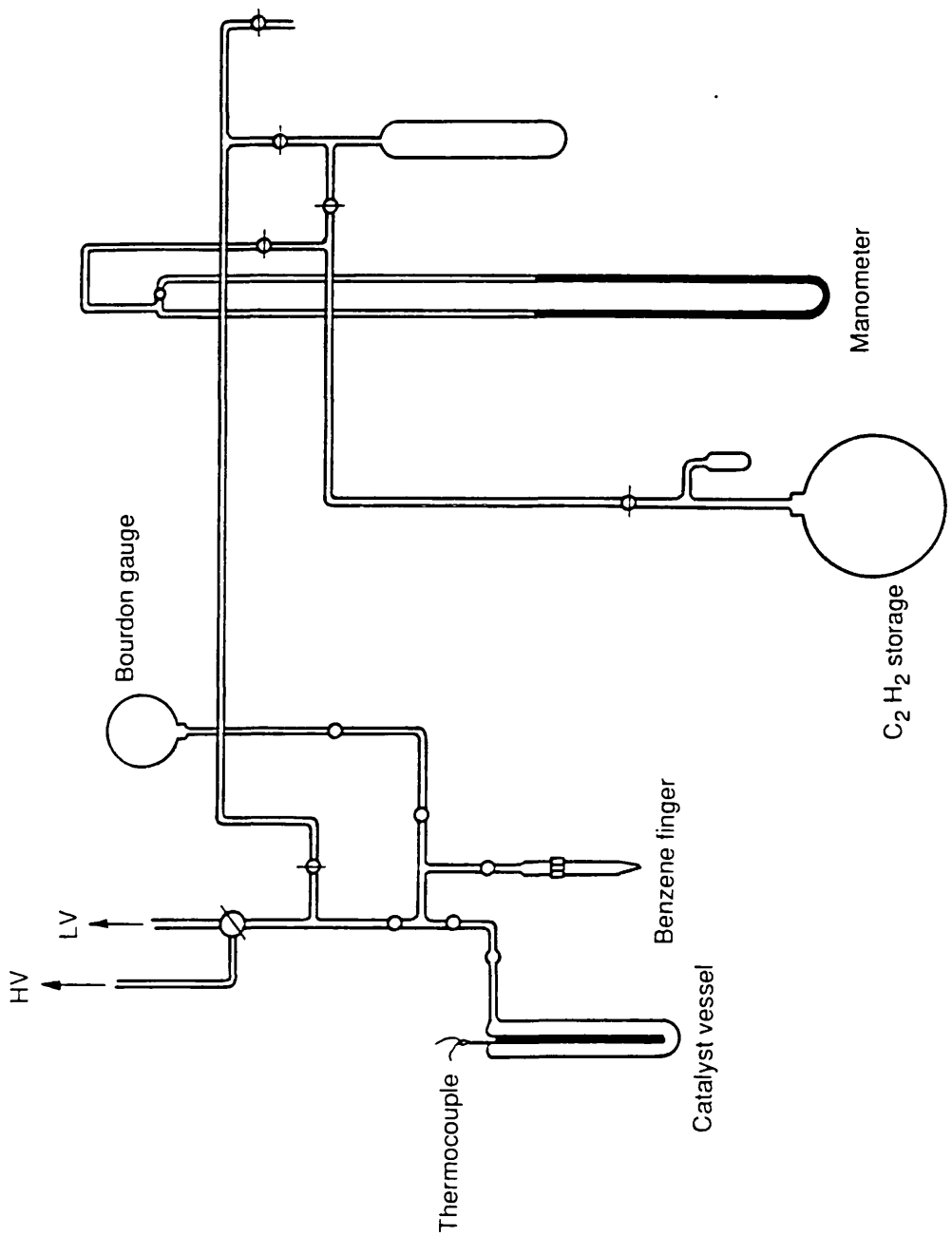

Figure 2.11: Benzene synthesis system.

2.2.5 Efficiency of sample preparation

The individual procedures carried out to convert sample carbon to benzene gave yields of >95% for the production of CO_2, ~90% for C_2H_2 production and >90% for the conversion to benzene. This resulted in an overall average yield of >80% with the greatest scope for loss of efficiency being in the conversion of CO_2 to C_2H_2.

2.3 ISOTOPIC FRACTIONATION MEASUREMENT

Isotopes of the same element, such as ^{14}C, ^{13}C and ^{12}C, have slightly different thermodynamic properties which can result in changes in the isotopic ratio of the element during chemical and physical processes in both the laboratory and the environment. As an example of environmental isotopic fractionation, Craig (1953) found a 2 ‰ depletion in the ^{13}C:^{12}C ratio of terrestrial organic plants relative to that of their carbon source *ie.* the atmosphere. As the mass difference is double for ^{14}C:^{12}C, relative to ^{13}C:^{12}C, Craig (1954) assumed an isotopic fractionation difference of the same magnitude (*ie.* a 4 ‰ depletion of ^{14}C).

Correcting measured ^{14}C activities for this isotopic effect, prior to age calculation, has been recommended by Stuiver and Polach (1977). To maintain this convention, all sample activities measured in this study have isotopic fractionation taken into account, although the majority of the samples did not derive their carbon from the atmosphere and marine samples have been shown to have an "apparent age". This apparent age is due to the slow mixing of water masses with different ages, which by coincidence compensates for any fractionation effect around the U.K. coastline (Harkness, 1983). The samples in this study, however, were not being dated, but, expressed as enhancements or depletions relative to the standard used, hence, isotopic fractionation corrections were included in the specific activity calculation for each sample.

The extent of isotopic fractionation for ^{14}C cannot be measured directly from ^{14}C:^{12}C ratios, hence, ^{13}C:^{12}C ratios are determined and used to calculate a fractionation factor by assuming a doubling of the deviation for ^{14}C. The sample of CO_2 for mass spectrometric analysis is collected prior to lithium carbide formation, with the assumption that no further fractionation is induced during the conversion to acetylene and benzene (Campbell, 1977). Carbon stable isotope ratios are reported in the $\delta^{13}C$ ‰ notation relative to PDB, where

PBD is a Cretaceous belemnite, *Belemnita americana*, from the Peedee formation in South Carolina and is the primary standard for $\delta^{13}C$ fractionation determinations. The isotopic composition of the samples are measured on a VG SIRA 10 or SIRA 11 instrument by comparing the m/z 45/44 and 46/44 ratios for sample CO_2 with those of a working, secondary standard CO_2 calibrated against NBS 22 oil ($\delta^{13}C$ = -29.61‰ PDB) and NBS 19 marble ($\delta^{13}C$ = +1.93‰ PDB), and making the usual instrumental correction factors (Craig, 1957a; Fallick, pers. comm., 1992). The deviation of the sample ^{13}C:^{12}C ratio relative to the standard ^{13}C:^{12}C ratio can be calculated from the equation:-

$$\delta^{13}C = [{}^{13}C:{}^{12}C_{sample}/{}^{13}C:{}^{12}C_{standard} - 1] \times 1000‰ \qquad (2.6)$$

Convention again results in all radiocarbon samples being corrected to a $\delta^{13}C$ of -25‰, which is the average $\delta^{13}C$ value of 19th century wood. The equation

$$F.F. = [1-2(\delta^{13}C + 25/1000)] \qquad (2.7)$$

produces a fractionation factor (F.F.) which can be directly applied to the sample activity as discussed in Section 2.5.6 to give an isotope fractionation corrected activity.

2.4 LIQUID SCINTILLATION COUNTING

The basic theory behind liquid scintillation counting has been described in great detail elsewhere (Birks, 1964,1975; Birks and Poullis, 1972; Knoll, 1979; Gupta and Polach, 1985) and will only be discussed generally in this section with the major emphasis placed on the application and reliability of the technique in relation to this work.

2.4.1 The Theory

As previously mentioned in the introduction to this chapter (Section 2.1), liquid scintillation counting requires the sample to be in direct contact with a solvent capable of absorbing the energy released during the emission of a beta particle. The beta particle will dissipate its energy by collisions with this solvent resulting in excitation of the solvent molecules. These excited solvent molecules are not readily detected hence a scintillation

solution contains not only a solvent, but, also a solute which is a scintillator. Once excited, the solvent molecules can transfer energy to other solvent molecules or to a solute molecule. Energy passed to the solute molecule disturbs the orbital electron cloud of the solute raising it to a state of excitation, and on its return to the ground state, a photon of light is released. The total number of photons from the excited scintillator molecules constitutes the scintillation in which the intensity of light is proportional to the initial energy of the beta particle. For ^{14}C, the scintillation intensity will range from 0 - 156 keV. The detection of this light is carried out by two photomultiplier tubes (PMTs, whose surfaces act as photocathodes) which transduce the detected photons into electrical pulses (see Section 2.4.3).

2.4.2 The Scintillation Medium

In the past, photomultiplier tubes were only responsive to certain wavelengths of light, hence, scintillation cocktails were made up using two scintillators - termed the primary and secondary scintillators. The primary scintillator emitted photons of light with a wavelength too short to be picked up by the PMTs, hence, a secondary scintillator was added to increase the optical efficiency of the system. Although modern bialkali PMTs respond to a wider range of wavelengths of light, the tradition of using two scintillators has been maintained as the cocktail has been found to be both efficient and convenient to use. With some "new technology" counters, which employ pulse shape analysis, the composition of the "scintillation cocktail" has been found to play an important role in the optical efficiency of the instrument (Cook *et al.*, 1990) with improved performance using two scintillators.

In this study the "scintillation cocktail" used was 12 g of butyl-PBD (2-(4'-tert-butylphenyl)-5-(4''-biphenylyl)-1,3,4-oxadiazole)), as the primary scintillant, and 6 g of bis-MSB (1,4-di(2-methylstyryl)-benzene), as the secondary scintillant, dissolved in one litre of toluene. Toluene was chosen as the solvent as it possesses all the properties required *ie.*

1) able to dissolve the scintillants in the required quantities
2) a good energy transfer agent
3) low freezing point (< 0°C).

2.4.3 The Detection System

The detection system of most modern liquid scintillation spectrometers consists of two photomultiplier tubes (PMTs) diametrically opposite each other and a centrally mounted optimising reflector. The inner faces of the PMTs are uniformly coated with a photosensitive material which converts the absorbed photons of light into electrical energy by the release of photoelectrons which are negatively charged. These photoelectrons are attracted to a positive electrode within the PMT resulting in the production of more electrons. These secondary electrons are attracted to a second electrode where a similar process occurs. Normally twelve of these electrodes (dynodes) are present within the PMTs, with the secondary electrons amplified at each electrode to give a cascade of electrons at the final dynode, thus creating an electrical pulse. PMTs are linear devices, therefore, the amplitude of the electrical pulse is directly proportional to the number of photons detected at the photocathode. By this means, the scintillation is detected and converted to an electrical pulse. By monitoring the occurrence of these electrical pulses in a given time period, an indication of the number of scintillations, hence, beta emissions, which are taking place in the sample is obtained. As PMTs are sensitive, the application of a voltage between the electrodes produces small noise pulses which contribute to the background of the system. In addition, ionisation effects due to incomplete vacuum within the PMTs contribute towards the total background count rate of the system. Noise pulses can also be induced due to thermal changes in the surroundings and the movement of these electrons is temperature dependent. These pulses are extraneous to the sample and resemble "true" pulses due to beta events.

The use of two PMTs and coincidence circuitry was introduced to reduce this component of background. Thus, nuclear decay events produce about 10 photons per keV of energy and the energy is dissipated in approximately 5×10^{-9} seconds. A beta decay event will stimulate both PMTs at the same instant - the output from both PMTs is compared and the event recorded only if both have detected the photon within the resolving time of the circuit *ie.* 20×10^{-9} seconds. Electrical noise from the PMTs is produced randomly, hence, the chances of a noise pulse occurring in each PMT within 20 nanoseconds is very small, therefore, they will not be recorded. This is termed as coincidence circuitry.

The location of an event within a vial determines the size of the signal at each PMT, and until the advent of pulse summation techniques this caused problems in determining pulse

amplitudes. Pulse summation adds the amplitude of the pulses at each PMT giving an output which is proportional to the total intensity of the scintillation.

Most modern commercial liquid scintillation counters now employ both pulse coincidence and pulse summation techniques with the more technologically advanced counters employing various other techniques to improve the system.

The use of linear amplification with three counting windows and discrete channels required a separate amplifier, pulse height analyser and scaler for each channel. The introduction in 1964 of logarithmic amplification eliminated the need for individual channel amplifiers *etc.* and by 1980, further advances resulted in counters with pulse height energy spectrum analysis facilities (Multi-Channel Analysis), which allowed windowless counting, in conjunction with linear amplification. The pulse height energy distribution spectrum is collected at a fixed gain over an energy range, normally 0 - 2000 keV, allowing the interpretation of any portion of the spectrum simultaneous to sample counting. A 4048 channel spectrum analyser facility has individual channels representing approximately 0.5 keV, hence, the spectrum for ^{14}C beta emissions will be stored in roughly the first 312 channels for an unquenched sample.

Many more advancements have been made in liquid scintillation technology within the last decade *eg.* three-dimensional spectrum analysis for the reduction of background by pulse shape analysis, vector qualitative analysis for the detection of heterogeneous samples and a number of methods of assessment of external standard spectra for the determination of counting efficiency, however, the study of these is outwith the scope of this work although more details can be found in the individual manufacturers manuals and the following texts (Gupta and Polach, 1985; van Cauter, 1986; Noakes and Valenta, 1989; Ross *et al.*, 1991).

2.4.4 The Counter

Throughout the period of this research, three liquid scintillation counters have been used - a Packard Tri-carb Model 3330, a Kontron/Intertechnique Model SL30 and finally a Packard Tri-carb Model 460C although "new technology" Packard Models 2250CA and 2260XL have also been available to count small samples. The major part of the work has been carried out on the final model (Packard Tri-carb 460C) but to ensure that all three instruments were comparable, eight samples were counted on each counter and the results obtained are detailed in Table 2.1. The results are reported in pM$\pm 1\sigma$ relative to the

international standard and show that all three counters were comparable with the measured activities all being within error.

SAMPLE No.	TRI-CARB 3330	INTERTECHNIQUE	TRI-CARB 460C
	(all results quoted as pM±1σ)		
F46	195.4±1.2	193.7±1.9	195.8±1.4
F48	138.8±1.1	137.4±1.9	139.4±1.2
F50	132.5±0.8	132.9±1.4	131.9±1.1
F52	165.2±0.9	166.0±1.6	164.9±1.1
F54	245.6±1.1	246.5±2.0	246.8±1.4
F56	154.7±0.8	154.2±1.5	152.9±1.2
F58	141.9±0.9	142.8±1.5	142.5±1.1
F60	131.0±0.8	130.5±1.4	130.7±0.9

Table 2.1: Comparison of the results obtained from the 3 counters used during this research.

2.4.4.1 Counter design

As the majority of the work has been carried out on the Packard Tri-Carb 460C, only the specifications for this model will be detailed although in general the basic design of "older technology" liquid scintillation counters is similar.

The 460C has the capacity for 460 samples in its belt driven sample cassettes within the main body of the counter. The sample chamber is maintained at a stable temperature (20°C) in an air conditioned room to aid reproducibility of count rates, while the actual optical chamber is shielded from background environmental radiation by 5 cm of lead.

The optical chamber consists of two diametrically opposed bi-alkali integrated photomultiplier tube assemblies, a reflector to ensure maximum beta event detection and

an elevator to raise and lower samples through a light-tight seal and shutter system. An external standard of ^{226}Ra of 10 μCi activity is counted for 15 seconds prior to each sample to determine the extent of quenching occurring in the vial (see Section 2.5.4).

2.4.4.2 Counter optimisation procedures

The Packard Tri-carb Model 3330 required pre-optimisation of the operational parameters (voltage and gain) prior to ^{14}C analysis. To achieve this, it is necessary to have a balance between the high voltage supply to the PMTs, the discriminator settings on all three counting channels and the amplifier gain (attenuation of the peak height) such that the "Figure of Merit" (E^2/B, where E is efficiency and B is background) is maximised.

Counter optimisation was carried out using a ^{14}C spike sample and a ^{3}H spike sample with activities ~10,000 cpm. With all the channels set at 0 - ∞ mV and 50% gain, the ^{14}C spike was counted over a range of high voltage settings and the resultant cpm plotted against the voltage to produce a curve reaching a plateau as the voltage increased. The high voltage was then set at 50 -100 V onto the plateau, channel 1 set at 0 - 1000 mV and the gain varied from 0% to a level where the count rate in Channel 1 was 98% of the open window count rate. As the ^{3}H spectrum overlaps the lower end of the ^{14}C spectrum by ~12%, any events due to ^{3}H present in the benzene, have to be discriminated out. This was achieved by setting the lower discriminator such that 99% of the ^{3}H spectrum was discarded. The final settings used on the Model 3330 were a gain of 72% and a counting window of 120 - 1000.

A similar optimisation procedure was carried out for the Kontron/Intertechnique SL30 prior to use although on these instruments the gain is fixed and only the voltage can be altered. In the case of the Packard Tri-Carb 460C, both the gain and the high voltage are factory set and hence, only the upper and lower discriminators can be altered to accommodate the isotope of interest. The "Figure of Merit" for the 460C is 690 at 70% efficiency with an average background value of 7.10 cpm. During this work the counting window was set at a lower level of 10 keV, which cut out 99% of the ^{3}H, and an upper level of 75 keV which cut out ~2% of the ^{14}C count rate at the high energy end of the spectrum.

2.5 MEASUREMENT OF THE ^{14}C SPECIFIC ACTIVITY

Once the counter has been optimised, samples are counted in batches in conjunction with

a series of background samples, modern reference standards and a high activity spike. The raw data from the counter for each sample are collected and corrected for the average background of the system, any dilution which was carried out and also any quenching which has occurred in the sample, before the specific activity is calculated. The procedures carried out prior to calculation of the final activity will be discussed briefly in the following sections and will be followed by an example of activity calculation.

2.5.1 Vials and Vialing

The geometry used throughout this work for samples, backgrounds and modern standards was 4.5 g of benzene placed into a 20 ml low potassium, borosilicate ampoule with 0.95 g of the scintillation cocktail. The necks of the vials are narrowed prior to 4.5 g of sample, background or standard benzene being added *via* a Pastuer pipette. If less than 4.5 g of benzene have been prepared, the sample weight is made up to 4.5 g by the addition of scintillation grade benzene which contains no ^{14}C. The scintillation cocktail (0.95 g) is then added and a rubber septum is placed over the neck. The ampoules are then placed on a bed of solid CO_2 to freeze down the contents. An oxy-gas flame is used to seal the neck of the ampoule once the contents are frozen, thus ensuring no loss of sample benzene through evaporation. Before the ampoule is placed in the counter, the upper half is masked using black paint to reduce optical "cross-talk" between the photomultiplier tubes.

2.5.2 Backgrounds

To ensure that scintillation events not attributable to ^{14}C in the sample are taken into account (*eg.* radioactive impurities in the glass vials, radioactivity in the laboratory and counter materials, cosmic rays or random electronic noise within the counter) a background count rate is monitored. This is done by preparing samples of scintillation grade benzene or synthesising samples which are known to contain no ^{14}C activity (*eg.* marble) in the same manner as *bona fide* samples and counting them in the batches together with samples. These background samples are monitored for any change in their count rate as an indicator of counter stability and are also used as a means of monitoring the vacuum line for carry-over and memory effects.

2.5.3 Modern Reference Standards

All radiocarbon results are calculated relative to an international standard which is 1890 wood (Broecker and Olson, 1959) which is assumed to have a natural ^{14}C specific activity of 226 Bq kg^{-1} C and is equivalent to 100 %Modern (pM). In the laboratory, a secondary standard supplied by the National Bureau of Standards is used - Oxalic Acid II which, when multiplied by 0.7459, equals the activity (corrected to $\delta^{13}C = -25‰$) of the primary standard.

This oxalic acid is converted to benzene, as in normal sample preparation although the method for generating CO_2 is a wet oxidation reaction using 50% H_2SO_4 and potassium permanganate solution. The reaction is carried out in the apparatus normally used for the hydrolysis of inorganic samples (Fig 2.3) with the reaction flask being placed in a heating mantle which is set to give a low heat throughout the reaction. 28 g of oxalic acid are placed in the reaction vessel which is then sealed and the system pumped to better than 10^{-1} torr *via* the low vacuum manifold. 112 ml of 50% H_2SO_4 is then added and the system repumped to 10^{-1} torr. Potassium permanganate solution (28 g in ~120 ml of distilled H_2O) is then added slowly *via* the acid reservoir and the generated CO_2 collected in liquid nitrogen-cooled spiral traps. During the addition of $KMnO_4$, the reaction mixture turns brown but the colour quickly disappears and more $KMnO_4$ can be added. Once a brown precipitate has formed, due to the formation of manganese dioxide, the reaction is complete and the CO_2 can be converted to benzene *via* acetylene in the normal manner. Throughout the period of research, a number of modern standards were prepared, with four normally being counted in the sample batches to enable accurate calculation of the sample specific activities.

2.5.4 Quenching

The counting efficiency of the solvent - solute system can be affected by both chemical and colour quenching. The first of these absorbs beta energy before photons of light are produced. In comparison, colour quenching occurs as the photons are passing through the medium resulting in changes in the wavelength of the light reaching the PMTs, thereby reducing the response.

All samples are quenched to some extent, resulting in a decrease in the number of photons per keV reaching the PMTs and, hence, the pulse amplitude is reduced for the same energy

of particle. This results in a shift of the whole spectrum to lower energies.

The method used in the Tri-Carb 460C to monitor the extent of quenching in each individual sample is the external standard technique which uses the movement of the external standard spectrum as an indicator of quenching. An external source of gamma radiation (10 μCi of ^{226}Ra) is placed adjacent to the sample vial for 15 seconds before sample counting commences. This produces electrons in the scintillation solution due to the Compton collision process. These electrons cause scintillations which can be detected and used to produce an external standard spectrum. The contribution from the sample count rate is deducted by counting for a similar time period in the absence of the external standard to provide an indication of quenching dependent only on the external standard spectrum. Analysis of the external standard spectrum produces an index which can be related to the measuring efficiency in the region of interest. This index is termed the SIE (Spectral Index of the External Standard). The association between the SIE and the measured efficiency in the sample region is obtained by measuring a series of standards of known activity which have all been quenched to varying degrees with acetone (a known quenching agent) and the regression equation used to calculate a quench factor for the sample relative to a baseline value. The regression equation obtained for the 460C was:

$$\text{Activity (cpm/g)} = -881 + 8172(\text{SIE}/1000) - 6339((\text{SIE}/1000)^2) \qquad (2.8)$$

with a baseline SIE value of 600.

The presence of quenching agents shifts the external standard spectra to lower energy levels as it does for actual samples.

Thus, the Compton spectrum is generated in the scintillation solution and monitors the occurrence of quenching. The external standard method cannot determine effects of inhomogeneity in the sample although this is not a concern when benzene is the sample. The index, SIE, is based on the Compton electron distribution, hence, it is relatively unaffected by the sample volume or the type of vial used.

2.5.5 Batch Composition

All batches contained four background and four modern samples and a high activity spike, as an added check on counter stability. Of the four backgrounds, two were scintillation

grade benzene based and the remaining two were prepared from marble chips or calcium carbide.

Samples were placed evenly between pairs of backgrounds and moderns - the number of samples varied but was usually between 8 and 14 - and the batch counted for 100 minutes (2x50) per sample and for 5 cycles to give a count time of 500 minutes for each sample, standard and background. Each batch was then counted in this way a further three times to achieve a total counting period of 2000 minutes.

2.5.6 Specific Activity Calculation

The raw data from the counter are entered into a spreadsheet for calculation of the average count rate per 5 cycles, the error associated with this count rate (standard error on the mean = standard deviation/$\sqrt{}$no. count periods) and the average SIE value. These values can then be fed into a specific activity calculation programme, in conjunction with the sample number, weight and fractionation factor (as calculated in equation 2.7), to produce the specific activity of the sample in both pM$\pm1\sigma$ and Bq kg^{-1} C$\pm1\sigma$.

The results$\pm1\sigma$ obtained for each of the four 500 minute counting periods are then entered into a programme which calculates the weighted mean$\pm1\sigma$ which is taken as the activity of the sample. Although most of the calculations have been carried out using computer programmes, the basics of the calculation are detailed below for one of the samples analysed (Set 58 counted on 19/7/91).

The first process carried out by the programme is the calculation of the average background count rate of the system, determined by the count rates observed in the four background samples in the counting batch. For Set 58 the average background was 6.67 cpm with a standard deviation of 0.09 obtained from individual count rates of 6.76, 6.71, 6.71 and 6.52. This is followed by the calculation of the average modern (standard) activity. Unlike the background calculation, the modern count rates are corrected for quenching and fractionation and then are divided by the weight of sample benzene to give a final activity in cpm/g. The activities of the four moderns in Set 58 were 9.52±0.06, 9.30±0.08, 9.40±0.08 and 9.27±0.08 which gave a weighted mean value of 9.39±0.04 cpm/g to be used in the subsequent calculations.

Table 2.2 details the information required to calculate the specific activity of a sample *ie.*

the weight of benzene, the quench factor, the fractionation factor, the background count rate and the modern count rate.

Set No. 58 counted on 19/7/91	
Sample No. F172	
Weight of sample	2.525 g
Quench Factor±1σ (Average SIE 609.5)	0.997±0.002
Fractionation Factor ($\delta^{13}C$ -14.06‰)	0.98
Average cpm±1σ	101.72±0.44
Background count rate±std. dev.	6.67±0.09
Modern count rate (wtd mean)±1σ	9.39±0.04

Table 2.2: The parameters required to calculate sample ^{14}C specific activity.

The overall equation for the calculation of specific activity (Bq kg^{-1} C) is:-

$$Specific\ Activity = \frac{F.F. \times Q.F. \times Net\ Count\ Rate \times 226}{Wt.Samp. \times Corr.\ Modern\ Count\ Rate} \quad (2.9)$$

which involves the following steps:-

1. Net count rate = sample count rate - background
   (101.72 - 6.67 = 95.05)
2. Multiply by quench factor = 94.76 cpm
3. Multiply by fractionation factor = 92.86 cpm
4. Divide by weight of sample benzene = 36.78 cpm/g
5. Divide by weighted mean modern = 3.917
6. Multiply by 100 = 391.7 % M

7. Multiply by 2.26 = 885.2 Bq kg^{-1} C

Within this calculation, three of the terms have associated errors which must be used in the calculation of the overall associated error.

For a function Z which has three variables *ie.* Z = h(x,y,T), where h is the function and x,y and T the variables, the associated error can be calculated from:-

$$e(Z) = \sqrt{\left(\frac{dZ}{dx}\right)^2\sigma_x^2 + \left(\frac{dZ}{dy}\right)^2\sigma_y^2 + \left(\frac{dZ}{dt}\right)^2\sigma_T^2} \qquad (2.10)$$

In the case of our calculation Z = Q.F. x net/mod, as it is assumed that no error is associated with the other parameters, and x = Q.F., y = net and T = mod. Hence, in the derivatised form of the equation

$$\frac{dZ}{d(QF)} = \frac{net}{\text{mod}}, \frac{dZ}{d(net)} = \frac{QF}{\text{mod}} and \frac{dZ}{d(\text{mod})} = \frac{-QF \times net}{\text{mod}^2} \qquad (2.11)$$

and the error associated with the function becomes:-

$$e(act.) = \frac{FF \times 226}{wt.samp} \times \sqrt{\left(\frac{net}{\text{mod}}\right)^2 \times [e(QF)]^2 + \left(\frac{QF}{\text{mod}}\right)^2 \times [e(net)]^2 + \frac{(QF \times net)^2}{\text{mod}^4} \times [e(\text{mod})]^2} \qquad (2.12)$$

where

$$e(net) = \sqrt{[e(gross)]^2 + [e(bkgd)]^2} \qquad (2.13)$$

The final calculated 1σ error for sample F172 counted in Set 58 was 2.5 %Modern (5.6 Bq kg^{-1} C).

These calculations are carried out on a further three sets of data (of 5 cycles) - the four results obtained are used to calculate the weighted mean for each sample. For F172, the

four results obtained using the computer programme were 391.7±2.5 (885.3±5.6), 389.6±2.7 (880.4±6.0), 394.2±2.7 (890.8±6.2) and 395.3±2.1 (893.5±4.7) which gave a weighted mean for the measured activity of 393.0±1.3 %Modern (888.2±2.9 Bq $kg^{-1}C$). Following the guidelines set out by Stuiver and Polach (1977) regarding the reporting of ^{14}C data, environmental studies require a correction for the decay of ^{14}C in the oxalic acid reference standard to be taken into account. This is achieved using the equation:-

$$pM = \%M \exp[-\lambda(y-1950)] \qquad (2.14)$$

where λ = 1/8267 yr^{-1} and y = the year of measurement. For the samples analysed during this study *ie.* during the years 1989 - 1991, all the results can be multiplied by 0.995 to take this into account (*eg.* for F172, pM = 391.0±1.3). All the results presented in this work are reported both as pM±1σ and specific activity (Bq kg^{-1} C±1σ).

2.6 RELIABILITY OF RESULTS

Reliability of the results obtained is a major concern in all scientific fields, and in the ^{14}C field, quality assurance of dating practices has become a growing international concern within the last decade. In an attempt to determine the reliability of dates produced from the many ^{14}C laboratories world-wide, a number of intercomparison and intercalibration studies have been undertaken. The latest of these intercalibration exercises, TIRI, (Third International Radiocarbon Intercalibration) is at present underway with ~90 laboratories taking part from ~30 countries (Scott, pers. comm., 1992).

2.6.1 In-house Reliability

The reliability of the final results is determined by a number of factors. The individual components of reliability range from the quality of the initial sample, through the collection and analytical procedures used, to the stability and reproducibility of the chosen counting technique. Each of these factors and processes will allow the introduction of uncertainty into the measurement and steps must be taken to keep this to a minimum. It is necessary, however, to determine the extent of this introduced uncertainty within individual ^{14}C laboratories.

A number of protocols for good laboratory practice and quality assurance/quality control were discussed at an international workshop in 1989 (Long and Kalin, 1990; Switsur, 1990) in an attempt to improve the reliability within laboratories and, hence, the public image of ^{14}C dating as perceived by the "users". Long (1990) proposes a quality assurance protocol which summarises the guidelines accepted not only by the directors of numerous radiocarbon laboratories but also by the IAEA. The basic principles of this protocol include:-

(1) Written procedures incorporating diagrams of the equipment used and details of any changes/modifications to procedures or equipment.

(2) Sample documentation and traceability which ensures that any person can use laboratory records to determine what, when and by whom any procedure has been carried out on the sample.

(3) Analysis of standards and counting backgrounds. Established count rates of backgrounds and NBS oxalic acid samples measured at regular intervals should be plotted on calendric scales to illustrate system reliability and/or to indicate problems.

(4) Replication of reference materials. Both in-house and IAEA standard materials should be analysed regularly to check system accuracy and indicate any analytical problems. These can also be used to determine analytical precision of procedures. Overall, ~20% of counting time should be devoted to quality assurance determination.

(5) Regular intercomparisons using natural (unknown activity) samples. These will be run every 2-3 years to provide an objective and independent check on analytical accuracy and precision.

(6) Recognition and correction of problems. Quality assurance analyses should be plotted on calendric scales and any statistical deviation from established ^{14}C age should be examined.

(7) Establishment of total analytical precision. This is obtained by repeat analyses (~20), through the entire chemical and physical system, of a homogeneous material similar in nature to those materials normally analysed in the laboratory.

In this study the ultimate aim of reliability was assumed from the beginning *ie.* at the sampling stage. The samples were collected randomly to obtain a sample which would reflect the mean ^{14}C activity at each site. To this end, biota samples were collected with

no regard to age or size, intertidal surface sediment scrapes were collected from a large area and the bottom sediments were subsampled from a much larger Kaston core.

During pretreatments and conversion of the sample carbon to CO_2, care was taken to ensure that no contamination of the sample occurred *eg.* acid washing of biota samples (Section 2.2.1.1) and preparation of CO_2-free 4M NaOH (Section 2.2.1.5(a)). To monitor the conversion of CO_2 to C_6H_6, background samples (marble chips) were analysed periodically to determine the extent, if any, of carry-over from previous high activity samples run through the vacuum line. No memory effects were found in these background samples, indicating that adequate measures had been taken during the pumping of the line to ensure no contamination of subsequent gas samples. Another step taken to reduce the risk of carry-over from previous samples involved regularly renewing the orthophosphoric acid and phosphorus pentoxide traps in the acetylene clean-up stage.

In an attempt to determine the reliability of the sampling, pretreatment and benzene preparation procedures, replicate analysis of a bulk seaweed sample (*Fucus* spp.), collected from north-west Scotland (Aldmuir), was carried out. In addition to this, several other sample types were analysed more than once *eg.* Ravenglass mussels, Sellafield winkles and for two of the sites selected for DIC analysis two or three samples were collected to determine the variability in the sampling technique.

The results from all these analyses are shown in Tables 2.3, 2.4 and 2.5. Most analyses have been carried out on the bulk seaweed sample and the results obtained (Table 2.3) indicate that the sample itself is fairly homogeneous and representative of the current ambient ^{14}C level. Reproducibility in the results also indicates that the methods used to prepare the sample benzene are not introducing contamination and that the end results are a true reflection of the activity in the seaweed at the time of sampling.

SAMPLE No.	DATE ANALYSED	pM± 1σ	Bq kg^{-1}C±1σ
FSA1	2/12/88	115.4±0.3	260.7±0.6
F15	20/2/89	117.0±0.5	264.3±1.1
F61	3/10/89	115.5±1.0	261.0±2.4
F62	4/10/89	115.0±0.2	259.9±0.5
F122	16/8/90	117.4±0.6	265.4±1.2
F144	7/1/91	117.9±0.5	266.5±1.1
F161	22/3/91	116.8±0.6	263.9±1.4
Overall Mean±standard error		**116.4±0.4**	**263.1±1.0**

Table 2.3: Replicate analysis results for Aldmuir seaweed.

The mussels and winkles collected close to the Sellafield discharge point also show good agreement between replicate samples indicating that sampling has been representative, even at sites subject to large variations in their source of ^{14}C (Table 2.4).

SAMPLE No.	DATE ANALYSED	pM±1σ	Bq kg^{-1} C±1σ
F2	13/1/89	683.5±2.0	1544.8±4.4
F65	30/10/89	683.4±2.7	1544.5±6.1
F66	1/11/89	681.2±3.2	1539.5±7.3
Overall Mean±standard error		**682.7±0.6**	**1542.9±1.7**
F10	3/2/89	438.1±1.8	990.2±4.0
F67	10/11/89	432.1±2.0	976.5±4.6
F68	13/11/89	435.5±1.8	984.3±4.1
Overall Mean±standard error		**435.3±1.8**	**983.7±4.0**

Table 2.4: Replicate analysis of Ravenglass mussels (F2,F65 and F66) and Sellafield winkles (F10,F67 and F68).

Replicate samples of surface seawater were collected at two sites to determine the reproducibility of the isolation technique for DIC, while determining whether the activity measured at one particular site was representative of the water in the area. Table 2.5 shows the activities measured at two sites, one of which is in St. Georges Channel, and the other in the North Channel. The activities measured in the water column are in fairly good agreement with one another indicating that the techniques being used produce reliable data.

SAMPLE No.	DATE ANALYSED	pM±1σ	Bq kg^{-1}C±1σ
F75	12/2/90	118.6±1.0	268.0±2.2
F76	2/4/90	119.1±0.4	269.1±0.8
F137	28/11/90	121.5±0.4	274.5±1.4
Overall Mean±standard error		**119.7±0.9**	**270.5±2.0**
F87	21/5/90	118.7±0.5	268.4±1.0
F136	23/11/90	120.4±0.8	272.0±1.7
Overall Mean±standard error		**119.6±0.8**	**270.2±1.8**

Table 2.5: Replicate analysis of water sampling stations C7 (F75,F76 and F137) and C18 (F87 and F136).

The reliability of the data produced does not only depend on the chemical treatment of the samples, but also on counter stability, accurate quench correction, the length of the counting period to incorporate background fluctuations, in addition to the treatment of the raw data. To investigate the effects of variable counting periods and different data handling techniques, one batch of samples was subjected to changes in the procedures normally followed. Three counting periods were chosen - 1000, 2000 and 4000 minutes and the raw data were treated in one of two ways - either all the data were used to determine a mean of the total counts obtained, or the data were treated in batches of 500 minutes counting time and the results used to calculate a weighted mean which was taken

as the final activity.

Table 2.6 details the results obtained for the batch of samples F141, F142, F143, F144 and F146 which contained both depleted and enriched samples relative to the modern reference standard. All activities are reported in pM ± 1σ with the upper values calculated from the complete data set (*) and the lower values representing the weighted mean for the 500 minute batches.

SAMPLE	1000 MINS.	2000 MINS.	4000 MINS.
	(all results quoted as pM±1σ)		
F141	36.9±0.7*	36.7±0.7*	36.5±0.6*
	37.1±1.2	36.8±0.4	36.5±0.3
F142	32.2±0.5*	32.6±0.5*	32.4±0.6*
	32.3±0.4	32.7±0.3	32.4±0.3
F143	33.3±0.8*	32.8±0.6*	33.0±0.8*
	33.3±0.6	32.7±0.4	32.9±0.3
F144	117.2±0.8*	118.0±0.9*	118.1±2.5*
	117.1±0.6	117.9±0.5	118.1±0.3
F146	49.3±1.4*	50.0±1.0*	50.3±3.2*
	49.4±1.0	49.9±0.5	50.2±0.6

Table 2.6: Investigation of the effects of counting time and data handling technique on the final activities.

The results in Table 2.6 show that all three counting periods give activities which are very similar and that for samples which are enriched in ^{14}C, very little is gained by counting for longer periods when the data is being considered as one large data set. However, when the data are accumulated and analysed in 500 minute batches, the errors obtained do decrease as the counting period is increased. There is very little difference in the values obtained when calculated as a complete set or as a weighted mean, although the errors

associated with the weighted mean are smaller.

These data show that for the chosen counting periods the results are all within the quoted error of each other - both for the mean and weighted mean results. In addition, there is little, if any, difference between the two data handling methods. Due to convenience, the time period and data handling methods used in this study were a total counting time of 2000 minutes per sample counted in four 500 minute batches and then a weighted mean calculated from the four results (see Section 2.5.6).

2.6.2 Intercalibrations

All the practices described above have determined the in-house ability to produce reliable data, but, to relate this to the results and precision attained at other ^{14}C laboratories the "IAEA ^{14}C Quality Assurance Materials" were also analysed. These IAEA calibration samples consist of a suite of samples which were analysed by 70 laboratories and their results used to determine "consensus" values. The samples available as IAEA ^{14}C Quality Assurance Materials are:-

(1) C-1 Carbonate - Carrara marble milled to 1.6 - 5.0 mm.

(2) C-2 Carbonate - fresh water travertine.

(3) C-3 Cellulose - produced in 1989 from one season's harvest of ~40 year old trees.

(4) C-4 Subfossil Wood - excavated from peat bogs in New Zealand.

(5) C-5 Subfossil Wood - from buried bed forest in Eastern Winsconsin, U.S.A.

(6) C-6 Sucrose - ANU sucrose.

For this study, all six samples were analysed, although, only the sucrose and the cellulose have activities close to those being analysed in this project. The results obtained, in conjunction with the "consensus" values, are detailed in Table 2.7.

SAMPLE No.	REPLICATE 1	REPLICATE 2	CONSENSUS VALUE*
	(all results quoted as pM±1σ)		
C1	0.32±0.16	0.32±0.18	0.00±0.02
C2	40.82±0.61	40.69±0.86	41.14±0.03
C3	129.94±1.31	129.66±1.06	129.41±0.06
C4	0.11±0.17	-0.26±0.17	0.20-0.44
C5	23.54±0.38	23.51±0.26	23.05±0.02
C6	150.69±1.29	150.74±1.44	150.61±0.11

Table 2.7: IAEA ^{14}C quality assurance materials (* data from IAEA (1991b)).

Overall, the measured activities agree well with those of the "consensus" values confirming that the techniques, both analytical and statistical, employed during this study are of an acceptable standard.

2.6.3 Conclusion

Overall, the in-house and intercomparison results indicate that the results produced throughout the period of this research are reliable and representative of the ^{14}C activities present in the environmental samples analysed.

2.7 GAMMA-RAY SPECTROMETRY

During this study samples of Nori (*Porphyra umbilicalis*) collected at Seascale were analysed by gamma-ray spectrometry for the anthropogenic radionuclides ^{137}Cs and ^{241}Am. This was carried out to determine whether these samples reflected the annual discharges from Sellafield in the period 1967 - 1988 hence assisting in the attempts to reconstruct the discharge record for ^{14}C over this time period.

The theory of γ-ray spectrometry has been detailed elsewhere (Debertin and Helmer, 1988; Knoll, 1989; MacKenzie, 1991), hence, this section will be restricted to discussing the

system installed at S.U.R.R.C. and employed during this work.

A 25% (w.r.t. a 3" x 3" NaI crystal), n-type high purity germanium (HpGe) detector with a carbon-epoxy thin window is used. This has a resolution of better than 2 keV at the ^{60}Co peak at 1332 keV. Events produced in the detector are amplified and stored using a Canberra Series 85 MCA and analysed with SpectranAT software run on an IBM PC-AT. The geometry size is kept constant by using petri dishes which hold on average 25 g of dried, ground sample. The counting time for all samples is 80000 seconds.

Prior to sample counting, both energy and efficiency calibrations are carried out on the detector. These calibrations are carried out by homogenising a known weight of mixed gamma standard (NPL Sample No. E1533) with a comparable matrix (*ie.* seaweed) and counting in the standard 25 g geometry. The channel numbers at which the peaks occur and the relative sizes of these peaks can then be assigned to the known energy and activity of each of the nuclides present in the standard. To ensure the reliability of these calibrations, a standard of marine algae issued by the IAEA (Sample No. IAEA AG-B-1) can be counted. This sample has known activities of ^{40}K, ^{137}Cs and ^{60}Co hence enabling a simple check on detector calibrations.

2.8 ISOLATION AND ANALYSIS OF ^{137}Cs FROM THE WATER COLUMN

To determine whether ^{14}C behaved conservatively in the water column, a known conservative radionuclide, ^{137}Cs, was also isolated and analysed during cruise CH62B/89 from the ^{14}C sampling sites within the Irish Sea. For such analysis, 50 l of seawater were collected and filtered through 0.45 μm membrane filter. The filtered water was then acidified and pumped through a column of either KCFC (potassium cobaltihexacyanoferrate) or ASG (ammonium-duo-deca-molybdophosphate) depending on how close the sampling station was to Sellafield. KCFC is specific for radiocaesium and was used at the sites closest to Sellafield to ensure no interference from ^{95}Zr and ^{95}Nb which are also retained by ASG resin. Once the sample had been pumped through the resin, the cartridges were dried and placed in a well-type NaI scintillation detector which had been calibrated for the geometry size used. Calibration of such detectors is carried out be passing a known activity of ^{137}Cs, incorporated into an "artificial" seawater matrix, through a column of resin of the required geometry. Both resins give quantitative removal

of the ^{137}Cs which allows the counting efficiency of the detector to be determined. During this study all the ^{137}Cs samples collected from the Irish Sea were processed on board ship, but counted at the MAFF laboratory in Lowestoft.

CHAPTER 3

^{14}C RELEASE TO THE AQUATIC ENVIRONMENT:

LOCAL OBSERVATIONS

3.1 INTRODUCTION

As discussed in Chapter 1, the sites selected for this study include BNFL's nuclear fuel reprocessing plant at Sellafield, Cumbria and the radiochemical establishments at Cardiff and Amersham, Buckinghamshire, owned by Amersham International plc (Fig 1.11). At each of these sites, the main aim was to establish the extent of ^{14}C dispersal from the point of release and to determine its distribution within the numerous carbon containing reservoirs of the aquatic environment. Such distribution studies also permit the calculation of the radiological significance of these releases to the local population and published global carbon cycle models can be used to interpret these data on a global scale. These can be used to investigate whether liquid discharges of ^{14}C from nuclear and radiochemical installations significantly alter the ^{14}C specific activities of the global carbon reservoirs.
In order to determine the chemical behaviour and fate of this anthropogenic ^{14}C, an extensive suite of samples was collected from the vicinity of each of the release points and the ^{14}C specific activities measured. In addition to these distribution studies of present ^{14}C discharges, archived intertidal biota samples have the potential for use in reconstructing past discharges of ^{14}C from Sellafield. Prior to 1985, discharges were not measured, merely estimated. Finally, the Irish Sea and Scottish coastal waters have been extensively studied using Sellafield-derived ^{137}Cs as a tracer (McKinley *et al.*, 1981; Jeffries *et al.*, 1982; Prandle, 1984; McKay and Baxter, 1985; Hallstadius *et al.*, 1987; Bradley *et al.*, 1987; Bradley *et al.*, 1991). However, as ^{137}Cs discharges from Sellafield have been greatly reduced with the introduction of the SIXEP plant, the future of these models is limited, therefore similarities in ^{14}C and ^{137}Cs distributions may allow the continued use and further development of such models based on ^{14}C measurements.
For the two coastal sites of Sellafield and Amersham International plc, Cardiff, samples were taken from both the intertidal environment and the water column, whereas at

Amersham, Buckinghamshire, sampling was restricted to the water column only.
Prior to analysis of samples from the study areas, the current ambient specific activities in similar sample types were determined. For this study, samples of mussels, winkles and seaweed were collected from sites in northwest Scotland where it is known that no local anthropogenic inputs occur. The results obtained are detailed in Table 3.1 and are used to calculate an overall mean value of 115.4±0.4 pM (260.8±0.8 Bq kg^{-1} C). This value will be used as a best estimate of the current ambient ^{14}C specific activity for the study period in subsequent discussions.

LOCATION	SAMPLE TYPE	pM±1σ	Bq kg^{-1} C±1σ
Loch Laxford	Mussels -flesh	114.4±0.3	258.6±0.7
	Mussels -shell	115.2±0.3	260.2±0.6
Tarbert	Winkles -flesh	116.1±0.3	262.4±0.6
	Winkles -shell	114.9±0.5	259.8±1.1
Aldmuir*	Seaweed	116.4±0.4	263.1±1.0
Overall Mean		**115.4±0.4**	**260.8±0.8**

Table 3.1: ^{14}C specific activities measured in samples from Northwest Scotland.
(* from Table 2.3)

In the following sections, the results obtained at each of the three locations will be detailed and discussed individually. These results will then be considered collectively in the determination of carbon behaviour in both coastal and freshwater systems.

3.2 SELLAFIELD AND THE IRISH SEA AREA

This was the most extensively studied area during the research period. The study area stretched from St. Georges Channel in the south, to the Clyde Sea area in the north, with most sampling carried out in the area to the east of the Isle of Man.
The study area and positions of the sampling sites are shown in Figure 3.1. In the

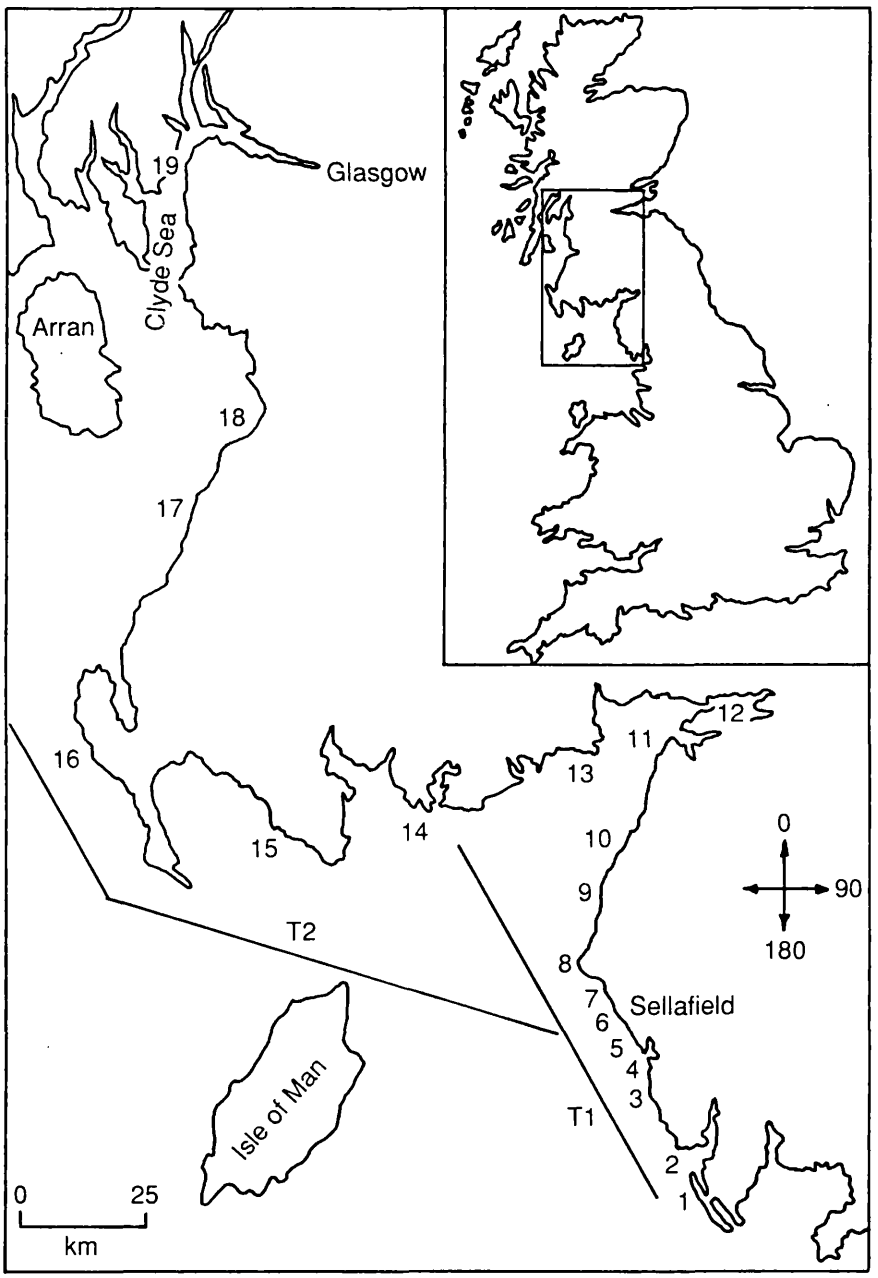

Figure 3.1: The Sellafield study area and sampling sites.

following sections, information from the intertidal biota studies will assist in the interpretation of the activities found in the water column and other carbon pools under consideration. All the results will then be considered collectively to present an overall view of the distribution of Sellafield-derived ^{14}C.

3.2.1 Intertidal Biota

Intertidal samples of mussels (*Mytilus edulis*), winkles (*Littorina littorea*) and seaweed (*Fucus* spp.) were collected from a number of sites both to the north and south of Sellafield (Fig 3.1) to determine the dispersion and help identify the chemical form of Sellafield-derived ^{14}C. The biota, because of differences in their feeding behaviour, will indirectly help to provide information on the form of the discharge, in addition to the chemical form and extent of ^{14}C transport in the area.

3.2.1.1 Spatial survey

These samples were collected during November 1988 - February 1989 at 19 sites from Earnse Point, 40 km south of Sellafield, northwards into the Clyde Sea area (Fig 3.1). The sample types were selected because of differences in their feeding behaviour. Mussels are sedentary organisms which filter particulate material out of seawater (Hawkins, 1983) and hence they should reflect the ^{14}C specific activity of particulate carbon present in the water column. Winkles are herbivorous and selectively graze on large seaweeds and algae-covered rocks (Newell, 1979; Watson and Norton, 1985). The material ingested can include both organic and inorganic material deposited from the surrounding water as well as algae growing on the rocks, therefore, the specific activity found in winkles should reflect that found in both the inorganic and organic pools. Seaweeds obtain their carbon supply from the dissolved inorganic carbon in the water column, although, during periods of low water, atmospheric CO_2 may be utilised. The ^{14}C specific activity found in seaweeds would be expected to be similar to that found in the DIC from the water column. The results obtained at all 19 sites for the three biota types are shown in Table 3.2. Distances from Sellafield are also shown for those sampling sites on the south-north coastal transect. These distances are taken as direct measurements along the coast from Sellafield and do not take into consideration the direction of the water currents in the area. Obviously, the direction of the currents will influence the distribution of Sellafield-derived ^{14}C and this will be taken into account in the discussion of the observations.

SITE	LOCATION	DISTANCE (km)	MUSSELS	WINKLES	SEAWEED
			(all results quoted as pM±1σ)		
1	Earnse Point	37.8(S)	266.0±0.9	221.8±0.8	156.2±0.7
2	Haverigg	30.3(S)	-	-	157.8±0.7
3	Annaside	19.8(S)	-	-	191.7±0.8
4	Ravenglass	10.8(S)	682.7±0.6	-	334.7±1.5
5	Drigg	6.5(S)	756.1±2.2	613.4±2.0	-
6	Sellafield	0	787.2±3.1	435.3±1.8	414.8±1.5
7	Nethertown	5.0(N)	625.1±1.9	437.3±2.1	233.4±1.5
8	St. Bees	10.2(N)	-	-	207.8±0.7
9	Workington	30.0(N)	-	200.6±1.0	151.9±1.0
10	Maryport	38.5(N)	-	-	146.5±0.9
11	Silloth	52.0(N)	-	-	144.0±0.5
12	Bowness-on-Solway	58.0(N)	-	-	124.6±0.6
13	Rockcliffe	77.0(N)	198.7±0.8	146.4±0.6	131.8±0.5
14	Auchenlarie	-	177.5±0.7	155.8±0.6	137.7±0.8
15	Port William	-	-	-	139.3±0.6
16	Port Patrick	-	-	-	124.7±0.5
17	Girvan	-	120.6±0.4	124.2±0.6	121.6±0.4
18	Ayr	-	123.5±0.5	-	125.6±0.5
19	Inverkip	-	124.8±0.6	124.0±0.5	120.8±0.5

Table 3.2: ^{14}C specific activities measured in the intertidal biota samples collected from Earnse Point to the Clyde Sea Area.

All the biota samples analysed from this area have ^{14}C activities above the baseline value of 115.4±0.4 pM. Figure 3.2 shows the ^{14}C concentrations found in the three sample types collected at the sites closest to Sellafield (sites 1-13). The most obvious point is that the activity of ^{14}C present in the organic material is dependent on the type of organism analysed and the distance from the discharge location.

At each site, mussels consistently have the highest observed ^{14}C activities and seaweeds the lowest. McDonald *et al.*, (1991) have observed a similar trend in the concentrations

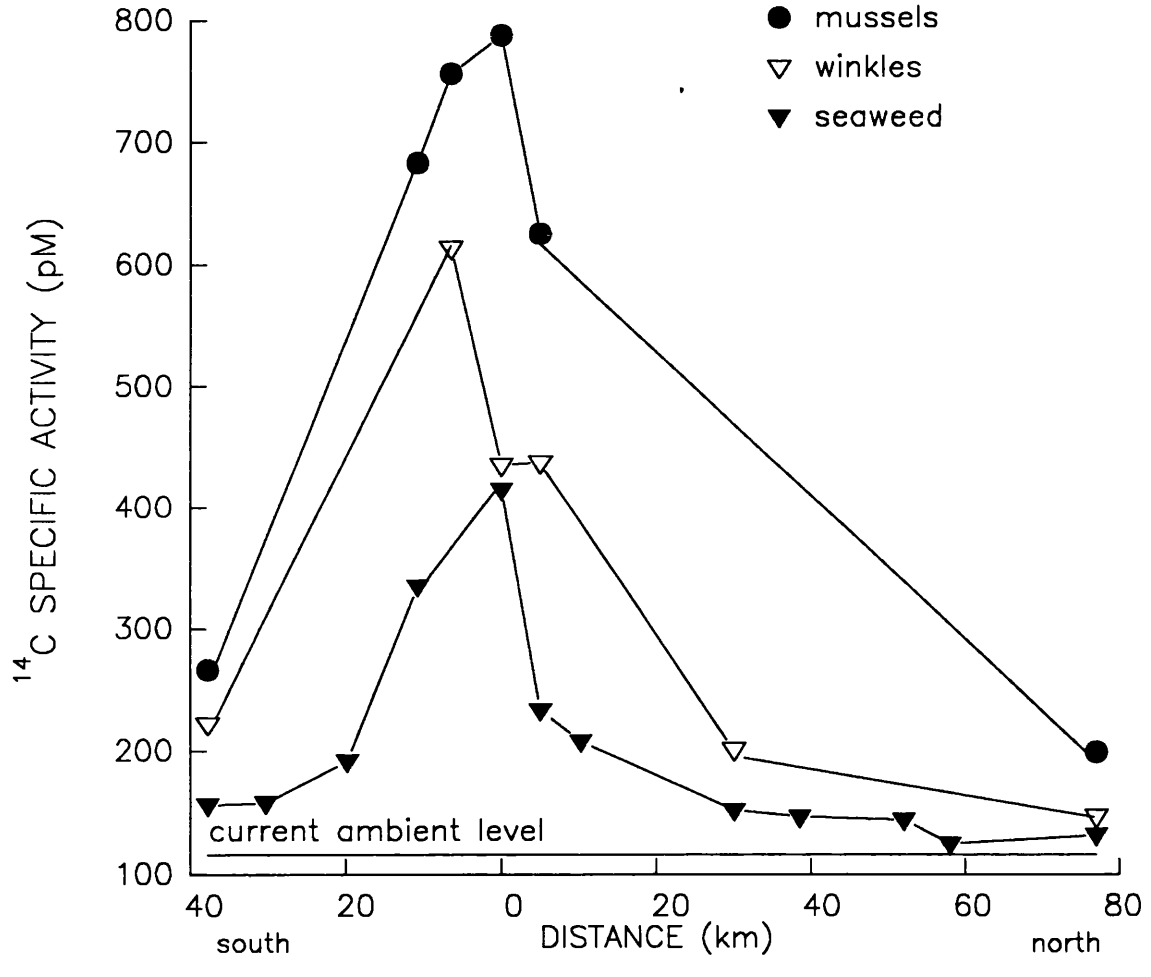

Figure 3.2: The ^{14}C activity measured in intertidal biota from the Sellafield area.

of ^{210}Pb and ^{210}Po in intertidal organisms collected at Ravenglass and Whitehaven which they have attributed to differences in feeding mechanisms. This trend decreases somewhat with distance from the point of release with all three sample types reaching a common activity of 120 - 125 pM at sampling sites within the Clyde Sea area (sites 17 - 19). A value which is still above the baseline level. This common activity is not observed at sampling stations to the south where organism selectivity is still apparent. However, as the predominant surface water currents flow southwards (Dickson and Boelens, 1988), extrapolation of the results in Figure 3.2 would indicate that a common activity would be reached if the sampling transect was extended to 50 - 60 km south from Sellafield.

The highest observed ^{14}C activities for mussels (787.2 pM) and seaweed (414.8 pM) were found at Sellafield while that for winkles (613.4 pM) was found 6.5 km to the south at Drigg. These values correspond to activities of approximately 7, 3.5 and 5 times the estimated baseline value of 115.4 pM and indicate some degree of organism selectivity occurring in the uptake of anthropogenic ^{14}C due to differences in feeding behaviour, this may have implications for local radiological calculations. In addition to the analysis of organic flesh from mussels and winkles, a limited number of analyses were carried out on the inorganic shell material of organisms collected in the vicinity of Sellafield. The results obtained from these analyses are shown in Table 3.3, in conjunction with the ^{14}C specific activities found in the corresponding organic material.

LOCATION	SITE No.	SAMPLE TYPE	INORGANIC SHELL	ORGANIC FLESH
Sellafield	6	Mussels	534.3±1.5	787.2±3.1
		Winkles	488.5±1.1	435.3±1.8
Drigg	5	Mussels	539.5±1.4	756.1±2.2
		Winkles	487.2±1.8	613.4±2.0
Ravenglass	4	Mussels	426.0±2.2	682.7±0.6

Table 3.3: ^{14}C activities measured in the inorganic and organic fractions of biota collected in the vicinity of Sellafield.

The results demonstrate that ^{14}C activities greater than the baseline value are also to be found in the shell material. However, these activities were less than those in the corresponding organic material (except for winkles collected at Sellafield). The lower activity in the inorganic material may reflect the fact that the shell carbon is accumulated throughout the entire lifespan of the organism, whereas the organic tissue is subject to turnover at a rate which is organism-specific. Also, the shell material of molluscs has been shown to be a combination of both metabolic organic carbon and inorganic carbon from the water column (Tanaka *et al.*, 1986) and this may help explain the observed differences. These results indicate that the likely form of the discharges of ^{14}C from Sellafield are as dissolved inorganic carbon (DIC) as the seaweeds are enriched. However, the results for the mussels point to considerable activity in the particulate phase (possibly both the inorganic and organic). This particulate enrichment must be greater than that of the DIC since mussel activities are enriched relative to the DIC. This is supported by the ^{14}C activities in the shell material being lower than that in the organic material. Winkles have intermediate activities as they are feeding on the same particulates as the mussels but they are also grazing on algae and seaweeds. This, therefore, suggests that the discharges could be in both the dissolved inorganic and the particulate (inorganic/organic) phases.

The annual ^{14}C discharges from Sellafield, since 1952 when operations commenced, to 1985, when actual discharges were monitored, are thought to have been relatively constant (Baxter, pers comm., 1988). Therefore, differences in the lifespans of the three biota types are unlikely to be major contributory factors in bringing about the observed activity trends. These results may be explained by postulating that the activity of ^{14}C in the particulate phase of the water column should be higher than that of the DIC. To determine whether this is the case, the water column and its carbon pools must be examined in greater detail.

As already stated, Sellafield-derived ^{14}C can be measured in molluscs and seaweed as far north as the Clyde Sea area although the inter-organism variation at these sites is negligible. The highest levels are found in the immediate vicinity of Sellafield (Fig 3.2) with enrichment occurring to the north and south of the discharge point. For mussels and seaweed, the ^{14}C activities sharply decrease immediately to the north of Sellafield - much more obviously than to the south - indicating that the transport of ^{14}C in the water column reflects the predominant residual currents in the area (Fig 3.3). In the case of winkles,

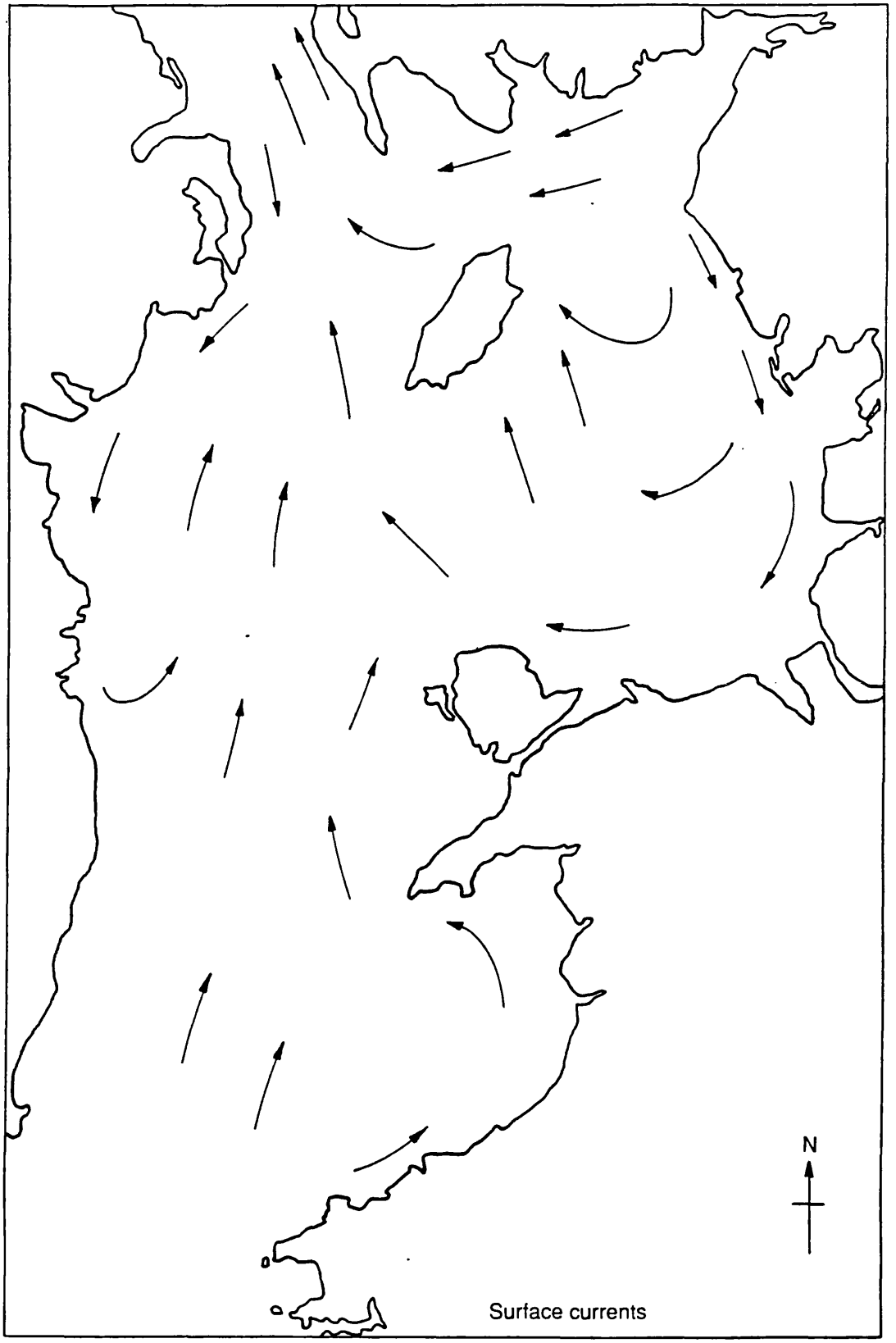

Figure 3.3: The predominant residual surface currents in the Irish Sea.

a similar sharp decline in the ^{14}C specific activity is observed to the north of Sellafield although the maximum activity is observed to the south. Additional sampling locations would need to be considered to determine the rate of this decline to the south and whether the winkles exhibit a similar ^{14}C distribution as mussels and seaweed.

In an attempt to empirically model the distribution found in the biota, distance and direction from the discharge location were considered. For the mussels and winkles, nearly all of the observed variation could be explained in terms of distance alone by the equations

$$\ln {}^{14}C_{mussels} = 6.80 - 0.0190 \text{ distance} + 0.000043 \text{ distance}^2 \quad (R^2\text{-adj} = 99.6\%) \qquad (3.1)$$

$$\ln {}^{14}C_{winkles} = 6.28 - 0.0161 \text{ distance} + 0.000040 \text{ distance}^2 \quad (R^2\text{-adj} = 89.7\%) \qquad (3.2)$$

respectively. However, for the seaweed, the concentrations were best explained when both distance and direction were taken into account *ie.*

$$\ln {}^{14}C_{seaweed} = 6.34 - 0.289 \ln \text{distance} + 0.0834 \cos \text{dir} \quad (R^2\text{-adj} = 88.7\%) \qquad (3.3)$$

Obviously, these are only crude representations of the data, but they do give some indication of how the observed distribution of ^{14}C specific activity in intertidal biota is related to simple parameters such as the distance and direction from Sellafield.

3.2.1.2 Annual Nori and the temporal distribution of ^{14}C

In addition to determining the spatial distribution of Sellafield-derived ^{14}C, the temporal distribution was also of interest. Discharges of ^{14}C from Sellafield have only been reported since 1985 with any prior data being estimated. In an attempt to determine past discharges to the Irish Sea, archival samples of Nori (*Porphyra umbilicalis*) collected at Seascale were obtained from MAFF for analysis.

The samples selected for this temporal study had all been collected between March and June of each year (back to 1967) to minimise any seasonal effects. Prior to ^{14}C analysis, each sample was counted on a high-resolution reverse electrode germanium (HpGe) γ-ray detector to determine the activity of radionuclides such as ^{137}Cs and ^{241}Am to ascertain whether the samples did reflect Sellafield discharges during that time period. ^{137}Cs and ^{241}Am were selected as they are two of the most abundant radionuclides in the discharges from Sellafield and they exhibit two extreme forms of behaviour in the water column.

^{137}Cs is known to be conservative in the water column (Pierson, 1988), whereas ^{241}Am is very particle-reactive and accumulates in areas of active sedimentation (MacKenzie *et al.*, 1987; McDonald *et al.*, 1990). The discharge data available for this time period and the results obtained from the Nori samples are shown in Table 3.4. To ensure that the ^{14}C data for Nori is directly comparable to that for the ^{137}Cs and ^{241}Am, the ^{14}C activity (pM) has been converted to Bq per kg of sample by assuming an average carbon content of 38% (based on a number of carbon analyses). Prior to this calculation, the ^{14}C activity measured in each sample must be corrected for the ambient ^{14}C level present at that time. As there is no direct means of determining these activities, an average value of 110 pM (Nydal *et al.*, 1980; Nydal and Lovseth, 1983, Nydal *et al.*, 1984) with an associated error of 1.0 pM has been used. This may slightly under estimate the ^{14}C activity in the DIC in the late 1960's but this should not significantly influence any trend present in the samples.

YEAR	^{14}C			^{137}Cs		^{241}Am	
	ACTIVITY pM±1σ	EXCESS ^{14}C Bq kg^{-1}±1σ	RELEASE* TBq	ACTIVITY Bq kg^{-1}±1σ	RELEASE TBq	ACTIVITY Bq kg^{-1}±1σ	RELEASE+ TBq
1967	167.7±0.7	49.6±1.1	0.50	34.5±2.4	150	40.6±9.5	17.94
1968	199.8±0.7	77.1±1.1	0.75	131.5±3.0	371	528.1±3.2	22.62
1969	239.5±1.5	111.2±1.6	0.83	175.9±3.3	444	450.1±5.4	16.92
1970	246.2±0.8	117.0±1.2	1.1	609.2±6.1	1154	68.7±2.7	22.66
1971	215.6±0.8	90.7±1.2	1.2	753.9±6.8	1325	407.8±5.3	43.37
1972	171.3±0.7	52.6±1.1	1.4	405.8±4.5	1289	1290.7±5.2	88.23
1973	315.4±0.9	176.4±1.2	0.9	874.3±6.1	768	1269.7±12.7	120.77
1974	164.9±0.6	47.2±1.1	0.79	2355.9±9.4	4061	1661.1±5.0	132.10
1975	204.4±0.8	77.6±1.2	1.1	1310.6±7.9	5231	698.5±23.1	52.49
1976	147.4±0.6	32.1±1.1	1.1	1586.9±7.9	4289	202.9±3.7	29.29
1977	186.4±0.6	65.6±1.1	0.77	2759.2±11.0	4478	502.5±18.6	21.96
1978	198.8±0.8	76.3±1.2	0.83	1715.3±8.6	4088	297.1±4.8	27.54
1979	208.7±0.7	84.8±1.1	1.1	1192.8±8.4	2562	359.9±23.0	29.19
1980	447.0±1.2	289.4±1.4	1.1	1294.8±9.1	2966	289.3±4.6	30.13
1981	300.3±1.0	163.4±1.3	na	650.2±5.9	2357	559.6±52.6	30.65
1982	237.9±0.7	109.9±1.1	na	277.1±5.0	2000	77.3±2.4	27.97
1983	266.4±0.9	134.3±1.2	na	357.8±4.3	1200	98.3±19.6	23.29
1984	na	na	0.7	280.4±3.6	434	98.9±13.1	22.79
1985	240.9±0.8	112.4±1.2	1.3	233.9±3.8	325	96.2±19.3	21.34
1986	233.4±0.9	106.0±1.2	2.6	204.3±2.9	17.9	53.2±2.1	20.04
1987	204.6±0.7	81.2±1.1	2.1	68.9±1.9	11.88	58.1±2.6	18.47
1988	268.4±0.9	136.0±1.2	3.0	42.7±1.6	13.3	62.3±2.1	17.65

Table 3.4: ^{14}C, ^{137}Cs and ^{241}Am activities measured in Nori (*Porphyra umbilicalis*) from Seascale with the appropriate Sellafield discharge records and a calculated ^{14}C activity in Bq per kg dry sample.

na = not available

* prior to 1985, ^{14}C releases were not monitored by BNFL hence values reported are estimated (Baxter, per. comm., 1988)

+ these release rates incorporate the contribution of ^{241}Am due to in-growth from ^{241}Pu

All samples are decay corrected to the year of sample collection.

Both the ^{137}Cs and ^{241}Am activities obtained by γ-ray spectroscopy show excellent agreement with the published discharge data (Figs 3.4 and 3.5), providing correlation

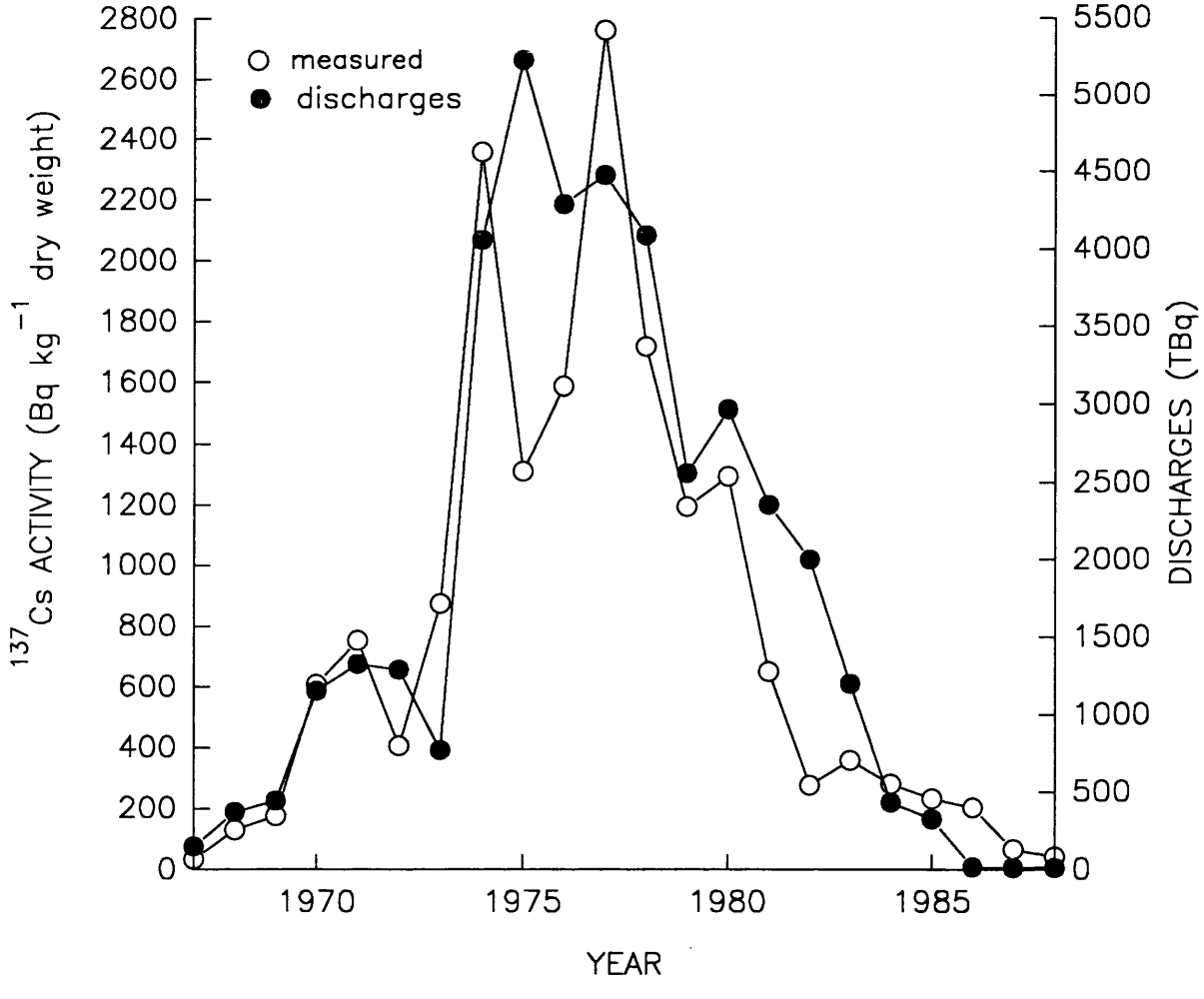

Figure 3.4: Measured ^{137}Cs activity in annually collected samples of Nori and reported annual discharges of ^{137}Cs from Sellafield (1967-1988).

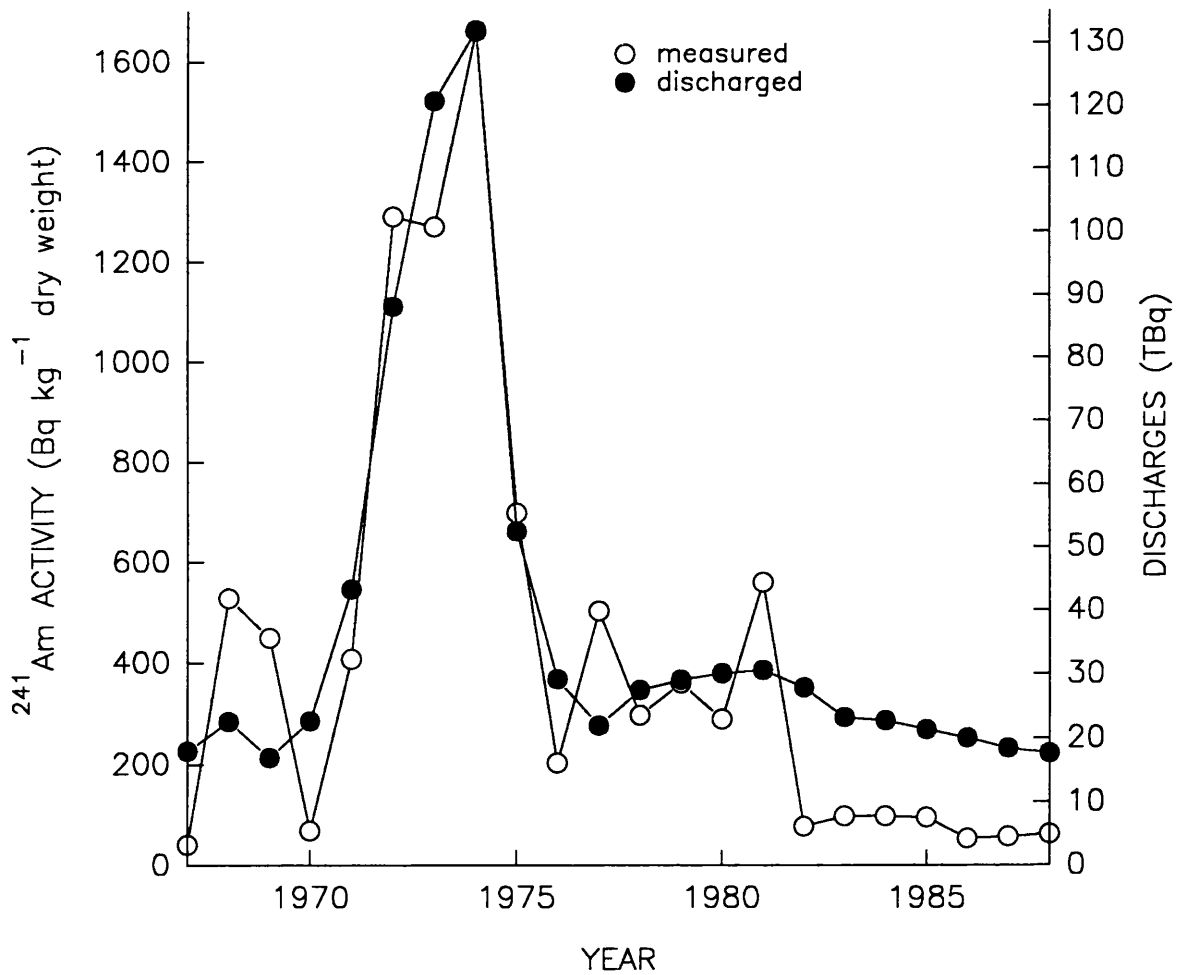

Figure 3.5: Measured ^{241}Am activity in annually collected samples of Nori and reported annual discharges of ^{241}Am from Sellafield (1967-1988).

coefficients (r) of 0.877 and 0.925, respectively. These significant correlations indicate that Nori samples do reflect the levels of discharge in any given year for these particular nuclides. However, the relationship observed between ^{14}C activities measured in the Nori and the estimated discharges (Fig 3.6) for the same time period appear not to be correlated (r=0.153), which indicates either that these samples cannot be used as a means of measuring past inputs of ^{14}C or that the estimated discharge data available are inaccurate. The plot of observed ^{14}C specific activities *vs.* estimated discharges does however show some similarities, pointing to the correlation coefficient not being the best measure of the relationship present. This relationship may be more complex *ie.* the observed values may reflect several years discharges rather than those just attributable to the year of sampling *ie.*

$$level_i = a + b\ level_{i-1} + c\ level_{i-2} \qquad (3.4)$$

where i = year and a, b and c are constants.

The samples selected were all collected between March and June in each year to reduce any seasonality effects, however, no information is available on the regularity and timing of ^{14}C discharges from Sellafield. As carbon is much more "biologically" involved than either caesium or americium, the seasonality of discharges may play an important role and could account at least in part for the poor correlation. If samples had been available back to 1945-1950 it would have been possible to determine the initial activity and the subsequent accumulation of ^{14}C in Nori due to the releases from Sellafield. This would allow the determination of the relationship present between the ^{14}C specific activity observed in Nori and the ^{14}C discharges from Sellafield and, hence, permit calculation of the parameters associated with an equation of the type shown as Equation 3.4. One apparent feature is that while the discharges of ^{137}Cs and ^{241}Am have decreased considerably, those for ^{14}C have increased three-fold since the start of monitoring in 1985. Analytically, ^{137}Cs and ^{241}Am discharges are relatively easily quantified whereas those for ^{14}C are not. The excellent correlation of the measured ^{137}Cs and ^{241}Am with their discharge records may in part be due to the very characteristic discharge patterns (*ie.* a large peak in the early 1970's with a subsequent rapid decrease). The estimated discharges for ^{14}C are more uniform, hence good correlations may be relatively more difficult to obtain.

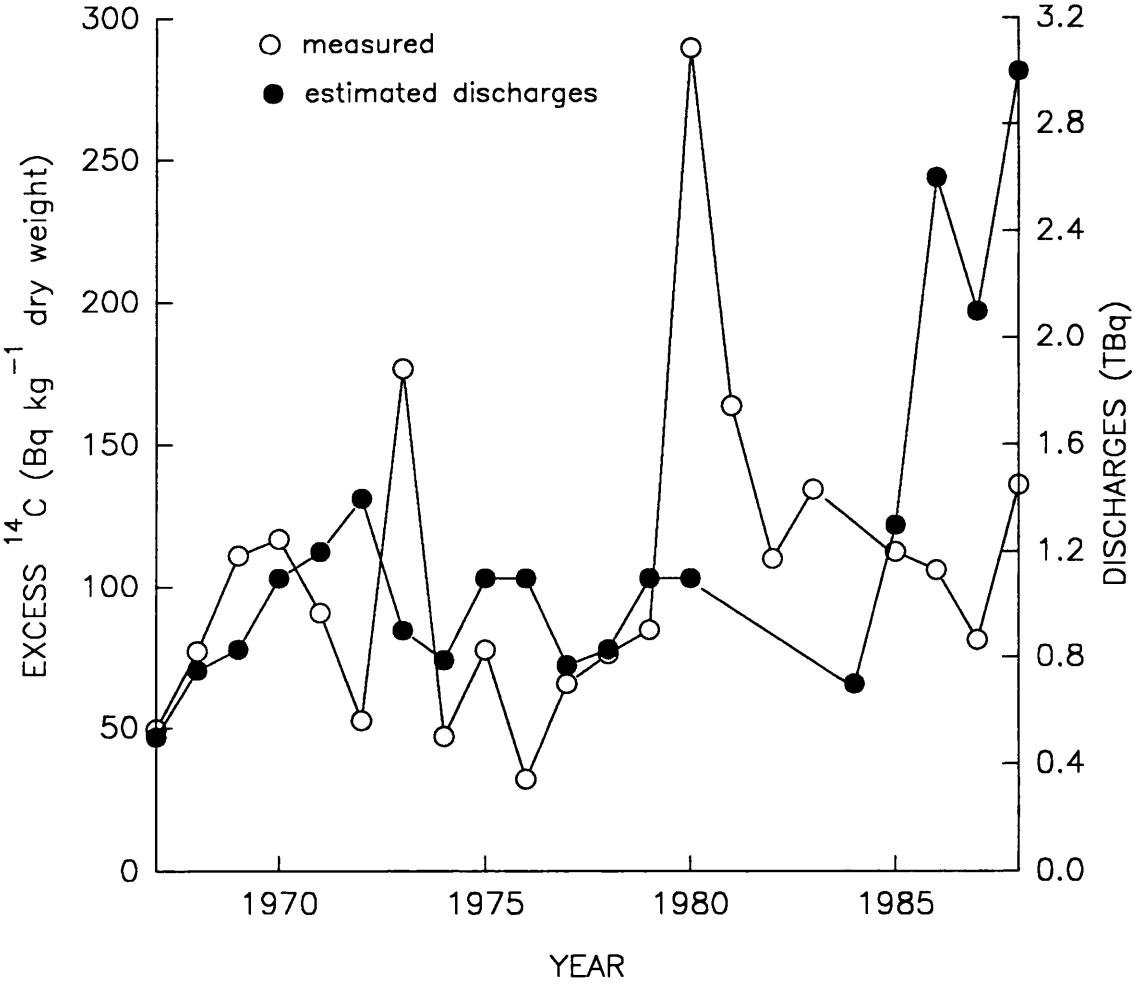

Figure 3.6: Measured ^{14}C activity in annually collected samples of Nori and reported annual estimated discharges of ^{14}C from Sellafield (1967-1988).

However, if the seasonal and cumulative effects discussed previously were not present, it would be reasonable to assume that ^{14}C activities should reflect the discharges. Therefore, if such a simple relationship is postulated, discharges which would explain the ^{14}C activities observed in Nori can be calculated. To do this, the results for ^{137}Cs and ^{241}Am in Nori were normalised to activity per unit discharge in an attempt to determine any similarities between these and the observed ^{14}C activities (Table 3.5).

YEAR	Normalised ^{14}C ($^{14}C^*$)	Normalised ^{137}Cs ($^{137}Cs^*$)	Normalised ^{241}Am ($^{241}Am^*$)	$^{14}C^*/^{137}Cs^*$	$^{14}C^*/^{241}Am^*$
1967	99.2	0.23	2.26	431.30	43.89
1968	102.8	0.35	23.35	293.71	4.40
1969	134.0	0.40	26.60	335.0	5.04
1970	106.4	0.53	3.03	200.75	35.12
1971	75.6	0.57	9.40	132.63	8.04
1972	37.6	0.31	14.63	121.29	2.57
1973	196.0	1.14	10.51	171.93	18.65
1974	59.8	0.58	12.57	103.10	4.76
1975	70.6	0.25	13.31	282.40	5.30
1976	29.2	0.37	6.93	78.92	4.21
1977	93.7	0.62	22.88	151.13	4.10
1978	91.9	0.42	10.79	218.81	8.52
1979	77.1	0.47	12.33	164.04	6.25
1980	263.1	0.44	9.60	597.95	27.41
1981	na	0.28	18.26	na	na
1982	na	0.14	2.78	na	na
1983	na	0.30	4.22	na	na
1984	na	0.65	4.34	na	na
1985	86.5	0.72	4.51	120.14	19.18
1986	40.8	11.41	2.65	3.58	15.40
1987	38.7	5.80	3.15	6.67	12.29
1988	45.3	3.21	3.53	14.11	12.83

Table 3.5 : Observed radionuclide activities in Nori normalised to unit discharge and $^{14}C^*$ related to $^{137}Cs^*$ and $^{241}Am^*$ (na=not available).

These results indicate that, overall, the ^{137}Cs activity normalised to the discharge in that year in Nori is within a relatively narrow range (0.23 - 1.14 in 1967-1985) compared to the normalised ^{241}Am activity (2.26 - 26.60). Figures 3.7 and 3.8 illustrate the normalised values for ^{137}Cs and ^{241}Am, respectively.

Within the ^{137}Cs data there are a few exceptions to the range quoted, notably, those for 1986 - 1988. In 1986 ^{134}Cs was also measurable; a ratio of approximately 0.4 was obtained for $^{134}Cs/^{137}Cs$. Sellafield discharges in this year had a $^{134}Cs/^{137}Cs$ ratio of 0.07 indicating that this was not the only source of caesium in the Irish Sea at that time. The releases of caesium from the incident at Chernobyl had a ratio of approximately 0.55 at the time of release which was only two weeks before the Nori sample was collected. This indicates that the high normalised value observed in 1986 is due to the incorporation of Chernobyl-derived caesium. However, ^{134}Cs was not measurable in the following two years suggesting that the high normalised values observed may be a reflection of the flushing time of the Irish Sea basin. Hence, the activities are due to carry-over from previous years discharges and are more noticeable because of the marked decrease in ^{137}Cs discharges due to the SIXEP plant coming into operation. Alternatively, they indicate desorption of ^{137}Cs from the relatively highly contaminated sediment (Hunt and Kershaw, 1990). The higher values and wider range found for the ^{241}Am may be a reflection of its' particle reactivity whereby Nori will be exposed for longer time periods to a larger source as a result of accumulation in, and resuspension from, the sediments of the "mud patch". ^{137}Cs released from Sellafield will be readily transported away from the area by water movement whereas ^{241}Am will become incorporated into the sediments and particulates within the water column.

There appears to be no relationship between the measured ^{14}C activities normalised to estimated discharges and these normalised values for ^{137}Cs or ^{241}Am, hence neither ^{137}Cs nor ^{241}Am can confirm the estimated discharges of ^{14}C from Sellafield. An estimate of ^{14}C discharges can however be obtained if the discharges published for 1985 - 1988 are assumed to be accurate. Normalising the observed excess ^{14}C activity (in Bq kg^{-1} dry weight) to unit discharge provides values of 86, 41, 39 and 45 for each of the four years. Given the good agreement between the last three, an average value of 42 Bq kg^{-1} per TBq released can be used to reconstruct the past discharges from the activities observed in the Nori. Table 3.6 summarises the observed data, the estimated and calculated releases and

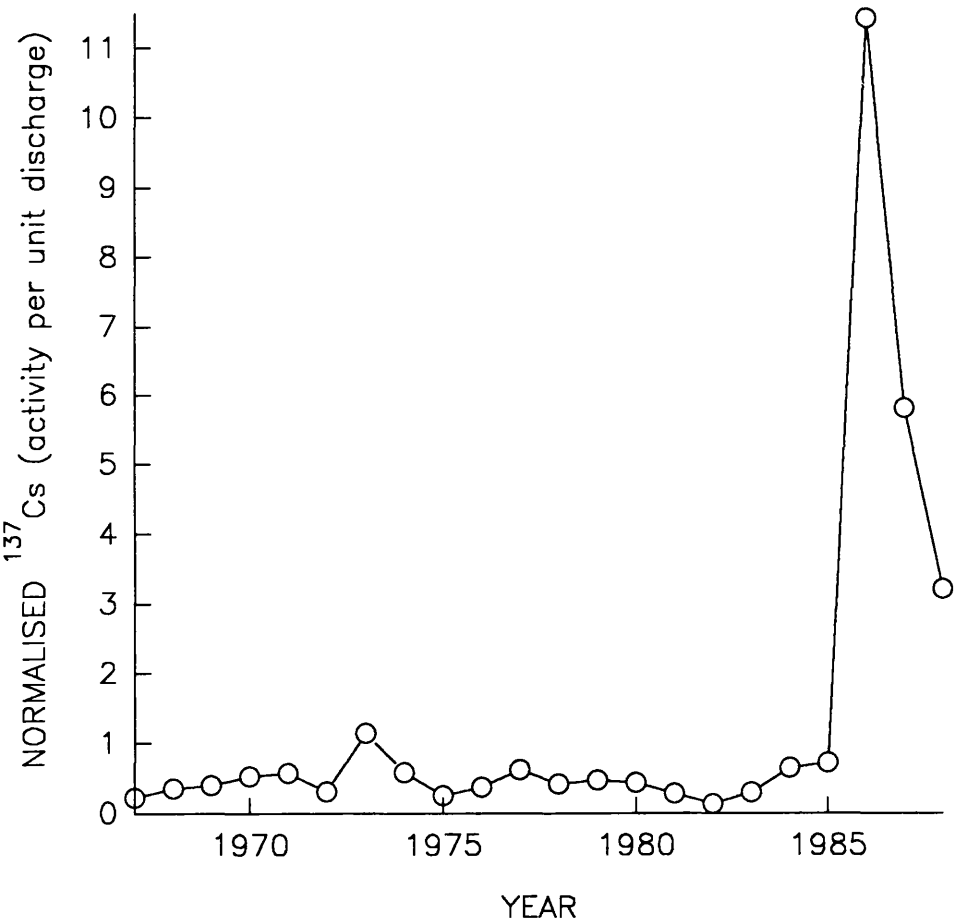

Figure 3.7: Normalised ^{137}Cs activities (*ie.* activity per unit discharge) in Nori (1967-1988).

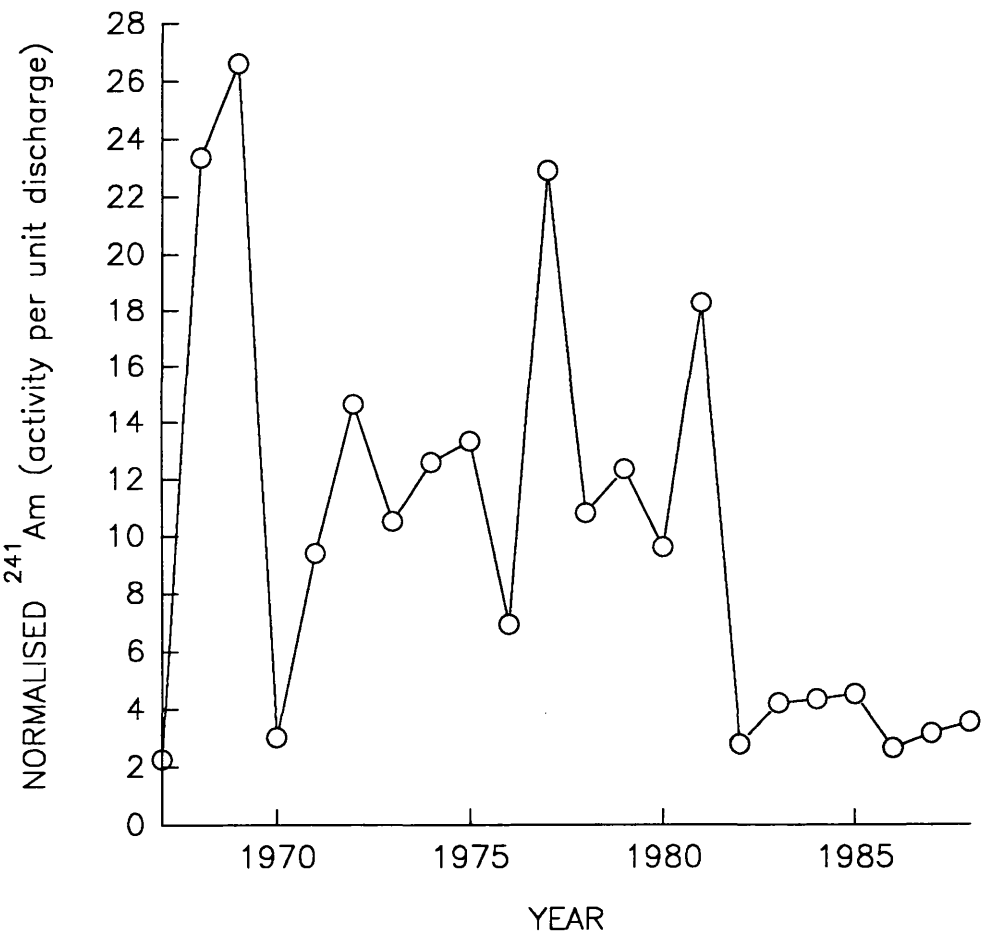

Figure 3.8: Normalised ^{241}Am activities (*ie.* activity per unit discharge) in Nori (1967-1988).

also the % of the total ^{14}C discharges from Sellafield which are released into the water column. Figure 3.9 illustrates the differences between the estimated ^{14}C discharge data and those values calculated from the results obtained during this study.

YEAR	^{14}C OBSERVED (pM)	EXCESS ^{14}C (Bq kg^{-1})	^{14}C RELEASES (TBq) ESTIMATED*	CALCULATED**	% TOTAL DISCHARGES+
1967	167.7	49.6	0.5	1.2	19
1968	199.8	77.1	0.75	1.9	21
1969	239.5	111.2	0.83	2.7	27
1970	246.2	117.0	1.1	2.8	17
1971	215.6	90.7	1.2	2.2	18
1972	171.3	52.6	1.4	1.3	10
1973	315.4	176.4	0.9	4.2	23
1974	164.9	47.2	0.79	1.1	20
1975	204.4	77.6	1.1	1.9	16
1976	147.7	32.1	1.1	0.8	7
1977	186.4	65.6	0.77	1.6	18
1978	198.8	76.3	0.83	1.8	18
1979	208.7	84.8	1.1	2.0	17
1980	447.0	289.4	1.1	7.0	47
1981	300.3	163.4	na	3.9	na
1982	237.9	109.9	na	2.6	na
1983	266.4	134.3	na	3.2	na
1984	na	na	0.7	na	na
1985	240.9	112.4	1.3	2.7	28
1986	233.4	106.0	2.6	2.6	33
1987	204.6	81.2	2.1	2.0	17
1988	268.4	136.0	3.0	3.3	52

Table 3.6 : Estimated and calculated discharge record of Sellafield ^{14}C from Nori samples.

na=not available

* BNFL estimated discharges

** calculated discharges from the results of this study

+ based on calculated discharges and estimated atmospheric releases (Baxter, pers. comm., 1988).

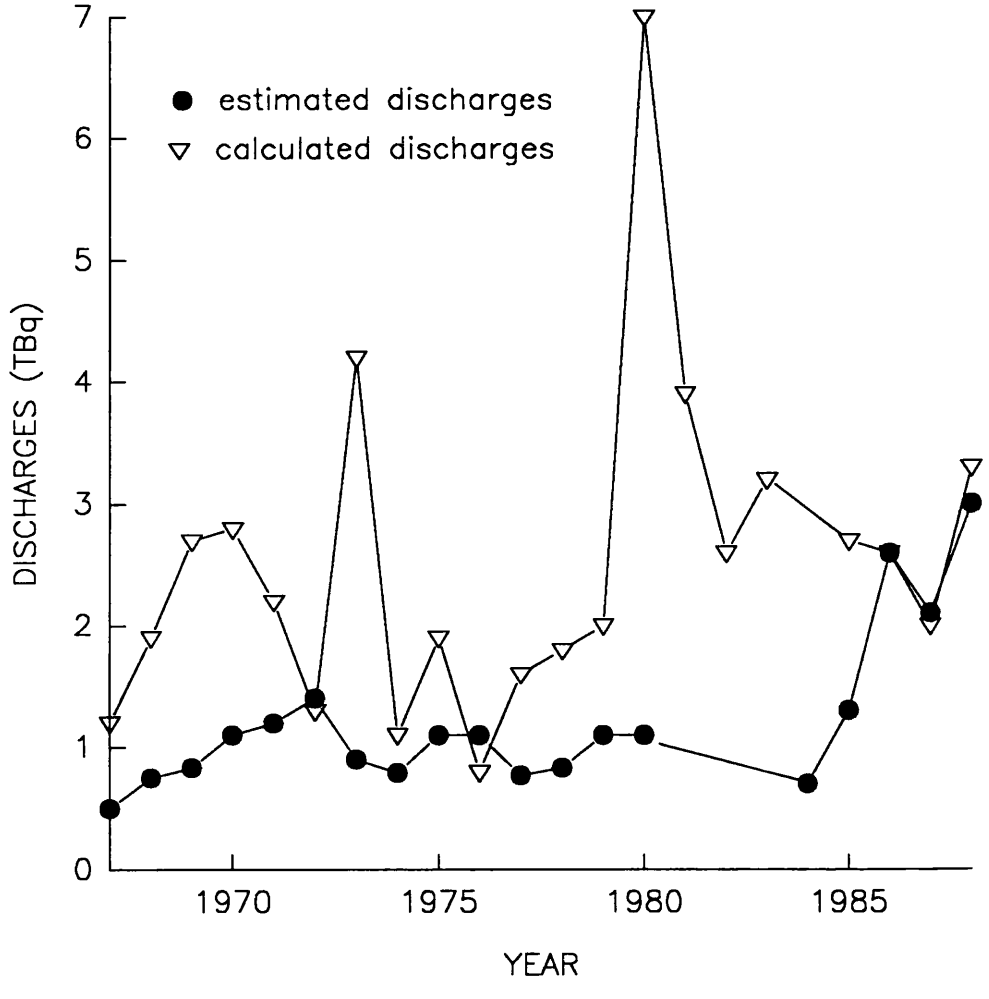

Figure 3.9: Estimated and calculated ^{14}C discharge data (1967-1988).

While these calculated values can at best be considered rough estimates of discharges from Sellafield, they do give some indication of the inputs required to bring about the observed activities if a "simple" relationship is present between the level of ^{14}C released and the activity measured in Nori. On the whole the calculated values are considerably higher than those previously considered as best estimate values, with a range of 7-52% of the total discharge for each year. This in essence indicates that either previous estimates of ^{14}C discharges from Sellafield have been inaccurate or that Nori is not a good indicator of the level of such discharges.

3.2.2 The Water Column

Intertidal biota samples provided both a spatial (1988-1989) and temporal study (1967 - 1988) of ^{14}C discharges from Sellafield, allowing the determination of the geographical extent of ^{14}C transport and a possible indication of past discharge levels from Sellafield. While these studies can provide valuable information, the fate of Sellafield-derived ^{14}C will be determined by processes occurring within the water column. Movement of ^{14}C within the geographical area was determined by analysis of the dissolved inorganic carbon fraction, while transfer within the carbon cycle was considered by comparing the ^{14}C specific activities of the four biogeochemical fractions present (dissolved organic and inorganic carbon, particulate organic and inorganic carbon).

Of the four fractions, the DIC has been most extensively studied as it is the largest carbon pool in the aquatic environment and as such, allows the use of conventional radiometric techniques in the analysis of ^{14}C as opposed to the AMS technique which is required for the PIC, POC and DOC.

3.2.2.1 DIC

The collection of samples coincided with the timing of MAFF research cruises to the Irish Sea area. During this research period, samples were collected on four such cruises from a total of 30 stations (Fig 3.10). Of the DIC samples analysed, 80% were collected in December 1989 on cruise CH62B/89. Samples collected on previous cruises (CIR 9/88 and COR 3B/89) provided the opportunity not only to gain an insight into the likely ^{14}C specific activities present in the area but also the chance to perfect the analytical techniques to be used on the main suite of samples. Furthermore, the results obtained allowed the structuring of the sampling strategy employed on the main cruise of the project

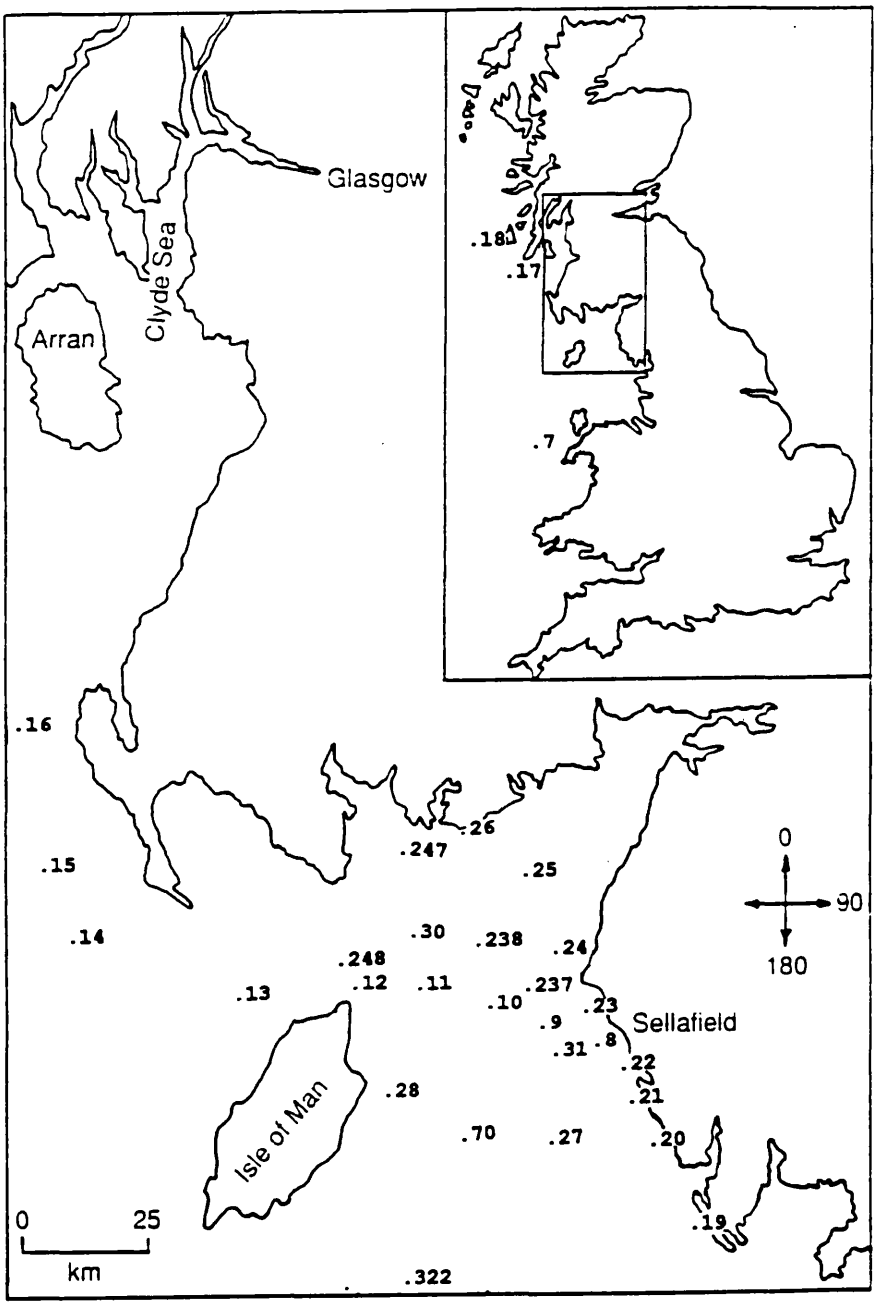

Figure 3.10: The water sampling stations within the Irish Sea area.

(CH62B/89).

The results from these samples indicated that, as with the biota, enhanced levels of ^{14}C were to be found both to the north and south of the discharge point up to 50 km from Sellafield (Table 3.7), confirming the theory that the discharges were, at least in part, in the dissolved inorganic form. As a result of these findings, sampling undertaken on cruise CH62B/89 encompassed an extensive area, with sampling stations up to 245 km from Sellafield, with the samples being collected primarily along two transects (T1 and T2 in Fig 3.1). The first of these followed the Cumbrian coastline from north-south while the second ran east to west from Sellafield into the North Channel. The final cruise (CIR 2/91) allowed the sampling of some additional stations, as well as the resampling of a previous site, to assist in the verification of the results.

STATION	LOCATION	DISTANCE (km)	pM±1σ	Bq kg^{-1} C±1σ
31*	54°25.0'N03°37.3'W	5.0	218.6±0.8	494.0±1.8
70*	54°15.0'N03°50.2'W	23.5	228.8±1.0	517.1±2.2
237+	54°26.1'N03°47.9'W	15.5	194.8±0.7	440.3±1.5
238+	54°30.9'N03°53.1'W	25.0	157.3±0.6	355.4±1.4
322+	54°03.1'N04°06.9'W	50.5	138.5±0.6	313.0±1.4

Table 3.7: ^{14}C specific activity in DIC samples collected on cruises CIR 9/88(*) and COR3B/89(+).

Before reporting and discussing the results obtained during this study, the hydrography of the area must be considered. The Irish Sea is a body of water bounded by St. Davids Head in the south (52°N) and the Mull of Galloway in the north (55°N) (Fig 3.11). The sea has a width of 75-200 km, decreasing to 30 km in the North Channel with an overall volume of approximately 2400 km^3. To the west there is a deep channel, 300 km long and 30 - 50 km wide, which has a minimum depth of 80 m and a maximum in Beauforts Dyke of 275 m. This deep channel is open ended and connected to the Celtic Sea in the south, and the Malin Shelf to the north, by the St. Georges and North Channels, respectively.

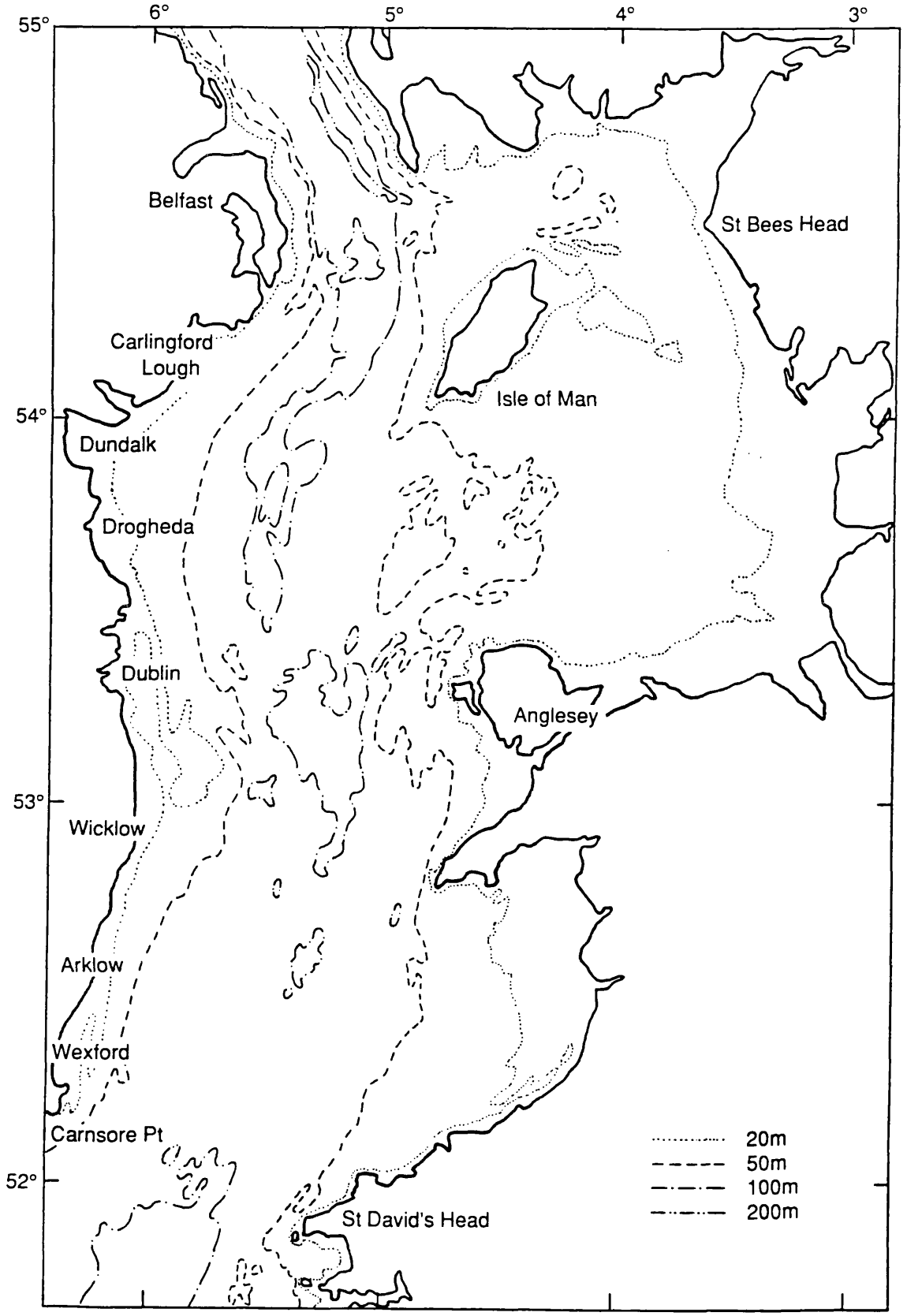

Figure 3.11: The bathymetry of the Irish Sea.

Atlantic water can enter the Irish Sea *via* either of these channels. To the east of this deep channel there are two areas of shallow water (<50 m) - Cardigan Bay to the south and the Eastern Irish Sea to the north.

Over the years, the flow of Atlantic water into the Irish Sea has been extensively studied, with fluxes of 2.2 km^3 d^{-1} being deduced from salinity data for inflow *via* St. Georges Channel (Bowden, 1950) and 2.7 - 8 km^3 d^{-1} for outflow *via* the North Channel from caesium distributions (Jeffries *et al.*, 1982; McKay and Baxter, 1985). However, flow through the North Channel occurs in both directions and fluxes of 10.3 km^3 d^{-1} and 3.0 km^3 d^{-1} have been postulated for the north and southward flows respectively (Dickson and Boelens, 1988).

Within the area there are only two main sites at which the water column is not homogenously mixed throughout the year. The first of these is to the south west of the Isle of Man where deeper waters, weak currents and the warming of surface waters result in the presence of a thermocline (20 - 30 m) from April to October. Density differences present on the entry of freshwater *via* river run-off produces stratification in the Eastern Irish Sea but this is seen primarily in winter and spring (Dickson and Boelens, 1988). The time-averaged circulation pattern within the Irish Sea is weak, but Dickson and Boelens (1988) have produced a map of predominant residual surface currents (Fig 3.3) which is in agreement with direct current measurements and radioactive tracer distributions. These indicate that the principal flow in the Western Irish Sea is northwards through the North Channel with some southward flow of Atlantic water occurring along the north east coast of Ireland. In the Eastern Irish Sea there is a southward drift of surface water along the Cumbrian coastline from off St. Bees Head. This current turns to flow northwards through the North Channel but it is unknown whether the main flow occurs to the east or the west of the Isle of Man. Due to large variations in the flow within the area, the residence time of anthropogenic inputs in the Irish Sea is dependent on the circulation conditions both at the time of release and in the subsequent few months. Regardless of these uncertainties, the predominant residual surface current pattern postulated by Dickson and Boelens (1988) will assist in the interpretation of the observed data.

The ^{14}C results obtained for those samples collected in the Irish Sea during cruise CH62B/89 are detailed in Table 3.8 with the distance and direction from Sellafield.

STATION	LOCATION	DIST km	DIR °	^{14}C pM±1σ	EXCESS ^{14}C pM±1σ	^{137}Cs Bq l^{-1}	$^{14}C/^{137}Cs^{*}$
C08	54°25.0'N03°33.9'W	1.5	280	252.5±0.5	137.1±0.6	0.531±0.003	258.2
C09	54°25.1'N03°40.3'W	8.0	271	248.7±0.5	133.3±0.6	0.460±0.002	289.8
C10	54°25.0'N03°51.1'W	19.0	270	239.3±0.9	123.9±1.0	0.403±0.001	307.4
C11	54°28.0'N04°04.9'W	35.0	277	157.3±0.4	41.9±0.6	0.215±0.001	194.9
C12	54°28.0'N04°23.0'W	53.5	274	156.2±0.4	40.8±0.6	0.211±0.001	193.4
C13	54°28.0'N04°42.1'W	74.5	274	137.4±0.4	22.0±0.6	0.138±0.001	159.4
C14	54°32.0'N05°07.0'W	102.0	278	145.3±0.4	29.9±0.6	0.166±0.001	180.1
C15	54°47.0'N05°24.4'W	126.5	289	135.9±0.3	20.5±0.5	0.130±0.001	157.7
C16	54°57.0'N05°33.0'W	140.0	294	133.8±0.6	18.4±0.9	0.128±0.001	143.8
C17	55°16.0'N05°51.8'W	176.0	299	127.6±0.5	12.2±0.6	0.102±0.001	119.6
C18	55°33.0'N06°50.4'W	245.0	296	118.7±0.5	3.3±0.6	0.056±0.001	58.9
C19	54°07.0'N03°22.9'W	32.5	162	217.8±0.9	102.4±1.0	0.386±0.002	265.3
C20	54°13.1'N03°27.0'W	20.5	175	394.3±1.2	278.9±1.3	0.527±0.002	529.2
C21	54°18.0'N03°30.3'W	11.0	184	248.9±1.2	133.5±1.3	0.470±0.002	284.0
C22	54°22.0'N03°32.0'W	3.5	205	242.8±1.0	127.4±1.1	0.490±0.003	260.0
C23	54°27.0'N03°37.0'W	7.0	292	253.4±1.1	138.0±1.2	0.478±0.003	288.7
C24	54°33.0'N03°41.0'W	18.5	320	233.3±1.4	117.9±1.5	0.420±0.002	280.7
C25	54°40.0'N03°49.5'W	34.0	322	197.6±0.7	82.2±0.8	0.311±0.002	264.3
C26	54°44.0'N04°03.9'W	46.5	315	218.1±0.7	102.7±0.8	0.393±0.002	261.3
C27	54°15.9'N03°34.0'W	15.0	195	166.7±0.8	51.3±0.9	0.289±0.001	177.5
C28	54°17.0'N04°11.9'W	42.5	252	139.2±0.5	23.8±0.6	0.152±0.001	156.6
C30	54°32.0'N04°05.9'W	38.5	286	142.5±0.8	27.1±0.9	0.145±0.001	186.9

Table 3.8 : ^{14}C and ^{137}Cs activities measured at the sampling sites of cruise CH62B/89 used to calculate $^{14}C/^{137}Cs$ ratio.

* ratio is calculated using the excess ^{14}C specific activity *ie.* quoted value less current ambient level of 115.4±0.4 pM

As with the biota samples, the distance from Sellafield has not taken into account the direction of the water currents in the area but has been measured on a straight line basis. Direction measurements assume that due north of Sellafield is 0°, hence, most stations are located in the 180 - 360° range (Fig 3.1). While the direction of the sampling stations from the release point will influence the activity observed, due to the flow of the currents in the area, this was effectively removed by collecting the samples along the two transects which mirrored the major flow patterns.

In addition to ^{14}C analyses, samples were also collected at each station for the analysis of radiocaesium (^{137}Cs). The analytical procedures used in the isolation of caesium from the water column are detailed in Section 2.8. All the samples were analysed at the MAFF laboratory in Lowestoft. ^{137}Cs is a well known and extensively used radioactive tracer of water movement and hydrography, due to its conservative behaviour in the water column (McKinley *et al.*, 1981; Jeffries *et al.*, 1982; Prandle, 1984; McKay and Baxter, 1985; Hallstadius *et al.*, 1987; Bradley *et al.*, 1987). Sampling of ^{14}C and ^{137}Cs at the same sites will allow comparison of their distributions; a significant correlation will enable mathematical models originally designed for ^{137}Cs transport to be modified to reflect the observed ^{14}C distribution. The ^{137}Cs results obtained are also presented in Table 3.8 and are used to calculate a $^{14}C/^{137}Cs$ ratio.

In the discussions which follow, the ^{14}C activities used are the actual measured values except in the calculation of the $^{14}C/^{137}Cs$ ratio where an ambient value of 115.4±0.4 pM is first deducted. For most of the work in this study it is the overall trends in the ^{14}C distribution which are of interest; these are measurable without the subtraction of a current ambient activity. However, the ambient activity must be taken into account in the calculation of the $^{14}C/^{137}Cs$ ratio as it is only the Sellafield-derived ^{14}C which is of interest in the determination of whether the ^{14}C and ^{137}Cs distributions are similar.

Although the samples were collected as two transects, the complete data set can be used to determine the overall distribution of ^{14}C in the Irish Sea area. Figures 3.12 and 3.13 illustrate the distribution of ^{14}C and ^{137}Cs relative to the distance and direction from the point of release. These diagrams indicate that the ^{14}C and ^{137}Cs distributions are similar. This similarity in behaviour between ^{14}C and ^{137}Cs can be further illustrated by plotting ^{14}C activities against those for ^{137}Cs at the same sites (Fig 3.14). A correlation coefficient (r) of 0.909 is obtained for the complete data set. Only one point in the diagram does not lie along the correlation line (Station C20) and if this point is removed the correlation coefficient is improved (r=0.989).

Figures 3.15 and 3.16 illustrate the data further by mapping the observations as contours of similar activity. The data for the nuclides is presented in four activity bands; 100 - 149, 150 - 199, 200 - 249 and >250 pM for ^{14}C and 0.1 - 0.2, 0.2 - 0.3, 0.3 - 0.4 and >0.4 Bq l^{-1} for ^{137}Cs. As expected, the highest levels are observed at those sites closest to the discharge point. For both nuclides, the band of highest activity stretches from St. Bees

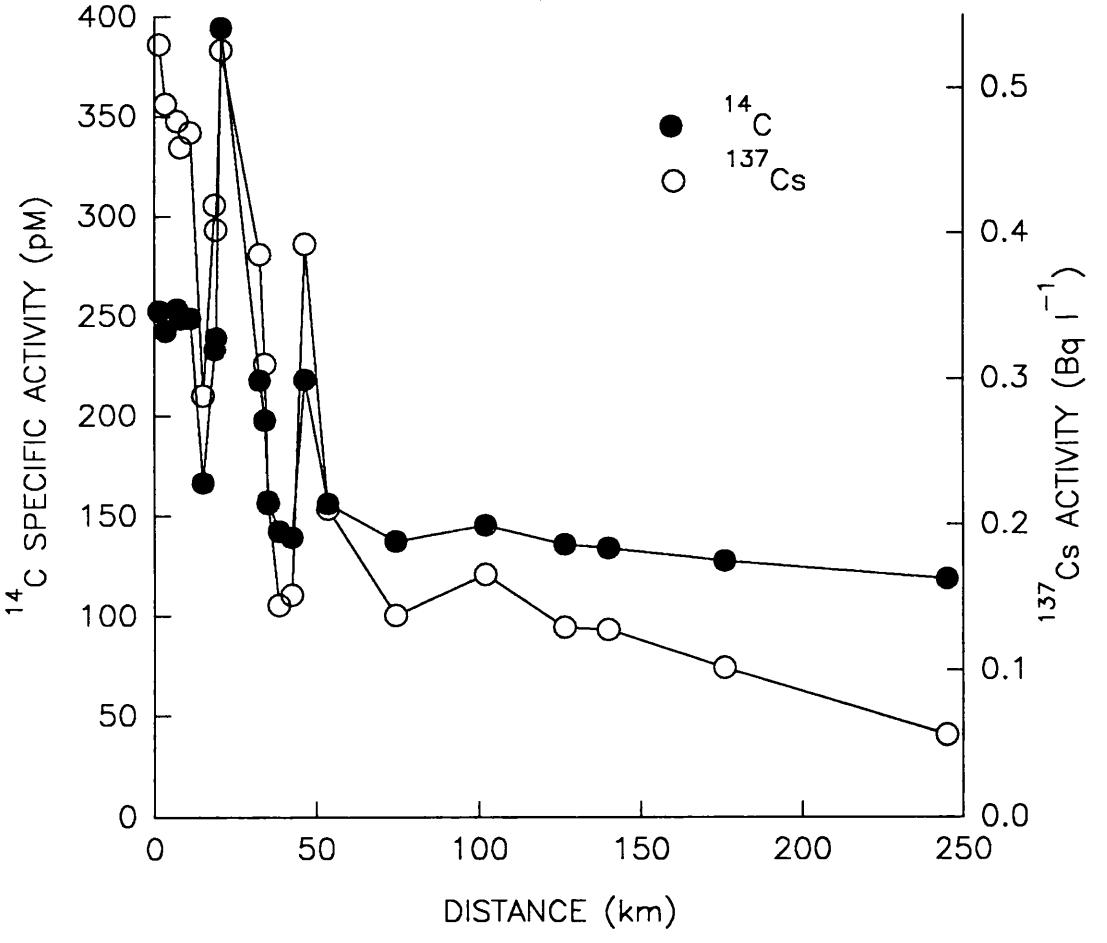

Figure 3.12: Observed ^{14}C and ^{137}Cs activities in seawater *vs.* distance from Sellafield.

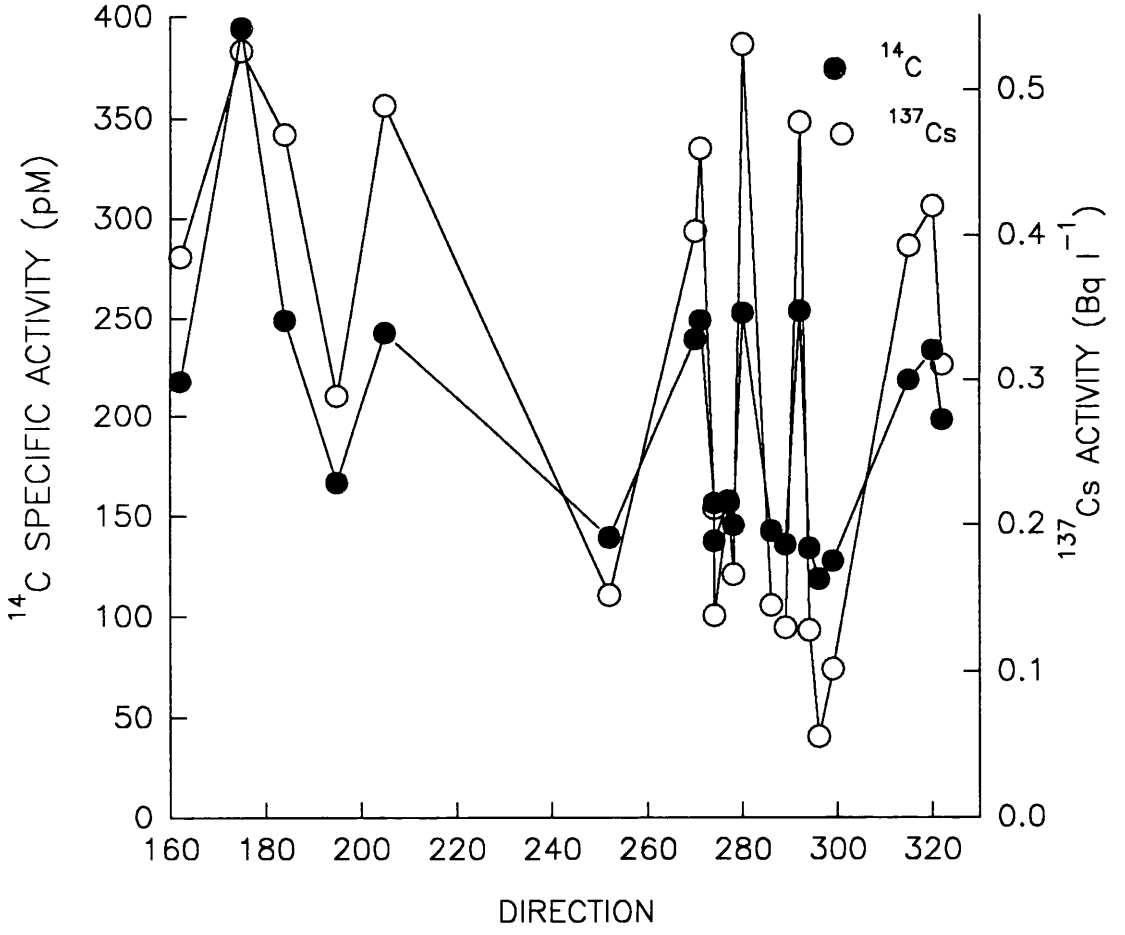

Figure 3.13: Observed ^{14}C and ^{137}Cs activities in seawater *vs.* direction from Sellafield.

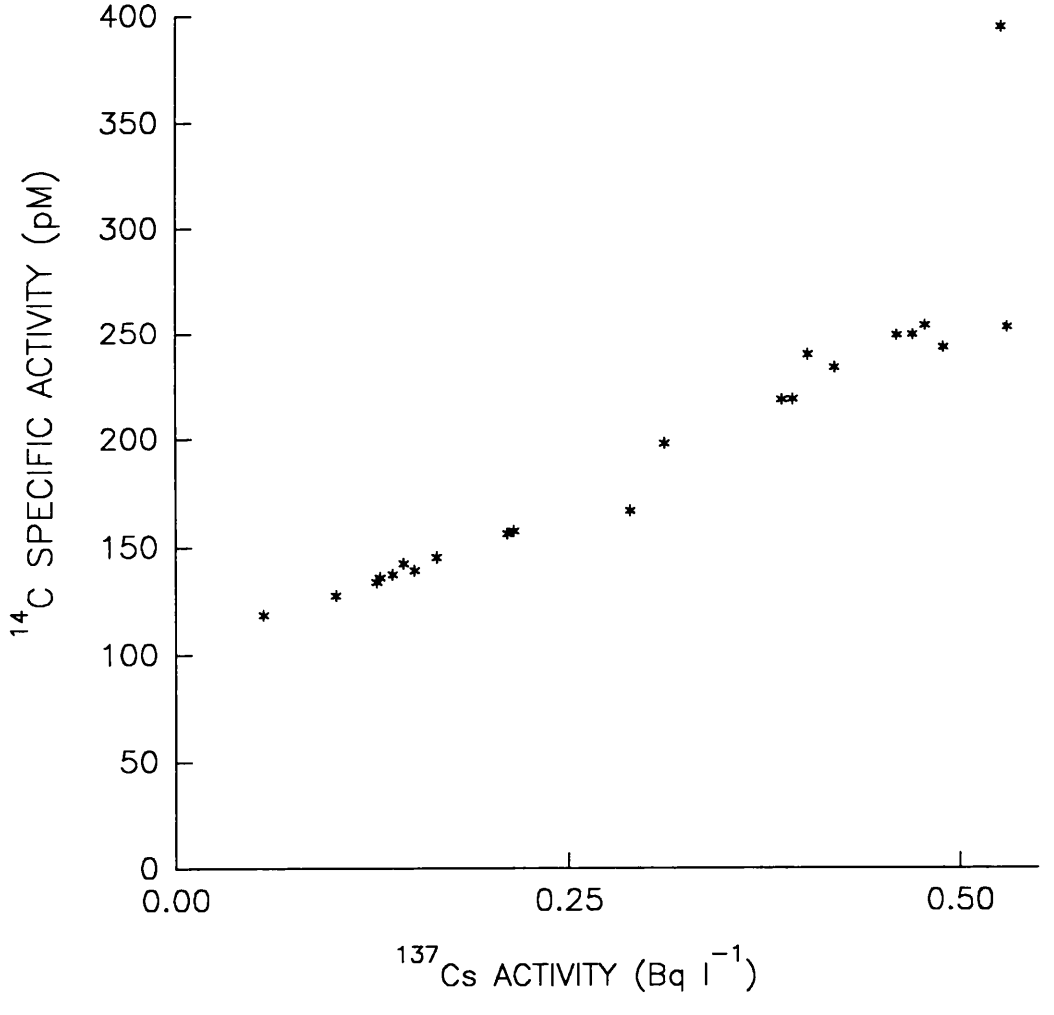

Figure 3.14: ^{14}C *vs.* ^{137}Cs activities in seawater at the same sampling locations.

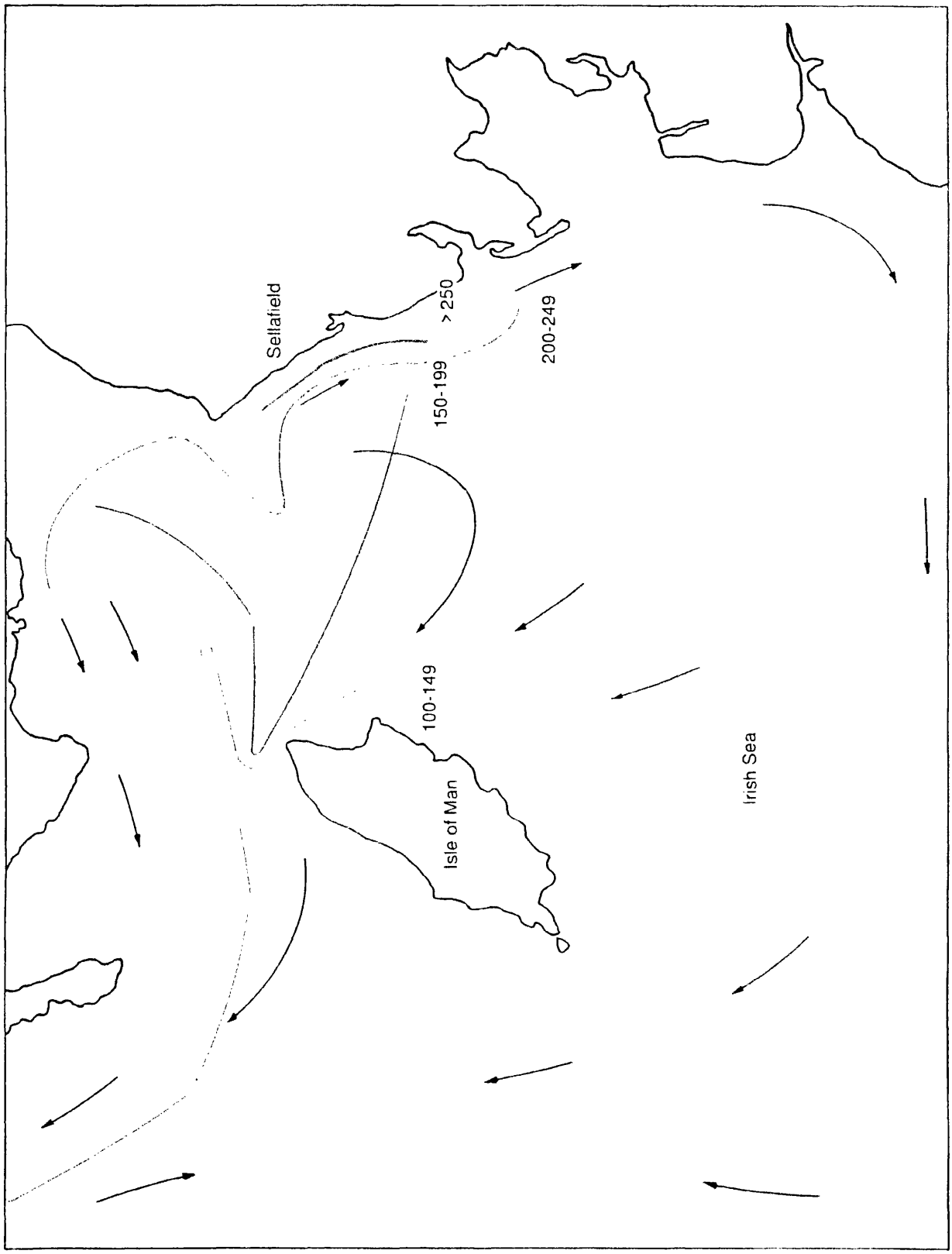

Figure 3.15: Contour diagram to illustrate ^{14}C distribution in the Irish Sea.

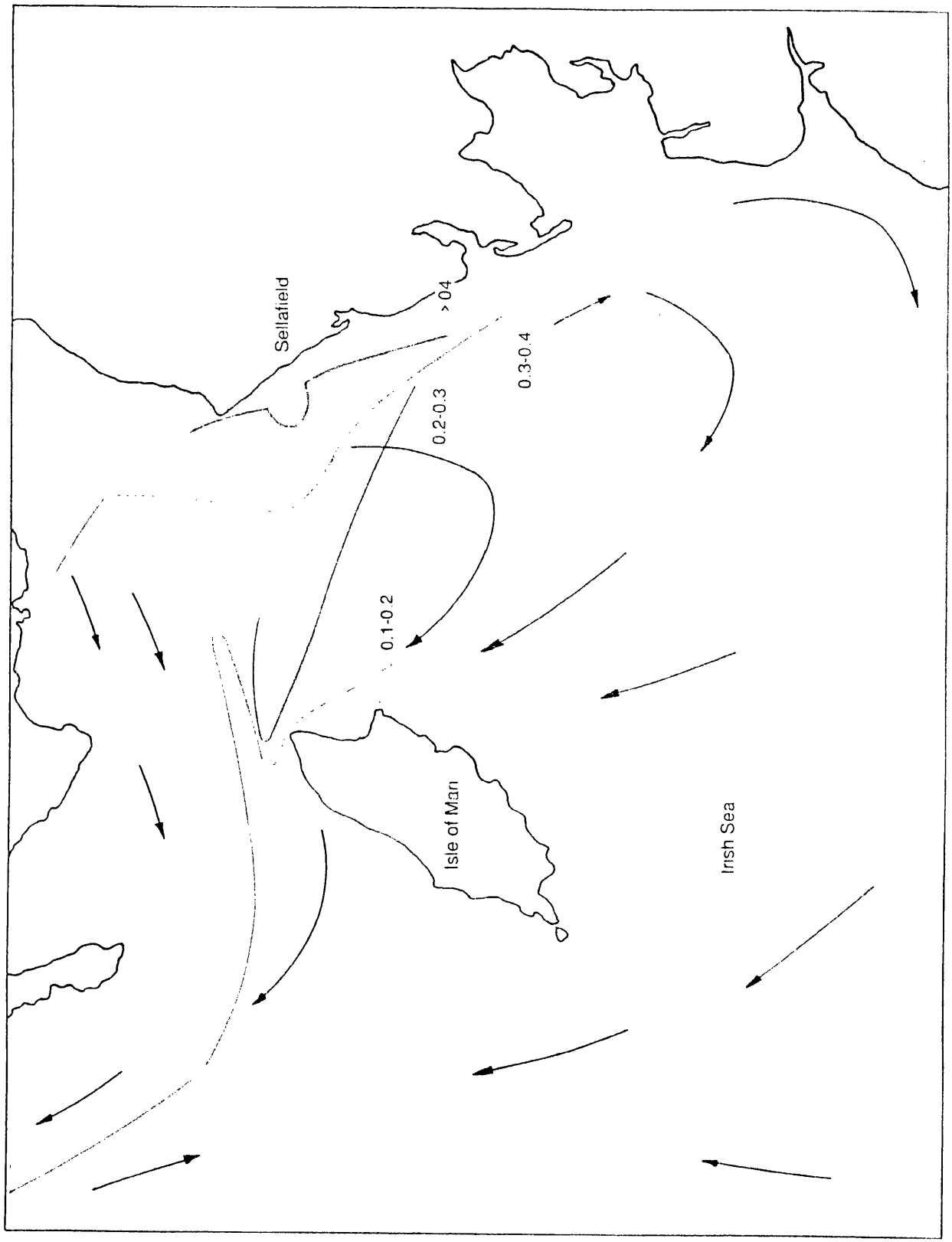

Figure 3.16: Contour diagram to illustrate ^{137}Cs distribution in the Irish Sea.

Head in the north to 20 km south of Sellafield following the Cumbrian coastline. While the distribution of the two nuclides appears to differ immediately to the northwest of Sellafield, this can be attributed to the range of activity bands chosen as one ^{14}C observation (C9) is at the upper limit of the 200 - 249 pM band. Apart from this point, the distribution of the two nuclides is very similar. The activity bands run parallel to the Cumbrian coast, decreasing in activity with increasing distance from the discharge point. A tongue of high activity water is observed just north of Sellafield. This pocket of water is transported northwestwards, towards the North Channel, passing the north of the Isle of Man *en route*.

From these contour maps and the predominant residual surface current pattern postulated by Dickson and Boelens (1988) (Fig 3.3) it would appear that the distribution of ^{14}C and ^{137}Cs is governed by water movement in the area. Although the predominant coastal currents are thought to flow southwards, the high activities observed to the north of Sellafield indicate that water movement in the area occurs in both directions. Overall, the observations demonstrate reasonable agreement with the distribution of surface currents, implying that Sellafield-derived ^{14}C behaves in a relatively conservative manner in the water column. However, the changing ratio of ^{14}C activity to ^{137}Cs activity in the water column (Fig 3.17) indicates that there are possible differences in the behaviour of the two nuclides. This ratio is highest when the sampling stations are closest to Sellafield, decreasing with distance from the discharge point; at station C18 (245 km) the ratio is almost 4.5 times smaller than that observed at station C8 (1.5 km). A pattern such as this indicates either that ^{14}C is being influenced by biological activity *ie.* uptake *via* photosynthesis or that the proportion of ^{137}Cs in the water column is being increased due to desorption from the sediments.

Regardless of this, the distribution patterns appear to be very similar for the two radionuclides indicating that the dispersal pathways are the same although some differences are apparent at those sites furthest from Sellafield. Decreasing releases of ^{137}Cs from Sellafield have already resulted in much lower water column activities within the Irish Sea with the further possibility of these reaching such levels that they are below detectable limits. ^{137}Cs has been a very useful tracer in the past for hydrographic studies and has been the basis of numerous modelling exercises. The observed correlation between ^{14}C and ^{137}Cs distributions may potentially allow ^{14}C to be used as an alternative tracer of

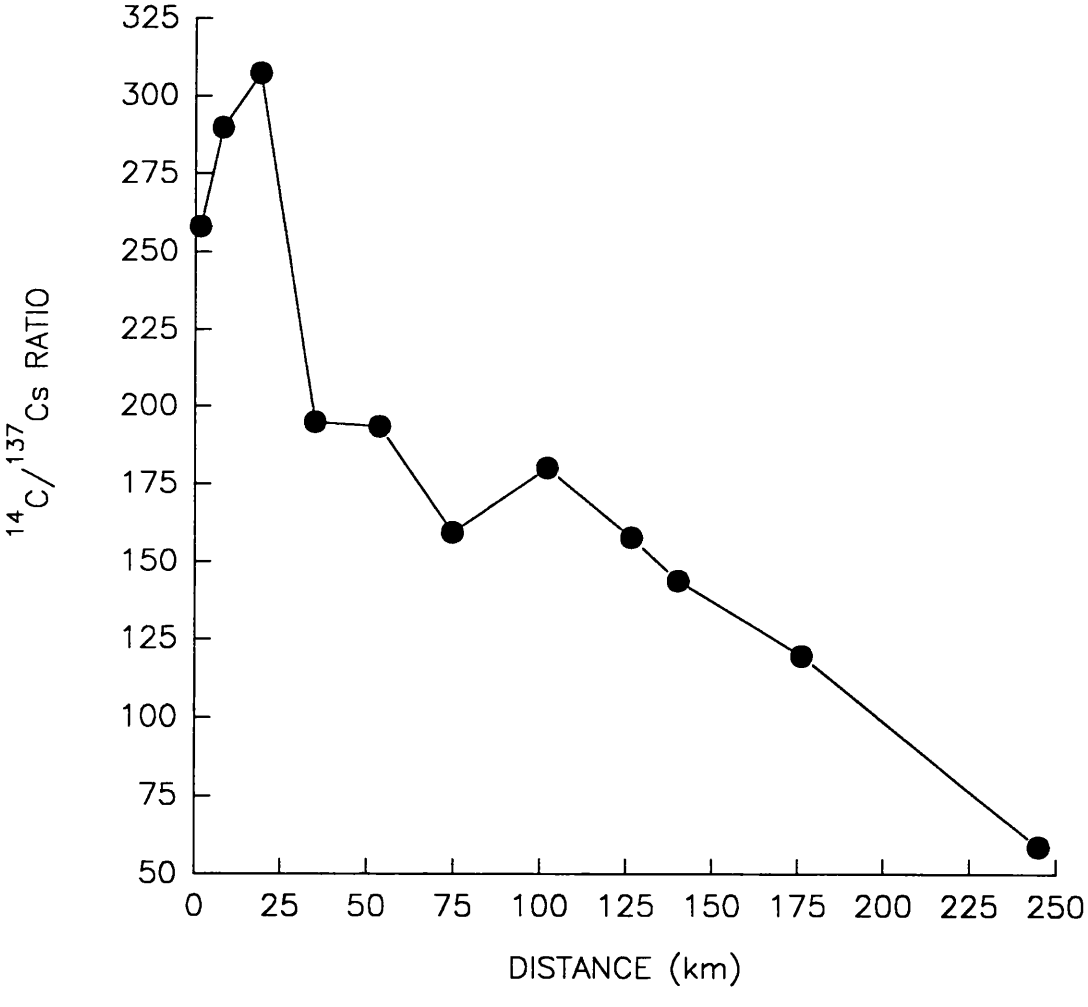

Figure 3.17: The variation observed in the $^{14}C/^{137}Cs$ ratio with distance from Sellafield.

water movement. This would require modification of existing ^{137}Cs models to include biological processes, to ensure that the model structure was representative of the processes controlling ^{14}C distribution.

While the two nuclides show an overall reasonable agreement in their distributions, indicating similar behaviour in the water column, it was also of interest to determine how the activities observed were dependent on parameters such as the distance and direction from the discharge location. The contour maps (Figs 3.15 and 3.16) indicated that the distributions observed were dependent on both of these parameters, hence a number of mathematical functions were considered to explain the observed activities. Table 3.9 details the equations considered and the regression values (R^2-adj) obtained for each of the relationships.

EQUATION	R^2-adj
$^{14}C = 233 - 0.659$ km	37.1%
$^{137}Cs = 0.410 - 0.00194$ km	58.0%
$^{14}C = 357 - 0.609$ dir	15.4%
$^{137}Cs = 0.639 - 0.00128$ dir	10.7%
$^{14}C = 316 - 0.568$ km $- 0.335$ dir	39.4%
$^{137}Cs = 0.510 - 0.00183$ km $- 0.0004$ dir	57.2%
$^{14}C = 258 - 1.70$ km $+ 0.00489$ km^2	45.6%
$^{137}Cs = 0.478 - 0.00481$ km $+ 0.000013$ km^2	71.3%
$\ln^{14}C = 5.43 - 0.00358$ km	49.6%
$\ln^{137}Cs = -0.868 - 0.00893$ km	76.1%
$\ln^{14}C = 5.95 - 0.00272$ dir	12.9%
$\ln^{137}Cs = -0.028 - 0.00510$ dir	10.0%
$\ln^{14}C = 5.72 - 0.00327$ km $- 0.00114$ dir	49.9%
$\ln^{137}Cs = -0.642 - 0.00868$ km $- 0.00091$ dir	75.3%
$\ln^{14}C = 5.55 - 0.00853$ km $+0.000023$ km^2	58.7%
$\ln^{137}Cs = -0.731 - 0.0148$ km $+ 0.000027$ km^2	78.7%

Table 3.9 : Functions considered to explain the observed ^{14}C and ^{137}Cs activities in surface seawater.

In most of the relationships considered, the ^{14}C data produced a poorer fit than the ^{137}Cs data which may be a further indication that biological activity is playing an important role in the overall distribution of the ^{14}C. From the equations and values listed in Table 3.9 the distribution of both nuclides can best be explained when the natural log of the activity is used in an equation incorporating a distance and distance-squared term *ie.*

$$\ln (\text{activity}) = a - b (\text{distance}) + c (\text{distance})^2 \qquad (3.5)$$

However, only ~60% of the ^{14}C and ~80% of the ^{137}Cs observations are explained in this way, respectively. When the measured data are plotted together with the predicted data from an equation of this type (Figs 3.18 and 3.19), the observed activities of both nuclides up to 75 km from Sellafield are variable around the best fit line, whereas after this point the observed activities are much higher than the predicted levels. Equations of this type cannot reproduce large variations such as those observed in the first 75 km, hence the predicted line is based on an average of the points.

Figure 3.20 illustrates the differences in the predicted values obtained from equations incorporating distance only, direction and distance and distance and distance-squared. This shows that while the distance, distance-squared equation under-estimates the activities, the other two over-estimates them. There is no significant improvement in the fit of the line when a direction term is included. The relatively poor match of the predicted and observed values may be due to not taking the predominant surface currents into account in addition to random noise in the data. Therefore, while this type of interpretation can attempt to explain observed data in terms of simple mathematical equations the extent to which it can be used is restricted by the impracticalities of including such parameters as current direction.

Collecting the samples on two transects was an attempt to overcome this directional problem. The first of the transects followed the coastline from Earnse Point, 40 km south of Sellafield, north to the Scottish coastline and included 9 sampling stations (C19 -C26 plus C8). The second transect, encompassing 11 sampling stations (C8 - C18), ran westwards from Sellafield through the North Channel into Scottish coastal waters (T1 and T2 in Figure 3.1, respectively).

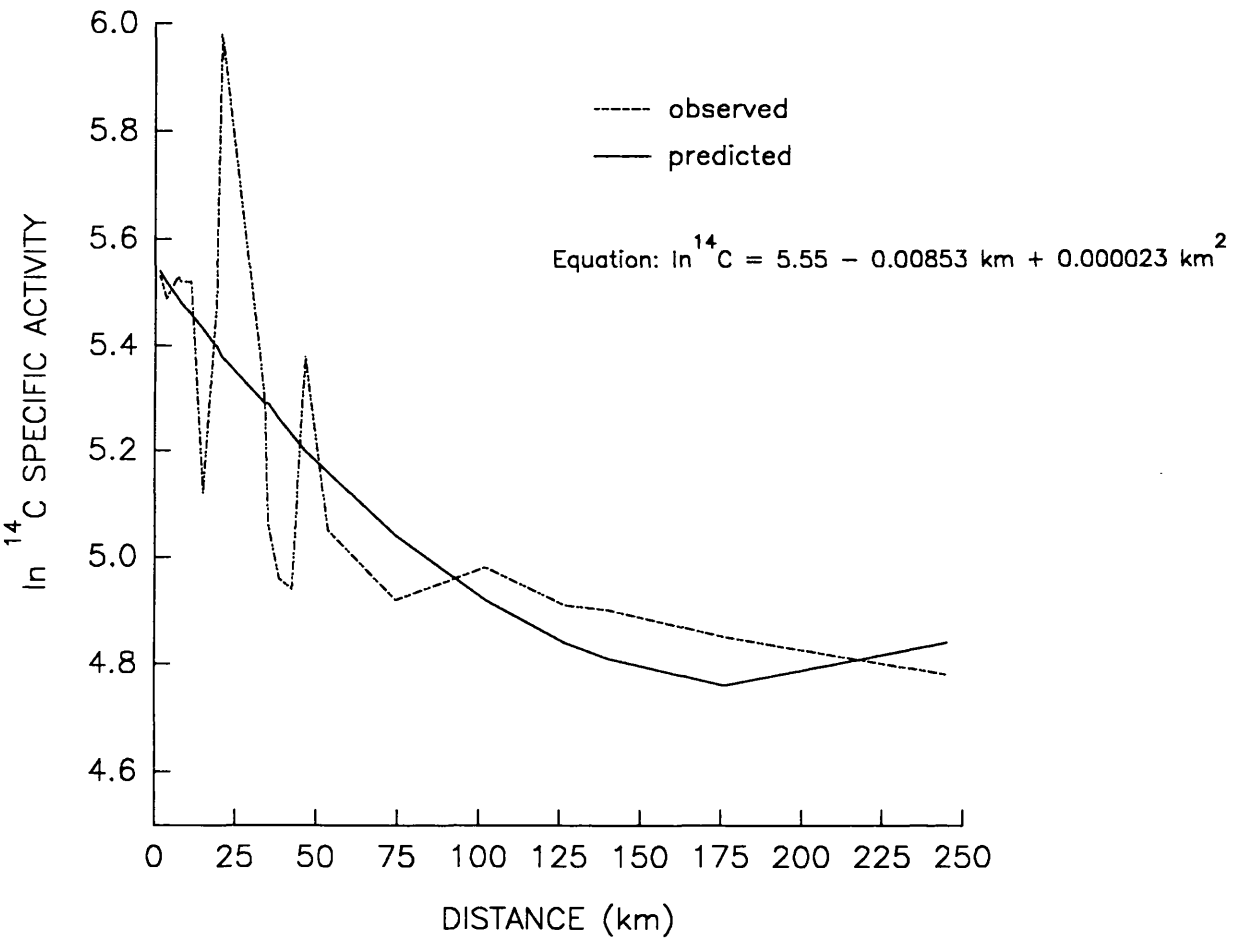

Figure 3.18: Observed ^{14}C activities *vs.* best fit curve.

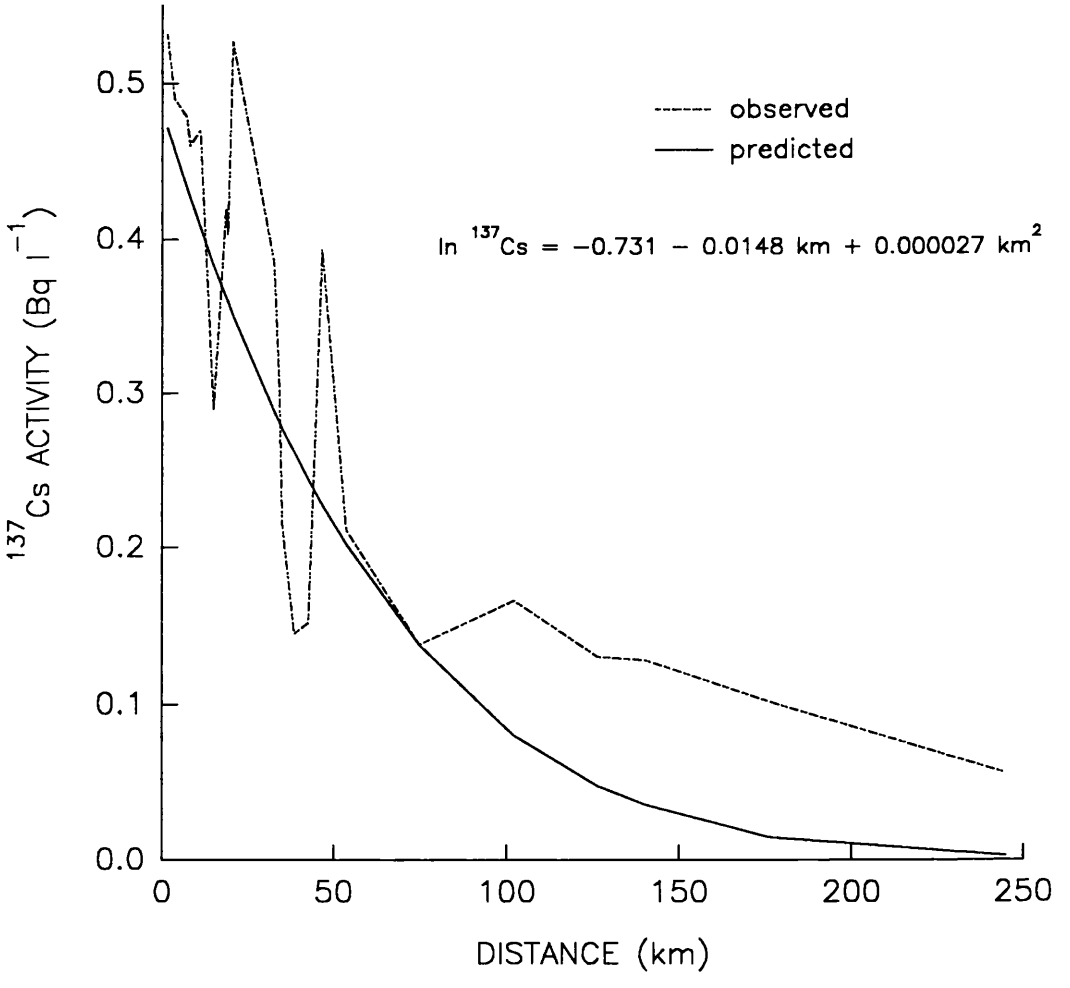

Figure 3.19: Observed ^{137}Cs activities *vs.* best fit curve.

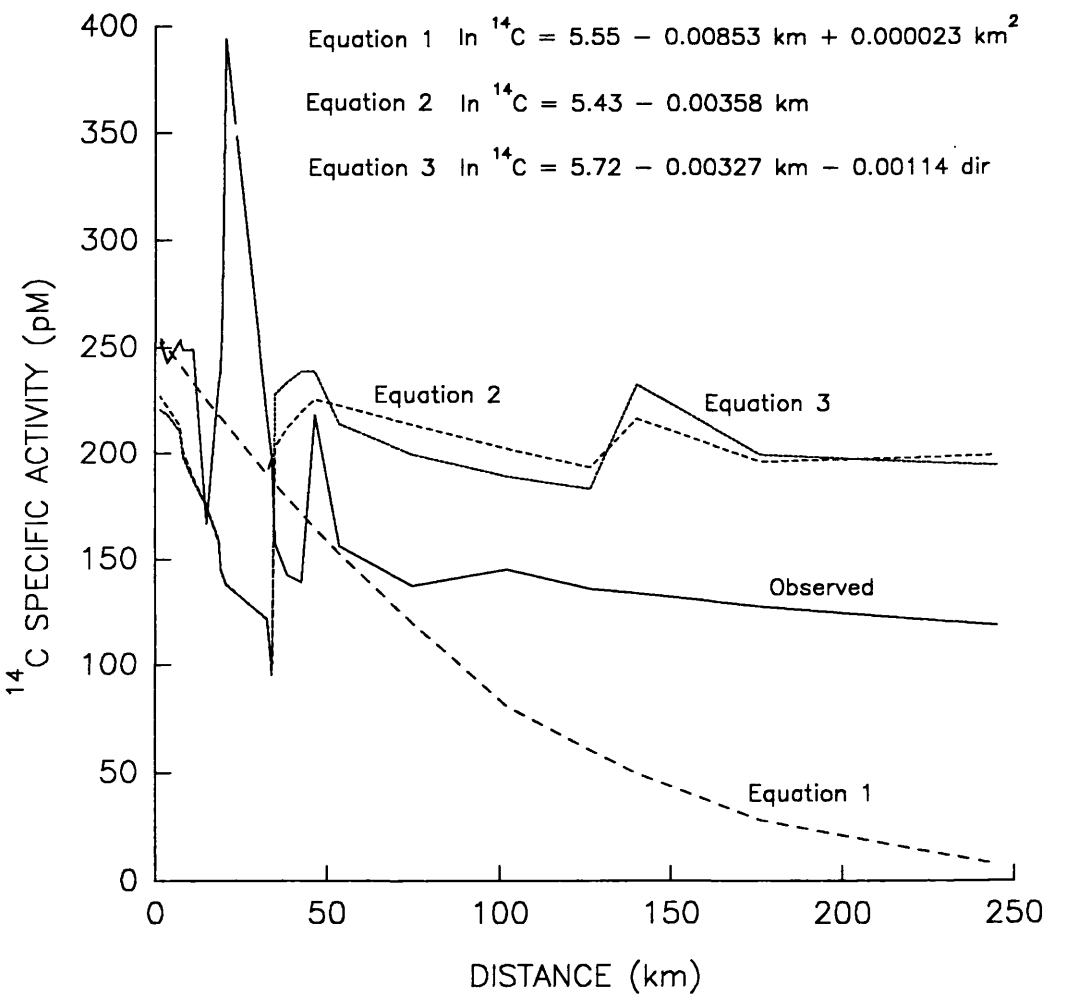

Figure 3.20: Measured ^{14}C activities *vs.* curves from three equations.

The results for the first transect are illustrated in Figure 3.21 which shows the distribution of both ^{14}C and ^{137}Cs in the coastal waters approximately 2.5 km offshore *ie.* parallel to the shore, at a distance which is level with the end of the discharge pipe. In the ^{14}C data, it is apparent that concentrations are fairly constant, except at one point 20.5 km to the south of Sellafield. If this point is discounted, the activity of ^{14}C in the DIC is generally within the range 200 - 250 pM which is higher than that found in water entering the Irish Sea through St. Georges Channel (119.7±0.9 pM at Station C7, data from Table 2.5). Consequently, ^{14}C discharged from Sellafield must be transported both to the north and south of the release point in the form of DIC with the anomaly at 20 km likely to be due to the pulsed nature of discharges from Sellafield superimposed upon the advective flow of water in the area. The ^{137}Cs data also indicate transport to the north and south of the release point. The sharp decline in the measured concentration of ^{137}Cs between 7 and 34 km north of the discharge point indicates that ^{137}Cs is being moved away from the coastal region as a result of water movement. A similar decline, although not as obvious, is also apparent in the ^{14}C data.

Again, the general distribution pattern is similar for the two nuclides although regression analysis between the two produces a correlation value (r) of 0.686 (Fig 3.22). This observed correlation can be improved, if the result from C20 is discounted, to give a correlation value of 0.960, reinforcing the similarity in the behaviour of ^{14}C and ^{137}Cs in the water column. The specific activity observed at this station (C20) is considerably higher than any of the others measured at that time. This may be due to some localised event occurring which is releasing higher activity material into the water column. To determine the exact nature of this would require additional sampling but would provide some indication of whether this was a one-off event, or a permanent feature of ^{14}C distribution in the area.

Interpretation of the observed data by simple mathematical equations was again carried out, however, the ^{14}C activities appeared not to be related to the distance from Sellafield. This seemed to be due to the anomalous point C20 because, on its removal, the relationship between ^{14}C activity and distance improved to give a correlation coefficient (r) of 0.860 as opposed to the 0.261 previously obtained. Unlike the complete data set, the distribution of ^{14}C activity along this south-north transect is best explained by either an equation incorporating distance alone or distance and distance-squared *ie.*

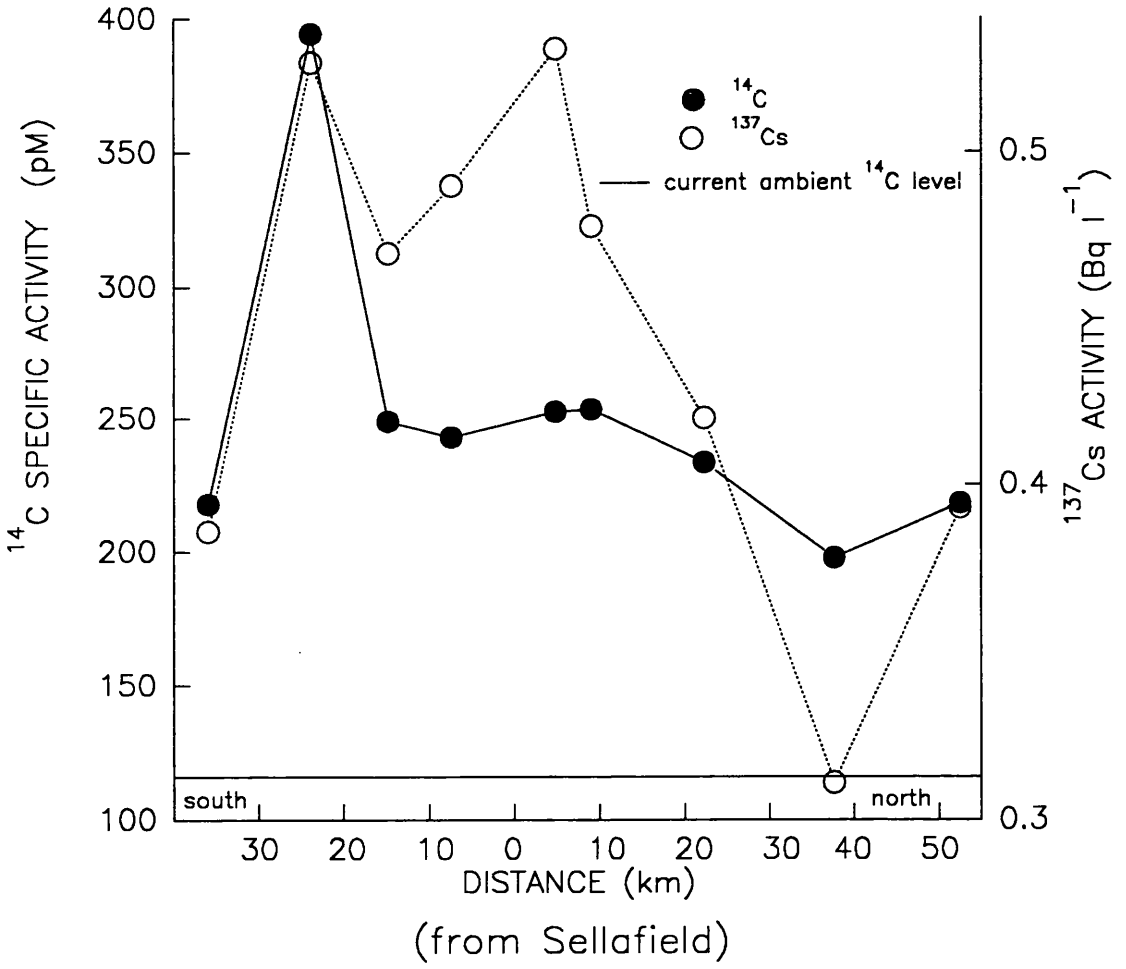

Figure 3.21: Measured ^{14}C and ^{137}Cs activities on the north-south coastal transect.

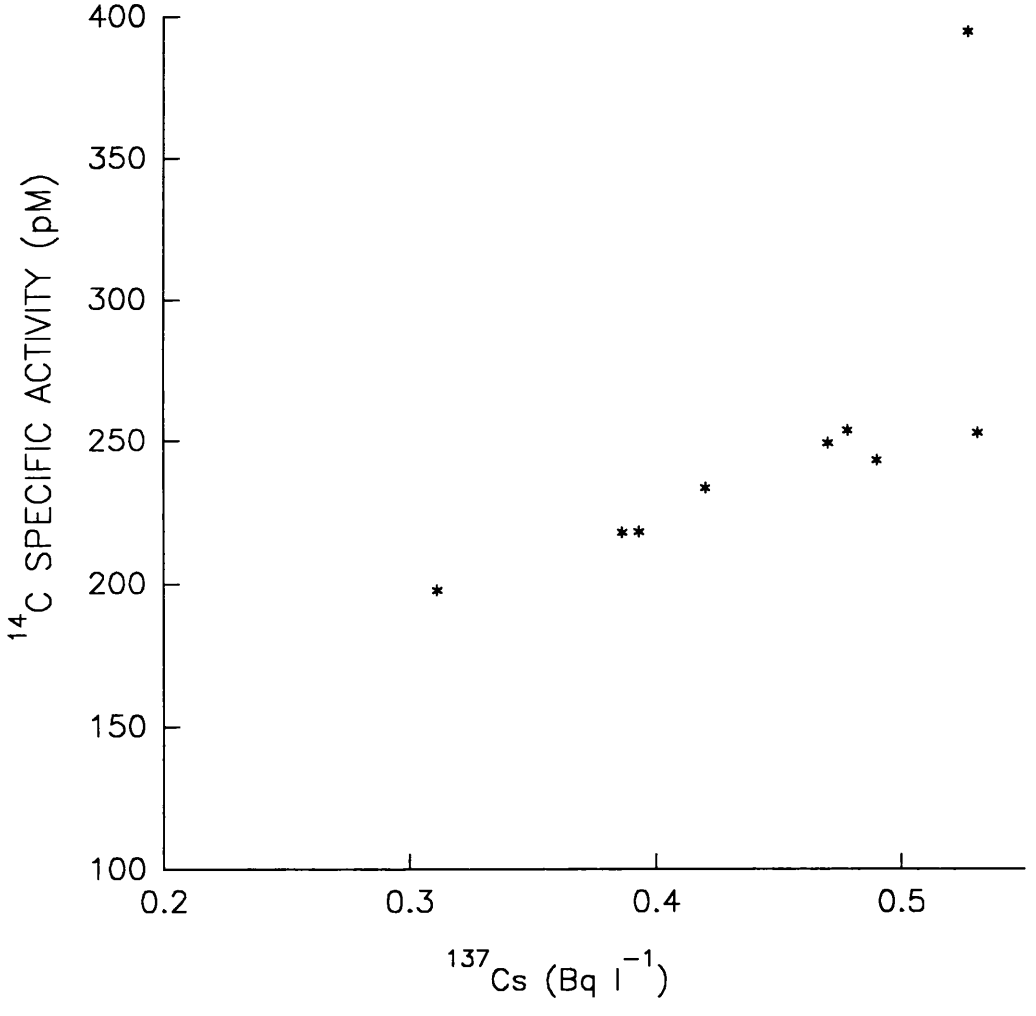

Figure 3.22: Correlation of ^{14}C and ^{137}Cs on a north-south coastal transect in the Irish Sea.

$$^{14}C \text{ activity} = 253\text{-}1.05 \text{ km} \quad (R^2=69.7\%) \quad (3.6)$$

$$^{14}C \text{ activity} = 259\text{-}2.04 \text{ km}+0.0216 \text{ km}^2 \quad (R^2=69.6\%) \quad (3.7)$$

whereas the ^{137}Cs distribution requires the distance-squared term to be included *ie.*

$$^{137}Cs \text{ activity} = 0.543\text{-}0.0101 \text{ km}+0.00014 \text{ km}^2 \quad (R^2=82.3\%) \quad (3.8)$$

No significant improvement is made by using the natural log of the activity in the equations.

In the case of the second transect, westwards from Sellafield, interpretation of the results is again aided by plotting the results against distance from the point of release (Fig 3.23). Unlike the coastal transect, the ^{14}C activities measured on this transect decrease considerably with increasing distance from the discharge point. This distribution is mirrored by the ^{137}Cs concentrations and a correlation value (r) of 0.989 is obtained (Fig 3.24), indicating that the behaviour of the two nuclides is similar.

While the ^{14}C activity closest to the discharge location is enhanced relative to the current ambient level by a factor of >2, the furthest point sampled has an activity within error of that measured in St. Georges Channel indicating dilution by incoming Atlantic or fresh water. In an attempt to empirically model the observed distribution of ^{14}C on this transect, in a manner directly comparable to the complete data set treatment, distance and direction were again considered as the determining parameters. Almost 85% and 90% of the observed variation in the ^{14}C and ^{137}Cs data, respectively, can be explained empirically by the equations:-

$$\ln^{14}C = 5.50\text{-}0.00758 \text{ km}+0.00002 \text{ km}^2 \quad (R^2=83.7\%) \quad (3.9)$$

$$\ln^{137}Cs = -0.785\text{-}0.0131 \text{ km}+0.000021 \text{ km}^2 \quad (R^2=90.1\%) \quad (3.10)$$

which does not take into account the direction of the sampling site in relation to the discharge location. This apparent irrelevance of direction may be in part due to the transect following the direction of the predominant residual surface currents in the area (Dickson and Boelens, 1988) *ie.* northwesterly through the North Channel. Therefore, the observed activity is determined by the distance from Sellafield only, as any directional

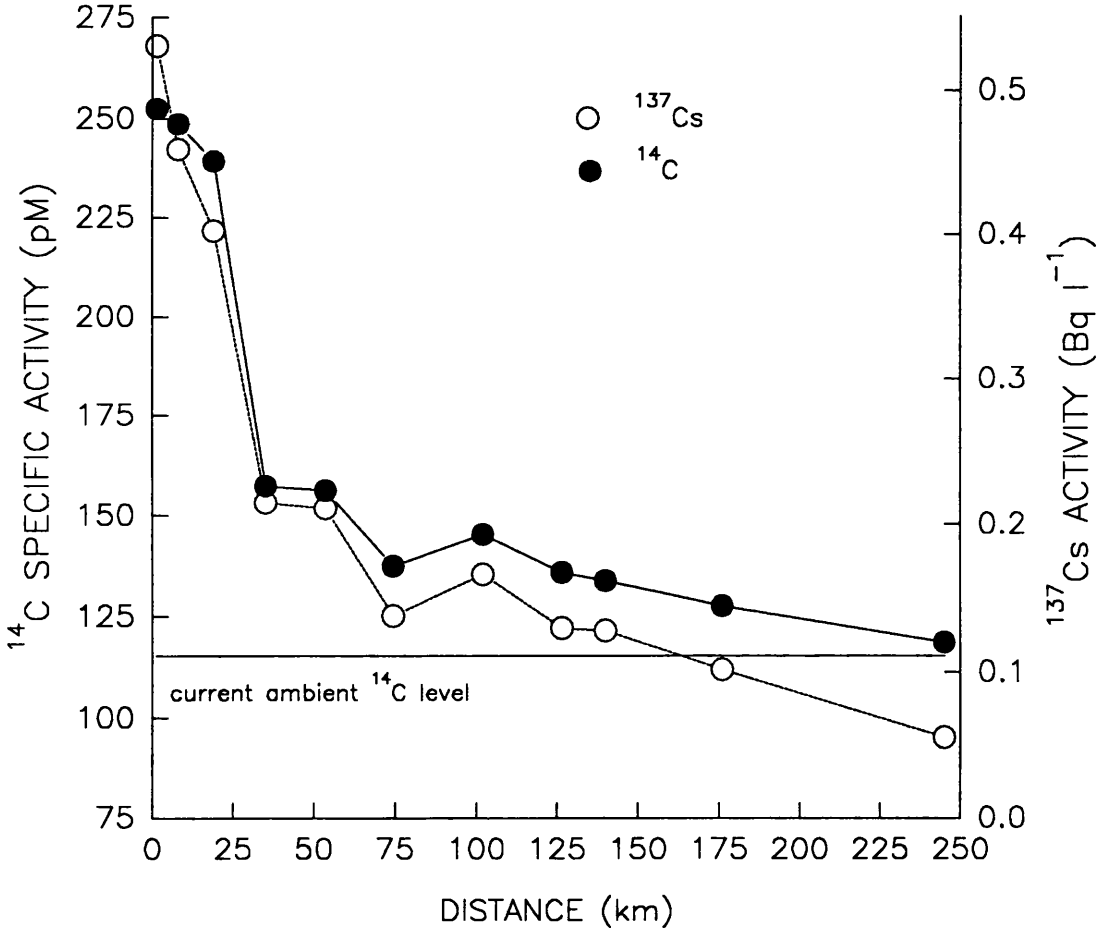

Figure 3.23: Measured ^{14}C and ^{137}Cs activities in seawater on an east-west transect in the Irish Sea.

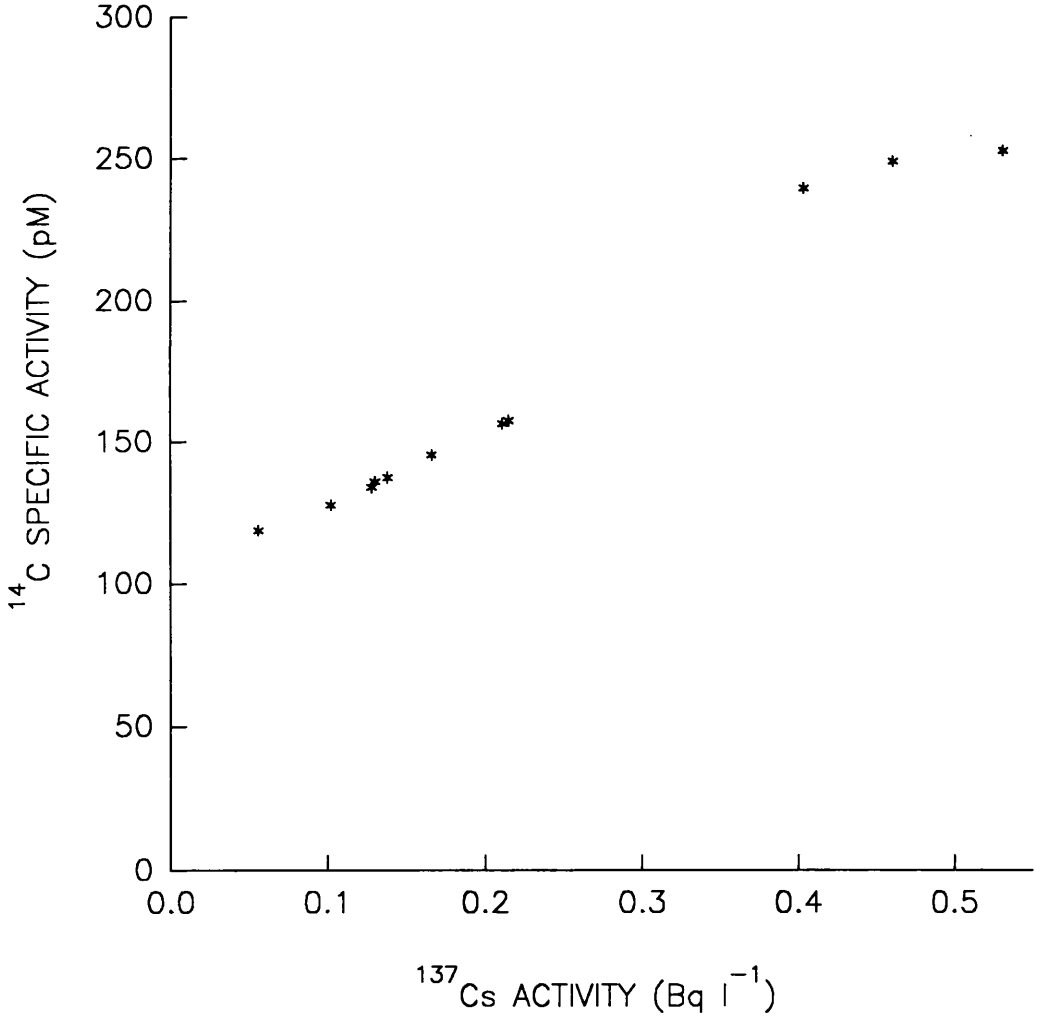

Figure 3.24: Correlation of ^{14}C and ^{137}Cs activities in seawater on an east-west transect in the Irish Sea.

effect has been removed.

Although such simple models provide no physical/hydrographic understanding, they do show that with such simple relationships it may be possible to predict concentrations at locations not sampled without relying on more complex model structures.

The final cruise was in February 1991 and, although it provided an additional four samples for DIC analysis, the main priority was to collect more samples to be analysed as individual biogeochemical fractions. The results obtained for the DIC samples were similar to those measured previously at nearby sites and are detailed in Table 3.10 which presents the biogeochemical data for all the locations sampled.

Station 208 was intended to be a resampling of Station C9 to determine to what extent temporal differences occurred in the measured activity. A slight decrease in the ^{14}C activity, which may just be a reflection of the timing of Sellafield releases, is apparent. Although various attempts have been made to determine the regularity and timing of Sellafield discharges, no information has been obtained to date. From all the results of DIC samples collected during this work, it would appear that the timing of sampling cruises has made little difference to the activity found, which would indicate frequent and relatively uniform releases, as opposed to spasmodic large releases of ^{14}C. In addition, the good agreement observed between ^{14}C and ^{137}Cs distributions would indicate release at similar time intervals and information on monthly discharges of ^{137}Cs for 1987 (Baxter, pers. comm., 1988) show fairly constant release rates throughout the year on a monthly basis.

3.2.2.2 Biogeochemical fractions

Previous sections of this work have focussed on the distribution of Sellafield-derived ^{14}C within intertidal biota and the DIC from the water column. These have both indicated that enhanced levels of ^{14}C can be found up to 200 km from the discharge location due to the conservative behaviour of carbon in the water column. However, the enhancements within the intertidal biota are dependent on the type of organism and its feeding behaviour. Mussels consistently show higher ^{14}C specific activities than either winkles or seaweed, pointing to the presence of enhanced particulate material. In an attempt to determine the validity of this, and also to determine the cycling of carbon within the coastal marine system, a preliminary investigation was undertaken of the four biogeochemical fractions isolated from the water column for analysis of their ^{14}C content.

Within the study area, five sites were selected for the collection and analysis of the biogeochemical fractions; DIC, PIC, POC and DOC (Fig 3.25). Of these sites, three were sampled in December 1989 - one in St. Georges Channel, one in the North Channel and one just off the Sellafield pipeline. These sampling sites provided an indication of the ^{14}C specific activity in the biogeochemical fractions as the water entered and exited the study area, in addition to the levels close to the point of release. A further two sites were sampled in February 1991, with the previous site at Sellafield being resampled in order to confirm the trends observed in the initial results. The two additional sites were sampled to give an indication of the rate at which the ^{14}C specific activities in the various fractions might change within the immediate zone of ^{14}C contamination from Sellafield. The results obtained during both sampling cruises are shown in Table 3.10; those from the December cruise in part (a) with those from the February cruise in part (b). The $\delta^{13}C$ values (per mil deviation relative to the PDB standard) for each sample are shown in Table 3.11 in a similar manner to the ^{14}C results.

SITE	LOCATION	FRACTION			
		DIC	PIC	POC	DOC
		(all results quoted as pM±1σ)			
(a) December 1989					
C7	54°48.6'N05°09.7'W	119.8±0.8	55.0±0.5	51.9±0.6	82.7±0.9
C9	54°25.1'N03°40.3'W	243.3±1.7	47.9±0.5	73.1±0.7	63.4±0.8
C15	54°47.0'N05°24.4'W	135.9±0.3	63.8±0.6	57.5±0.5	74.0±0.8
(b) February 1991					
S208	54°24.9'N03°40.2'W	200.0±0.6	59.1±1.2	80.4±1.1	38.5±0.7
S247	54°43.1'N04°07.9'W	183.9±0.7	100.3±1.5	66.6±0.7	33.2±0.5
S248	54°28.1'N04°25.1'W	168.9±0.7	51.4±1.0	59.4±1.0	30.2±0.5

Table 3.10: ^{14}C activities measured in the biogeochemical fractions from the Irish Sea.

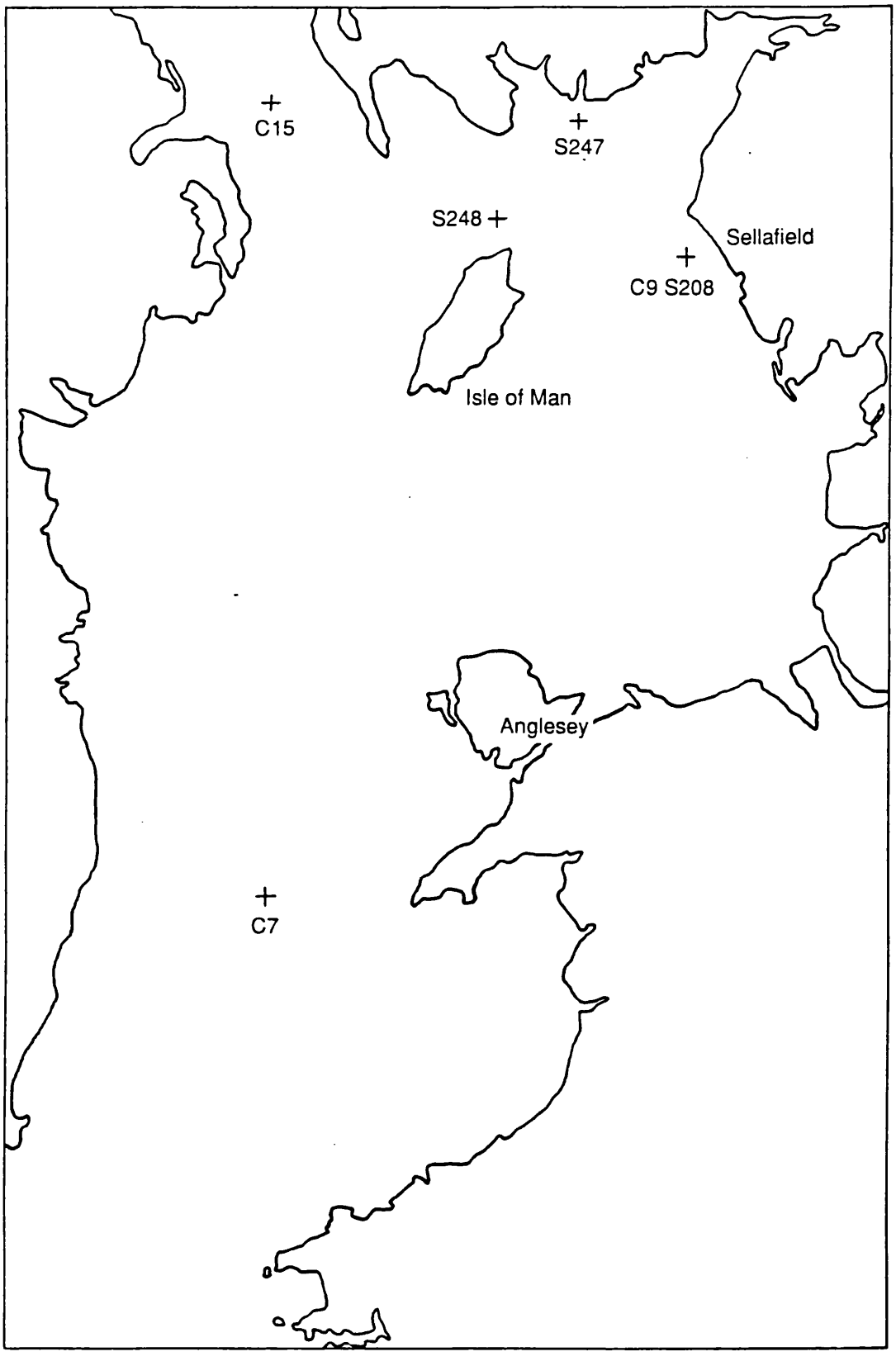

Figure 3.25: Sampling sites of the biogeochemical fractions within the Irish Sea.

SITE	FRACTION			
	DIC	PIC	POC	DOC
	(all results reported as ‰)			
(a) December 1989				
C7	+0.6	+0.4	-26.4	-25.1
C9	-0.7	+0.4	-25.6	-25.9
C15	+0.6	+0.4	-25.7	-26.7
(b) February 1991				
S208	+0.4	+0.6	-25.4	-23.8
S247	+0.2	+0.4	-25.3	-25.6
S248	+0.1	-0.8	-19.3	-29.9

Table 3.11: $\delta^{13}C$ values (per mil deviation relative to PDB standard) obtained for the biogeochemical samples.

In an attempt to ensure that the two techniques used (radiometric and AMS) would provide comparable results, duplicate DIC samples were analysed from two sites in the Sellafield area (C7 and C9). These gave ^{14}C activities of 119.7 and 119.8 pM for C7 and 248.7 and 243.3 pM for C9 by radiometric and AMS analysis, respectively. The good agreement permits discussion of the results for the biogeochemical fractions in relation to those obtained by the radiometric method.

In the following discussion of the results presented in Table 3.10 and 3.11, the two sets of samples (*ie.* December 1989 and February 1991) will firstly be considered in isolation to determine any trends present. These will then be studied together to ascertain any similarities/discrepancies which may help to determine the distribution of Sellafield-derived ^{14}C in the water column. To help in the interpretation of the measured activities, the results for the PIC, POC and DOC at each sampling site have been normalised to that for the DIC. These are presented in Table 3.12.

SITE	DIC	PIC	POC	DOC
(a) December 1989				
C7	1	0.46	0.43	0.69
C9	1	0.20	0.30	0.26
C15	1	0.47	0.42	0.54
(b) February 1991				
S208	1	0.30	0.40	0.19
S247	1	0.55	0.36	0.18
S248	1	0.30	0.35	0.18

Table 3.12: ^{14}C activity in the biogeochemical fractions normalised to the ^{14}C activity in the DIC at each site.

At all three sites sampled in December 1989 the DIC fraction is enriched in ^{14}C relative to the modern standard as a result of both rapid equilibrium with the atmosphere and the incorporation of Sellafield-derived ^{14}C. The activity measured in St. Georges Channel of 119.8±0.8 pM is slightly higher than the estimated current ambient level of 115.4±0.4 pM. This could be due to a southward flow from Sellafield or the northward transport of ^{14}C from the Amersham International radiochemical plant in Cardiff. The enrichment in ^{14}C in the DIC observed close to Sellafield is more than double the activity observed in St. Georges Channel. For the site in the North Channel the measured ^{14}C activity in the DIC is considerably less than that observed at Sellafield but is still enriched relative to that in St. Georges Channel. This indicates that the concentration of ^{14}C leaving the Irish Sea is greater than that entering due to the input from Sellafield.

With respect to the DIC, the three other fractions are depleted in ^{14}C. This is a reflection of the residence time of the ^{14}C within the reservoir, the activity of the material entering the reservoir and to a lesser extent, fractionation effects. These results tend to indicate that transfer of carbon between the reservoirs occurs at a very slow rate with the activities measured in these fractions likely to reflect natural cycling of carbon, in addition to inputs from external sources such as river runoff. The $\delta^{13}C$ data (Table 3.11) indicate the

incorporation of terrestrial material in the isolated POC and DOC fractions - *in situ* marine production would give $\delta^{13}C$ values of -15 to -22‰ (Section 1.7.2.2(b)) as opposed to the -24 to -30‰ found on average for the samples in this study.

The DOC sample collected in St. Georges Channel has a higher ^{14}C activity than the other two samples collected at this time. The chemical form of the discharges from Amersham are unknown but if they were in an organic form they may help explain the slight enrichment found at this site. However, these observed differences may be due to natural processes such as river run-off and may reflect the natural variability in the ^{14}C content of this reservoir. Relative to this site in St. Georges Channel and the other in the North Channel, the ^{14}C activity measured in the POC at the Sellafield site is enriched, indicating the incorporation of higher activity material in the vicinity of Sellafield. There is no obvious trend in the measured activities for the PIC except that they consistently appear to be the most depleted material sampled at the three sites.

Overall, it seems that the DIC fraction is the only one readily influenced by discharges of ^{14}C from Sellafield. Apart from some indication of incorporation of enriched material into the POC at Sellafield, the other three fractions are depleted in ^{14}C. If there is a distribution pattern present it is being overshadowed by natural processes such as river run-off which will add both particulate and dissolved material of differing ^{14}C activities.

For those samples collected in February 1991, a similar pattern emerges *ie.* the DIC is enriched relative to the modern standard while the other three fractions are depleted relative to the activity observed in the DIC and to the modern standard. The highest activity in the DIC is again seen at the sampling site closest to Sellafield although the enrichment is not as high as that seen on previous sampling. This is likely to be due to differences in the discharges from Sellafield. For the other three fractions, the measured activities are again depleted with respect to the current ambient level. However, the PIC collected close to the Solway coast is less depleted than those collected at the other sites. The breakdown and resuspension of shell material, from intertidal organisms with ^{14}C activities similar to those found in the DIC, may help to explain this higher activity. The area of sampling is known to be subjected to storms which result in considerable movement of both bottom and intertidal sediments, providing the opportunity for the incorporation of more contemporary material into the water column. The activities measured in the DOC at all three sites during this sampling cruise appear to be

considerably more depleted than those previously measured which may, in part, be due to the inherent difficulties in isolation and oxidation of the material, or as postulated previously, be due to increased river runoff and the incorporation of terrestrial DOC.

Overall, the biogeochemical fractions analysed show that the DIC is enhanced in ^{14}C due to discharges from Sellafield and, relative to this and to the current ambient value, the other three fractions all have depleted ^{14}C activities. This in essence means that there appears to be no enriched particulate material in the water column to support the enriched activities found in the mussels and winkles which are feeding in the area. From the initial data collected during December 1989 (Table 3.10 (a)), the higher ^{14}C activity found in the POC fraction at the Sellafield site, in comparison to that at the other two sites, suggests transfer of carbon from the DIC to the POC. The results obtained for February 1991 support this theory as lower ^{14}C activities are found in POC samples with increasing distance from Sellafield - similar to the distribution seen in the DIC. For the DOC samples, there is no obvious explanation for the activity measured in water entering and leaving the area to be higher than that observed at all the other sites.

Hence, an anomaly exists in that macro-invertebrates, especially mussels, which feed by removing particulate material from the water column, are enriched in ^{14}C yet there is no obvious enriched particulate material present in the water column. The most likely route for transfer of carbon from the DIC to the POC, as indicated at Sellafield, is due to photosynthetic uptake by phytoplankton which introduces a seasonal component which may help explain some of the observations. This possible seasonal dependency was only really uncovered towards the end of this study at a time outwith the season for phytoplankton collections. A number of institutes were approached in an attempt to obtain such material. Several samples were obtained from MAFF with the one collected closest to Sellafield being chosen for analysis by AMS. This sample had been collected in April 1989 and stored in formalin. Despite thorough cleaning, there is a small possibility that some formalin could be incorporated into the sample, hence the measured activity is likely to be a minimum value, assuming that the formalin has no ^{14}C activity. The ^{14}C specific activity of the phytoplankton sample was 270.0±2.1 pM indicating that there is a source of enhanced particulate material within the study area. This material is seasonal in nature but the level of enhancement present will be governed by the timing of discharges from Sellafield with respect to the occurrence of phytoplankton blooms.

The influence of phytoplankton on the activity of the POC could be determined by a temporal study in which samples would be collected and analysed periodically over a complete seasonal cycle. During this work, time did not allow for such a study, hence, further research is required to determine the exact influence of phytoplankton on the cycling of carbon in the biogeochemical fractions of the water column. A temporal study of this nature could also be used to determine whether the good agreement observed between ^{14}C in the DIC and ^{137}Cs would hold during periods of increased biological activity.

3.2.3 Sediments

Within the study area, the bottom sediments are predominantly coarse sands and gravels with finer particle-sized muddy sediments being restricted to two areas (Fig 3.26). One of these areas is to the west of the Isle of Man in a fairly deep basin, whereas the other is parallel to the Cumbrian coast and extends from Liverpool Bay, in the south, to the Solway Firth, in the north. This easterly "mud patch" has been the subject of much discussion concerning the removal and remobilisation of radionuclides discharged from Sellafield. A large proportion of particle-reactive, long-lived, Sellafield-derived radionuclides are associated with the seabed sediment, and hence the mud patch, in the vicinity of the discharge pipe (Kershaw, 1986). These muddy areas have been thought of as zones of active sedimentation (Belderson, 1964; Belderson and Stride, 1969; Pantin, 1977, 1978; Mauchline, 1980; Johnson, 1983) although more recent research has challenged these views. Kirby *et al.* (1983) concluded that there was no direct evidence that net sedimentation had been or was presently occurring, while Sills and Edge (1989) found that the mud patch was overconsolidated due either to loss of the top sediment by erosion or because of creep in the seabed sediments. In an attempt to determine likely sedimentation rates for this area, Kershaw and co-workers (Kershaw, 1986; Kershaw *et al.*, 1988) undertook ^{14}C dating of both bulk sediments (inorganic fraction) and marine shells (*Turritella communis*) from cores up to 2.5 m deep. They found that the bulk sediments gave a uniform age of 12,500±1000 years B.P. for the whole length of the core due to extensive re-working of the sediment which overshadows any measurable indicators of sedimentation. In comparison, the results obtained for the *T. communis* samples indicated active sedimentation occurring at two sites on the mud patch at rates of 0.02-0.08 cm yr^{-1}

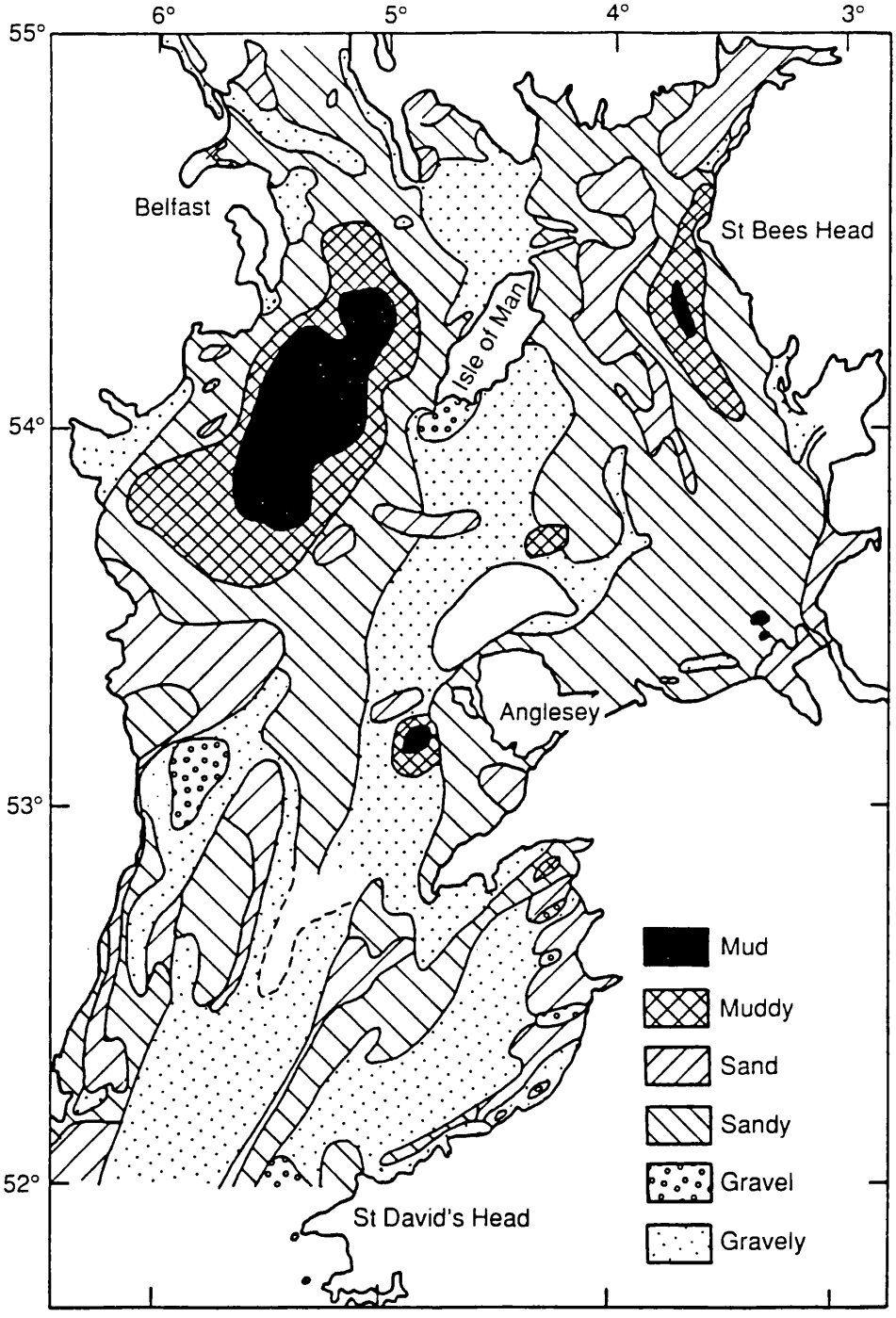

Figure 3.26: Distribution of sediment types within the Irish Sea.

for the past 3000-4000 years.

In this study, it was not determination of sedimentation rates which was of interest, but, whether Sellafield-derived ^{14}C was being incorporated into the sediments in the study area and, if so, in what form. Due to the coarse sand and gravel composition of most of the seabed in the study area, a core sample could only be collected from the mud patch, with grab samples collected from a number of other sites. However, it was felt that due to the composition of the material in these grab samples, that accurate ^{14}C analysis by radiometric techniques would not be feasible and that the core sample would provide the information required. The core was collected in December 1989 at a sampling station close to the Sellafield discharge pipeline (C8). Both the inorganic and organic fractions were analysed in 5 cm sections of the core down to a depth of 25 cm. The results obtained (Table 3.13) are similar to those obtained for northeast Atlantic sediments (Kershaw, 1985) but not those reported by Kershaw and co-workers for the Eastern Irish Sea (Kershaw, 1986, Kershaw *et al.*, 1988).

DEPTH INTERVAL (cm)	INORGANIC		ORGANIC
	pM±1σ	AGE±1σ	pM±1σ
0 - 5	53.8±0.7	4980±100	211.5±1.1
5 - 10	53.3±0.5	5060±80	192.2±1.3
10 - 15	36.8±0.4	8030±90	233.4±0.8
15 - 20	32.7±0.3	8980±70	256.1±1.5
20 - 25	32.7±0.4	8980±100	233.8±0.9

Table 3.13: ^{14}C specific activities and corresponding ages measured in sediment core from station C8 (54°25.0'N03°33.9'W).

The ^{14}C specific activities of the inorganic and organic sedimentary carbon pools are markedly different. The inorganic pool is depleted in ^{14}C while the organic pool is enriched. Figures 3.27 (a) and (b) show the distribution of ^{14}C within the two fractions of the sediment core. The degree of ^{14}C depletion in the inorganic fraction is greatest at

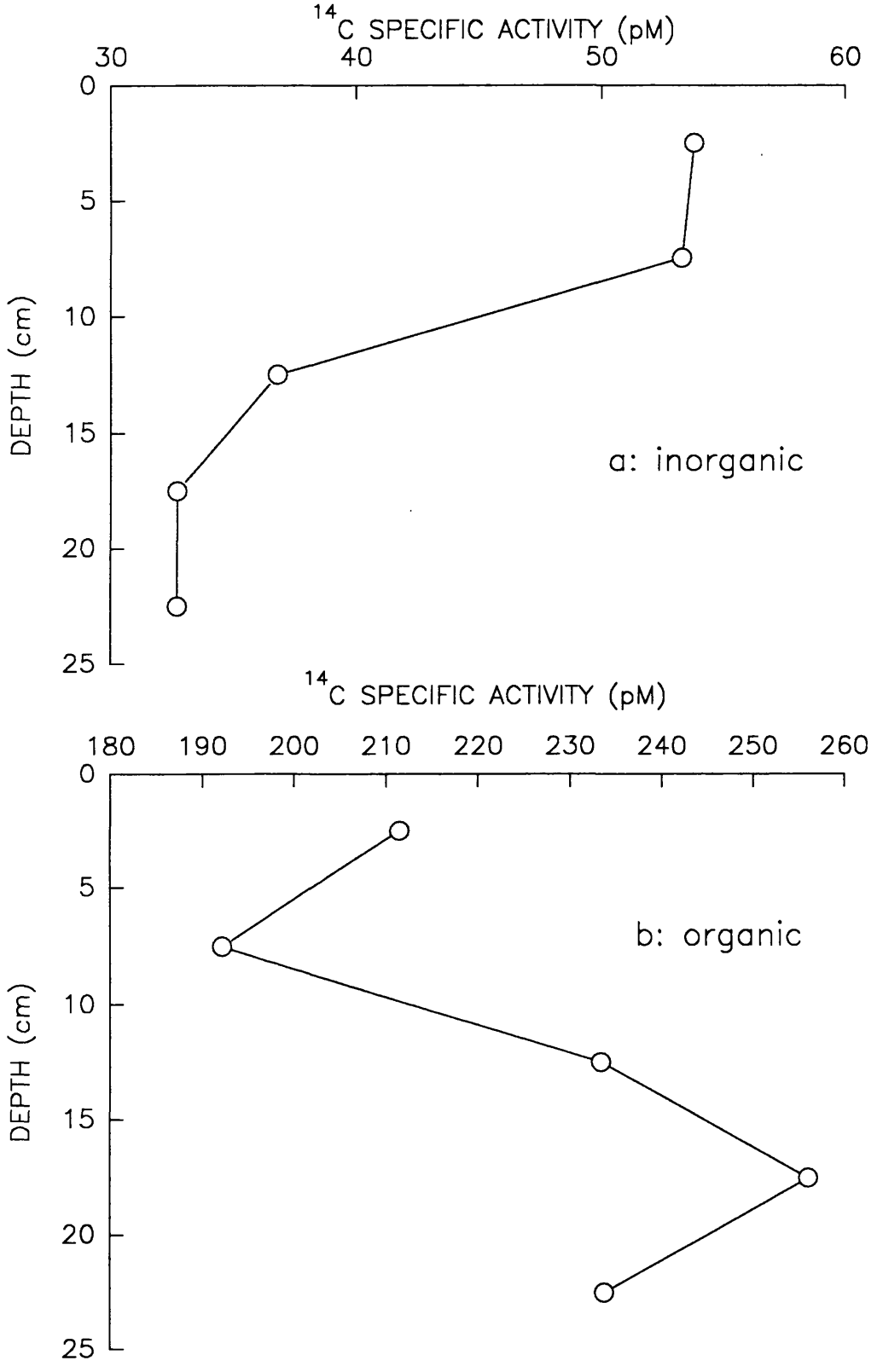

Figure 3.27: Measured ^{14}C activity in the inorganic and organic fractions of the sediment core (0-25 cm).

depths of 15 - 25 cm with the highest activity material found in the top 10 cm. An intermediate activity is found in the 10 - 15 cm interval. In comparison, the organic fraction appears to be enriched in ^{14}C to depths of ≥25 cm. The lowest activity samples are found within the top 10 cm of the core while the highest activity material seems to be sandwiched between two areas of intermediate activity at 15 - 20 cm.

While the ^{14}C distribution in the inorganic fraction would indicate the occurrence of sedimentation in the area, this is not supported by the distribution seen in the organic fraction. The activities in the inorganic fraction are similar to those which have been found in the PIC of the water column (Table 3.10) providing some indication that these have a common source. Assuming that this is also the case for the organic material, evidence of enriched organic material should be present in the water column. Suspended particulate organic carbon sampled from the water column does not appear to be enriched in ^{14}C (Table 3.10) but these samples were collected from surface water and do not rule out the presence of enriched POC further down the water column.

Phytoplankton sampled during April 1989 had a ^{14}C activity of 270 pM indicating that there is a potential source of enriched organic carbon in the water column. Sellafield-derived ^{14}C, released as dissolved inorganic carbon, would be converted into organic material during photosynthesis by phytoplankton and could then fall to the sea floor as faecal material and/or on death of the organisms. In addition to the production of particulate organic carbon in surface waters by this method, particulate inorganic carbon would also be produced from the DIC by organisms, hence the flux of inorganic carbon to the sediments should also be enriched in ^{14}C. While this ensures a supply of material enriched in ^{14}C to the sediments, some other mechanism must be responsible for the distribution pattern observed in the core. The data obtained for the organic fractions support the accepted theory that the mud patch is subject to bioturbation (Kirby *et al.*, 1983; Kershaw *et al.*, 1983; Kershaw *et al.*, 1984; Kershaw, 1986) which will ensure the incorporation of fresh material to depth in the sediment. Therefore, the distribution of ^{14}C observed in the sedimentary inorganic carbon is not a function of the decay of ^{14}C, as it first appears, but is more likely to be due to enriched material arriving at the surface being mixed with older, ^{14}C depleted carbonates. The organic fraction will undergo oxidation, hence the turnover time is shorter than that for the inorganic fraction and the time available for decay of ^{14}C is negligible, resulting in specific activities above the current ambient

level.

Although the sedimentary organic carbon and the phytoplankton indicate that there are enriched particulates in the water column, the level of enrichment is still not as high as that observed in the mussels. This implies that either there is a source of highly enriched particulate material that has not been measured or that the sources have been measured but are sensitive to the timing of Sellafield discharges.

Attempts were made in February 1991 to obtain two cores from the mud patch in which the water - sediment interface was undisturbed. This would have allowed the determination of the ^{14}C specific activity of the material reaching the sea bed from the water column. Unfortunately, weather conditions at the time of sampling prevented coring and grab samples were collected instead. The top 2 cm were removed from each grab sample for ^{14}C determination in the inorganic and organic fractions (Table 3.14).

STATION	LOCATION	INORGANIC		ORGANIC
		pM±1σ	AGE±1σ	pM±1σ
208	54°24.9'N03°40.2'W	31.7±0.9	9230±230	224.0±4.6
206	54°29.8'N03°42.4'W	34.9±1.1	8460±250	223.5±5.0

Table 3.14: ^{14}C specific activity and the corresponding ages measured in 0-2 cm sediment samples from the mud patch.

These show reasonable agreement with each other for both fractions but not with the inorganic fraction of the samples collected with the corer. This may be a result of mixing on entrance of the grab sampler into the sediment. While unable to determine the ^{14}C specific activity of material reaching the sea bed from these samples, they do indicate that the mud patch sediment is fairly well mixed. Station 206 is situated just off St. Bees Head whereas Station 208 is close to the discharge pipe at Sellafield and yet a very similar pattern is observed in the two fractions of the sediment. Bioturbation will mix the sediment vertically but either mixing occurs horizontally as well or the source of material to the sea bed is of a similar activity at both sites. The ^{14}C specific activity found in the DIC at sites close to each of these stations is fairly similar, hence this might indicate that

the source material is of a similar activity. This however does not rule out the movement of sediment within the area, as particulate transport is thought to be the major mechanism for radionuclide transfer to the Solway coast (MacKenzie *et al.*, 1987; Garland *et al.*, 1989; McDonald *et al.*, 1990). The specific activity of the radionuclides ^{137}Cs, ^{241}Am and $^{239,240}Pu$ measured on a transect from Sellafield to the Solway is thought to be a function of particle size rather than the distance from Sellafield (McDonald *et al.*, 1990) with the relative influence of particulate transport decreasing towards the North Channel where transport in the dissolved phase becomes more important (MacKenzie *et al.*, 1987).

In an attempt to determine whether ^{14}C enriched particulate material was being transported, two sites on the Solway and three on the Cumbrian coast were chosen for the collection of intertidal surface sediment samples. The chosen sites and observed ^{14}C specific activities are shown in Table 3.15.

SITE	No.*	FRACTION	pM±1σ	AGE±1σ
Earnse Point	1	Inorganic	49.9±0.5	5580±80
Ravenglass	4	Inorganic	76.2±1.1	2180±115
Ravenglass	4	Organic	194.7±1.4	-
Sellafield	6	Inorganic	65.3±0.8	3420±100
Rockcliffe	13	Inorganic	24.8±0.5	11200±160
Creetown	14-15**	Inorganic	68.3±0.5	3060±60

Table 3.15: ^{14}C specific activities found in intertidal sediments from the Solway and Cumbrian coasts.

* Site Nos. taken from Figure 3.1

** mid-way between sites 14 and 15 in Figure 3.1

From the results shown, the ^{14}C activity in the intertidal sediments is extremely variable. At all sites, the inorganic fraction was depleted in ^{14}C with respect to the current ambient level, whereas, the one organic sample analysed was enriched. Unfortunately, in most of

the samples there was insufficient organic matter present to allow measurement of the ^{14}C specific activity. However, from the sample which did have sufficient organic matter present, the distribution between the two phases is similar to that already observed in bottom sediments collected from the mud patch.

The inorganic sample collected at Ravenglass has a higher activity than that seen at either Earnse Point or Sellafield indicating possible incorporation of Sellafield-derived ^{14}C. The degree of enhancement in the organic sediment is less than that seen in either the intertidal biota or the DIC from the water column in that area which indicates that the higher activity material being added to the surface sediments, by the death of organisms *etc.*, may be diluted by older, less active material already present. From the limited number of samples collected and analysed it is very difficult to determine whether the intertidal sediments will act as a sink for Sellafield-derived ^{14}C although it would appear that the organic fraction is participating in carbon transfer in the coastal environment. This, in fact, could increase the availability of ^{14}C to organisms which feed off the intertidal sediments which may in time return ^{14}C to the local human population.

3.2.4 Supplementary carbon containing reservoirs

So far, this work has considered the ^{14}C specific activity present in intertidal biota samples, the biogeochemical fractions of the water column and both the bottom and intertidal sediments of the study area. While these have been the most studied reservoirs in this determination of the environmental distribution of ^{14}C, a number of other carbon containing pools have been studied in less detail. These will be discussed briefly in the following sections.

3.2.4.1 Fish

Flatfish such as plaice and dab feed on the surface of bottom sediments (Pentreath, 1984), hence, ^{14}C enhancements found in such samples must have originated in the sediment on which the fish feed. In this study, samples of fillet from both dab and plaice, collected 2 km south of the Sellafield pipeline in November 1989, were obtained from MAFF. Both species are enhanced relative to ambient background levels (502.3±1.2 and 398.4±1.2 pM, respectively) with the activities measured being similar to those previously found in mussels and winkles. This indicates that the surface sediments must have a source of carbon enriched in ^{14}C which is easily incorporated into organisms feeding on the

sediment. Although not ruling out the possibility of particulate releases, this indicates that Sellafield-derived ^{14}C, although initially inorganic in nature, is rapidly incorporated into organic material in the water column and may be retained by organisms, *eg.* fish, and returned to man.

3.2.4.2 Air

An air sample was collected along a transect in the Eastern Irish Sea in February 1991 to ensure that any enhancements found in the marine environment were a direct result of inputs from the installations being studied, as opposed to transfer of enhanced atmospheric CO_2 into surface waters. The measured activity in air above the Irish Sea, after fractionation was taken into account, was 116.1±2.0 pM (262.4±4.5 Bq kg^{-1} C) which is in agreement with the overall value calculated from the samples considered in Table 3.1. Hence, enhanced levels of ^{14}C in the Irish Sea are conclusively the result of direct inputs into the aquatic system.

3.2.4.3 Terrestrial vegetation

Although this study is concerned primarily with ^{14}C inputs *via* low level liquid wastes into coastal waters, atmospheric discharges account for 55-80% of the total ^{14}C released from Sellafield. Determination of ^{14}C specific activities in vegetation from the area will allow comparison with those found in marine biota to help assess the relative risks to the local population. For this study, grass was collected on two transects - one to the east of Sellafield and the other northeast from Sellafield. The results obtained are shown in Table 3.16 with the distance of the sampling site from the discharge location. Figure 3.28 illustrates the differences in the distribution along the two transects.

SITE	DISTANCE (km)	pM±1σ	Bq kg^{-1} C±1σ
		East Transect	
1	0.7	129.0±0.7	291.2±1.5
2	0.8	132.6±0.5	299.6±1.3
3	1.35	143.4±0.8	324.1±1.8
4	2.0	165.5±0.5	373.9±1.2
5	2.85	263.0±0.8	594.4±1.7
6	3.85	245.8±0.9	555.5±2.0
		Northeast Transect	
1	1.0	185.0±0.3	418.1±0.8
2	1.35	154.7±0.5	349.7±1.1
3	1.75	153.6±0.8	347.2±1.8
4	2.6	142.2±0.8	321.3±1.7
5	3.2	141.8±0.4	320.4±1.0
6	4.15	131.0±0.6	295.9±1.4

Table 3.16: ^{14}C specific activities obtained for the two grass transects in the vicinity of Sellafield.

All the samples were collected in November 1988 when ~14% of the wind during the growing season had been to the east and the total atmospheric discharge for the year was 3.6 TBq. These results are considerably less than those measured in seaweed at comparable distances, indicating greater dilution of the atmopheric discharges when released.

Previous work by McCartney (1987), studied the dispersion of gaseous ^{14}C discharges from Sellafield by analysing grass growing in the area. The maximum observed activity was found 0.4 km northeast of the discharge point and was over four times higher than the ambient background level at that time. Atmospheric dispersion models utilising wind rose data for the year of interest were then used to determine the direction and value of maximum ^{14}C enhancements based on the observed data. These allowed the calculation of the radiological risk to local populations. In part, the grass samples collected in this study were to determine the accuracy of such predictions. However, the predictions were based on the observations made to the northeast of Sellafield and the format of the wind

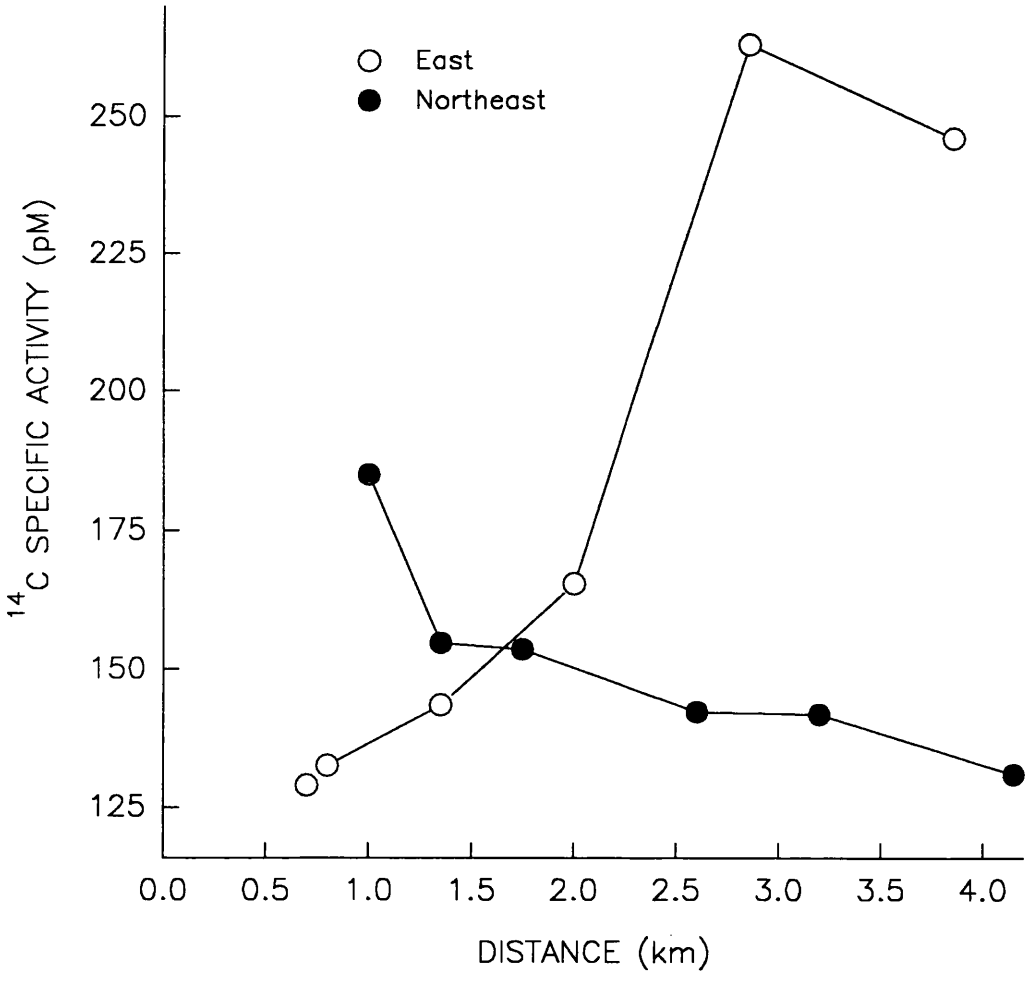

Figure 3.28: Measured ^{14}C activity in the grass samples from two transects.

rose data available for 1988 did not allow the direct application of the model used in previous studies. The data collected during this study indicated that the maximum ^{14}C specific activity observed in grass for 1988 was approximately twice the ambient background level and found 2.85 km to the east of Sellafield whereas McCartney (1987) found levels of ~500 pM to the northeast of Sellafield at a distance of 0.34 km in 1985. These observed levels are obviously dependent on the levels of ^{14}C discharged, with 3.6 and 7 TBq released during 1988 and 1985 respectively, explaining the lower observed values in this study. The wind conditions at the time of release will determine the direction and distance to which enhanced levels are found.

Due to the length of the transects on which terrestrial vegetation was collected, a direct comparison of the ^{14}C distribution in the terrestrial and aquatic environments cannot be carried out. However, McCartney (1987) observed enhanced levels of 131 pM in grass up to 37.5 km north of the discharge location in 1985 when the atmospheric discharges were double the present day liquid releases. In the present study, this level of activity was found approximately 140 km from the discharge point, again indicating that Sellafield-derived ^{14}C is subject to much greater atmospheric dispersion. In addition to this, if atmospheric discharges are spasmodic, they are quickly dispersed by the wind, whereas, spasmodic releases to the marine system would not be as readily dispersed because of the water currents previously described. This could potentially be important in radiological studies as marine biota will be subject to enhancements in their environment for a longer time period after release.

3.2.5 Overview of the Data

The data presented in the previous sections are all relevant to determining the chemical form and distribution of ^{14}C discharged from Sellafield into the Eastern Irish Sea, hence this section will bring these results together and set out the main findings of this study. Firstly, intertidal biota samples have enrichments in ^{14}C at least as far north as the Clyde Sea area. In the immediate vicinity of the releases, inter-organism selectivity is apparent, with mussels consistently having higher ^{14}C specific activities than winkles which in turn have higher levels than seaweeds. This suggests the presence of enriched particulate and DIC material; as mussels retain particulate material from the water column and seaweeds obtain their carbon from the DIC. Winkles have intermediate values as they utilise both

the particulate and indirectly the dissolved inorganic carbon pool *via* algae consumption. These results led to the isolation and analysis of four biogeochemical fractions from the water column; DIC, DOC, PIC and POC. However, although evidence of enriched DIC was found, the particulate material and the DOC were depleted in ^{14}C. Initial sampling provided some indication of a link between the DIC and the POC which propelled the study towards looking at processes which may account for these observations. One of the most obvious processes is the uptake of DIC during photosynthesis by phytoplankton, leading to the incorporation of inorganic carbon into organic matter. However, all the sampling carried out during this study was in winter months, *ie.* when virtually no phytoplankton were present. A phytoplankton sample obtained from MAFF had a ^{14}C specific activity comparable to that observed in the DIC but was not high enough to explain the level of enrichment observed in the intertidal biota. This, therefore, indicates that a more highly enriched environment has been present in the recent past, certainly within the lifespan of the mussels and winkles, or that there is a supply of enriched particulate material from Sellafield. Of the two, the former is more likely as an enriched particulate source from Sellafield would manifest itself throughout the entire year. In addition, the discharges calculated during this work from Nori samples (Fig 3.9) suggest that higher levels of ^{14}C were discharged in the past, which could help explain the observations.

When the sediments were studied, there was a definite partitioning between the inorganic and organic fractions. The inorganic fraction was depleted in ^{14}C, whereas, the organic fraction was enriched. This is not only a reflection of the ^{14}C specific activity of the material reaching the sediment surface but is also a consequence of the relatively rapid oxidation and turnover of the organic material. Fish which feed on these sediments were more highly enriched in ^{14}C than the organic fraction, indicating that there must be areas where the activity in the sediment is higher than that measured during this study.

In summary, these results imply that ^{14}C discharges from Sellafield are in a dissolved inorganic form which is taken up by phytoplankton and subsequently distributed throughout the food chain.

As an additional part of this work, the ^{14}C distribution within the DIC fraction of the water column was studied in relation to measured activities of ^{137}Cs in seawater. The results indicate that the two nuclides behave similarly; both reflecting the predominant residual

surface currents in the area. However, analysis of a $^{14}C/^{137}Cs$ ratio implies that the ^{14}C is not behaving as conservatively as the ^{137}Cs which may be a result of biological activity within the water column or the ratios may be influenced by the desorption of ^{137}Cs from the sediments.

To determine the influence exerted by phytoplankton on carbon distribution, both stable and ^{14}C, a temporal study over a 12 or 24 month period is required. Analysis of ^{137}Cs in a similar study would provide additional information on the degree of conservatism shown by ^{14}C in the DIC, and whether biological activity was responsible for the variations observed in the $^{14}C/^{137}Cs$ ratio.

3.2.6 Sellafield-derived ^{14}C Distribution: Interpretation Using Mathematical Modelling

Mathematical models are empirical representations of natural systems and their determining and important processes, *ie.* they provide a "simple" empirical description of a typically complex environmental system. Model structures permit, not only the prediction of future distribution patterns, but also on comparison with actual observations, may help identify the most important and influential processes within the system. Models of environmental systems range from the very simple one or two box representations to relatively complex compartmental models, such as the ^{137}Cs model developed by Bradley *et al.*, (1991) or the global carbon cycle models discussed in Chapter 4, which average over space, time and the volume of the compartment. More complex, physical, two and three dimensional models (Bryan and Lewis, 1979; Toggweiler *et al.*, 1989a,b) also exist for both the atmosphere and ocean and are widely used in climatic studies.

The development of any model structure requires firstly a description of the system to be modelled, *ie.* a definition of the compartments to be considered. The structure of the compartments is based on a number of criteria including a good physical description of the situation *eg.* in hydrographic models this would include known information on the currents and depths *etc.* in the area. In addition, the structure should at least approximately satisfy the assumption of homogeneity of the pollutant of interest within each of the compartments. Once the structure of the model has been defined, the parameters must be determined. These include the initial starting conditions, the concentration of the component of interest in each compartment and the transfer coefficients between the various compartments. These values will obviously be determined from both the literature

and experimental results. Finally, the model structure and parameter values should be validated against experimental results to confirm that the model adequately represents reality and that the predictions are credible.

Within this section there are two main aims in the modelling work *ie.*

1. to consider the behaviour of the ^{14}C in the dissolved inorganic carbon phase *ie.* its dispersal and distribution in the region of interest

2. to consider the more complex biogeochemical cycling occurring within the water column to provide a description, in physical terms, of the inter-relationships between the various phases, and to begin the development of an appropriate model structure. During such work, the system will be described and the parameters determined. Validation of the model structure will not be possible, due to current lack of appropriate experimental data, but producing the basic structure and evaluating parameters will indicate the areas where current knowledge is limited and requiring additional study.

3.2.6.1 DIC dispersal

A considerable portion of this work studied the distribution of ^{14}C in the dissolved inorganic carbon phase of the water column in a number of widely distributed locations, to determine its geographical distribution and chemical behaviour. In addition, ^{137}Cs - a conservative radioactive tracer - was also measured. ^{137}Cs observations over an extensive time period have previously been used to determine water movement within the Irish Sea and Scottish coastal waters and thus ^{137}Cs results give a good indication of water movement within the area. A model developed by Bradley *et al.* (1991) has used this extensive data set in conjunction with inverse compartmental analysis (ICA) to determine transfer coefficients between the defined compartments within the model structure. The model structure is detailed in Figure 3.29 and comprises 10 compartments connected by 20 transfer coefficients. This model has been shown to:-

1) exploit logistic sense in its construction as it is based on known hydrographic flow patterns and distributions,

2) demonstrate a good fit between observed and predicted values and

3) have parameters which are similar to measured environmental parameters.

These permit the model to be used to describe the complex hydrography of the western Scottish coastal current system to predict future radionuclide levels in Scottish waters in response to continuing Sellafield discharges of ^{137}Cs and potentially for other radionuclides.

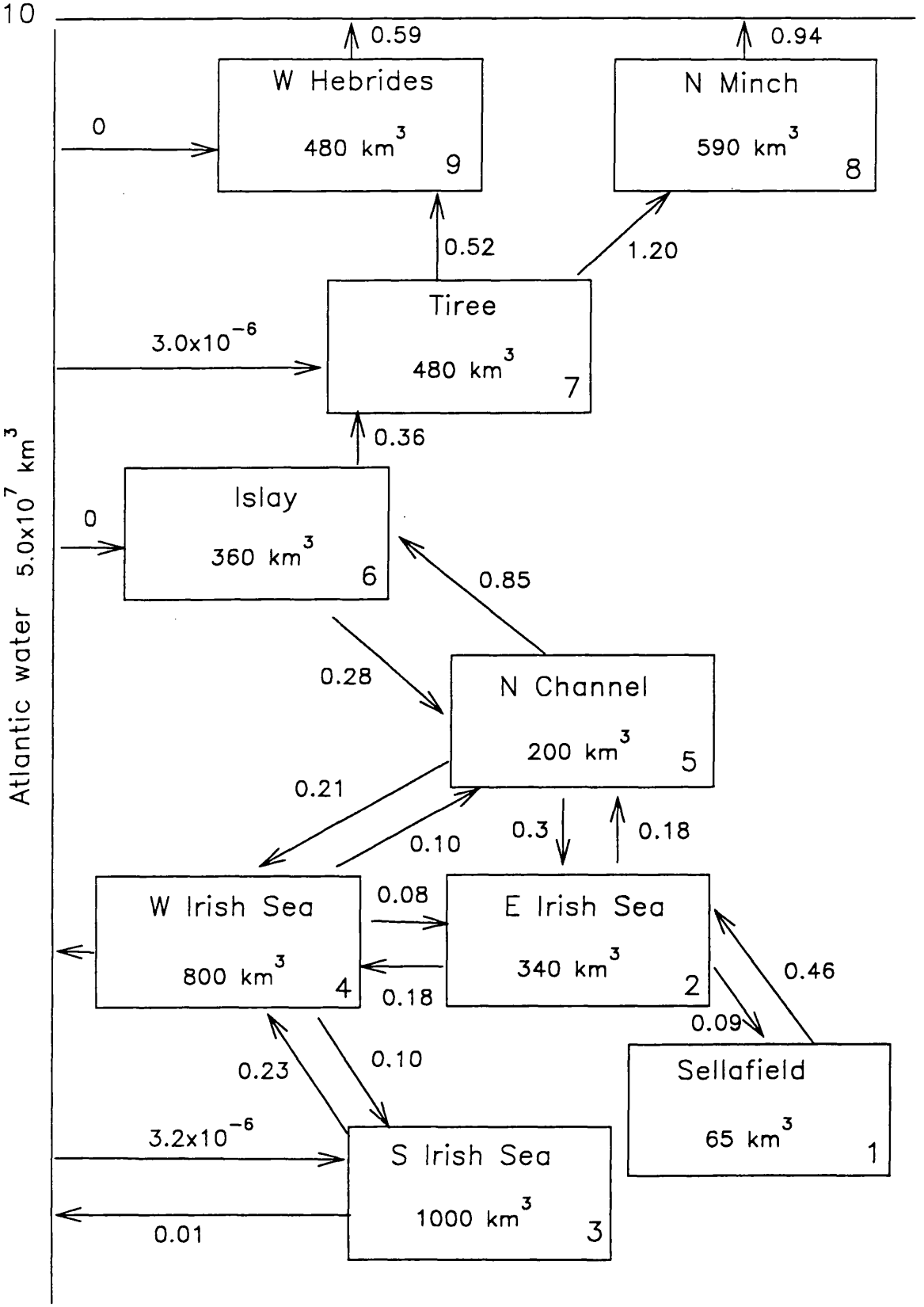

Figure 3.29: The ^{137}Cs compartmental model developed by Bradley *et al.*, (1991).

This study will provide a preliminary assessment of its use for ^{14}C.

To incorporate the transfer of carbon into this model structure it is necessary to define starting parameters *ie.* the initial mass of ^{14}C in each compartment. This quantity must be calculated from the mass of stable carbon and an assumed initial specific activity in each compartment. In this case, where the compartment contents are given as volume of water, the carbon content is calculated from a DIC concentration of 24-30 mgC l^{-1} (Lassey *et al.*,1988; Chester, 1990) and the mass of ^{14}C from a specific activity of 226 Bq $kg^{-1}C$ for the year 1953. The influence of nuclear weapon-derived ^{14}C can be incorporated, once the model has been run, by adding a value which corresponds to the approximate excess over the baseline value in each year that the model covers. As all the quantities within the model structure must be in the same units, *ie.* mass is in grams of ^{14}C while the time factor is months, the annual discharges of ^{14}C from Sellafield are assumed to occur at a constant rate throughout the year.

Initial studies involved the model being run with no ^{14}C in the compartments and an input of 1 TBq of ^{14}C from Sellafield. The results from this show that in the year of discharge, less than 5% of the input remains in the Sellafield compartment with 17%, 16% and 29% being found in the Eastern Irish Sea, the Western Irish Sea and the Atlantic waters, respectively. After 5 years, only 0.2% remains in the Sellafield compartment with 97% incorporated into the Atlantic waters. It takes over eight years for the total input of 1 TBq to be flushed out of the Irish Sea and Scottish coastal waters into the Atlantic.

Further studies used the estimated discharges from Sellafield into the Irish Sea for the time period 1953 to 1990. The mass of ^{14}C and ^{12}C considered to be in each compartment is detailed in Table 3.17.

BOX No.	NAME	VOLUME (km^3)	MASS OF ^{12}C (g)	MASS OF ^{14}C (g)
1	Sellafield	65	1.79×10^{12}	2.45
2	Eastern Irish Sea	340	9.35×10^{12}	12.81
3	Southern Irish Sea	1000	2.75×10^{13}	37.66
4	Western Irish Sea	800	2.2×10^{13}	30.13
5	North Channel	200	5.5×10^{12}	7.53
6	Islay	360	9.9×10^{12}	13.56
7	Tiree	480	1.32×10^{13}	18.08
8	North Minch	590	1.62×10^{13}	22.22
9	Western Hebrides	480	1.32×10^{13}	18.08
10	Atlantic waters	5.0×10^{7}	1.38×10^{18}	1.88×10^{6}

Table 3.17: The parameters used in the model to determine Sellafield-derived ^{14}C distribution.

Figure 3.30 illustrates the results obtained using the model and the estimated discharge data for five of the ten compartments. This demonstrates, as one would expect, that the specific activity in each year is highest in the Sellafield compartment and decreases as a function of distance from Sellafield. The predicted values for the Eastern Irish Sea and the North Channel are consistently higher than those for the Southern Irish Sea. Although the Atlantic waters appear to increase slightly from the baseline value (226 Bq $kg^{-1}C$) this, in the main, is due to the inputs of ^{14}C from nuclear weapons tests rather than the influence of Sellafield. To assess the model validity, we compare the model predictions for 1989 with the data determined during this study (Tables 3.8 and 3.10). Assuming that Stations C8, C12, C15 (Table 3.8) and C7 (Table 3.10) represent Sellafield, the Eastern Irish Sea, the North Channel and the Southern Irish Sea, respectively, the model predictions can be compared to actual measured ^{14}C specific activities (Table 3.18).

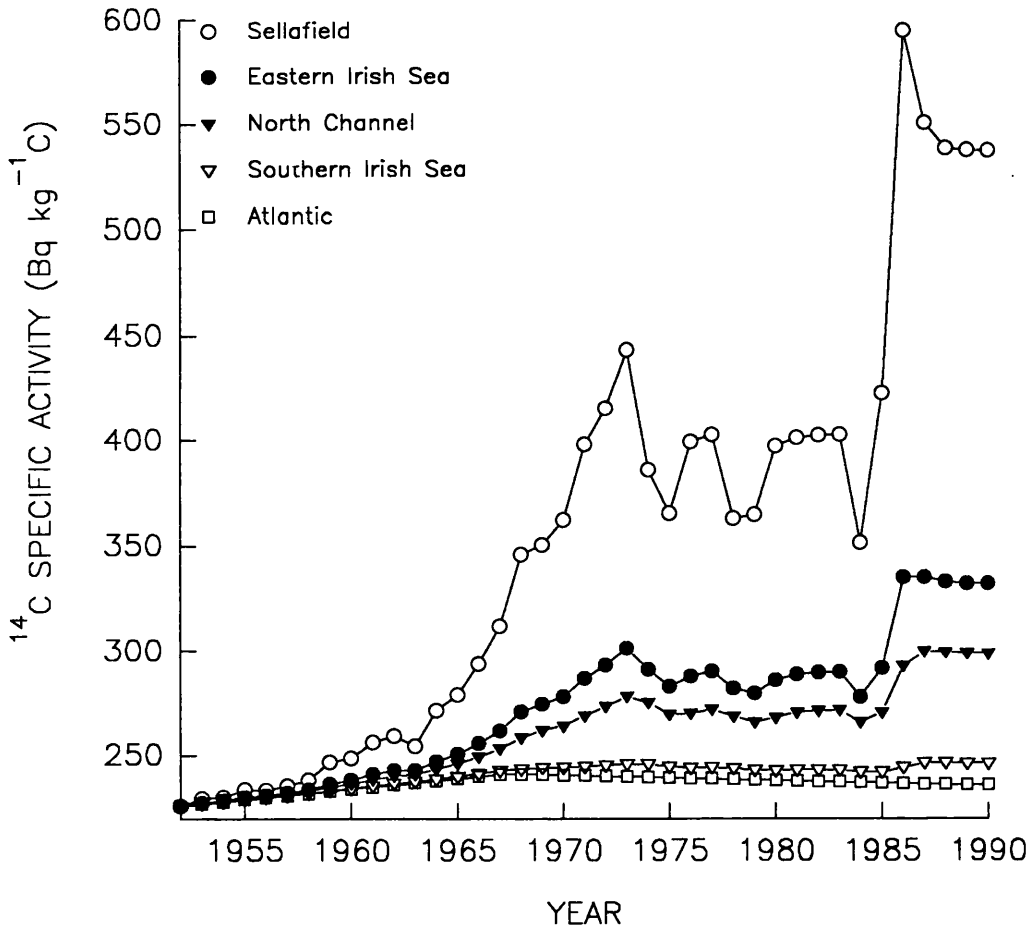

Figure 3.30: Model predictions for the ^{14}C specific activities in generalised areas of the Irish Sea.

BOX No.	STATION No.	PREDICTED ACTIVITY (Bq $kg^{-1}C$)	OBSERVED ACTIVITY (Bq $kg^{-1}C$)
1 - Sellafield	C8	537.1	571.1±1.1
2 - Eastern Irish Sea	C12	332.1	353.0±0.9
5 - North Channel	C15	298.6	307.1±0.7
3 - Southern Irish Sea	C7	246.1	270.7±1.8

Table 3.18: Predictions of ^{14}C specific activity in 1989 using the model developed by Bradley *et al.* (1991) with actual measured values in 1989.

The agreement between the two sets of data is excellent remembering that the model is smoothing the distributions in the compartments and that it is producing "averaged" ^{14}C specific activities. Time has only allowed a brief study on the use of such models to determine ^{14}C distribution, but the data obtained so far are promising and indicate that further work in this area would be viable. However, until more information is available about biological influences on the dispersal of ^{14}C and/or more observations are made to allow further validation of the model structure, the simple $^{14}C/^{137}Cs$ ratio calculated in Section 3.2.2 provides a simple and reasonable interpretation of ^{14}C behaviour in the Irish Sea and Scottish coastal waters.

3.2.6.2 Biogeochemical cycling

While a model of the type described in the previous section permits the determination of the distribution pattern of certain nuclides with respect to water movement it has no provision for processes, such as biological activity, which this work has indicated will influence the dispersal of ^{14}C. As a result of the sampling and analyses carried out during this study, it appears that the biogeochemical fractions, the phytoplankton and the sediments are all influenced by anthropogenic inputs of ^{14}C from nuclear and radiochemical establishments, hence, these reservoirs must be included in any model developed to represent the marine carbon cycle. The model structure developed in this study is detailed in Figure 3.31. In the diagram, the present day mass of stable carbon (in grams) is presented as the top figure in each compartment with the lower figure representing the mass of ^{14}C in grams. The fluxes between each of the compartments are shown in

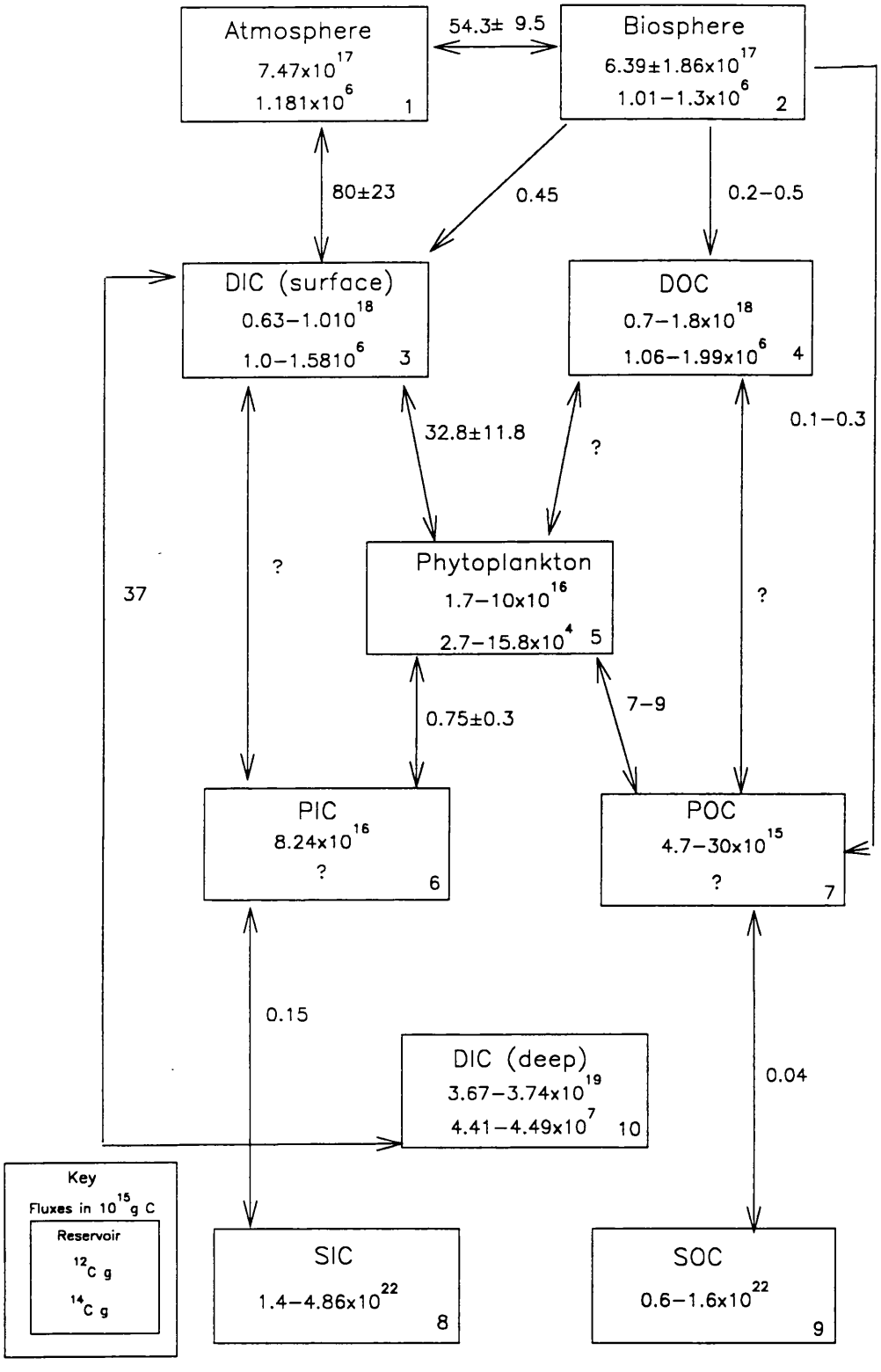

Figure 3.31: The structure of the marine biogeochemical carbon cycle.

petagrams (and hence have to be multiplied by 10^{15}). The structure consists of 10 compartments, three of which represent the atmosphere, the terrestrial biosphere and the deep ocean to ensure that the the flux of carbon to the surface ocean is regulated. Two compartments represent the sediment - one for the organic component and the other for the inorganic component. The remaining five compartments represent the biogeochemical fractions of surface water including the phytoplankton. The phytoplankton reservoir in this model structure is present in an attempt to mimic biological uptake of DIC and its conversion to organic material. The biogeochemical fractions have not been subdivided on the basis of depth in the water column, thus we assume that the majority of determining processes occur within the surface water. Druffel and Williams (1990) have shown that this is not the case as rapidly sinking POC, such as faecal pellets, ensures the transfer of carbon enriched in ^{14}C to deep waters. However, the data collected for the biogeochemical fractions from the Irish Sea were all collected from surface waters as the Irish Sea is relatively shallow and considered to be well-mixed, therefore, initial model structures were restricted to surface water processes with the sediment and deep water DIC boxes added later to try and maintain the total mass of carbon in the model.

While the carbon content of some of the compartments is fairly well known, such as the atmosphere, the biosphere and the DIC of the deep and surface waters, there are others which are at present still under debate, in particular the DOC (Sugimura and Suzuki, 1988; Bauer *et al.*, 1992; Kepkay and Wells, 1992; Martin and Fitzwater, 1992; Ogawa and Ogura, 1992), or have been essentially ignored in previous studies, *eg.* the PIC. The amount of ^{14}C data available is limited, therefore, in this study the ^{14}C content of the compartments is deduced from this limited data and general assumptions regarding the potential ^{14}C specific activity for each compartment. The data used to generate this structure have been taken from a number of sources including those referred to in Chapter 1 plus several, more in-depth studies of the biogeochemistry of the oceans (Williams, 1975; Williams and Druffel, 1987; Druffel and Williams, 1990; Longhurst, 1991; Martin and Fitzwater, 1992; Toggweiler, 1992). Most texts tend to quote a total inorganic particulate concentration rather than one for inorganic carbon, hence the mass of carbon in the PIC fraction presented here is based on a concentration of 0.061 mgC l^{-1} determined from the biogeochemical work carried out during this study. This figure is obviously a rough estimate but gives some idea of the level of carbon present in this reservoir. As the

model is based on present day stable carbon levels, the mass of ^{14}C in each compartment has been based on the current ambient level measured during this work of 260.8 Bq $kg^{-1}C$ for both the atmosphere and surface oceans. Both the biosphere and phytoplankton which are considered to be in rapid equilibrium with their carbon sources, *ie.* the atmosphere and surface oceans respectively, are also assumed to have a ^{14}C specific activity of 260.8 Bq $kg^{-1}C$. Williams and Druffel (1987) indicated that DIC and DOC distributions were similar with depth; the DOC being depleted in ^{14}C relative to the DIC by approximately 30%. This relationship can be used to calculate the mass of ^{14}C required to exhibit a specific activity of 182.6 Bq $kg^{-1}C$ (*ie.* 70% of that present in the surface DIC) for the DOC in surface water. In the same study (Williams and Druffel, 1987), the measured ^{14}C activity for deep water DIC was -240‰ ($\Delta^{14}C$) allowing a similar calculation to be made to ascertain the mass of ^{14}C required in the deep water DIC to equate to a specific activity of 198.2 Bq $kg^{-1}C$.

The fluxes between the compartments are based on the figures presented by Longhurst (1991) and are the best estimates available at present. However, many of them are net transfer rates only and further development of the model would require these net transfers to be divided into their constituent two-way flows. A number of the parameters between the reservoirs are unknown, especially those associated with the phytoplankton and DOC. These may become available reasonably soon as a great deal of interest has arisen in the study of DOC; its sources, reactivity and its role in the cycling of carbon in surface and deep waters. A DOC Working Group recommends that the DOC considered in biogeochemical models should be represented by three pools - a labile fraction which has a turnover time of days, a refractory fraction with a turnover rate of centuries and a semi-refractory fraction which may be more seasonal in nature (Scott, pers. comm., 1992). However, this degree of fractionation was not the impetus behind the biogeochemical modelling carried out in this study. The main interest here was to produce a carbon cycle model which could explain the distribution of anthropogenic ^{14}C, in terms of chemical form, within the biogeochemical fractions. While the model structure postulated is not at the stage to allow its use, it has brought together some of the necessary information, in addition to indicating areas where further research is required.

Further work required before validation of such a model would involve obtaining a temporal sequence of observations in each of the compartments to determine the influence

of biological activity. To reduce some of the variation present in the data, further study needs to include determining the concentration of the different biogeochemical fractions present and their ^{14}C specific activity. In addition, ^{14}C data needs to be acquired from a site at which anthropogenic inputs are not affecting the observed specific activities so that the influence of discharges from Sellafield and Amersham could be ascertained. It would also be beneficial to such studies if there was more detailed information on the timing, quantity and chemical form of the releases from the installations of interest.

3.3 AMERSHAM INTERNATIONAL plc, CARDIFF

Apart from Sellafield, the only other U.K. establishment which monitors its ^{14}C releases separately from total beta discharges is the radiochemical plant owned by Amersham International plc in Cardiff. The sampling undertaken in this area was less extensive than that carried out in the vicinity of Sellafield, but again it included both intertidal areas and the water column in the determination of the spatial distribution of the ^{14}C releases. MAFF indicate (Hunt, 1992) that Amersham International plc discharge ^{14}C into Cardiff Bay and from the position of the plant, on the banks of the River Taff, it is assumed that the discharges are into the river which flows into Cardiff Bay just north of Penarth Head. Figure 3.32 shows the study area and the positions of the sampling sites used during this study.

3.3.1 Intertidal

A total of three intertidal samples were collected from Swanbridge, approximately 7.5 km southwest from the point where the River Taff enters Cardiff Bay (Fig 3.32). The samples available at this site were winkles (*Littorina littorea*), seaweed (*Fucus* spp.) and intertidal sediment of which both the inorganic and organic fractions were analysed. The results obtained for these samples are shown in Table 3.19.

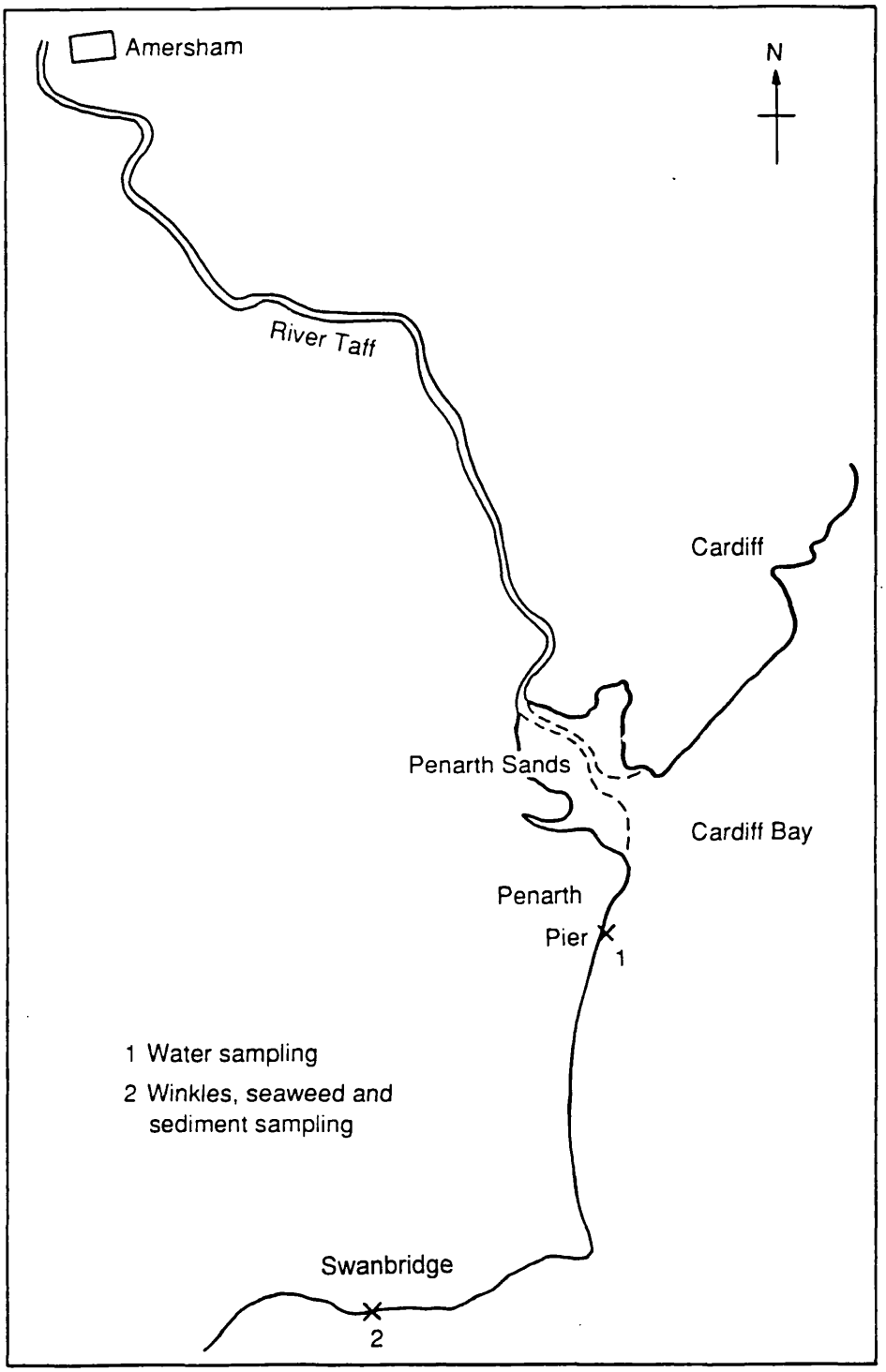

Figure 3.32: Study area and sampling sites of intertidal and shoreline samples in the Bristol Channel.

SAMPLE TYPE	FRACTION	pM±1σ	Bq kg^{-1}C±1σ
Winkles	Organic	391.0±1.3	883.7±2.9
Seaweed	Organic	146.8±0.7	331.8±1.5
Sediment	Inorganic	25.3±0.2	57.1±0.5
Sediment	Organic	137.4±0.8	310.5±1.9

Table 3.19: ^{14}C specific activities measured in intertidal biota samples from the Bristol Channel.

The organism selectivity observed within the Irish Sea sampling area is also apparent at this site in the Bristol Channel. Winkles have a specific activity of approximately four times the current ambient level while seaweed is just above the ambient value of 115.4±0.4 pM. When considered in relation to activities reported by Hunt (1989, 1990, 1992), a fairly good agreement is observed, assuming that seaweed is 15% dry matter (of which 40% is carbon) to convert the results into a comparable format.

Due to the incomplete set of data for both study areas, it is difficult to compare the results from both sites to determine similarities/differences in the distribution within the intertidal biota. However, the ratio of activity in winkles to the activity in seaweed at the sampling sites within the Irish Sea is on average ~1.2, whereas, the ratio at this site in the Bristol Channel is 2.7, indicating that the ^{14}C present may be in a form more readily available to the winkles *ie.* organic particulate. This difference in the ratio also indicates that within the Bristol Channel, the grazing on seaweeds and algae by the winkles is less important in terms of ^{14}C uptake, suggesting that the discharges of ^{14}C from Amersham are in a different chemical form from those released by Sellafield.

Unfortunately, bottom sediments were not collected during cruise CH62B/89 as the sea bed at all sampling stations was too stony to allow the penetration of the grab sampler. However, intertidal sediments which were collected indicate a similar distribution to that observed in the bottom and intertidal sediments of the Irish Sea area *ie.* a depleted inorganic fraction and an enriched organic fraction. The activity in the inorganic fraction is equivalent to a radiocarbon age of 11,040±60 years B.P. which is considerably older than most of those measured in the Irish Sea area.

Overall, the activities found in the sediment and seaweed are comparable, whereas, that for the winkles is considerably higher, indicating that the winkles are being exposed to higher activity material during their lifespan. This could be a reflection of the discharges being particulate in nature. As at Sellafield, the discharges from Amersham appear to be in a form which is readily taken up and incorporated into the organic carbon cycle.

3.3.2 The Water Column

Having studied the intertidal areas and found indications of the incorporation of Amersham-derived ^{14}C, the spatial distribution was considered by a study of the water column DIC. The DIC fraction of the water column was the most extensively studied, with seven of the fourteen samples collected for analysis of ^{14}C being in this fraction. The other three biogeochemical fractions were studied in the remaining seven samples. A transect of six sampling stations was taken from Cardiff, along the Bristol Channel, in December 1989 (CH62B/89). Table 3.20 depicts the results obtained for the DIC samples collected on this transect.

STATION	LOCATION	DISTANCE (km)	pM±1σ	Bq kg^{-1}C±1σ
C0	51°25.3'N03°09.2'W	1.0	476.7±3.3	1077.4±7.6
C1	51°21.0'N03°20.7'W	14.5	304.3±2.6	687.7±6.0
C2	51°20.2'N03°27.3'W	21.0	281.2±2.1	635.4±4.8
C3	51°19.0'N03°38.6'W	34.0	239.8±1.6	542.0±3.5
C5	50°28.0'N04°53.9'W	115.0	120.9±1.4	273.2±3.6
C6	51°38.4'N05°17.0'W	145.0	116.9±0.9	264.5±1.9

Table 3.20: ^{14}C specific activities in DIC from Bristol Channel Transect.

The distribution shown in the ^{14}C activity of the DIC in the Bristol Channel (Fig 3.33) indicates the presence of a point source which is subject to water flow predominantly away from the area. Initial high activities found close to the discharge location (> 4 times the current ambient level) appear to decrease exponentially with distance until reaching current ambient levels at a distance of 145 km from the discharge location. These initial activities are higher than those seen at Sellafield despite the published discharges being smaller in

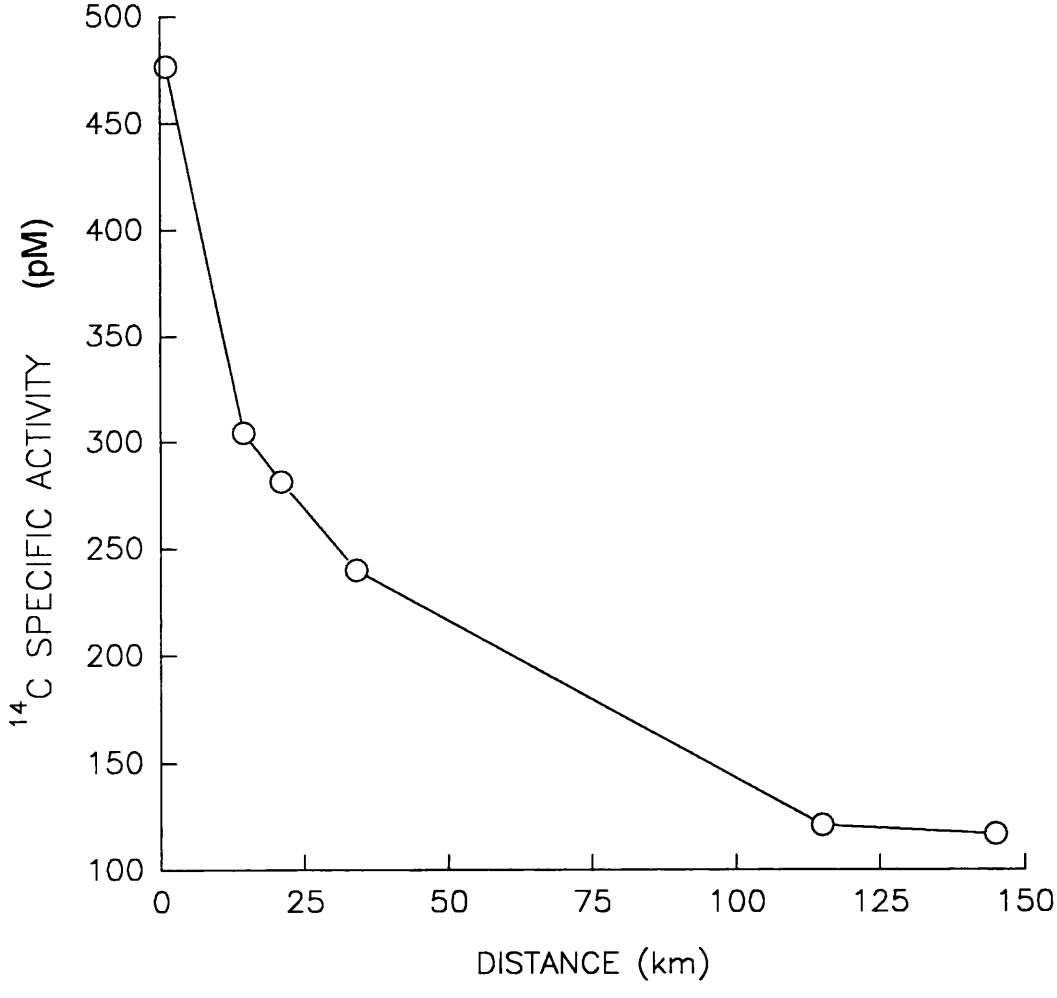

Figure 3.33: Measured ^{14}C activities in DIC on a transect in the Bristol Channel.

magnitude, indicating less initial mixing and dilution. The rate of decrease in activity appears to be higher, with the current ambient level being reached within 145 km as opposed to 245 km in the Irish Sea, but this is likely to be the result of incoming Atlantic water at the mouth of the Bristol Channel. As at Sellafield, it appears that the ^{14}C activity in the DIC at a particular site is determined by the distance from the discharge location and hence, ultimately the local currents.

At one of the sites on the transect (C2), a sample was collected for isolation into the four biogeochemical fractions, to determine the transfer of ^{14}C within the carbon cycle. Due to the loss of one of these samples during analysis at Oxford, a second sampling trip was undertaken where another sample was collected for fractionation into the biogeochemical phases - this time from the shore at Penarth rather than from the middle of the channel. Penarth pier was chosen as the shoreline sampling location not only because of the ease of access but also because it was close to the sampling location C0 on the original transect. Table 3.21 demonstrates the results obtained for the biogeochemical fractions at both the mid-channel and shoreline sampling locations. The distribution observed in these is completely different from that at sites within the Irish Sea, indicating that perhaps the chemical form of the discharges may differ between the two establishments. As stated in Section 3.2.5, the discharges from Sellafield are thought to be dissolved and inorganic in nature, whereas the intertidal biota collected in the Bristol Channel suggest organic particulate releases may occur from Amersham International plc.

FRACTION	MID-CHANNEL (51°20.2'N03°27.3'W) December 1989	SHORE (51°25.9'N03°09.6'W) June 1991
	(all results reported as pM±1σ)	
DIC	271.2±1.8	139.4±1.2
PIC	40.4±0.5	46.3±0.7
POC	151.6±1.0	439.2±4.3
DOC	na	287.3±2.4

Table 3.21: ^{14}C activities measured in the biogeochemical fractions from the Bristol Channel.

(na=not available)

Samples collected in mid-channel differ greatly in their ^{14}C activity from those collected at the shore, apart from the PIC's which are depleted in ^{14}C by 55-60% relative to the international standard. This depletion may be due to the resuspension of sedimentary carbonate which will be "old". The ^{14}C activity of the DIC has almost halved between the two sampling periods and if the shoreline sample is compared to that from C0 on the transect, the activity has decreased by a factor of 3.5. This indicates that releases of ^{14}C from Amersham are not extensively diluted when they enter Cardiff Bay. The organic samples collected and analysed are all enhanced in ^{14}C, relative to the standard, with the highest activities present in the shoreline samples. Whether this is due to the actual sampling locations, or to the time of sampling, is unclear. Relative to the activities found in the intertidal samples, the POC sample collected in mid-channel is similar to the activities observed in both the intertidal seaweed and sediment but is considerably less than that found in the winkles. However, the shoreline POC sample is more active than the winkles indicating that a source of high activity material is available for incorporation into the foodchain. The winkles obviously show an average of the ^{14}C specific activity of the material consumed during their lifespan.

These enhancements observed in the POC and DOC must be due either to the inputs of organic ^{14}C from Amersham or higher discharges in the past which are at present

undergoing oxidation and resuspension. If these high activities are due to present discharges they must differ in chemical form from those at Sellafield to explain the differences observed in the distribution. This would suggest that the discharges from Sellafield are mainly inorganic in nature whereas those from Amersham contain ^{14}C in both an inorganic (DIC) and organic (POC and DOC) form. The enriched ^{14}C activities observed in the POC during the December sampling is a further indication that the discharges from Amersham are partly organic in nature as this enrichment is not seen in the vicinity of Sellafield in the winter months.

3.4 AMERSHAM INTERNATIONAL plc, BUCKINGHAMSHIRE

The final sampling location considered in this research was a second radiochemical plant owned by Amersham International plc. This installation is situated in Buckinghamshire and differs from the other two sites in that it does not discharge to a marine coastal environment but to a fresh water system. Liquid discharges are passed to the Maple Cross sewage works from which releases enter the Grand Union canal and the River Colne within the Thames catchment area.

Samples collected in this area were taken from the Grand Union canal below the outlet from Maple Cross and consisted of water for DIC, DOC, PIC and POC analysis, river weed, sediment and fish (Chub). The ^{14}C specific activities found in each of these samples are detailed below in Table 3.22.

SAMPLE TYPE	pM±1σ	AGE±1σ
DIC	68.4±0.9	3050±100
PIC	56.6±0.6	4570±90
POC	87.3±1.0	1095±90
DOC	28.5±0.5	10080±140
Sediment - Inorganic	102.4±1.2	-
River Weed	92.8±1.2	600±105
Fish - Chub	159.6±0.5	-

Table 3.22: ^{14}C specific activities measured in samples from the Grand Union canal.

Of the seven samples collected from this area, only the fish is enhanced relative to the current ambient level of 115.4±0.4 pM. From the results, it would appear either that discharges of ^{14}C from Amersham are removed from the effluent as it passes through the sewage works, hence are not released into the carbon cycle of the local aquatic environment, or more likely that at the time of sampling there had been a lull in discharges from the plant. The fish may have been exposed to higher activity ^{14}C in the past and, hence, still retain an enriched ^{14}C signal which may have been extensively diluted in the other reservoirs considered.

Regardless of the lack of enhancements, it is still apparent that the ^{14}C activity present in the biogeochemical fractions is variable. The POC appears to have the highest activity with the DOC having the least, perhaps indicating extensive recycling of the DOC within the water column. The POC and river weed have comparable ^{14}C specific activities, therefore, river weed may supply particulate organic matter to the system. The sedimentary inorganic carbon, although not enhanced, has a higher ^{14}C activity than observed elsewhere indicating a source of slightly higher activity material which is particulate in nature. Unfortunately, there was insufficient sedimentary organic material to allow analysis; this may have helped to determine whether past discharges of ^{14}C had occurred.

The most likely explanation for the observed variation in the activity of the fractions is the natural cycling of carbon. This will obviously be influenced by external processes such as leaching of dissolved organics from surrounding soils, particulate material washed into the canal during heavy rain, leaf fall and degradation during autumn *etc.* which will add carbon of variable activity and origin to the system. Because of this, interpretation of so few results is difficult with the most outstanding feature being the lack of enhancement.

3.5 RADIOLOGICAL IMPLICATIONS

The nomenclature and calculation associated with the determination of the radiological dose to human populations has already been introduced in Section 1.6. In that discussion it was found that for equilibrium conditions, the dose received by man due to ingestion and inhalation of ^{14}C can be related to the specific activities in the atmosphere and food at that time. The equation relating dose to the specific activity in the foodstuff for Reference

Man is:-

$$H_x^{ing}(t) = (6.3 \times 10^{-8})\ A_f(t) \qquad (3.11)$$

where $H_x^{ing}(t)$ is the dose equivalent in Sieverts per year from ingestion of food with the specific activity $A_f(t)$, which takes into account the average beta energy per decay, the mass of carbon and the total mass in the body considered, the quality factor and a time conversion factor (seconds to years). Equation 3.11 assumes that the total food intake is terrestrial in nature. To incorporate the aquatic foodchain it is assumed that each foodchain source will contribute proportionally to the total dose *ie.*

$$H_{ges} = n\ H_{terr} + (1-n)\ H_{aquat} \qquad (3.12)$$

where H_{ges} is the total dose rate equivalent (Sv yr^{-1}), H_{terr} and H_{aquat} are the dose rate equivalents from the terrestrial and aquatic pathways respectively and n is the contribution of the terrestrial pathway to the total carbon content of man.

However, for a conservative estimate of the total dose it is sufficient to consider only the pathway with the highest specific activity. The terrestrial samples analysed during this work have shown enhancements which are considerably less than those found in intertidal biota samples collected in the vicinity of the release points, hence, the results obtained for mussel and winkle samples will be used to determine the potential radiological dose received by local people within the three study areas.

Table 3.23 shows the results obtained for those samples with the highest activity at the sites of interest in relation to a potential effective dose equivalent from atmospheric ^{14}C (without further anthropogenic inputs) of 0.014 - 0.016 mSv per year.

SAMPLE	^{14}C SPECIFIC ACTIVITY (Bq kg^{-1} C)	EFFECTIVE DOSE EQUIVALENTS (mSv yr^{-1})
Pre-industrial	226	0.014
Current Ambient	260.8	0.016
Sellafield Grass	594.4	0.037
Sellafield Mussels	1779.1	0.112
Drigg Winkles	1386.2	0.087
Sellafield Plaice	900.4	0.057
Sellafield Dab	1135.3	0.072
Cardiff Winkles	883.7	0.056
Grand Union Canal Chub	360.6	0.023

Table 3.23: Effective dose equivalents calculated from the ^{14}C specific activity of samples collected from the three sampling locations assuming 100% consumption.

The terrestrial foodchain in the vicinity of Sellafield, as indicated by the grass samples, produces a doubling of the potential effective dose equivalent to the local population but this is overshadowed by that from locally harvested fish and shellfish. An increase in the potential dose is also observed at Cardiff when the specific activity found in winkles is considered, but this is less than that seen at Sellafield. The only sample collected in the Grand Union Canal that was enhanced was the Chub and this gives a much lower potential dose equivalent per year than any of the samples collected at the other two sites.

It must be remembered that these results are overestimates of the potential dose to members of the public as they assume the worst scenario *ie.* the local population have only one source of food with the ^{14}C specific activities noted in the table. To take into account the small proportion of the diet that shellfish occupy Equation 3.12 can be used in conjunction with some assumptions regarding consumption rate *etc.*. McDonald *et al.* (1991) estimated that a representative consumption rate of mussels or winkles in the U.K. was 10 kg per year fresh weight. To fit into Equation 3.12 this weight must be converted into the proportion of the total carbon in the diet. Reference Man is assumed to consume

0.3 kg of carbon per day (*ie.* 110 kg of carbon yr^{-1}) (ICRP, 1975), hence, 10 kg fresh weight of mussels (85% water, 40% of the dry matter being carbon) is equivalent only to 0.6 kg of carbon and 0.5% of the total diet. Using Equation 3.12 with these proportions and the specific activities of atmospheric and Sellafield mussel samples produces an effective dose equivalent of 0.0169 mSv yr^{-1}. This is only slightly higher than the dose received from current ambient levels, indicating that the consumption of shellfish with a ^{14}C specific activity such as that observed in Sellafield mussels does not increase the annual dose by a significant amount. However, fish sampled close to Amersham, Cardiff by MAFF had ^{14}C specific activities in excess of 21,000 Bq $kg^{-1}C$ (Hunt, 1988). Assuming the same consumption rate *etc.* these would result in a higher dose to consumers (0.0230 mSv yr^{-1}) than that measured due to the consumption of Sellafield mussels. When these results (Table 3.23) are considered in relation to the NRBP recommended limit of 1 mSv per year for members of the general public (NRPB, 1987) they are low and show that the releases of ^{14}C from the three establishments under consideration are well within the recommended limits.

CHAPTER 4

^{14}C RELEASES TO THE AQUATIC ENVIRONMENT:

GLOBAL IMPLICATIONS

4.1 INTRODUCTION

The main emphasis of this study has been on the local, spatial and temporal distributions of ^{14}C discharges from both nuclear and radiochemical establishments. However, due to its mobility in the environment and its long half-life ^{14}C can become globally dispersed and act as a long-term source of irradiation to the world's population. To complete this study, a brief consideration of the global implications of ^{14}C releases to the aquatic environment will be undertaken.

McCartney *et al.* (1988a) carried out a study on the global effects of ^{14}C discharges from the nuclear fuel cycle based on gaseous releases. Their study determined the radiological dose received by global populations, assuming a range of scenarios for future nuclear and fossil fuel-derived energy demands. The authors also considered briefly the influences on the predicted dose due to a proportional release to the oceans. In summary, they predicted an atmospheric ^{14}C specific activity of 234 Bq kg^{-1} C in the year 2050 using the "most probable" scenario for nuclear and fossil fuel use (*ie.* medium predictions for both), assuming 50% waste reprocessing and a negligible contribution from fast breeder reactors. This figure was reduced by only 1.3% when 20% of the discharges were released to the oceans.

The aim of this section is not to repeat these studies, but to use the "most probable" scenario in conjunction with the data determined during this study to ascertain the influence of liquid ^{14}C releases from the nuclear fuel cycle on the resultant specific activity in each of the carbon reservoirs.

To predict the influence of such anthropogenic releases, the system into which they are released must be modelled. Models which mathematically attempt to mimic natural processes are widely used in a number of scientific fields including ocean circulation studies using tracers such as ^{3}H, ^{14}C, alkalinity, DIC, salinity (Kuo and Veronis, 1970; Fine

et al., 1981; Bolin *et al.*, 1983; Toggweiler *et al.*, 1989 a,b), sediment interactions in the oceans (Camplin and Gurbutt, 1985), the dispersion of radioactive wastes dumped to sea (Shepherd, 1976) plus the influence of anthropogenic perturbations on the global carbon cycle (Craig, 1957b; Revelle and Suess, 1957; Bolin and Ericksson, 1959; Keeling, 1973; Bush *et al.*, 1983, Emanuel *et al.*, 1984). The latter topic will be discussed more fully within this chapter.

These mathematical models must represent the determining processes within the system so that, with the appropriate input data, they can adequately predict future, and reflect past and present, distributions. Within this work, two models of the global carbon cycle have been used and these will be discussed in detail in subsequent sections. Both of these will then be used to determine the future ^{14}C specific activities in the major reservoirs of the carbon cycle when liquid discharges from the nuclear fuel cycle are incorporated and their results compared.

4.2 GLOBAL CARBON CYCLE MODELLING

As in the modelling of all natural systems, the basic structure of a carbon cycle model is determined by physical, chemical and biological processes which occur within the system. The validation and testing of such models should ideally be undertaken with data not used to determine the parameters within the basic structure of the model. However, this situation very rarely arises in environmental studies.

Over the years carbon cycle model structures have been developed and applied to topics such as the estimation of the future extent of the Suess effect (Revelle and Suess, 1957; Baxter and Walton, 1970), the uptake of bomb-^{14}C by the oceans and biosphere (Thommeret *et al.*, 1983), predictions of future atmospheric CO_2 levels (Keeling and Bacastow, 1977; Siegenthaler and Oeschger, 1978; Nienhaus and Williams, 1979; Edmonds *et al.*, 1984), the prediction of fossil fuel-derived CO_2 uptake by the oceans (Broecker and Peng, 1982; Crane, 1988) and also the prediction of the radiological impact of ^{14}C discharges from the nuclear fuel cycle (Kelly *et al.*, 1975; Killough and Till, 1978; Killough, 1980; Krishnamoorthy *et al.*, 1982; Matthies and Paretzke, 1982; Bush *et al.*, 1983; Kocher and Killough, 1984; IAEA, 1985; McCartney *et al.*, 1988a,b). As carbon cycle models have such a wide and varied application to topical scientific issues, the

selection of model structures available is extensive, although many of the incorporated features are similar. The general features of these models are detailed in the following sections.

4.2.1 The History of Global Carbon Cycle Modelling

Global carbon cycle modelling was initiated over 30 years ago by the development of simple box models (Craig, 1957b; Revelle and Suess, 1957; Bolin and Ericksson, 1959; Keeling, 1973) to determine the influences of fossil fuel on the atmospheric CO_2 levels and the exchange rate of CO_2 between the atmosphere and ocean.

These models divide the carbon cycle into three well-mixed compartments or reservoirs (atmosphere, surface ocean and deep ocean) with a known mass of carbon in each. Transfer of carbon between these compartments is by first order kinetics *ie.* the flux is proportional to the mass of carbon in the donating compartment. These fluxes take place such that steady state conditions are maintained *ie.* the outward flux from a box is always matched by that entering it from other compartments. To model the transfer between the boxes a set of linear equations can be produced in the form:-

$$\sum (n_{(i,j)}) \times N_i = \sum (n_{(j,i)} \times N_j) \qquad (4.1)$$

where N_i and N_j are the mass of carbon in boxes i and j respectively, $n_{(i,j)}$ is the transfer coefficient from box i to j and $n_{(j,i)}$ is that from box j to i. An equation of this type can be derived for each compartment of the model and a program developed to run the model with appropriate input data for prediction of future masses of carbon in each reservoir, or if ^{14}C data are available the ^{14}C specific activity in each reservoir. This design of model assumes that the contents of the compartments are well-mixed and that any new material entering the compartment is mixed instantaneously.

Over the years the complexity of these models has increased. Alterations to the basic structure have been introduced in an attempt to model the determining processes more accurately, hence, improving the fit of the predicted values to the actual observations. Within global carbon cycle models, the reservoirs subject to most alteration have been the terrestrial biosphere and the oceans. In some models the atmosphere has been split into a stratosphere and troposphere compartment (Walton *et al.*, 1970; Kelly *et al.*, 1975;

Matthies and Paretzke, 1982) which improves the response of the model to ^{14}C inputs due to nuclear weapons tests. The atmosphere can also be subdivided hemispherically, *ie.* into north and south hemispheres, which improves the response of the model by incorporating the rate of exchange between the hemispheres and the greater rate of exchange between the atmosphere and the oceans in the southern hemisphere (Bush *et al.*, 1983). While these representations of the atmosphere are used in certain model structures the most common approach is to consider the atmosphere as one, well-mixed reservoir.

The modifications incorporated into the terrestrial compartment have been many and varied to account for the residence time of carbon incorporated into the various pools present. In an attempt to account for these differences, the terrestrial biosphere has been divided into living and dead material *ie.* biota and humus (Craig, 1957b) or into fast and slow pools (Fig 4.1) (Machta, 1971; Keeling, 1973). Bacastow and Keeling (1973) introduced a fertilisation effect whereby they replaced the linear flux of carbon between the atmosphere and biosphere by a non-linear, logarithmic flux to improve the response of the model with respect to the CO_2 measurement records. Further developments have included subdivision into northern and southern hemispheres to assist in the modelling of the effects of large scale forest clearances (Chan *et al.*, 1979) but this still does not relate directly to the structural components found in the reservoir. Emanuel *et al.* (1981) refined these ideas and developed a much more intricate structure (Fig 4.2) which attempted to treat the terrestrial biosphere in a more realistic manner with compartments representing ground vegetation, trees, detritus/decomposers and active soil carbon.

This is only a brief resume of the model structures available to represent the terrestrial reservoir in global carbon cycle models, but overall, these are the structures most widely applied.

The reservoir which has received most attention is the oceans because over long periods of time they are assumed to be the primary sink for excess atmospheric carbon (Baes *et al.*, 1977). This has resulted in a large selection of oceanic carbon cycle models of varying complexity. The earliest of these was the two box approach by Craig (1957b) whereby the oceans were considered as a 75 metre deep surface layer adjoining a deep water reservoir. In a similar manner to the non-linear flux introduced into the terrestrial-atmosphere system, Keeling (1973) introduced a buffer factor into surface water uptake of CO_2 from the atmosphere. This takes into account surface water chemistry where the rate

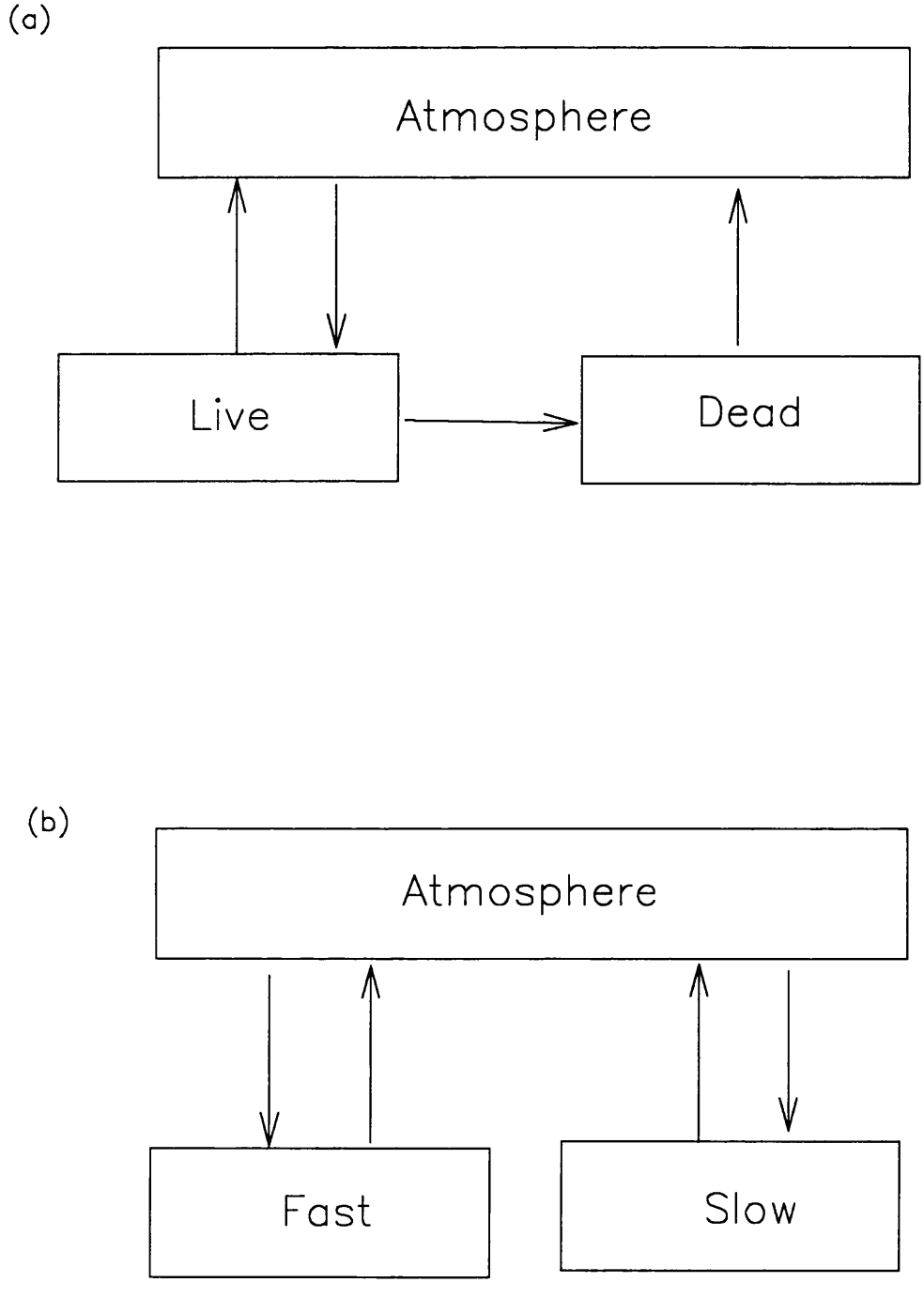

Figure 4.1: Model representations of the terrestrial biosphere.

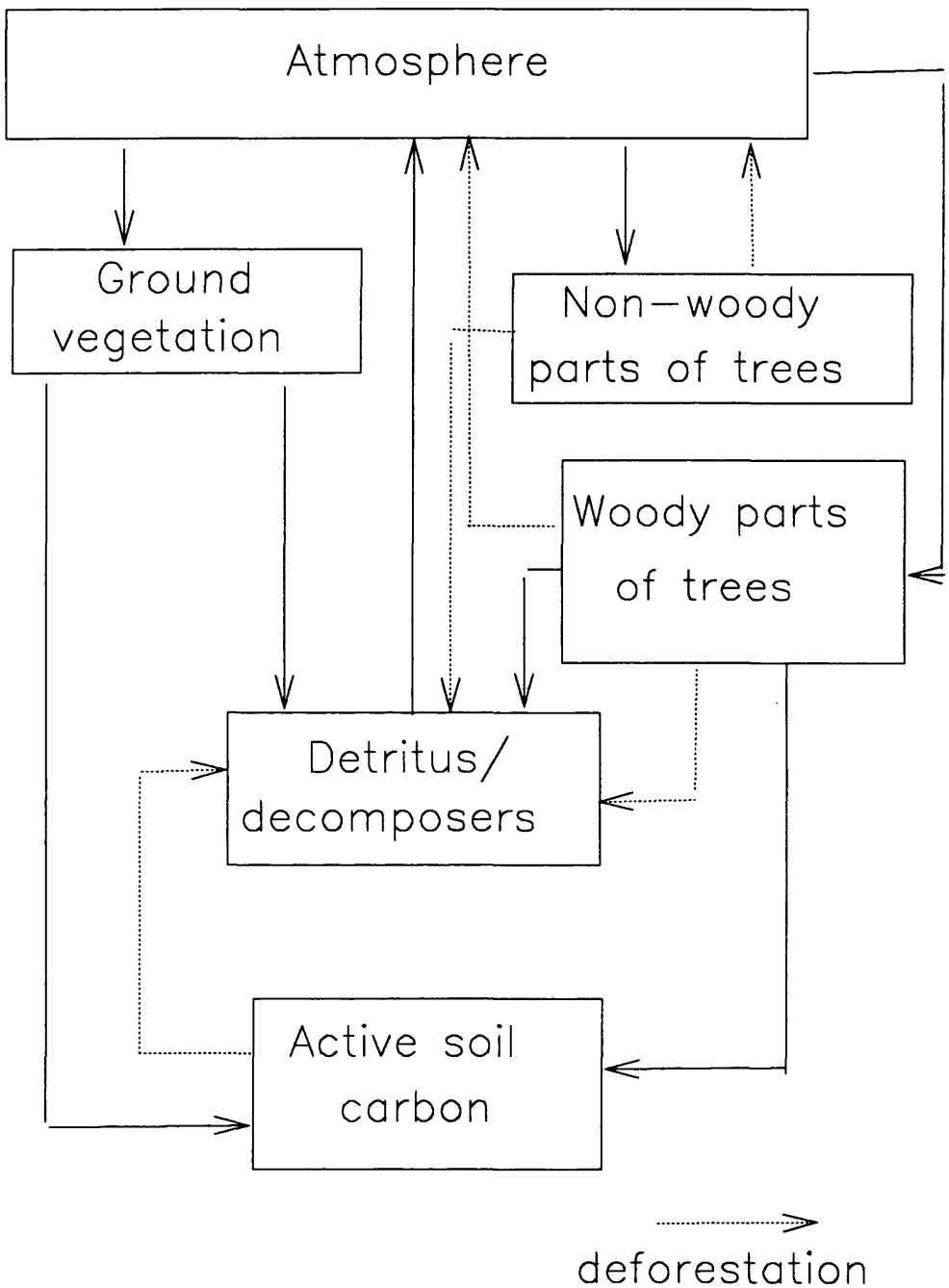

Figure 4.2: A model with 5 boxes representing the terrestrial biosphere.

of CO_2 uptake from the atmosphere is governed by properties such as pH, alkalinity and the partial pressure of CO_2 in the atmosphere and surface waters. While Keeling's buffer factor takes into account the chemistry of uptake, Oeschger *et al.* (1975) developed a box diffusion model to improve the representation of water movement below 75 m (Fig 4.3). This model was based on a diffusion equation to explain carbon turnover in deep water with the constant coefficient of diffusivity estimated to reflect ^{14}C distribution down the water column. However, when this was applied to the three box model, the predicted values only began to match the observed values when the mixed layer depth was taken down to 260 m. This is a consequence of the presence of the thermocline (or transition zone) between the surface and deep waters (75 - 600 m), hence, the boundary of the compartments should not be at the extremes of the zone but somewhere in between (Bacastow and Keeling, 1979). Since then, the box diffusion model of Oeschger *et al.* (1975) has been the basis of most ocean models developed within carbon studies. These have attempted to introduce more realism by incorporating such features as polar outcropping, biological activity, nutrient cycling and upwelling (Bjorkstrom, 1979; Broecker *et al.*, 1980; Hoffert *et al.*, 1981; Enting and Pearman, 1982; Crane, 1982; Peng *et al.*, 1983; Siegenthaler, 1983).

The model developed by Peng *et al.* (1983) included most of the alterations discussed above (Fig 4.4). They proposed a modified box diffusion model incorporating an oceanic photosynthesis-respiration cycle, the formation of deep water (by outcropping of intermediate water in polar regions, therefore increasing its density and sending it to the bottom of the water column from which it is returned to intermediate depths) and an increased eddy diffusion coefficient for the main thermocline. Within this structure the values for parameters such as diffusivity of the thermocline and deep water, the downward advective flux and the depth of the deep water source were selected to reflect the penetration of bomb-derived ^{3}H and the mean depth distribution of natural radiocarbon at the time of the GEOSECS surveys. The particulate cycling is based on the distribution of phosphate within the water column, assuming all phosphate reaching the surface ocean is incorporated into organic debris with a C:P ratio of 105:1. This PO_4 is released as the debris falls to the thermocline and deep sea. While these model designs can provide globally averaged values, the increased awareness of the "greenhouse effect" and potential climatic changes has meant a more realistic approach being advocated. General circulation

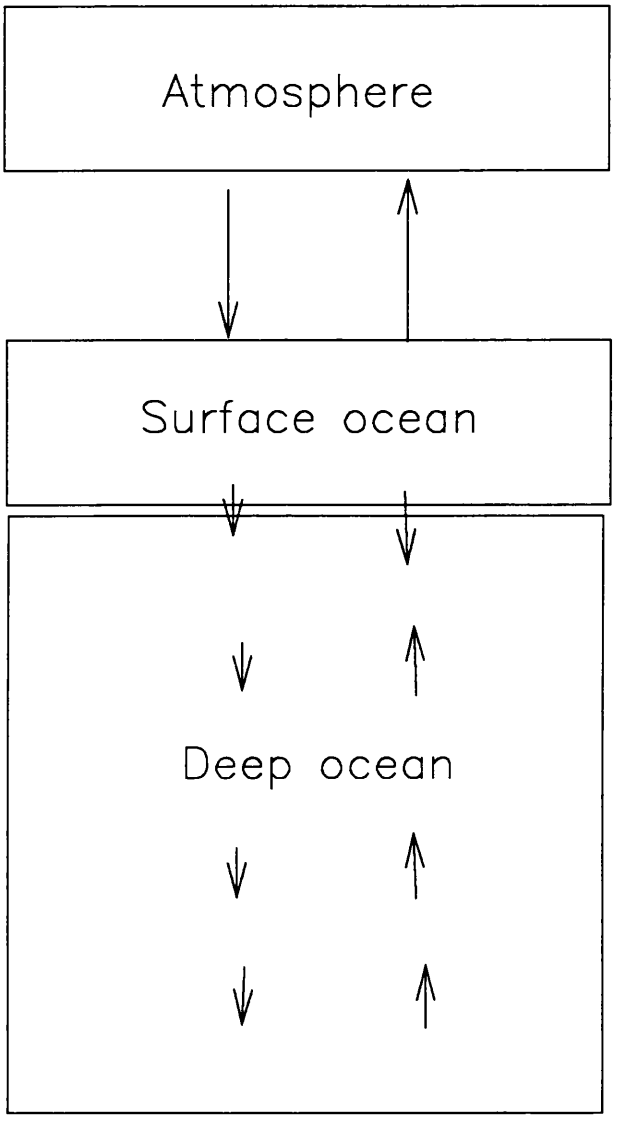

Figure 4.3: A model structure incorporating diffusion to represent water movement in the deep ocean.

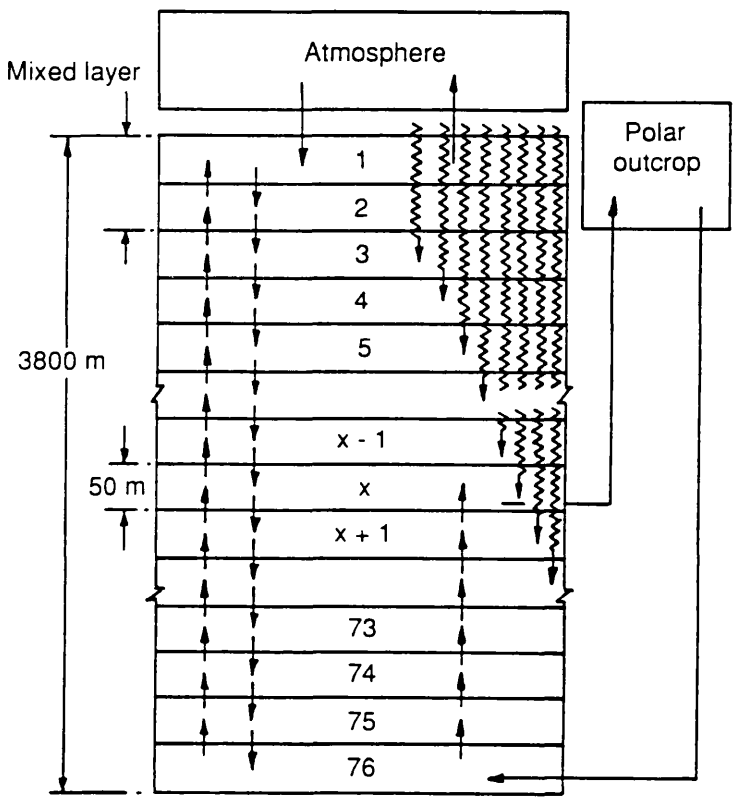

Figure 4.4: The modified box-diffusion model proposed by Peng *et al.* (1983).

models (Bryan, 1969) are now being validated on both the steady state pre-bomb and the nuclear weapons test radiocarbon distributions (Toggweiler *et al.*, 1989a,b) so that they may be used to predict future responses of the ocean to the anticipated levels of atmospheric CO_2 due to fossil fuel use. These models are still in the trial stages but appear to be an important development for global carbon modelling.

4.2.2 Description and validation of the chosen model structures

The previous section highlights the advances which have been made in global carbon cycle modelling in the last three decades. Of those models available in the literature, two have been used in this work to determine the global influences of liquid ^{14}C discharges from the nuclear fuel cycle. The models selected are an eight box representation which has a northern and southern hemisphere component and a more complex 25 box structure which treats both the terrestrial and oceanic reservoirs in greater detail.

Prior to using such models, their ability to maintain steady state conditions is checked by running the model with only natural ^{14}C production and radioactive decay taken into account. Anthropogenic inputs such as fossil fuel CO_2 and nuclear weapons ^{14}C can then be incorporated to ensure that the model can reconstruct past atmospheric ^{14}C specific activities before it can be used as a predictive tool.

4.2.2.1 The 8-box model

An eight box representation of the global carbon cycle was proposed by Kelly *et al.* (1975) and modified by Bush *et al.* (1983) to predict the possible effects of ^{14}C from the nuclear fuel cycle. McCartney used this eight box model in similar studies (McCartney, 1987; McCartney *et al.*, 1988a). The model structurally consists of 8 carbon reservoirs representing the deep ocean, the surface ocean, the humus and the circulating (*ie.* atmospheric and the fast turnover portion of the terrestrial biosphere) carbon in both the northern and southern hemispheres (Fig 4.5).

These reservoirs are linked by 18 linear transfer co-efficients which have been found to maintain steady state conditions in the absence of anthropogenic perturbations. Values for the parameters used within the structure of this model as proposed by Bush *et al.* (1983) are detailed in Table 4.1 with those values assigned to the mass of ^{14}C in each reservoir based on the pre-industrial specific activities detailed in Section 1.3.5.

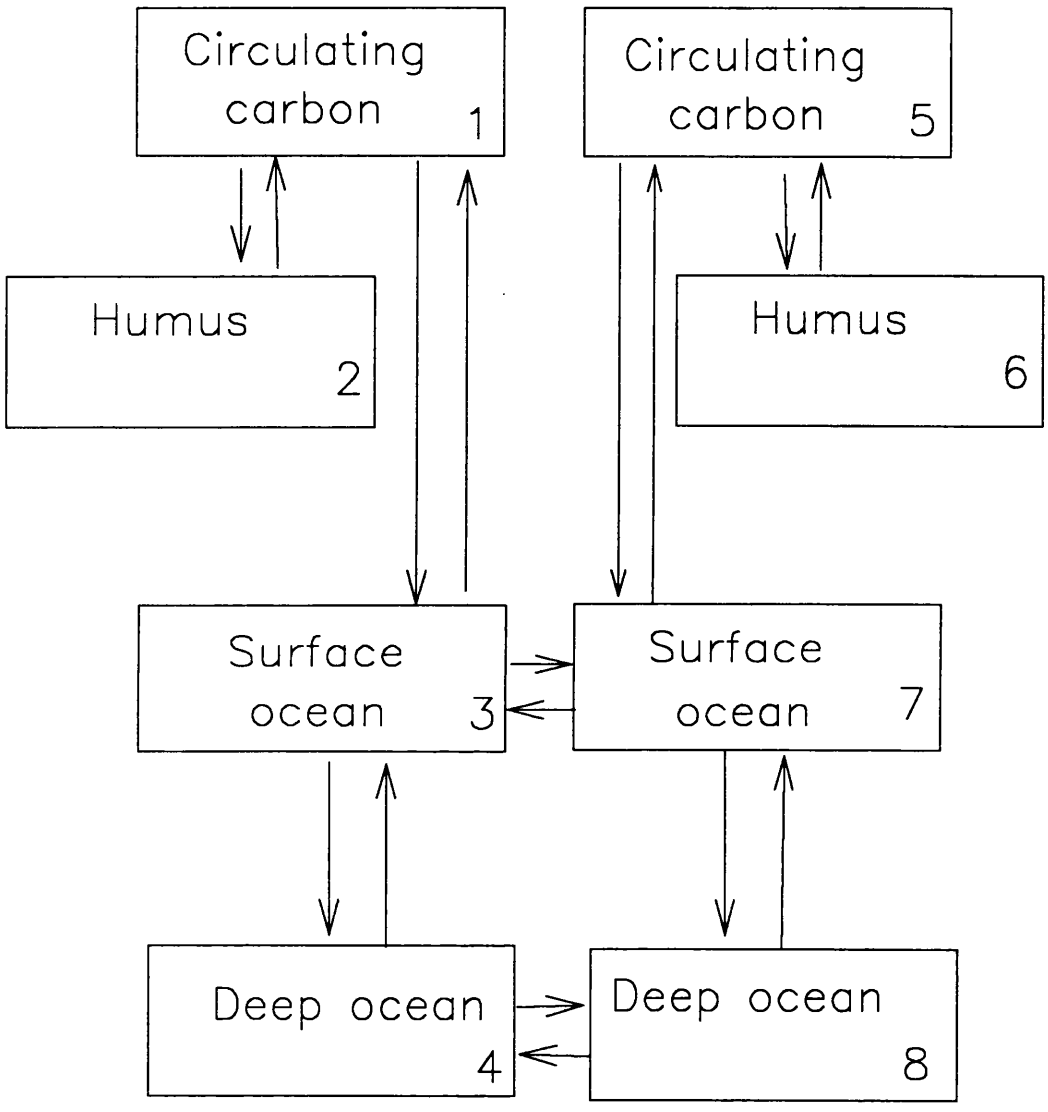

Figure 4.5: The 8-box model.

PARAMETER	STABLE CARBON	^{14}C
N_1	3.6×10^{17} g	5.051×10^5 g
N_2	11.6×10^{17} g	1.557×10^6 g
N_3	5.0×10^{17} g	6.665×10^5 g
N_4	136.4×10^{17} g	1.558×10^7 g
N_5	3.3×10^{17} g	4.630×10^5 g
N_6	4.0×10^{17} g	5.368×10^5 g
N_7	7.6×10^{17} g	10.131×10^5 g
N_8	245.7×10^{17} g	2.856×10^7 g
$k_{1,2}$	0.016	
$k_{1,3}$	0.14	
$k_{1,5}$	0.50	
$k_{2,1}$	0.005	
$k_{3,1}$	0.10	
$k_{3,4}$	0.10	
$k_{4,3}$	0.0036	
$k_{4,8}$	0.005	
$k_{5,1}$	0.56	
$k_{5,6}$	0.0061	
$k_{5,7}$	0.23	
$k_{6,5}$	0.005	
$k_{7,3}$	0.066	
$k_{7,5}$	0.10	
$k_{7,8}$	0.10	
$k_{8,4}$	0.0028	
$k_{8,7}$	0.0031	

Table 4.1: The values assigned to the parameters in the 8-box model.

These parameters are known to maintain steady state conditions when only natural production and radioactive decay are taken into account. All inputs, except natural

production, are entered into the model on an 80%:20% based split between the northern and southern hemispheres to reflect the present day population distribution (Bush *et al.*, 1983). In addition, this gives a more accurate reproduction of the inputs from nuclear weapons tests which took place primarily in the northern hemisphere (United Nations, 1982).

To ensure that this structure can adequately model past fluctuations in the carbon cycle, the predicted atmospheric ^{14}C specific activities can be plotted against observed values for both hemispheres. These are shown in Figures 4.6(a) and 4.6(b) for the northern and southern hemispheres respectively. For both hemispheres it is obvious that the model predictions show the same trends as the observed data although the predicted maximum in both cases is slightly higher and occurs earlier than actual measurements indicate. This discrepancy arises due to the model treating the atmosphere in each hemisphere as a single box *ie.* not differentiating between the troposphere and stratosphere. Most of the ^{14}C produced by nuclear weapons tests was injected into the upper atmosphere (stratosphere), whereas the observed ^{14}C levels correspond to values in the lower atmosphere (troposphere). This absence of a discrete stratosphere reservoir results in the model ignoring the finite mixing time between the stratosphere and troposphere and leads to the slight differences between the predicted and observed values. Regardless of this, the model can still prove useful as it has the ability to respond fairly accurately to anthropogenic inputs of carbon. As a result of this ability, the model will be considered and used as a predictive tool later on in this chapter.

4.2.2.2 The 25-box model

By definition, this model structure is considerably more complex than the 8-box model already considered. The 25-box model was originally designed by Emanuel *et al.*, (1984) to predict the future extent of the greenhouse effect. Figure 4.7 illustrates the model structure consisting of a single box atmosphere, a 19 box ocean and a 5 box terrestrial biosphere, all linked by a set of 54 different transfer coefficients.

The atmosphere-ocean system of the model is described by the box diffusion model proposed by Killough and Emanuel (1981) while the terrestrial biosphere utilises the complex structure detailed by Emanuel *et al.* (1981). In both cases (*ie.* atmosphere-ocean and atmosphere-terrestrial biosphere), the exchange rates are non-linear in nature.

Included in the original publication of this model (Emanuel *et al.*, 1984) was a

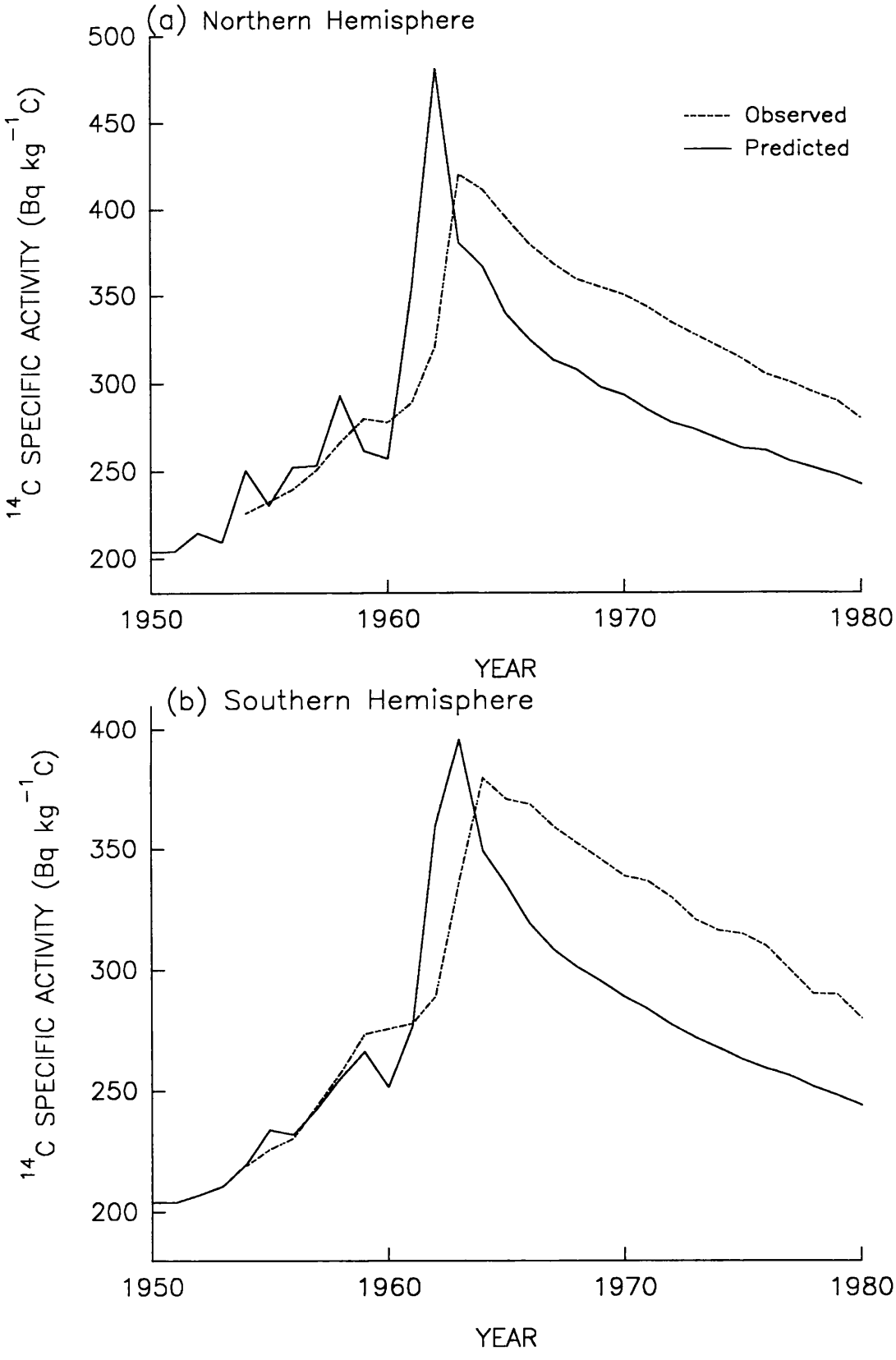

Figure 4.6: Observed *vs.* predicted atmospheric ^{14}C specific activities (8-box model).

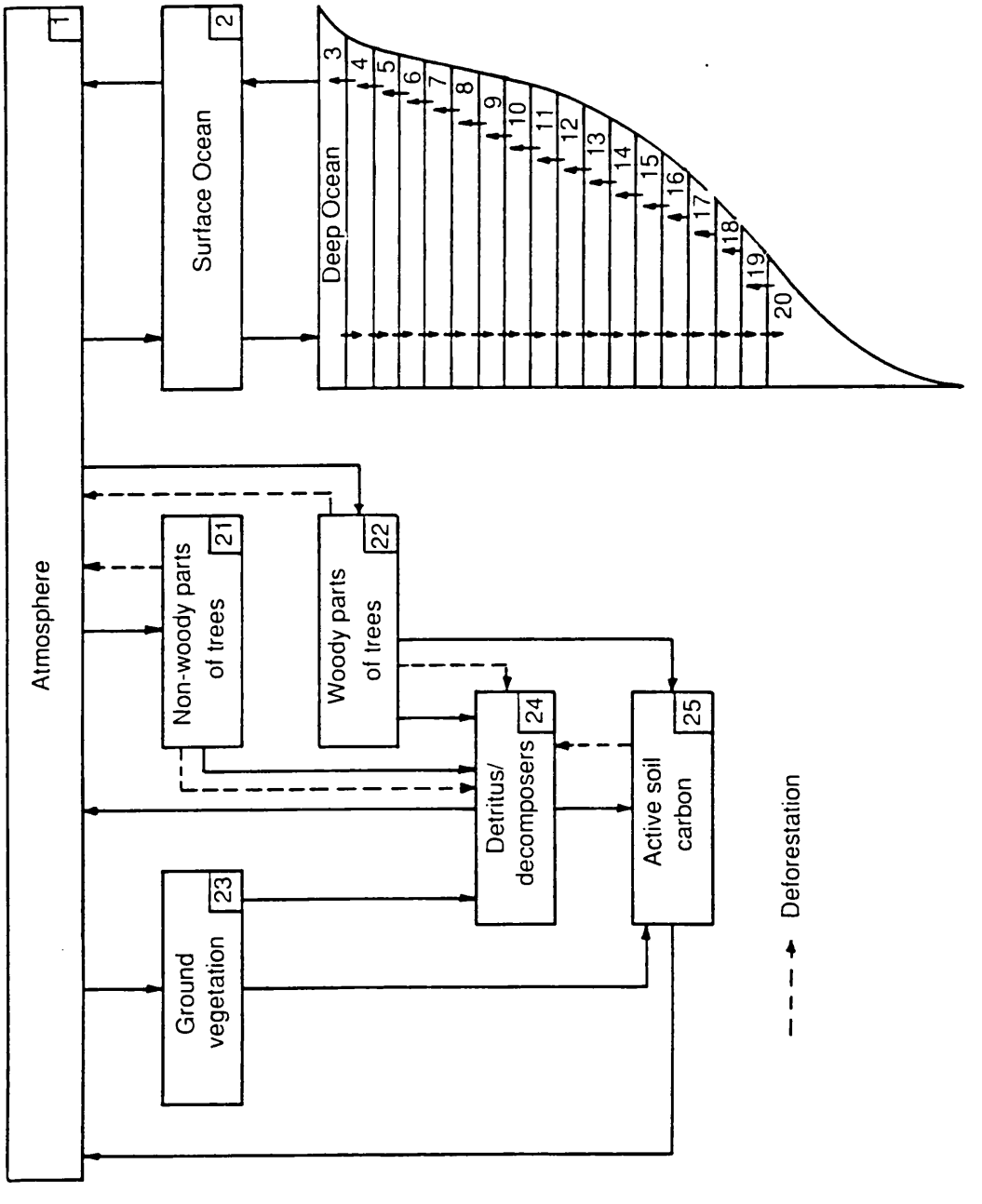

Figure 4.7: The 25-box model.

comprehensive calibration procedure, hence, the parameters suggested by the authors were used to test the model implementation. A selection of these parameters are detailed in Table 4.2 with the full set being available in the original publication.

PARAMETER	STABLE CARBON	^{14}C
N_1	5.2×10^{17} g	7.13×10^{5} g
N_2	6.6×10^{17} g	8.87×10^{5} g
$N_3+N_4....+N_{20}$	3.8×10^{19} g	4.41×10^{7} g
$N_{21}+N_{22}..+N_{25}$	2.0×10^{18} g	2.76×10^{6} g
$k_{1,2}$	0.19	
$k_{2,1}$	0.15	
$k_{2,3}$	5.8	
$k_{3,2}$	8.8	
$k_{1,(21,22,23)}$	0.12	
$k_{(24,25),1}$	0.05	

Table 4.2: The values assigned to a selection of the parameters in the 25-box model.

Once running, the performance of the model was checked by ensuring that the results obtained matched those achieved by the authors in their calibration procedures. The model original structure unfortunately did not incorporate an input mechanism for nuclear fuel cycle-derived ^{14}C which was therefore added for this application.

As with the 8-box model, the ability of the model to reconstruct past fluctuations in the carbon cycle was monitored by comparing the predicted atmospheric ^{14}C specific activities with those actually observed (Fig 4.8). The agreement between the two sets of data is extremely good, with the maximum activities occurring in the same year with only a slight discrepancy in the actual value. The model does, however, show a sharper decline in the atmospheric ^{14}C specific activity than is actually observed, but the extent of this

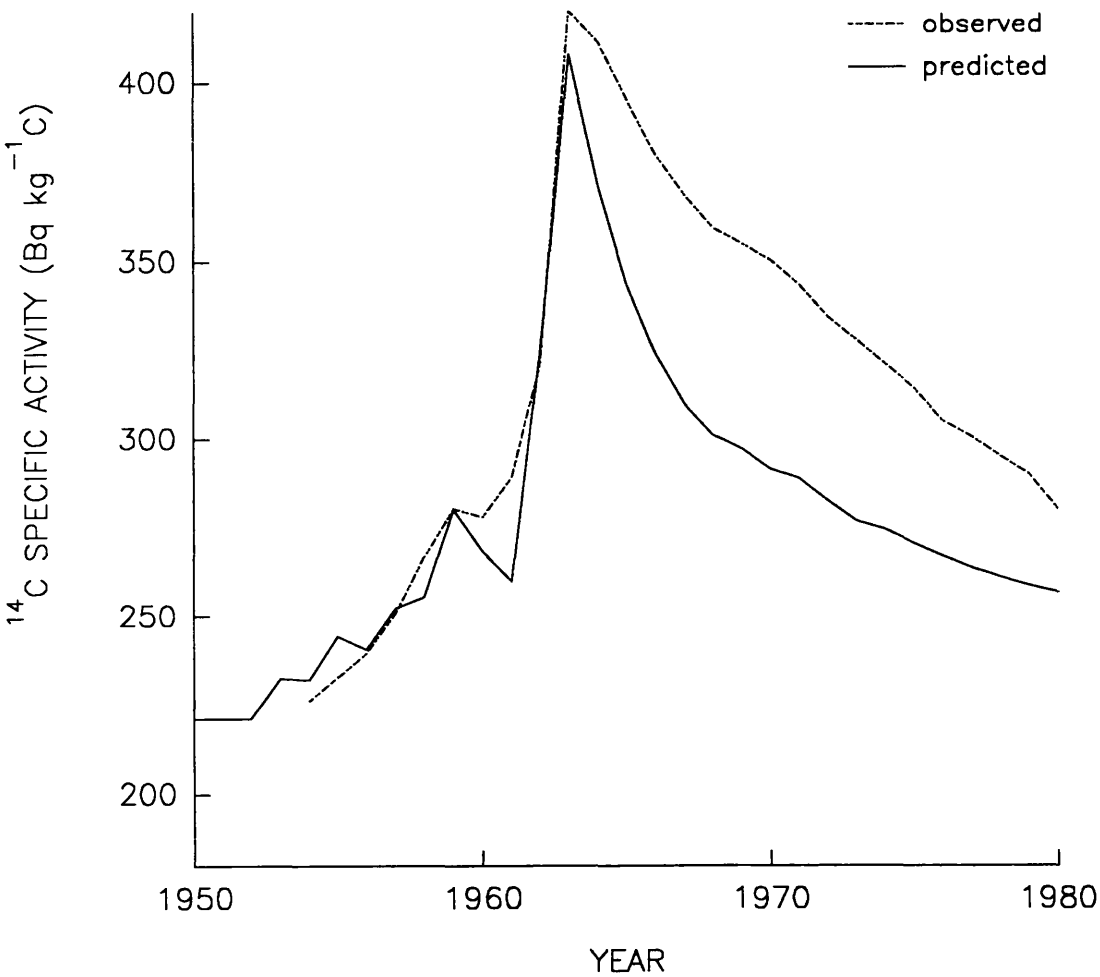

Figure 4.8: Observed *vs.* predicted atmospheric ^{14}C specific activities (25-box model).

discrepancy decreases, with excellent agreement apparent by 1980.

In addition to this comparison with atmospheric ^{14}C specific activities, it is also useful to look more closely at the water column and how the predicted ^{14}C specific activities compare with data from the Atlantic and Pacific oceans during the GEOSECS surveys. The data used for this comparison were collected between 10 and 50°N in both oceans during the period 1972 - 1974 and are based on an average of 9 and 20 stations, respectively (Stuiver *et al.*, 1981). These show the marked differences in the ^{14}C activity of the two oceans as a result of global deep water circulation. The results, with the predicted values for 1973, are shown in Figure 4.9. The model appears to produce slightly higher ^{14}C specific activities at the surface, indicating that perhaps the atmosphere-ocean exchange rate is slightly high. This would also account for the steep decline in the post-nuclear weapons test atmospheric ^{14}C specific activity. One other slight discrepancy occurs below 3000 m when the rate of decrease in the ^{14}C specific activity appears to be too rapid. However, the general trend of the three distributions is similar, with rapid decline in the top 1000 m followed by a more gradual change occurring throughout the rest of the water column. The values obtained from the 25-box model are globally averaged, hence, it is not surprising that some degree of discrepancy is apparent.

The good agreement with the observed trends in atmospheric ^{14}C specific activity, plus the additional agreement in the distribution of ^{14}C with the GEOSECS data, enables this model to be used as a predictive tool in further sections of this work with some confidence.

While this agreement between model and observed values appears to indicate that the model structure is accurate and represents the determining chemical and physical processes, this may not be the case. The more complex a model structure is, the more parameters are required to be known. This is not always possible, hence, parameters may be estimated introducing some degree of error into the predictions. Therefore, while mathematical models do have their applications, it must be remembered that they will only be as accurate as their input data. In carbon cycle modelling there is still a great deal of research to be carried out if the increasing complexity of models is to be supported. However, to ascertain the likely effects of anthropogenic additions into the carbon cycle, mathematical models are an essential requirement and as long as their limitations are kept in mind they can produce interesting and worthwhile results.

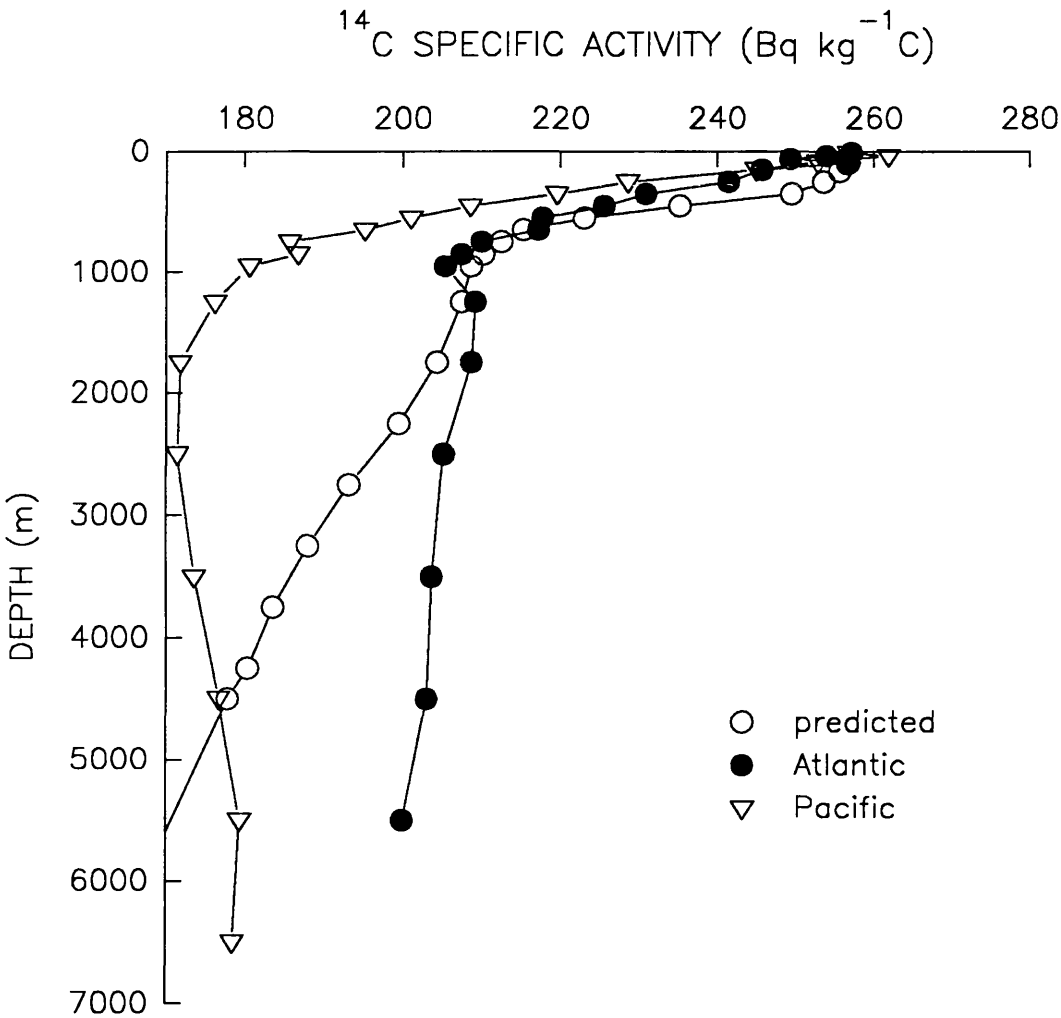

Figure 4.9: Observed *vs.* predicted ^{14}C specific activities in the water column (25-box model).

4.3 LIQUID DISCHARGES OF ^{14}C FROM THE NUCLEAR FUEL CYCLE

The validation of models such as the 8 and 25 box representations of the global carbon cycle permit their use as predictive tools. They will be used here to determine the effect of partitioning the ^{14}C releases from the nuclear fuel cycle between the gaseous and aqueous phases. Atmospheric ^{14}C discharges from the nuclear fuel cycle have been comprehensively studied (McCartney *et al.*, 1986; McCartney, 1987; McCartney *et al.*, 1988a,b) with the major conclusions being that in the short-term, ^{14}C from the nuclear fuel cycle would only contribute 0.2% in the year 2050 A.D. of the 1 mSv $year^{-1}$ limit set by the ICRP, but, in the long-term it is likely to be more significant, delivering one of the largest contributions to the dose to man from the generation of nuclear power.

While local radiological doses are related to the specific activity found in locally harvested foodstuffs, the calculations of global doses are based on the atmospheric ^{14}C specific activities. Therefore, greater proportions of the nuclear fuel cycle-derived ^{14}C released into the marine system should decrease the atmospheric burden and be manifest in lower global doses. However, the radiological implications of ^{14}C releases from the nuclear fuel cycle were not the main impetus behind this study, therefore, it seems more appropriate to concentrate on just how increasing releases to the marine environment will influence the specific activities found throughout the reservoirs of the global carbon cycle.

When determining future ^{14}C specific activities several assumptions must be made *ie.* the future natural production rate of ^{14}C will remain constant at its present day level and there will be no further detonation of nuclear weapons. This effectively means that future ^{14}C specific activities in the environment will be determined by the release of ^{14}C from the nuclear fuel cycle and its dilution by ^{14}C-free carbon from fossil fuel combustion. However, predictions of this type are based on likely economic and social policies which are not easily determined. Due to the inherent uncertainties within these predictions, the time limit of future projections of fossil fuel and nuclear energy productions are restricted to 2050 A.D.. Therefore, the modelling exercises undertaken will be restricted to predicting the specific activity in the global carbon reservoirs up to 2050 A.D..

Unlike the studies previously carried out, this work will deal only with the "most probable" scenario concerning the future projections of fossil and nuclear energy requirements based

on data of Edmonds and Reilly (1983a,b and c). In these projections both fossil fuel and nuclear energy requirements are thought to increase steadily until 2050 A.D. reaching an annual production of 14.5 x 10^{15} g of carbon and an installed capacity of approximately 6750 GW(e), respectively.

For incorporation into the models the input data have to be presented in mass of stable carbon or ^{14}C. The predictions presented by Edmonds and Reilly (1983a,b and c) for fossil fuel use are in this form while those for the nuclear fuel cycle are presented as installed capacity. It has already been calculated, in Chapter 1, that the ^{14}C production rate is 4.6 TBq $(GW(e))^{-1}$, based on the present distribution of reactor designs. However, only 1.8 TBq $(GW(e))^{-1}$ are released in the gaseous form, and if only 50% of the fuel is reprocessed this figure is reduced further to 1.4 TBq $(GW(e))^{-1}$. This is considerably higher than the 0.94 TBq $(GW(e))^{-1}$ used in previous calculations (McCartney *et al.*, 1988a) and should be reflected in higher ^{14}C specific activities. In the conversion of installed capacity to mass of ^{14}C, this figure of 1.4 TBq $(GW(e))^{-1}$ is used in conjunction with an assumed load factor of 0.7 (*ie.* the reactors were operational for only 70% of the time, hence the ^{14}C production has to be scaled down accordingly) (IAEA, 1983) to produce the predicted release of ^{14}C from the nuclear power industry to the year 2050 A.D..

Previous studies included a brief discussion on the effects of releasing 20% of the total gaseous wastes as liquid effluent (McCartney *et al.*, 1988a). Having already shown that liquid discharges from the nuclear fuel reprocessing plant at Sellafield in fact contribute 20 - 45% of the total releases (Section 1.8.1) it seemed appropriate to determine the influence, globally, on the ^{14}C specific activities of the individual carbon reservoirs if such partitioning occurred at all the sites of release *ie.* the reactor site itself and the reprocessing plant. To do this, the predicted global releases of ^{14}C were entered in varying proportions into the atmosphere and surface ocean boxes of the 8 and 25 box models.

Within the 8 box model structure, the projected inputs were split in the same manner as before; 80% to the northern hemisphere and 20% to the southern hemisphere. Figures 4.10(a) and (b) show the ^{14}C specific activity distribution within the eight reservoirs considered. These indicate that while the maximum atmospheric specific activity was considerably higher in the northern compared to the southern hemisphere, the values obtained for the surface ocean, humus and deep ocean appear to be very similar. The atmosphere and surface oceans are most responsive to the input of anthropogenic carbon,

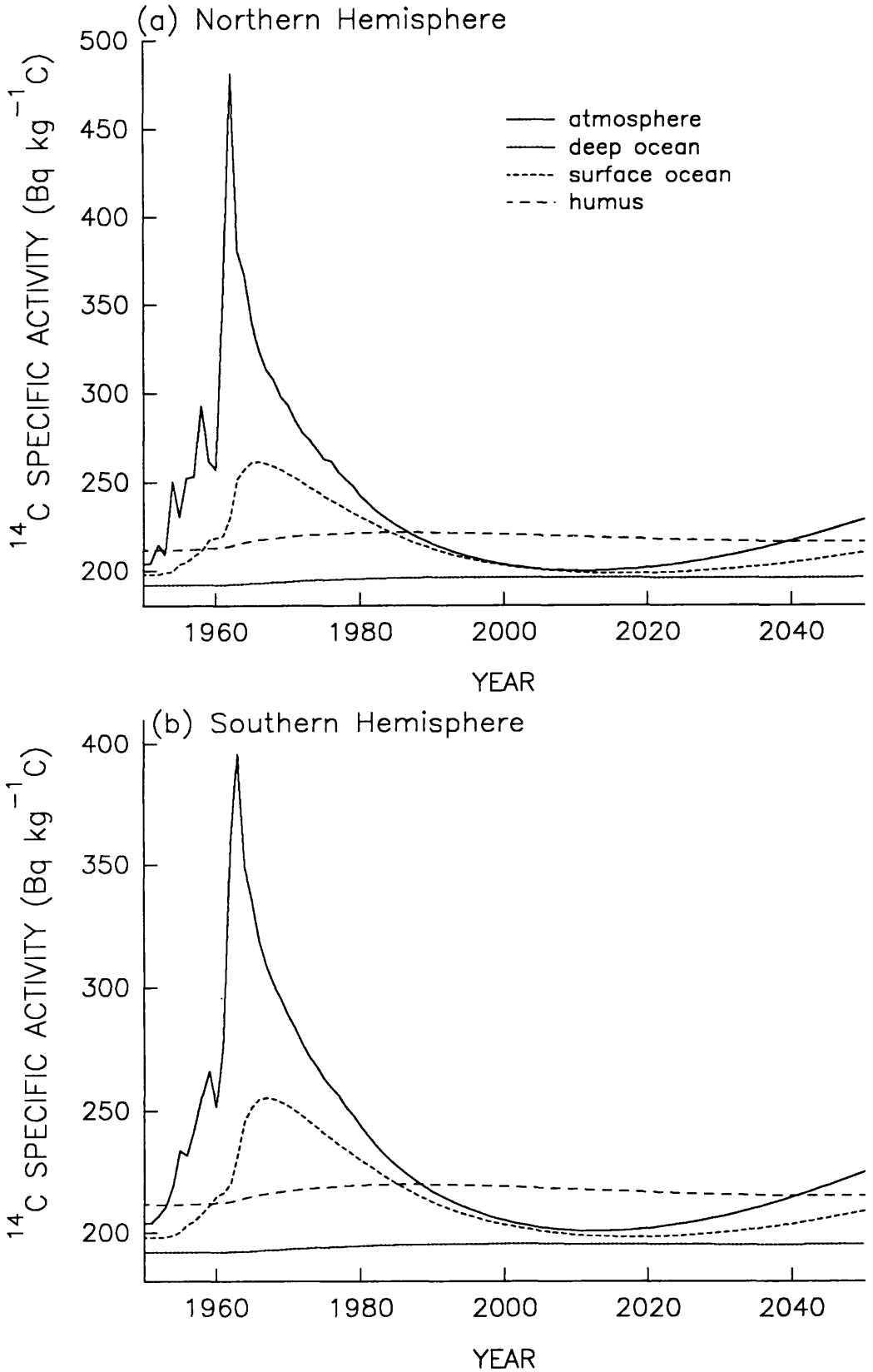

Figure 4.10: The ^{14}C specific activity observed in the reservoirs of the 8-box model.

with very little variation being observed in the humus or deep oceans due to the long residence time of carbon within them. The upturn in the specific activity post-2000 A.D. is due to the input of nuclear fuel-derived ^{14}C, resulting in an atmospheric specific activity of 229 Bq $kg^{-1}C$ and 225 Bq $kg^{-1}C$ for the northern and southern hemispheres, respectively. This is lower than the current ambient level of 265 Bq $kg^{-1}C$. The predicted specific activity for the surface oceans is 210 and 209 Bq $kg^{-1}C$, respectively; similar to the natural level reported in Chapter 1.

Figures 4.11(a) and (b) show the atmospheric ^{14}C specific activities for the northern and southern hemispheres as 0, 50 and 100% of the nuclear fuel cycle-derived ^{14}C is released to the surface oceans. The plots show the expected trend; the higher the input to the surface ocean, the lower both the northern and southern hemisphere's atmospheric ^{14}C specific activity. For every 10% of input into the surface ocean, a decrease of 1.6% and 1.2% in the atmospheric ^{14}C specific activities of the northern and southern hemispheres are observed. However, the subsequent increase in the ^{14}C specific activity of the northern surface oceans is only of the order of 0.8% per additional 10% input while there is no noticeable difference in the southern surface waters (Figs 4.12(a) and (b)). This is obviously a reflection of the greater mass of carbon present in the surface oceans compared to the atmosphere. As a result of this distribution effect, small releases of the total ^{14}C discharges to the surface oceans, rather than to the atmosphere, will be manifest in lower doses to the global population with relatively little change in the ^{14}C specific activity of the surface oceans. The magnitude of this effect in the northern hemisphere is slightly larger than the 1.3% decrease found by McCartney *et al.* (1988a) in their studies which may in part be due to their use of the 25 box model, as opposed to the 8 box model, for the calculations.

For the 25-box model, only certain compartments representing the major reservoirs, were studied. These included the atmosphere (box 1), the surface, the mid and the deep oceans (boxes 2, 10 and 20, respectively). This model is not split hemispherically, hence, partitioning of the input data such as that undertaken in the 8-box model is unnecessary. Figure 4.13 shows the results obtained for the four selected compartments and indicate that the nuclear fuel cycle-derived ^{14}C will maintain the ^{14}C specific activities of all the considered reservoirs, apart from the deep ocean, above their natural steady state values for the foreseeable future. This is of course dependent on the accuracy of the predictions

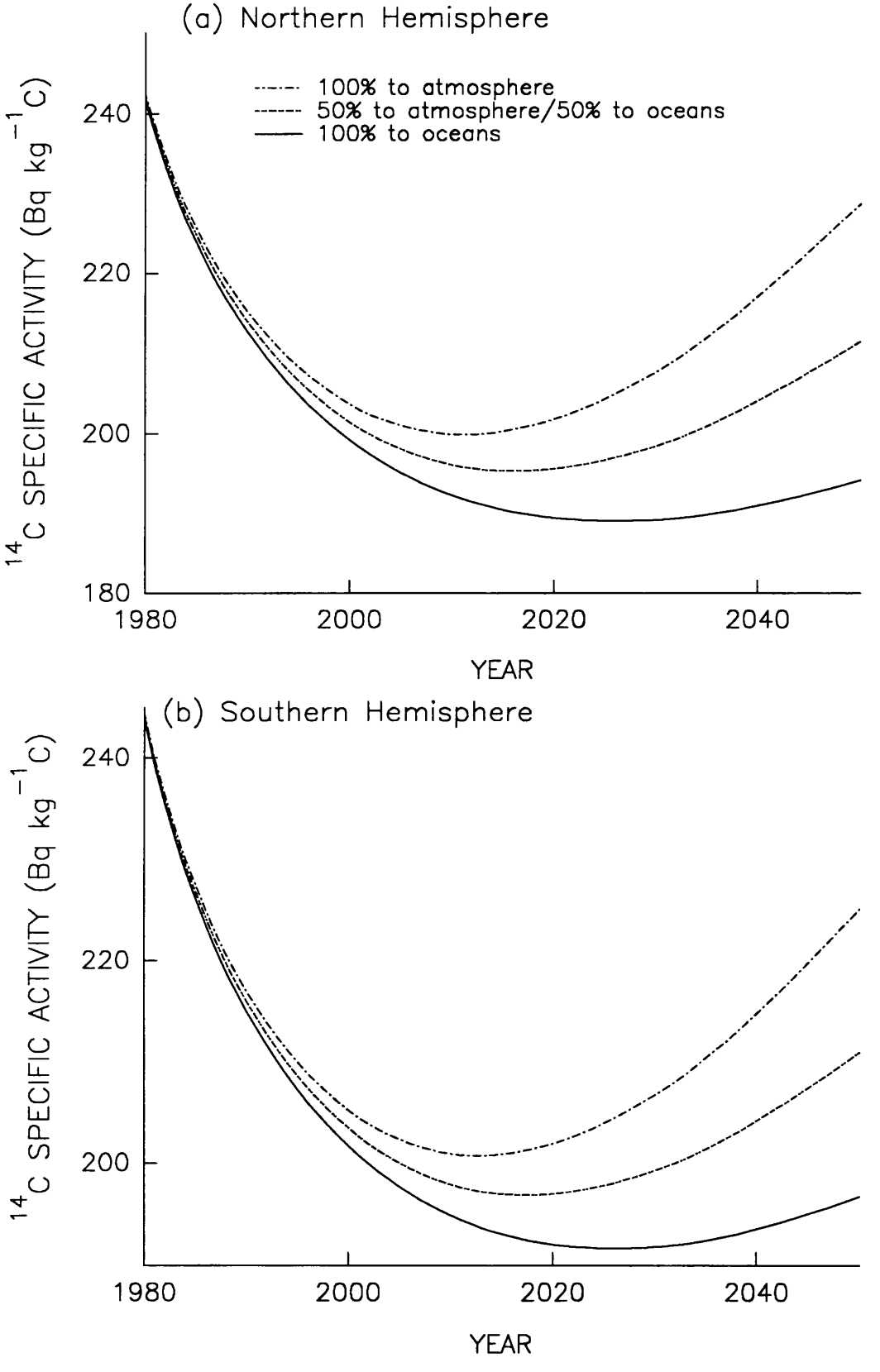

Figure 4.11: Predictions of partitioning (8-box model): The atmosphere.

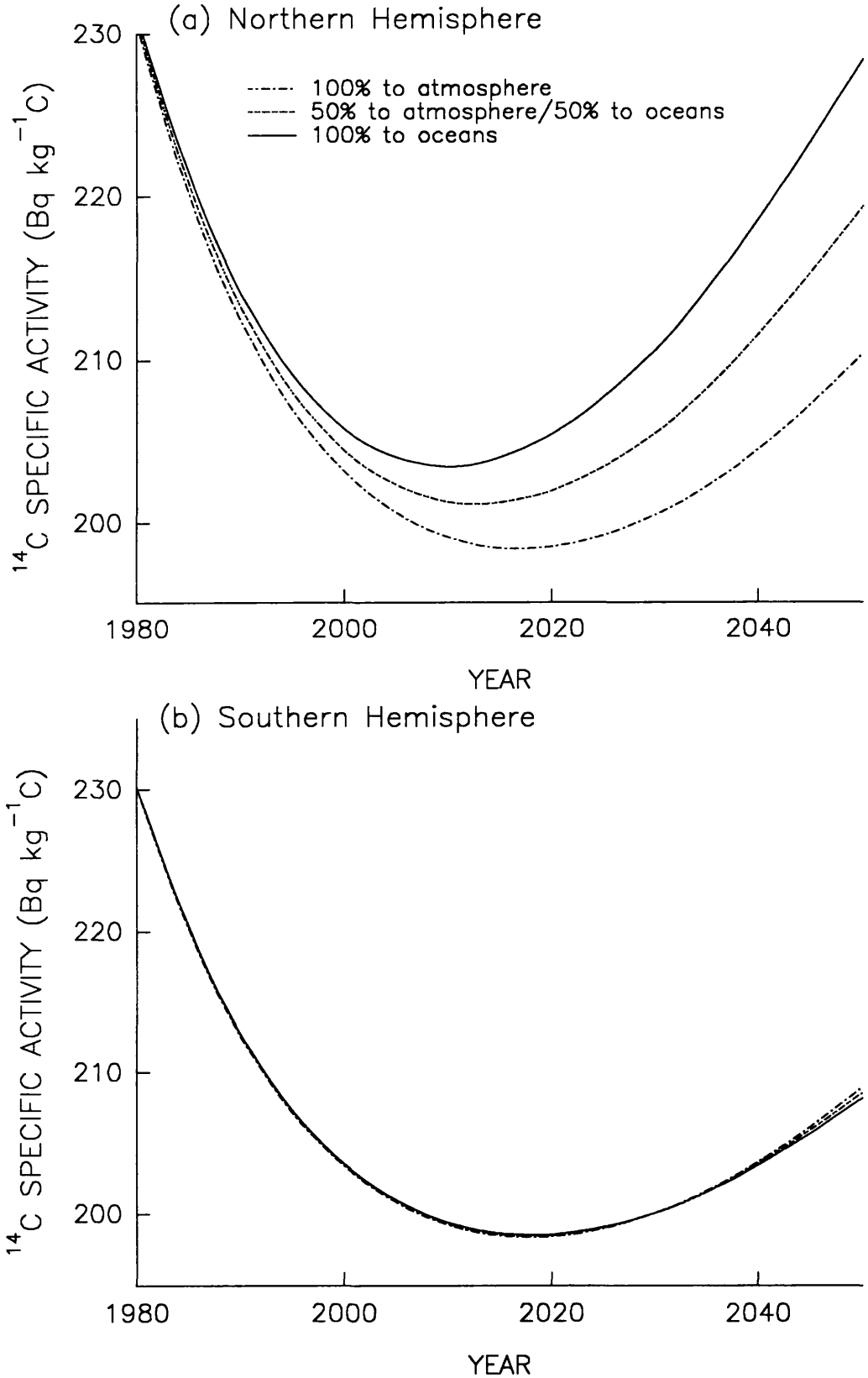

Figure 4.12: Predictions of partitioning (8-box model): The surface oceans.

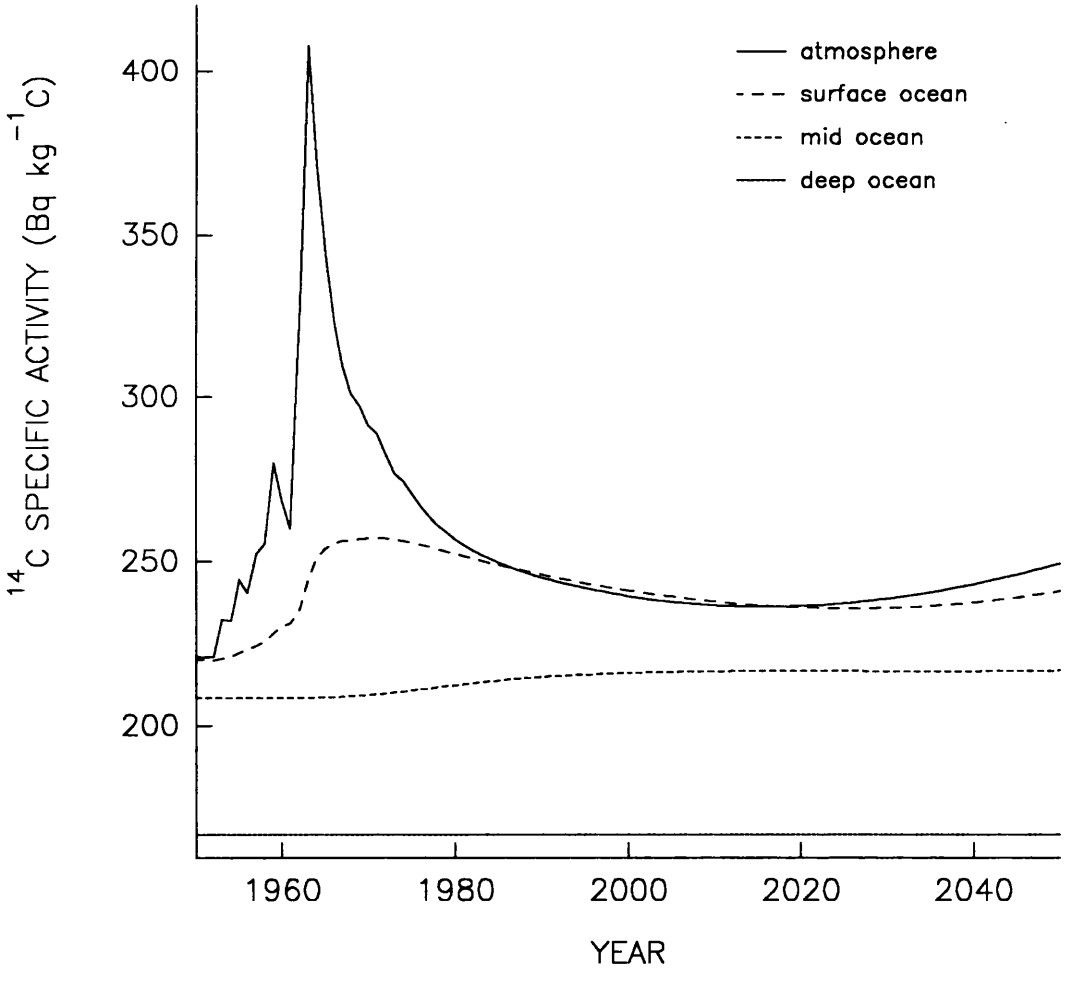

Figure 4.13: The predicted ^{14}C specific activity in selected reservoirs of the 25-box model.

of the chosen energy requirement scenario. In addition, these diagrams show that the atmosphere is the most responsive to inputs of carbon. Once again, the surface ocean shows an increase in its ^{14}C specific activity due to uptake of enhanced atmospheric CO_2. This is transported down the water column with enhancements being found in the mid ocean box which was selected (850 m) but not in the deep ocean. The deep ocean seems to have remained at its steady state activity throughout the timescale of the model, indicating carbon turnover times in excess of 200 years.

The atmospheric ^{14}C specific activity predicted for the year 2050 A.D. is 249 Bq $kg^{-1}C$ which is slightly higher than that obtained by McCartney *et al.* (1988a) of 234 Bq $kg^{-1}C$. This is due to two differences in the input data from the nuclear fuel cycle. In previous studies, a seven year lag period was included to accommodate the differences in the chemical form of ^{14}C releases, *ie.* to mimic the oxidation of CO, CH_4 *etc.* to CO_2. This was not carried out in this study, which will result in slightly higher ^{14}C specific activities. The second, and more important difference, is the incorporation of the higher rate of ^{14}C production per GW(e)) of installed nuclear capacity. However, the observed increase in the ^{14}C specific activities is relatively small compared to the almost 50% increase in the rate of ^{14}C production from the nuclear fuel cycle.

In a similar exercise to that carried out with the 8-box model, the inputs from the nuclear fuel cycle have been partitioned in varying proportions between the atmosphere and surface oceans. Figures 4.14(a) and (b) illustrate the distributions found in the atmosphere and surface oceans for the period 1980 to 2050 A.D.. The highest ^{14}C specific activity found in the atmosphere is 249 Bq $kg^{-1}C$ when 100% of the discharges are gaseous in nature. This drops to 230 Bq $kg^{-1}C$ when all the releases are in the liquid form. The rate of this decline is approximately 0.76% per 10% released in the aqueous form. This is more than half that predicted by the 8-box model but similar to that predicted by McCartney *et al.* (1988a). The corresponding values for the surface ocean are 241 Bq $kg^{-1}C$ and 249 Bq $kg^{-1}C$ for gaseous and aqueous discharges, respectively, with an average rate of increase of 0.37% per 10% additional release to the water column. Data available for the mid and deep oceans show that the rate of increase in the ^{14}C specific activity down the water column is considerably less, with no change occurring below 4500 m at all. The rate of increase in the specific activity for the mid ocean is only 0.05% per 10% as liquid waste. From these figures it would appear that the increased complexity of the 25 box model has

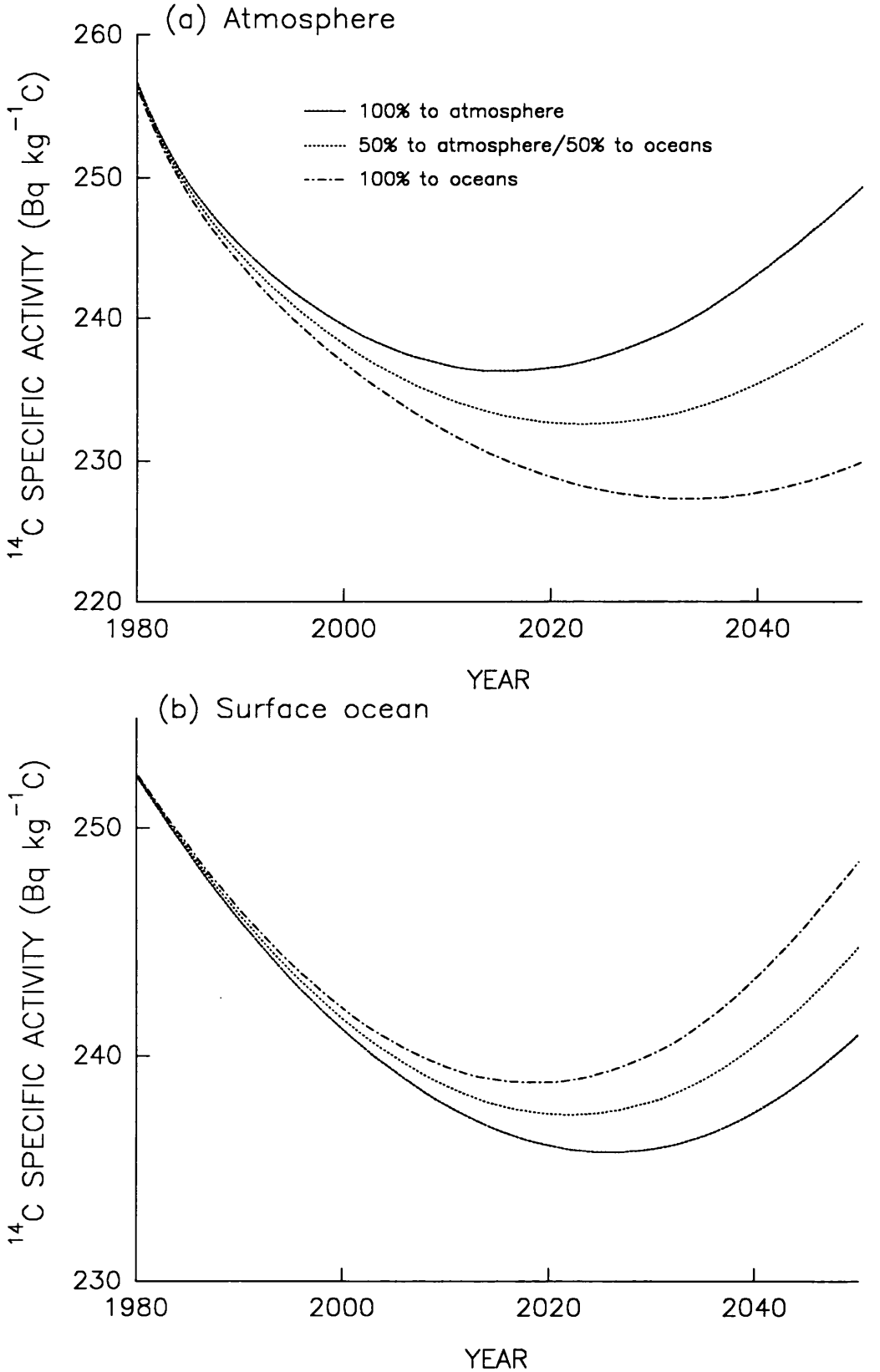

Figure 4.14: Predictions of partitioning (25-box model): Atmosphere and surface oceans.

halved the rate at which the ^{14}C specific activity of the atmosphere decreases on addition of nuclear fuel cycle-derived ^{14}C to the surface oceans compared to the 8 box model. A similar difference is observed in the rate of increase in the specific activity of the surface oceans, the 25 box model indicates a 0.37% increase per 10% release as opposed to the 0.8% per 10% of the 8 box model. Regardless of this, it is apparent, in both model structures, that relatively small discharges of ^{14}C to the oceans is manifest in proportionally higher decreases of atmospheric ^{14}C specific activity than the increases observed in the surface oceans.

This indicates that ^{14}C produced by the nuclear fuel cycle, if released to the surface oceans, will decrease the radiological dose received by the global population, with the greater mass of carbon present in the oceans diluting the inputs to a greater extent.

4.4. CONCLUSIONS

As stated in the introduction to this chapter, this work was mainly concerned with the local, spatial and temporal distribution of liquid discharges from the nuclear fuel cycle. However, the application of global carbon cycle models has permitted some basic predictions of the global effect of such releases up to the year 2050 A.D.. The two models used predict ^{14}C specific activities, in the year 2050 A.D., of 229 Bq $kg^{-1}C$ (8-box model) and 249 Bq $kg^{-1}C$ (25-box model) and 210 Bq $kg^{-1}C$ (8-box model) and 241 Bq $kg^{-1}C$ (25-box model) for the atmosphere and surface oceans, repectively. The deep ocean in each of the models appears to remain at a constant specific activity of 196 Bq $kg^{-1}C$ and 167 Bq $kg^{-1}C$ for the 8 and 25 box-models, respectively. In the 25-box model, the mid ocean box selected indicates the incorporation of nuclear weapons tests ^{14}C. These models, therefore, show some discrepancies in their predictions but overall, indicate that on partitioning of nuclear fuel cycle releases of ^{14}C between the atmosphere and surface oceans, the decrease in atmospheric ^{14}C specific activity is approximately 0.76 - 1.6% per 10% of additional release to the surface oceans. Subsequent increases in the surface ocean specific activities are less marked (0.37 - 0.8%) due to the greater mass of carbon present in the reservoir.

Assuming that the 25 box model, because of its increased complexity and detailed treatment of the oceanic reservoir, is more accurate than the 8 box model, it appears that

global atmospheric ^{14}C specific activities are going to be considerably less than those observed presently and in the past. If a larger proportion of the total ^{14}C discharged from the nuclear fuel cycle is released to the surface oceans, a further reduction in the radiological dose to the population would be observed.

CHAPTER 5

CONCLUSIONS

The main impetus behind this study was the determination of the behaviour and environmental distribution of anthropogenically produced ^{14}C released to the aquatic environment from the nuclear and radiochemical industries. To this end, a number of areas of study were undertaken, including studies of the intertidal biota, the biogeochemical fractions of the water column and bottom and intertidal sediments. The local implications of the results were presented in Chapter 3 with the extrapolation of them to the global scale detailed in Chapter 4. This concluding chapter will consider the main points to come out of each of these study areas and will discuss them in relation to potential areas for future work.

Preliminary studies within the project used intertidal organisms such as mussels, winkles and seaweed to provide an indication of the likely levels of ^{14}C present in the aquatic environment. In addition, this was a means of determining the possible chemical form of ^{14}C releases from the nuclear fuel reprocessing plant at Sellafield, Cumbria and the radiochemical plants owned by Amersham International plc in Cardiff and Buckinghamshire. At sites influenced by Sellafield-derived ^{14}C, mussels were consistently more highly enriched in ^{14}C than winkles or seaweed. In turn, the winkles were consistently more enriched than the seaweed. The enrichment observed in the seaweed points to the presence of ^{14}C enrichment in the dissolved inorganic fraction, whereas those in the mussels and winkles indicate the presence of enriched particulate material (inorganic/organic). As mussels are the most enriched, the particulate material on which they feed must have a ^{14}C activity greater than that derived from the incorporation of DIC into organic matter. Therefore, it suggests that Sellafield releases ^{14}C in both the dissolved and particulate forms.

To confirm this hypothesis, biogeochemical fractions present in the water column, *ie.* DIC, DOC, POC and PIC, were isolated and analysed. Such studies can also help in the determination of the rates of transfer of carbon between each of these reservoirs, providing important information on the cycling of carbon within coastal marine environments. Apart

from the DIC, all the biogeochemical fractions were depleted in ^{14}C although not to the same degree. The ^{14}C activities observed in the DIC were similar to, and hence could explain, those previously measured in seaweed. However, no evidence was found of enriched particulate material to explain the ^{14}C activities observed in mussels and winkles. Most of the sampling during this project was undertaken in the winter months when biological activity was at its lowest, hence providing some indication that there may be a seasonal influence in the distribution of ^{14}C. To determine whether this was the case, a phytoplankton sample collected by MAFF in April 1989 was analysed. This sample had a ^{14}C specific activity similar to that observed in DIC indicating that there is a source of enriched particulate material within the water column; although still not high enough to explain the activities measured in mussels. Obviously, one sample provides only a rough indication of the ^{14}C activities present. Further interpretation would require a more detailed study which would need to incorporate both a spatial and temporal element to ascertain whether biological activity is responsible for the distribution of Sellafield-derived ^{14}C observed within the study area during this work.

Preliminary investigations of the ^{14}C activities to be found in fish indicated a similar level of incorporation as observed in the intertidal biota; again this is not supported by information available for the ^{14}C activities of the water column fractions. The sediments in the area have a definite partitioning between the depleted, inorganic and the enriched, organic fractions. However, once more the activities observed in the sediments are not sufficiently high to explain the degree of enrichment found in the fish. This may of course be due to extensive dilution occurring within the sediments, with more highly enriched material being present, but not analysed, at the water column-sediment interface. To ascertain the exact nature and ^{14}C activity of the material available for uptake by bottom-dwelling fish a much more detailed study of the sediments in the area is required.

While intertidal samples have been used to determine the spatial distribution of Sellafield - derived ^{14}C, archival samples of Nori (*Porphyra umbilicalis*) provided the opportunity to determine a temporal record of ^{14}C distribution in the Irish Sea for the time period 1967-1988. To ascertain whether such samples could reflect past discharges from Sellafield, other, less biologically involved radionuclides were also measured. Both ^{137}Cs and ^{241}Am

concentrations observed in the Nori exhibited excellent correlations with published discharge data, intimating that Nori is a good indicator of past discharges of these radionuclides from Sellafield. However, this good correlation between measured activities and discharge data was not observed for ^{14}C. Prior to 1985, ^{14}C discharges were merely estimated and may be inaccurate, hence explaining the poor correlation. Conversely, Nori may not be a good indicator of ^{14}C discharges due to biological incorporation and retention of ^{14}C. A crude estimate of discharges, based on the final three years data, to explain the observed ^{14}C activities indicates that considerably higher discharges must have occurred in the past if such a simple relationship exists between discharges and measured activities.

In an attempt to determine the spatial distribution of ^{14}C from Sellafield an extensive suite of DIC samples were collected and analysed. ^{137}Cs, a conservative radionuclide in the water column and hence a widely used tracer of water movement, was also isolated at the sampling locations to ascertain any similarities in the distribution of the two nuclides. Such a study permitted the determination of the relatively conservative behaviour of ^{14}C in the DIC, although there was some evidence *via* calculation of a $^{14}C/^{137}Cs$ ratio that ^{14}C was influenced by biological activity and/or the ^{137}Cs activities measured included some contribution from desorption of ^{137}Cs from the sediments. This comparison of ^{14}C and ^{137}Cs was extended to include the use of a mathematical model, developed on the basis of ^{137}Cs distribution in the Irish Sea and Scottish coastal waters, to determine whether the observed ^{14}C distribution in the Irish Sea could be reproduced. Preliminary results indicated a reasonable agreement between predicted and observed values suggesting that the ^{14}C distribution observed can be explained to some degree by water movement in the area. However, until more observations have been made, and the extent to which biological activity influences the distribution has been determined, validation of such a model is not feasible.

The modelling aspects of this study were not restricted to just determining the spatial distribution of ^{14}C but aimed to ascertain the processes, and the rates at which they occur, within the marine carbon cycle. Insufficient experimental data and a worldwide uncertainty in the mass of carbon present in some of the reservoirs allowed only a review of the current available knowledge and the development of a possible model structure. For

this model structure to be verified a great deal more research is required. The mass of stable carbon and ^{14}C in each reservoir is required in conjunction with some indication of the important processes and their rates. Areas of known anthropogenic ^{14}C inputs, such as Sellafield and the Irish Sea area, may provide ideal locations for the study and determination of these processes and allow calculation of the rates at which carbon is transferred between reservoirs.

Similar studies were undertaken in the Bristol Channel to determine the distribution of ^{14}C released from the Amersham radiochemical plant in Cardiff. The intertidal biota samples exhibited ^{14}C activities indicative of uptake of enriched ^{14}C from both the dissolved and particulate fractions of the water column. However, unlike those collected from sites within the Irish Sea, the biogeochemical fractions were all enriched in ^{14}C, apart from the PIC. This marked enrichment in the biogeochemical fractions indicates that the discharges of ^{14}C from Amersham are in a different chemical form from those at Sellafield *ie.* Sellafield releases ^{14}C in the dissolved inorganic form whereas releases from Amersham into Cardiff Bay appear to be organic in nature (both particulate and dissolved). The intertidal sediments collected from the area show a similar depleted inorganic enriched organic pattern observed in the intertidal and bottom sediments within the Irish Sea area. Enrichments in the organic fraction of the sediments are thought to be due to the relatively rapid oxidation which occurs, whereas the ^{14}C specific activity of the inorganic fraction, which is not involved in such processes, is due to the slow rate of carbon turnover allowing radioactive decay to influence the specific activity of the reservoir.

^{14}C measured in the DIC on a transect stretching the length of the Bristol Channel demonstrated decreasing ^{14}C activities with increasing distance from the point of release. The activity measured at the mouth of the Bristol Channel, which is influenced by incoming Atlantic water, was comparable to the estimated current ambient specific activity indicating that Amersham-derived ^{14}C is not significantly influencing the activities measured within the Irish Sea.

At the final site, *ie.* the radiochemical plant owned by Amersham International plc in Buckinghamshire, the sampling carried out was limited to the water column. Apart from

fish, none of the samples analysed showed enriched levels of ^{14}C although discharges of ^{14}C are thought to occur. This may have been a direct consequence of the location of the sampling sites and/or the time of sampling. On reflection, it may have been more beneficial to base the study around the Maple Cross sewage works rather than further down the Grand Union canal with sampling undertaken at regular intervals to produce a more detailed picture of ^{14}C distribution in the area.

Overall, the three study sites illustrate that anthropogenic ^{14}C is readily incorporated into the natural carbon cycle and, hence, the food chain. The extent of this incorporation appears to be dependent on the chemical form of the releases from establishments such as Sellafield and Amersham, Cardiff. ^{14}C within the DIC fraction of the water column is dispersed by water movement, with enriched levels being observed up to 200 km from the point of release. Biological activity may be responsible for enriched levels found in intertidal biota and the organic fractions of sediments but to ascertain the extent of this influence would require a more detailed and controlled study with samples collected regularly throughout the year. If detailed biogeochemical models are to be developed, more experimental data is obviously required. However, if sites such as the Irish Sea are used for this purpose, the inflow of carbon in the various biogeochemical fractions *via* river run-off must also be considered and monitored, *ie.* the mass of carbon, its $\delta^{13}C$ signature and its ^{14}C activity, throughout a complete seasonal cycle. This would help in the interpretation of results from such a complex system and may, in future work, allow determination of the processes responsible for the observed distribution of ^{14}C within the marine carbon cycle.

Although the ^{14}C specific activities found in mussels, winkles and fish were greatly enhanced relative to the current ambient level, the proportion that they constitute in the diet is only in the order of 0.5% of total carbon intake, ensuring that the radiological significance of consumption of ^{14}C-enriched shellfish is only slightly greater than that attributable to the current ambient level.

The final area considered during this project was the global implications of releasing nuclear fuel cycle-derived ^{14}C into the surface oceans rather than to the atmosphere. Data

available for Sellafield suggest that up to 50% of the total ^{14}C discharges may be in the liquid form, hence such an occurrence throughout the nuclear industry would result in a lower radiological dose to global populations. Two global carbon cycle models were used - an 8-box model which differentiated between the northern and southern hemispheres and a more complex 25-box model which treated the oceans and terrestrial biosphere in greater detail. These models predicted an atmospheric ^{14}C specific activity of 229 Bq $kg^{-1}C$ and 249 Bq $kg^{-1}C$ for the year 2050 A.D., respectively. On partitioning the nuclear fuel cycle ^{14}C releases between the atmosphere and surface oceans, these values were reduced to 211 and 240 Bq $kg^{-1}C$, when 50% of the releases were to the surface oceans, and 194 and 230 Bq $kg^{-1}C$ when all the releases were to the oceans. The subsequent rise in the ^{14}C specific activity of the surface oceans occurred at half the rate of the decrease observed in the atmospheric ^{14}C specific activity. This is due to the greater mass of carbon present in the surface oceans, resulting in extensive dilution of the released ^{14}C.

Overall, this work has produced a comprehensive study of the environmental distribution of Sellafield and Amersham-derived ^{14}C within the Irish Sea and Bristol Channel, respectively. While it has answered many of the original aims it has also highlighted a number of areas worthy of further investigation which have been discussed previously in this chapter. Work of this nature would not only be relevant to local scale carbon distribution and cycling studies, but may assist in more general, globally based studies of the biogeochemical fractions and their importance in the marine carbon cycle.

Finally, the results presented indicate that biological activity is the principle mechanism responsible for the retention and transfer of anthropogenic ^{14}C within the study areas. Therefore, if discharges were restricted to the winter months, when biological activity was at its lowest, potentially there would be a reduction in the specific activities of the carbon reservoirs in the water column and, hence, the biota as the ^{14}C is dispersed and diluted by water movement before it can be incorporated into the food chain.

APPENDIX

As part of the global modelling work undertaken during this project, an 8-box model was used. The computer programme was written in FORTRAN and run on the University mainframe computer. The code for the programme is detailed below.

```
      PROGRAM BOX8
C     THIS PROGRAM CALCULATES THE SPECIFIC ACTIVITIES OF C-14 IN AN 8BOX+
C     MODEL FOR BOTH THE NORTHERN AND SOUTHERN HEMISPHERES.
      REAL N,NA,K,NFC,NFC1,NWT
      DIMENSION N(8)
      DIMENSION NA(8)
      DIMENSION SA(8)
      DIMENSION K(8,8),DN(8),DNA(8)
      FF2=0.0
      PFF2=0.0
      NFC2=0.0
      NWT2=0.0
      PNFC2=0.0
      PFF1=0.0
      FF1=0.0
      PNFC1=0.0
      NWT1=0.0
      NFC3=0.0
      NFC4=0.0
      PNFC3=0.0
      PNFC4=0.0
      NFC1=0.0
C     LEVEL OF NON-RADIOACTIVE CARBON PRESENT INITIALLY IN +
C     EACH BOX
      N(1)=3.6*(1E17)
      N(2)=11.6*(1E17)
      N(3)=5.0*(1E17)
      N(4)=136.4*(1E17)
      N(5)=3.3*(1E17)
      N(6)=4.0*(1E17)
      N(7)=7.6*(1E17)
      N(8)=245.7*(1E17)
C     LEVEL OF C14 PRESENT INITIALLY IN EACH BOX (G.OF C14)
      NA(1)=5.051*(1E5)
      NA(2)=1.557*(1E6)
      NA(3)=6.665*(1E5)
      NA(4)=1.558*(1E7)
      NA(5)=4.630*(1E5)
      NA(6)=5.368*(1E5)
      NA(7)=10.131*(1E5)
      NA(8)=2.856*(1E7)
C     INPUT VALUES OF NATURAL PRODUCTION OF C14 (G/YR)
      NP=2.933*(1E3)
      NP1=2.933*(1E3)
      DO 1 I=1,8
      DO 2 J=1,8
      K(I,J)=0.0
```

```
   2 CONTINUE
   1 CONTINUE
     K(1,2)=0.016
     K(1,3)=0.14
     K(1,5)=0.50
     K(2,1)=0.005
     K(3,1)=0.10
     K(3,4)=0.10
     K(3,7)=0.10
     K(4,3)=0.0036
     K(4,8)=0.005
     K(5,1)=0.56
     K(5,6)=0.0061
     K(5,7)=0.23
     K(6,5)=0.005
     K(7,3)=0.066
     K(7,5)=0.10
     K(7,8)=0.10
     K(8,4)=0.0028
     K(8,7)=0.0031
     T=1800
     DO 20 IT=1,251
C    CALCULATION OF THE FLUX BETWEEN COMPARTMENTS FOR THE STABLE CARBON
C    OFTHE SYSTEM
     DO 3 I=1,8
     DN(I)=0.0
     DO 4 J=1,8
     DN(I)=DN(I)-(K(I,J)*N(I))+(K(J,I)*N(J))
   4 CONTINUE
   3 CONTINUE
C    CALCULATION OF THE FLUX BETWEEN COMPARTMENTS FOR THE RADIOACTIVE
C    CARBON OF THE SYSTEM
     DO 5 M=1,8
     DNA(M)=0.0
     DO 6 L=1,8
     DNA(M)=DNA(M)-(K(M,L)*NA(M))+(K(L,M)*NA(L))
   6 CONTINUE
   5 CONTINUE
C    CALCULATION OF THE INPUTS INTO COMPARTMENTS ONE AND FIVE
C    80% INTO NORTHERN HEMISPHERE,20% INTO SOUTHERN HEMISPHERE
C    INPUT OF STABLE CARBON FROM FOSSIL FUEL COMBUSTION
     IF (1859.LT.T.AND.T.LT.1980) THEN
     READ(12,*)FF
     FF2=FF*1.0E12*0.8
     FF1=FF*1.0E12/5
     ENDIF
     IF (1979.LT.T.AND.T.LT.2051) THEN
     READ(16,*)PFF
     PFF2=PFF*1.0E12*0.8
     PFF1=PFF*1.0E12/5
     ENDIF
C    INPUT OF CARBON-14 FROM NUCLEAR WEAPONS TESTING
     IF(1944.LT.T.AND.T.LT.1981) THEN
     READ(13,*)NWT
     NWT2=NWT*2.44E3*0.8
```

```
      NWT1=NWT*2.44E3/5
      ENDIF
C     INPUT OF CARBON-14 FROM THE NUCLEAR FUEL CYCLE
      IF(1961.LT.T.AND.T.LT.1980) THEN
      READ(14,*)NFC
      NFC2=NFC*7.32*0.8
      NFC1=NFC*7.32/5
      NFC3=NFC2*0.5
      NFC4=NFC1*0.5
      ENDIF
      IF(1979.LT.T.AND.T.LT.2051) THEN
      READ(15,*)PNFC
      PNFC2=PNFC*7.32*0.8
      PNFC1=PNFC*7.32/5
      PNFC3=PNFC2*0.5
      PNFC4=PNFC1*0.5
      ENDIF
      N(1)=N(1)+FF2+PFF2
      N(5)=N(5)+FF1+PFF1
      NA(1)=NA(1)+NWT2+(NFC2*0.5)+(PNFC2*0.5)+NP
      NA(5)=NA(5)+NWT1+(NFC1*0.5)+(PNFC1*0.5)+NP1
      NA(3)=NA(3)+NFC3+PNFC3
      NA(7)=NA(7)+NFC4+PNFC4
C     CALCULATION OF THE NEW LEVELS IN EACH COMPARTMENT
      DO 10 I=1,8
      N(I)=N(I)+DN(I)
      NA(I)=NA(I)+DNA(I)-(NA(I)*1.21*(1E-4))
   10 CONTINUE
C     CALCULATION OF THE SPECIFIC ACTIVITY OF CARBON-14 IN EACH
C     COMPARTMENT (BQ.PER.KG.OF.C)
      DO 11 JK=1,8
      SA(JK)=(4.46*3.7E10*1.0E3*NA(JK))/(NA(JK)+N(JK))
   11 CONTINUE
      WRITE(17,*) T,(SA(JK),JK=1,8)
      IF (T.EQ.2050)  GOTO 500
      T=T+1
   20 CONTINUE
  500 STOP
      END
```

REFERENCES

Adams, J.M., Faure, H., Faure-Denard, L., McGlade, J.M. and Woodward, F.I. 1990. Increases in terrestrial carbon storage from the Last Glacial Maximum to the present. Nature, **348**, 711-714.

Allardice, R.H., Harris, D.W. and Mills, A.L. 1983. Nuclear Fuel Reprocessing in the U.K. In: *Nuclear Power Technology Vol 2: Fuel Cycle*, Ed. W.Marshall, 205-281, Clarendon Press, Oxford.

Anderson, E.C. and Libby, W.F. 1951. World-wide distribution of natural radiocarbon. The Physical Review, **81(1)**, 64-69.

Arrol, W.J. and Glascock, R. 1947. Conversion of carbon dioxide to acetylene on a micro scale. Nature, **159**, 810.

Bacastow, R.B. and Keeling, C.D. 1973. Atmospheric carbon dioxide and radiocarbon in the natural carbon cycle, II Changes from AD 1700 to 2070 as deduced from a geochemical model. In: *Carbon and the biosphere., Proceedings of the 24th Brookhaven Symposium in Biology*, Eds. G.M.Woodwell and E.V.Pecan, 86-135, U.S. Atomic Energy Commission Report CONF-720510, NTIS, Springfield, Virginia.

Bacastow, R.B. and Keeling, C.D. 1979. Models to predict future atmospheric CO_2 concentration. In: *Global effects of carbon dioxide from fossil fuels., Proceedings of an International Workshop*, Eds. W.P.Elliott and L.Machta, 72-90, U.S. Department of Energy report CONF-770385, NTIS, Springfield, Virginia.

Baes, Jr, C.F., Bjorkstrom, A. and Mulholland, P.J. 1985. Uptake of carbon dioxide by the oceans. In: *Atmospheric Carbon Dioxide and the Global Carbon Cycle*, Ed. J.R.Trabalka, 81-112, US Department of Energy Report DOE/ER-0239, NTIS, Springfield, Virginia.

Baes, C.F., Goeller, H.E., Olson, J.S. and Rotty, R.M. 1976. The Global Carbon Dioxide Problem. Oak Ridge National Laboratory, Oak Ridge, Tennessee, ORNL-5194.

Baes, C.F., Goeller, H.E., Olson, J.S. and Rotty, R.M. 1977. Carbon dioxide and climate: the uncontrolled experiment. American Scientist, **65**, 310-320.

Bard, E., Hamelin, B., Fairbanks, R.G. and Zindler, A. 1990. Calibration of the ^{14}C timescale over the past 30,000 years using mass spectrometric U-Th ages from Barbados corals. Nature, **345**, 405-409.

Barker, H. 1953. Radiocarbon dating: large-scale preparation of acetylene from organic material. Nature, **172**, 631-632.

Barker, H., Burleigh, R. and Meeks, N. 1969. New method for the combustion of samples for radiocarbon dating. Nature, **221**, 49-50.

Bauer, J.E., Williams, P.M. and Druffel, E.R.M. 1992. ^{14}C activity of dissolved organic carbon fractions in the north-central Pacific and Sargasso Sea. Nature, **357**, 667-670.

Baxter, M.S. and Farmer, J.G. 1973. Radiocarbon: short-term variations. Earth and Planetary Science Letters, **20**, 295.

Baxter, M.S. and Stenhouse, M.J. 1976. Glasgow University radiocarbon measurements VIII. Radiocarbon, **18**, 161-173.

Baxter, M.S. and Walton, A. 1970. A theoretical approach to the Suess effect. Proceedings of the Royal Society of London, Series A, **318**, 213-230.

Baxter, M.S. and Walton, A. 1971. Fluctuations of atmospheric carbon-14 concentrations during the past century. Proceedings of the Royal Society of London, Series A, **321**, 105-127.

Becker, B. and Kromer, B. 1986. Extension of the holocene dendrochronology by the preboreal pine series, 8800 - 10100 BP. Radiocarbon, **28(2B)**, 961-968.

Begg, F.H., Baxter, M.S., Cook, G.T., Scott, E.M. and McCartney, M. 1991. Anthropogenic ^{14}C as a tracer in western U.K. coastal waters. In: *Radionuclides in the study of marine processes*, Eds. P.J.Kershaw and D.S. Woodhead, 52-60, Elsevier Applied Science, London.

Begg, F.H., Cook, G.T., Scott, E.M., Baxter, M.S. and McCartney, M. 1992. Anthropogenic radiocarbon in the Irish Sea and Scottish coastal waters. Radiocarbon, **34**, 707-716.

Belderson, R.H. 1964. Holocene sedimentation in the western half of the Irish Sea. Marine Geology, **2**, 147-163.

Belderson, R.H. and Stride, A.H. 1969. Tidal currents and sand wave profiles in the north-eastern Irish Sea. Nature, **222**, 74-75.

Beninson, D.J. 1984. Production, release and means of control of C-14 in Heavy Water Reactors. Report to IAEA's Coordinated Research Programme from Nuclear Facilities, 3247/R2/CF, IAEA, Vienna.

Beninson, D.J and Gonzalez, A.J. 1981. Applications of the dose limitation system to the control of carbon-14 releases from heavy-water-moderated reactors. In: *The Dose Limitation System in the Nuclear Fuel Cycle and in Radiation Protection*, 1-19, IAEA-SM-258, IAEA, Vienna.

Berger, W.H. 1976. Biogenous deep sea sediments: production, preservation and interpretation. In: *Chemical Oceanography (Vol. 5)*, Eds. J.P.Riley and R.Chester, 265-388, Academic Press, London.

Bien, G.S., Rakestraw, N.W. and Suess, H.E. 1960. Radiocarbon concentrations in Pacific Ocean Water. Tellus, **12**, 436-443.

Bien, G.S., Rakestraw, N.W. and Suess, H.E. 1965. Radiocarbon in the Pacific and Indian Ocean and its relation to deep water measurements. Limnology Oceanography, **10 (suppl.)**, R25-R37.

Birks, J.B. 1964. *Theory and practice of liquid scintillation counting*. Pergamon Press, Oxford.

Birks, J.B. 1975. An introduction to liquid scintillation counting and solutes and solvents for liquid scintillation counting. Combined edition. Koch-Light Laboratories Ltd, Bucks., England.

Birks, J.B. and Poullis, G.C. 1972. Liquid scintillators. In: *Liquid scintillation counting, Vol. 2*, Eds. M.A.Crook, P.Johnson and B.Scales, 1-23, Heyden and Son Ltd.

Bjorkstrom, A. 1979. A model of CO_2 interaction between atmosphere, oceans and land biota. In: *The global carbon cycle, SCOPE 13.*, Eds. B.Bolin, E.T.Degens, S.Kempe and P.Ketner, 403-457, Wiley and Sons, New York.

Bolin, B., Bjorkstrom, A., Holmen, K. and Moore, B. 1983. The simultaneous use of tracers for ocean circulation studies. Tellus, **35B**, 206-236.

Bolin, B., Bjorkstrom, A., Keeling, C.D., Bacastow, R. and Siegenthaler, U. 1981. Carbon cycle modelling. In: *Carbon Cycle Modelling, SCOPE 16*, Ed. B. Bolin, 1-28, Wiley, New York.

Bolin, B., Degens, E.T., Duvigneaud, P. and Kempe, S. 1979. The global biogeochemical carbon cycle. In: *The Global Carbon Cycle, SCOPE 13*, Eds. B.Bolin, E.T.Degens, S.Kempe and P.Ketner, 1-56, Wiley, New York.

Bolin, B. and Ericksson, E. 1959. Changes in the carbon dioxide content of the atmosphere and sea due to fossil fuel combustion. In: *Atmosphere and sea in motion.*, Ed. B.Bolin, 130-142, The Rockefeller Institute Press, New York.

Bonka, H. 1980. Produktion und freisetzung von tritium und kohlenstoff-14 durch kernwaffenversuche, testexplosionen und kerntechnische anlagen, einschlieblich wiederaufarbeitungsanlagen. In: *Strahlenschutzprobleme im Zusammenhang mit der Verwendung von Tritium und Kohlenstoff-14 und Ihren Verbindungen*, Eds. F.E.Stieve and G.Kristner, 17-27, STH-Bericht 12/80, BGA, Neuherberg.

Bowden, K.F. 1950. Processes affecting the salinity of the Irish Sea. Monthly Notices Royal Astronomical Society Geophysical Supplement, **6(2)**, 63-90.

Bradley, P.E., Economides, B.E., Baxter, M.S. and Ellet, D.J. 1987. Sellafield radiocaesium as a tracer of water movement in the Scottish coastal zone. In: *Radionuclides: a tool for oceanography*, Eds. J.C.Guary, P.Guegueniat and R.J.Pentreath, 281-293, Elsevier, London.

Bradley, P.E., Scott, E.M., Baxter, M.S. and Ellet, D.J. 1991. Radiocaesium in local and regional coastal water modelling exercises. In: *Radionuclides in the study of marine processes*, Eds. P.J.Kershaw and D.S.Woodhead, 61-73, Elsevier Applied Science, London.

British Nuclear Fuels Limited 1991. Annual Report of Radioactive Discharges and Monitoring of the Environment 1990 Vol.1: Report on Discharges and Environmental Monitoring.

Broecker, W.S. 1963. $^{14}C/^{12}C$ ratios in surface ocean water. Nuclear Geophysics, US National Academy Science Publication, **1075**, 138-149.

Broecker, W.S. 1979. A revised estimate for the radiocarbon age of North Atlantic deep water. Journal of Geophysical Research, **84**, 3218-3226.

Broecker, W.S. and Olson, E.A. 1959. Lamont radiocarbon measurements VI. American Journal of Science (Radiocarbon Supplement), **1**, 111-132.

Broecker, W.S. and Olson, E.A. 1961. Lamont radiocarbon measurements VIII. Radiocarbon, **3**, 176-204.

Broecker, W.S. and Peng, T.-H. 1982. *Tracers in the Sea.* Eldigio Press, Lamont-Doherty Geological Observatory, Palisades, New York.

Broecker, W.S., Peng, T.-H. and Engh, R. 1980. Modelling the carbon system. Radiocarbon, **22**, 565-598.

Broecker, W.S., Peng, T.-H., Ostlund, G. and Stuiver, M. 1985. The distribution of bomb radiocarbon in the ocean. Journal of Geophysical Research, **90**, 6953-6970.

Broecker, W.S., Peng, T.-H and Stuiver, M. 1978. An estimate of the upwelling rate in the equatorial Atlantic based on the distribution of bomb radiocarbon. Journal of Geophysical Research, **83**, 6179-6186.

Broecker, W.S. and Walton, A. 1959. Radiocarbon from nuclear tests. Science, **130**, 309-314.

Bruns, M., Munnich, K.O. and Becker, B. 1980. Natural radiocarbon variations from AD 200 to 800. Radiocarbon, **22**, 273-277.

Bruns, M., Rhein, M., Linick, T.W. and Suess, H.E. 1983. The atmospheric ^{14}C level in the 7th millennium BC. In: *^{14}C and Archaeology, Proceedings of PACT 8*, Groningen, Netherlands, August 1982, Eds. W.G.Mook and H.T.Waterbolk, 511-516, Council of Europe, Strasbourg.

Bryan, K. 1969. A numerical model for the study of the circulation of the world ocean. Journal of Computational Physics, **4(3)**, 347-376.

Bryan, K. and Lewis, L.J. 1979. A water mass model of the World ocean circulation. Journal of Geophysical Research, **84**, 2503-2517.

Bucha, V. 1970. Influence of the earth's magnetic field on radiocarbon dating. In: *Radiocarbon Variations and Absolute Chronology, Proceedings of the 12th Nobel Symposium*, Uppsala, Sweden, 11-15 August 1969, Ed. I.U.Olson, 501-511, Wiley, New York.

Bucha, V. and Neustupny, E. 1967. Changes of the earth's magnetic field and radiocarbon dating. Nature, **215**, 261-263.

Burke, Jr, W.H. and Meinschein, W.G. 1955. ^{14}C dating with a methane proportional counter. The Review of Scientific Instruments, **26**, 1137-1140.

Bush, R.P., White, I.F. and Smith, G.M. 1983. Carbon-14 waste management. UK Atomic Energy Research Establishment Report R10543, Harwell.

Cambray, R.S., Lewin, G.N.J. and Playford, K. 1985. Radioactive fallout in air and rain: Results to the end of 1984. UK Atomic Energy Authority, Harwell, AERE-R11915.

Campbell, J.A. 1977. Past variations in natural radiocarbon as recorded in UK wood. Ph.D. Thesis, University of Glasgow.

Camplin, W.C. and Gurbutt, P.A. 1985. Sediment interactions in a new ocean model. In: *Proceedings of the scientific seminar on the application of distribution coefficients to radiological assessment models*, 381-390, Commission of the European Communities, Brussels.

Carter, M.W. and Moghissi, A.A. 1977. Three decades of nuclear testing. Health Physics, **33**, 55-71.

Cauwet, G. 1981. Non-living particulate matter. In: *Marine Organic Chemistry*, Eds. E.K. Duursma and R. Dawson, 71-89, Elsevier, Amsterdam.

Chan, Y.H., Olson, J.S. and Emanuel, W.R. 1979. Simulation of land use patterns affecting the global carbon cycle. Oak Ridge National Laboratory ORNL/TM-6651, Oak Ridge, Tennessee.

Chester, R. 1990. *Marine Geochemistry*. Unwin Hyman, London.

Commission of the European Communities 1979. Methodology for evaluating the radiological consequences of radioactive effluents released in normal operations. Joint Report by the National Radiological Protection Board and the Commissariat A L'Energie Atomique. Commission of the European Communities, Luxembourg, V/3865/1/79-EN,FR.

Cook, G.T., Naysmith, P., Anderson, R. and Harkness, D.D. 1990. Performance optimisation of the Packard 2000CA/LL liquid scintillation counter for ^{14}C dating. Nuclear Geophysics, **4(2)**, 241-245.

Copin-Montegut, C. and Copin-Montegut, G. 1973. Comparison between two processes of determination of particulate organic carbon in sea water. Marine Chemistry, **1**, 151-156.

Craig, H. 1953. The geochemistry of the stable carbon isotopes. Geochimica et Cosmochimica Acta, **3**, 53-92.

Craig, H. 1954. Carbon-13 in plants and the relationship between carbon-13 and carbon-14 variations in nature. Journal of Geology, **62**, 115-149.

Craig, H. 1957a. Isotopic standards for carbon and oxygen and correction factors for mass-spectrometric analysis of carbon-dioxide. Geochimica et Cosmochimica Acta, **12**, 133-149.

Craig, H. 1957b. The natural distribution of radiocarbon and the exchange time of carbon dioxide between atmosphere and sea. Tellus, **9**, 1-17.

Crane, A.J. 1982. The partitioning of excess CO_2 in a five-reservoir atmosphere-ocean model. Tellus, **34**, 398-401.

Crane, A.J. 1988. The use of tracers in modelling the oceanic uptake of carbon dioxide. Philosophical Transactions of the Royal Society of London, **A325**, 23-42.

Damon, P.E., Long, A. and Wallick, E.I. 1973. On the magnitude of the 11-year radiocarbon cycle. Earth and Planetary Science Letters, **20**, 300-306.

Davis, W. 1979. Carbon-14 production in nuclear reactors. In: *Management of Low-Level Radioactive Waste*, Eds. M.W.Carter, A.A.Moghissi and B.Kahn, 151-191, Pergammon Press, Oxford.

Debertin, K. and Helmer, R.G. 1988. *Gamma- and X-ray spectrometry with semiconductor detectors*. North Holland, Amsterdam.

de Geer, G. 1940. Geochronologica suecia principles. Kungliga Svenska Vetenskapsakademiens Handlingar, Series A, **18**.

Degens, E.T. and Mopper, K., 1976. Factors controlling the distribution and early diagenesis of organic matter in the marine sediments. In: *Chemical Oceanography Vol5*, Eds. J.P.Riley and R.Chester, 59-113, Academic Press, London.

de Jong, A.F.M., Mook, W.G. and Becker, B. 1979. Confirmation of the Suess wiggles: 3200-3700 BC. Nature, **280**, 48-49.

de Jong, A.F.M., Becker, B. and Mook, W.G. 1986. High-Precision Calibration of the Radiocarbon Timescale, 3930 - 3230 Cal BC. Radiocarbon, **28(2B)**, 939-942.

de Vooys, C.G.N. 1979. Primary production in aquatic environments. In: *The Global Carbon Cycle, SCOPE 13*, 259-292, Chichester, Wiley.

de Vries, H.I. 1958. Variation in concentration of radiocarbon with time and location on earth. Proceedings of the Koninkl Nederlandse Akademi Wetenschap, Series B, **61**, 94-102.

de Vries, H.L. and Barendsen, G.W. 1953. Radiocarbon dating by a proportional counter filled with carbon dioxide. Physica, **19**, 987-1003.

Dickson, R.R. and Boelens, R.G.V. 1988. The status of current knowledge of anthropogenic influences in the Irish Sea. International Council for the exploration of the sea (Denmark), Cooperative Research Report 155.

Druffel, E.M. 1981. Radiocarbon in annual coral rings from the eastern tropical Pacific Ocean. Geophysical Research Letters, **8**, 59-62.

Druffel, E.M. and Linick, T.W. 1978. Radiocarbon in annual coral rings of Florida. Geophysical Research Letters, **5**, 913-916.

Druffel, E.M. and Suess, H.E. 1983. On the radiocarbon record in banded corals: exchange parameters and net transport of $^{14}CO_2$ between atmosphere and surface ocean. Journal of Geophysical Research, **88**, 1271-1280.

Druffel, E.R.M. and Williams, P.M. 1990. Identification of a deep marine source of particulate organic carbon using bomb ^{14}C. Nature, **347**, 172-174.

Duce, R.A. 1978. Speculations on the budget of particulate and vapour phase non-methane organic carbon in the global troposphere. Pure and Applied Geophysics, **116**, 244-273.

Duce, R.A. and Duursma, E.K. 1977. Inputs of organic matter to the ocean. Marine Chemistry, **5**, 319-339.

Duursma, E.K. 1961. Dissolved organic carbon, nitrogen and phosphorus in the sea. Netherlands Journal of Sea Research, **1**, 1-148.

Duursma, E.K. 1965. The dissolved organic constituents of sea water. In: *Chemical Oceanography, Vol.1*, Eds. J.P. Riley and G. Skirrow, 433-475, Academic Press, New York.

Eadie, B.J., Jeffrey, L.M. and Sackett, W.M. 1978. Some observations on the stable carbon isotope composition of dissolved and particulate organic carbon in the marine environment. Geochimica et Cosmochimica Acta, **42**, 1265-1269.

Edmonds, J.A., Reilly, J., Trabalka, J.R. and Reichle, D.E. 1984. An analysis of possible future atmospheric retention of fossil fuel CO_2. U.S. Department of Energy Report DOE/OR/21400-1, NTIS, Springfield, Virginia.

Edmonds, J. and Reilly, J. 1983a. A long-term global energy-economic model of carbon dioxide release from fossil fuel use. Energy Economics, **5(2)**, 74-88.

Edmonds, J. and Reilly, J. 1983b. Global energy and CO_2 to the year 2050. The Energy Journal, **4(3)**, 27-47.

Edmonds, J. and Reilly, J. 1983c. Global energy production and use to the year 2050. Energy, **8(6)**, 419-432.

Elsasser, W., Ney, E.P. and Winckler, J.R. 1956. Cosmic-ray intensity and geomagnetism. Nature, **178**, 1226-1227.

Emanuel, W.R., Killough, G.G. and Olson, J.S. 1981. Modelling the circulation of carbon in the world's terrestrial ecosystems. In: *Carbon cycle modelling, SCOPE 16.*, Ed. B.Bolin, 335-353, Wiley and Sons, New York.

Emanuel, W.R., Killough, G.G., Post, W.M. and Shugart, H.H. 1984. Computer implementation of a globally averaged model of the world carbon cycle. U.S. Department of Energy Report DOE/NBB-0062. NTIS, Springfield, Virginia.

Enting, I.G. and Pearman, G.I. 1982. Description of a one-dimensional global carbon cycle model. Technical Paper No. 42, Division of Atmospheric Research, CSIRO, Canberra, Australia.

Ertel, J.R., Hedges, J.I., Devol, A.H., Richey, J.E. and Ribeiro, M. 1986. Dissolved humic substances in the Amazon river system. Limnology Oceanography, **31**, 739-754.

Fellows, D.A., Karl, D.M. and Knauer, G.A. 1981. Large particle fluxes and the vertical transport of the living carbon in the upper 1500m of the northeast Pacific Ocean. Deep Sea Research, **28**, 921-936.

Ferguson, C.W. 1968. Bristlecone pine: science and esthetics. Science, **159**, 839-846.

Ferguson, C.W. 1969. A 7104-year annual-tree ring chronology for Bristlecone pine, *Pinus aristata* from the White Mountain California. Tree-ring Bulletin, **29**, 3-29.

Ferguson, C.W. 1970. Dendrochronology of bristlecone pine, *Pinus aristata*: establishment of a 7484 year chronology in the White Mountains of eastern central California, USA. In: *Radiocarbon Variations and Absolute Chronology, Proceedings of the 12th Nobel Symposium*, Uppsala, Sweden, 11-15 August 1969, Ed. I.U.Olson, 237-259, Wiley, New York.

Ferguson, C.W. 1972. Dendrochronology of bristlecone pine prior to 4000 BC. In: *Radiocarbon Dating, Proceedings of the 8th International Conference*, Lower Hutt, New Zealand, 18-25 October 1972, Eds. T.A.Rafter and T.Grant-Taylor, **A1-A10**, Royal Society of New Zealand, Wellington.

Fergusson, G.J. 1958. Reduction of atmospheric radiocarbon concentration by fossil fuel carbon dioxide and the mean life of carbon dioxide in the atmosphere. Proceedings of the Royal Society of London, Series A, **243**, 561-574.

Fine, R.A., Reid, J.L. and Ostlund, H.G. 1981. Circulation of tritium in the Pacific Ocean. Journal of Physical Oceanography, **11**, 3-14.

Fowler, T.W., Clark, R.L., Gruhlke, and Russel, J.L. 1976. Public health considerations of Carbon-14 discharges from the light-water-cooled nuclear power industry, US Environmental Protection Agency Report ORP-TAD-76-3, Springfield, Virginia.

Friedli, H., Lotscher, H., Oeschger, H., Siegenthaler, U. and Stauffer, B. 1986. Ice core record of the $^{13}C/^{12}C$ ratio of atmospheric CO_2 in the past two centuries. Nature, **324**, 237-238.

Gammon, R.H., Sundquist, E.T. and Fraser, P.J. 1985. History of carbon dioxide in the atmosphere. In: *Atmospheric Carbon Dioxide and the Global Carbon Cycle*, Ed. J.R. Trabalka, 25-62, US Department of Energy Report DOE/ER-0239, NTIS, Springfield, Virginia.

Garland, J.A., McKay, W.A., Cambray, R.S. and Burton, P.J. 1989. Man made radionuclides in the environment of Dumfries and Galloway. UKAEA, Harwell, AERE-R13223, HMSO, London.

Godwin, H. 1962. Half-life of radiocarbon. Nature, **195**, 984.

Gordon, Jnr, D.C. and Sutcliffe, Jnr, W.H. 1973. A new dry combustion method for the simultaneous determination of total organic carbon and nitrogen in seawater. Marine Chemistry, **7**, 289-306.

Gross, M.G. 1990. *Oceanography*, 6th edition. Merrill Publishing Company, Columbus.

Gupta, S.K. and Polach, H.A. 1985. *Radiocarbon dating practices at ANU*. Handbook, Radiocarbon Laboratory, Research School of Pacific Studies, ANU, Canberra.

Hallstadius, L., Garcia-Montano, E. and Nilsson, U. 1987. An improved and validated dispersion model for the North Sea and adjacent waters. Journal of Environmental Radioactivity, **5**, 261-274.

Harkness, D.D. 1983. The extent of natural ^{14}C deficiency in the coastal environment of the United Kingdom. In: *^{14}C and Archaeology, Proceedings of Pact 8*, Groningen, Netherlands, August 1982, Eds. W.G.Mook and H.T.Waterbolk,,Council of Europe, Strasbourg.

Harvey, G.R. and Boran, D.A. 1985. Geochemistry of Humic Substances in Seawater. In: *Humic substances in Soil, Sediment and Water*, Eds. G.R.Aitken, D.M.McKnight, R.L.Kershaw and P. MacCarthy, 233-247.

Harvey, G.R., Boran, D.A., Chesal, L.A. and Tokar, J.M. 1983. The structure of marine fulvic and humic acids. Marine Chemistry, **12**, 119-132.

Hawkins, A.J. 1983. Metabolic strategy in the marine mussel *Mytilus edulis (L)*. PhD. Thesis, University of Exeter.

Hayes, D.W. and McMurdo, K.W. 1977. Carbon-14 production by the nuclear industry. Health Physics, **32**, 215-219.

Hayes, F.N., Williams, D.L. and Rogers, B. 1953. Liquid scintillation counting of natural ^{14}C. Physical Review, **92**, 512-513.

Hedges, J.I., Clark, W.A., Quay, P.D., Richey, J.E., Devol, A.H. and Santos, U. deM. 1986. Compositions and fluxes of particulate organic material in the Amazon river. Limnology Oceanography, **31**, 717-738.

Hedges, R.E.M. and Gowlett, J.A.J. 1986. Radiocarbon dating by Accelerator Mass Spectrometry. Scientific American, **254(1)**, 100-107.

Hoffert, M.I., Callegari, A.J. and Hsieh, C.-T. 1981. A box-diffusion carbon cycle model with upwelling, polar bottom water formation and a marine biosphere. In: *Carbon cycle modelling, SCOPE 16.*, Ed. B.Bolin, 287-305, Wiley and Sons, New York.

Holm-Hansen, O., Williams, P.M. and Strickland, J.D.H. 1966. A detailed analysis of biologically important substances in a profile off southern California. Limnology Oceanography, **11**, 548-558.

Houghton, R.A., Boone, R.D., Melills, J.M., Palm, C.A., Woodwell, G.M., Myers, N., Moore, B. and Skole, D.L. 1985. Net flux of carbon dioxide from tropical forests in 1980. Nature, **316**, 617-620.

Houtermans, J.C. 1971. Geophysical interpretations of Bristlecone pine radiocarbon measurement using a method of Fourier analysis of unequally spaced data. PhD Thesis, University of Bern.

Houtermans, J., Suess, H.E. and Munk, W. 1967. Effect of industrial fuel combustion on the carbon-14 level of atmospheric CO_2. In: *Radioactive Dating and Methods of Low-Level Counting*, 57-68, IAEA, STI/PUB/152.

Hunt, G.J. 1988. Radioactivity in surface and coastal waters of the British Isles, 1987. Aquatic Environment Monitoring Report, MAFF Directorate of Fisheries research, Lowestoft, **19**, 1-67.

Hunt, G.J. 1989. Radioactivity in surface and coastal waters of the British Isles, 1988. Aquatic Environment Monitoring Report, MAFF Directorate of Fisheries Research, Lowestoft, **21**, 1-69.

Hunt, G.J. 1990. Radioactivity in surface and coastal waters of the British Isles, 1989. Aquatic Environment Monitoring Report, MAFF Directorate of Fisheries Research, Lowestoft, **23**, 1-66.

Hunt, G.J. 1992. Radioactivity in surface and coastal waters of the British Isles, 1990. Aquatic Environment Monitoring Report, MAFF Directorate of Fisheries Research, Lowestoft, **29**, 1-68.

Hunt, G.J. and Kershaw, P.J. 1990. Remobilisation of artificial radionuclides from the sediment of the Irish Sea. Journal of Radiological Protection, **10**, 147-151.

International Atomic Energy Agency 1983. Energy, electricity and nuclear power estimates for the period up to 2000. IAEA-RDS-1/3, IAEA, Vienna.

International Atomic Energy Agency 1985. The radiological impact of radionuclides dispersed on a regional and global scale: Methods for assessment and their application. IAEA-TRS-250, IAEA, Vienna.

International Atomic Energy Agency 1991. IAEA Bulletin, **33(4)**, 1991. Quarterly Journal of the IAEA, Vienna.

International Atomic Energy Agency 1991. Report on Consultants Group Meeting on C-14 reference materials for Radiocarbon Laboratories. February 18-20, 1991, Vienna.

International Commission on Radiological Protection 1975. Report of the task group on Reference Man. ICRP Publication 23, Pergamon Press, Oxford.

Jeffries, D.F., Steele, A.K. and Preston, A. 1982. Further studies on the distribution of ^{137}Cs in British coastal waters. 1. Irish Sea. Deep Sea Research, **29**, 713-738.

Johnson, L.R. 1983. The transport mechanisms of clay and fine silt in the north Irish Sea. Marine Geology, **52**, M33-M41.

Joshi, M.L., Ramamirtham, B. and Soman, S.D. 1987. Measurement of ^{14}C emission rates from a pressurised heavy water reactor. Health Physics, **52(6)**, 787-791.

Kabat, M.J. 1979. Monitoring and removal of gaseous carbon-14 species. In: *Proceedings of the 15th DOE Nuclear Air Cleaning Conference*, 208-230, US Department of Energy Report CONF-780819-P1, NTIS, Springfield, Virginia.

Karlen, I., Olsson, I.U., Karlberg, P. and Killicci, S. 1964. Absolute determination of the activity of two ^{14}C dating standards. Archiv for Geofysik, **4**, 465-471.

Keeling, C.D. 1973. The carbon dioxide cycle: reservoir models to depict the exchange of atmospheric carbon dioxide with the oceans and land plants. In: *Chemistry of the lower atmosphere.*, Ed. S.I.Rasool, 251-329, Plenum Press, New York.

Keeling, C.D. and Bacastow, R.B. 1977. Impact of industrial gases on climate. In: *Energy and Climate*, 72-95, National Academy Press, Washington D.C..

Keeling, C.D., Bacastow, R.B. and Whorf, T.P. 1982. Measurements of the concentration of carbon dioxide at Mauna Loa Observatory, Hawaii. In: *Carbon Dioxide Review*, Ed. W.C. Clark, 377-385, Oxford University Press, New York.

Keir, R.S. 1983. Reduction of thermohaline circulation during deglaciation: the effect on atmospheric radiocarbon and CO_2. Earth and Planetary Science Letters, **64**, 445-456.

Kelly, G.N., Jones, J.A., Bryant, P.M. and Morley, F. 1975. The predicted radiation exposure of the population of the European Community resulting from discharges of Krypton-85, Tritium, Carbon-14 and Iodine-129 from the nuclear power industry to the year 2050. Commission of the European Communities, Luxembourg, V/2676/75.

Kempe, S. 1979. Carbon in the Freshwater Cycle. In: *The Global Carbon Cycle, SCOPE 13*, Eds. B.Bolin, E.T.Degens, S.Kempe and P.Ketner, 317-342, Wiley, New York.

Kepkay, P.E. and Wells, M.L. 1992. Dissolved organic carbon in North Atlantic surface waters. Marine Ecology Progress Series, **80**, 275-283.

Kershaw, P.J. 1985. ^{14}C and ^{210}Pb in NE Atlantic sediments: Evidence of biological reworking in the context of radioactive waste disposal. Journal of Environmental Radioactivity, **2**, 115-134.

Kershaw, P.J. 1986. Radiocarbon dating of Irish Sea sediments. Estuarine and Coastal Shelf Science, **23**, 295-303.

Kershaw, P.J., Swift, D.J. and Denoon, D.C. 1988. Evidence of recent sedimentation in the eastern Irish Sea. Marine Geology, **85**, 1-14.

Kershaw, P.J., Swift, D.J., Pentreath, R.J. and Lovett, M.B. 1983. Plutonium redistribution by biological activity in Irish Sea sediments. Nature, **306**, 774-775.

Kershaw, P.J., Swift, D.J., Pentreath, R.J. and Lovett, M.B. 1984. The incorporation of plutonium, americium and curium into the Irish Sea seabed by biological activity. The Science of the Total Environment, **40**, 61-81.

Killough, G.G. 1980. A dynamic model for estimating radiation dose to the world population from releases of ^{14}C to the atmosphere. Health Physics, **38**, 269-300.

Killough, G.G. and Emanuel, W.R. 1981. A comparison of several models of carbon turnover in the oceans with respect to their distributions of transit time and age and responses to atmospheric CO_2 and ^{14}C. Tellus, **33**, 271-290.

Killough, G.G. and Till, J.E. 1978. Scenarios of ^{14}C releases from the world nuclear power industry from 1975 to 2020 and the estimated radiological impact. Nuclear Safety, **19**, 602-617.

Kirby, R., Parker, W.R., Pentreath, R.J. and Lovett, M.B. 1983. Sedimentation studies relevant to low-level radioactive effluent dispersal in the Irish sea. Part III. An evaluation of possible mechanisms for the incorporation of radionuclides into marine sediments. Report Institute Oceanographic Science, **178**, 63pp.

Knoll, G.F. 1979. *Radiation detection and measurement.* Wiley and Sons, New York.

Knoll, G.F. 1989. *Radiation detection and measurement.* Wiley and Sons, New York.

Kocher, D.C. and Killough, G.G. 1984. A review of global environmental transport models for ^{3}H, ^{14}C, ^{85}Kr and ^{129}I. In: *Radioactive waste management., Proceedings of an IAEA Conference*, 157-179, IAEA-CN-43, IAEA, Vienna.

Krishnamoorthy, T.M., Sastry, V.N. and Sarma, T.P. 1982. Model calculations for the projected estimates of ^{14}C burden on earth. Indian Journal of Pure and Applied Physics, **20**, 119-123.

Krogh, A. 1934. Conditions of life at great depths in the ocean. Ecology Monograph, **4**, 430-439.

Kromer, B., Rhein, M., Bruns, M., Schoch-Fischer, H., Munnich, K.O., Stuiver, M. and Becker, B. 1986. Radiocarbon calibration data for the 6th to the 8th millennia BC. Radiocarbon, **28(2B)**, 954-960.

Kuc, T. 1987. ^{14}C traced in Krakow after the Chernobyl accident. Radiocarbon, **29(3)**, 319-322.

Kulp, J.L. 1954. Advances in radiocarbon dating. Nucleonics, **12(12)**, 19-21.

Kunz, C.O., Mahoney, W.E. and Miller, T.W. 1975. Carbon-14 gaseous effluents from boiling water reactors. Transactions of the American Nuclear Society, **21**, 91-92.

Kuo, J.J. and Veronis, G. 1970. Distribution of tracers in the deep oceans of the world. Deep Sea Research, **17**, 29-46.

Lal, D. and Rama, ., 1966. Characteristics of global tropospheric mixing based on man-made ^{14}C, ^{3}H and ^{90}Sr. Journal of Geophysical Research, **71**, 2865-2874.

Lassey, K.R., Manning, M.R. and O'Brien, B.J. 1988. Assessment of the inventory of carbon-14 in the oceans: an overview. In: *Inventories of selected radionuclides in the oceans*, IAEA-TECDOC-481. IAEA, Vienna.

Lee, C. and Bada, J.L. 1977. Dissolved amino acids in the equatorial Pacific, Sargasso Sea and Biscayne Bay. Limnology Oceanography, **22**, 502-510.

Leenheer, J.A. 1981. Comprehensive approach to preparative isolation and fractionation of dissolved organic carbon from natural waters and waste waters. Environmental Science and Technology, **15(5)**, 578-587.

Levin, I., Kromer, B., Barabas, M. and Munnich, K.O. 1988. Environmental distribution and long-term dispersion of reactor $^{14}CO_2$ around two German nuclear power plants. Health Physics, **54(2)**, 149-156.

Li, Y.-H., Takahashi, T. and Broecker, W.S. 1969. Degree of saturation of $CaCO_3$ in the oceans. Journal of Geophysical Research, **75**, 3545-3552.

Libby, W.F. 1946. Atmospheric helium-three and radiocarbon from cosmic radiation. Physical Review, **69**, 671-672.

Libby, W.F., Anderson, E.C. and Arnold, J.R. 1949. Age determination by radiocarbon content: world-wide assay of natural radiocarbon. Science, **109(2827)**, 227-228.

Light, E.S., Merker, M., Verschell, H.J., Mendell, R.B. and Korff, S.A. 1973. Time dependence worldwide distribution of atmospheric neutrons and of their products. 2: Calculation. Journal of Geophysical Research, **78**, 2741-2762.

Linick, T.W. 1978. La Jolla measurements of radiocarbon in the oceans. Radiocarbon, **20**, 333-359.

Linick, T.W. 1980. Bomb-produced carbon-14 in the surface water of the Pacific Ocean. Radiocarbon, **22(3)**, 599-606.

Linick, T.W., Long, A., Damon, P.E. and Ferguson, C.W. 1986. High-Precision Radiocarbon Dating of Bristlecone Pine from 6554 - 5350 BC. Radiocarbon, **28(2B)**, 943-953.

Long, A. 1990. A quality assurance protocol for radiocarbon laboratories. Radiocarbon, **32(3)**, 393-397.

Long, A. and Kalin, R.M. 1990. A suggested quality assurance protocol for radiocarbon dating laboratories. Radiocarbon, **32(3)**,329-334.

Longhurst, A.R. 1991. Role of the marine biosphere in the global carbon cycle. Limnology Oceanography, **36(8)**, 1507-1526.

Machta, L. 1971. The role of the oceans and biosphere in the carbon dioxide cycle. In: *The changing chemistry of the oceans.*, Eds. D.Dryssen and D.Jagner, 121-145, Wiley and Sons, New York.

MacKenzie, A.B. 1991. Radiochemical methods. In: *Instrumental analysis of pollutants*, Environmental management series, Ed. C.N.Hewitt, 243-286, Elsevier Applied Science.

MacKenzie, A.B., Scott, R.D. and Williams, T.M. 1987. Mechanisms of northwards dispersal of Sellafield waste. Nature, **329**, 42-45.

MacKinnon, M.D. 1978. A dry oxidation method for the analysis of the T.O.C. in seawater. Marine Chemistry, **7**, 17-37.

Magno, P.J., Nelson, C.B. and Ellet, W.H. 1975. A consideration of the significance of C-14 discharges from the nuclear power industry. In: *Proceedings of the 13th AEC Air Cleaning Conference*, Ed. M.W.First, 1047-1055, US Atomic Energy Committee Report CONF-740807, Springfield, Virginia.

Mantoura, R.F.C. and Woodward, E.M.S. 1983. Conservative behaviour of riverine dissolved organic carbon in the Severn Estuary: chemical and geochemical implications. Geochimica et Cosmochimica Acta, **47**, 1293-1309.

Martin, J.E. 1986. Carbon-14 in low-level radioactive waste from two nuclear power plants. Health Physics, **50**, 57-64.

Martin, J.H. and Fitzwater, S.E. 1992. Dissolved organic carbon in the Atlantic, Southern and Pacific oceans. Nature, **356**, 699-700.

Martin, J.H., Knauer, D.M., Karl, D.M. and Broenkow, W.W. 1987. VERTEX: carbon cycling in the northeast Pacific. Deep Sea Research, **34**, 267-285.

Matthews, E. 1983. Global vegetation and land use: new high resolution data bases for climate studies. Journal of Climate and Applied Meteorology, **22**, 474-487.

Matthies, M. and Paretzke, H.G. 1982. Assessments of long-term effects of CO_2 and ^{14}C: Various energy scenarios. In: *Health impacts of different sources of energy., Proceedings of an IAEA Symposium*, 329-341, IAEA-SM-254, IAEA, Vienna.

Mauchline, J. 1980. Artificial radioisotopes in the marginal seas of north-western Europe. In: *The north-west European shelf seas: the sea bed and the sea in motion. II. Physical and chemical oceanography, and physical resources*, Eds., F.T.Banner, M.B.Collins and K.S.Massie, 517-542, Elsevier.

Mazaud, A., Laj, C., Bard, E., Arnold, M. and Tric, E. 1991. Geomagnetic field control of ^{14}C production over the last 80 KY: Implications for the radiocarbon timescale. Geophysical Research Letters, **18(10)**, 1885-1888.

McCartney, M. 1987. Global and local effects of ^{14}C discharges from the nuclear fuel cycle. PhD Thesis, University of Glasgow.

McCartney, M., Baxter, M.S., McKay, K. and Scott, E.M. 1986. Global and local effects ^{14}C discharges from the nuclear fuel cycle. Radiocarbon, **28(2A)**, 634-643.

McCartney, M., Baxter, M.S. and Scott, E.M. 1988a. Carbon-14 discharges from the nuclear fuel cycle: 1. Global effects. Journal of Environmental Radioactivity, **8**, 143-155.

McCartney, M., Baxter, M.S. and Scott, E.M. 1988b. Carbon-14 discharges from the nuclear fuel cycle: 2. Local effects. Journal of Environmental Radioactivity, **8**, 157-171.

McDonald, P., Cook, G.T. and Baxter, M.S. 1991. Natural and artificial radioactivity in coastal regions of U.K. In: *Radionuclides in the study of marine processes*, Eds. P.J.Kershaw and D.S.Woodhead, 329-339, Elsevier Applied Science, London.

McDonald, P., Cook, G.T., Baxter, M.S. and Thomson, J.T. 1990. Radionuclide transfer from Sellafield to south-west Scotland. Journal of Environmental Radioactivity, **12**, 285-298.

McEwan, M.J. and Phillips, L.F. 1975. *Chemistry of the Atmosphere*. Arnold, London.

McKay, W.A. and Baxter, M.S. 1985. Water transport from the north Irish Sea to western Scottish coastal waters: further observations from time trend matching of Sellafield radiocaesium. Estuarine and Coastal Shelf Science, **21**, 471-480.

McKinley, I.G., Baxter, M.S. and Jack, W. 1981. A simple model of radiocaesium transport from Windscale to the Clyde Sea area. Estuarine and Coastal Shelf Science, **13**, 69-82.

Menzel, D.W. and Ryther, J. 1968. Organic carbon and the oxygen minimum in the South Atlantic Ocean. Deep-Sea Research, **15**, 327-337.

Meybeck, M. 1982. Carbon, nitrogen and phosphorus transport by world rivers. American Journal of Science, **282**, 401-450.

Meyers-Schulte, K.J. and Hedges, J.I. 1986. Molecular evidence for a terrestrial component of organic matter dissolved in ocean water. Nature, **321**, 61-63.

Miyaki, Y., Saruhashi, K., Kanazawa, T. and Sagi, T. 1985. On the dissolved carbon in seawater. Bulletin of the Society of Seawater Science Japan, **38**, 353-367.

Munnich, K.O. 1963. Der kreislauf des radiokohlenstoffs in der natur. Naturwissenschafen, **50**, 211-218.

Munnich, K.O. and Roether, W. 1967. Transfer of bomb ^{14}C and tritium from the atmosphere to the ocean. In: *Radioactive Dating and Methods of Low-Level Counting*, 93-104, IAEA, Vienna.

National Council on Radiation Protection 1985. Carbon-14 in the Environment. Recommendations of the National Council on Radiation Protection and Measures. NCRP Report 81.

National Radiological Protection Board 1987. Committed doses to selected organs and committed effective doses from intakes of radionuclides. NRPB-GS7, National Radiological Protection Board, Oxford.

Neftel, A., Moore, E., Oeschger, H. and Stauffer, B. 1985. Evidence from polar ice cores for the increase in atmospheric CO_2 in the past two centuries. Nature, **315**, 45-47.

Newell, R.C. 1979. Biology of intertidal animals. Marine Ecological Surveys Ltd, Faversham.

Nienhaus, F. and Williams, J. 1979. Studies of different energy strategies in terms of their effects on the atmospheric CO_2 concentrations. Journal of Geophysical Research, **84**, 3123-3129.

Nienhius, P.H. 1981. Distribution of organic matter in the living marine organisms. In: *Marine Organic Chemistry*, Eds. E.K.Duursma and R.Dawson, 31-69, Elsevier, Amsterdam.

Noakes, J.E., Isbell, A.F., Stipp, J.J. and Hood, D.W. 1963. Benzene synthesis by low temperature catalysis for radiocarbon dating. Geochimica et Cosmochimica Acta, **27**, 797-804.

Noakes, J.E., Kim, S.M. and Stipp, J.J. 1965. Chemical and counting advances in liquid scintillation age dating. In: *Radiocarbon and Tritium Dating, Proceedings of the 6th International Conference*, 68-92, US Atomic Energy Commission Report CONF-650652. NTIS, Springfield, Virginia.

Noakes, J.E. and Valenta, R.J. 1989. Low background liquid scintillation counting using an active sample holder and pulse discrimination electronics. Radiocarbon, **31(3)**, 332-341.

Nozaki, Y., Rye, D.M., Turekian, K.K. and Dodge, R.E. 1978. A 200 year record of carbon-13 and carbon-14 variations in a Bermuda Coral. Geophysical Research Letters, **5**, 825-828.

Nydal, R. 1967. On the transfer of radiocarbon in nature. In: *Radioactive Dating and Methods of Low-Level Counting*, 119-128, UN DOC-SM-87, IAEA, Vienna.

Nydal, R. 1968. Further investigation on the transfer of radiocarbon in nature. Journal of Geophysical Research, **73**, 3617-3635.

Nydal, R., Gulliksen, S., Lovseth, K. and Skogseth, F.H. 1984. Bomb ^{14}C in the ocean surface 1966-1981. Radiocarbon, **26**, 7-45.

Nydal, R. and Lovseth, K. 1983. Tracing bomb carbon-14 in the atmosphere 1962-1980. Journal of Geophysical Research, **88**.

Nydal, R., Lovseth, K. and Gulliksen, S. 1979. A study of radiocarbon variation in nature since the Test Ban Treaty. In: *Radiocarbon Dating, Proceedings of the 9th International Conference*, University of Chicago, Los Angeles/San Diego, USA, Eds. R.Berger and H.E.Suess, 313-323, University of California Press, Berkeley, California.

Nydal, R., Lovseth, K. and Skogseth, F. 1980. Transfer of bomb ^{14}C to the ocean surface. Radiocarbon, **22(3)**, 626-635.

Oeschger, H., Siegenthaler, U., Schotterer, U. and Gugelmann, A. 1975. A box diffusion model to study the carbon dioxide exchange in nature. Tellus, **27**, 168-192.

Ogawa, H. and Ogura, N. 1992. Comparison of two methods for measuring dissolved organic carbon in sea water. Nature, **356**, 696-698.

Ogura, N. 1970. The relation between dissolved organic carbon and apparent oxygen utilisation in the western North Pacific. Deep Sea Research, **17**, 221-231.

Olson, J.S. 1974. Terrestrial Ecosystem. In: *Encyclopedia Britannica 15th Edition, Vol. 2*, 144-149, H.H. Benton, Chicago.

Olson, J.S. 1985. Cenozoic fluctuations in biotic parts of the global carbon cycle. In: *The Carbon Cycle and Atmospheric CO_2: Natural Variations Archean to Present*, Eds. E.T. Sundquist and W.S. Broecker, 377-396, American Geophysical Union, Washington D.C..

Olson, J.S., Garrels, R.M., Berner, R.A., Armentano, T.V., Dyer, M.I. and Yaalon, D.H. 1985. In: *Atmospheric Carbon Dioxide and the Global Carbon Cycle*, Ed. J.R. Trabalka, 175-214, US Department of Energy Report DOE/ER-0239, NTIS, Springfield, Virginia.

Olsson, I.U. and Karlen, I. 1965. Uppsala radiocarbon measurements VI. Radiocarbon, **7**, 331-335.

Olsson, I.U. and Klasson, M. 1970. Uppsala radiocarbon measurements X. Radiocarbon, **12**, 281-284.

Ostlund, H.G. and Engstrand, L.G. 1963. Stockholm natural radiocarbon measurements V. Radiocarbon, **5**, 203-227.

Ostlund, H.G. and Stuiver, M. 1980. GEOSECS Pacific Radiocarbon. Radiocarbon, **22**, 25-53.

Otlet, R.L., Huxtable, G., Evans, G.V., Humphreys, D.G., Short, T.D. and Conchie, S.J. 1983. Development and operation of the Harwell small counter facility for the measurement of ^{14}C in very small samples. Radiocarbon, **25**, 565-575.

Pantin, H.M. 1977. Quaternary sediments of the northern Irish Sea. In: *The Quaternary History of the Irish Sea*, Eds., C.Kidson and M.J.Tooley, 27-54, Seel House, Liverpool.

Pantin, H.M. 1978. Quaternary sediments from the northern Irish Sea: Isle of Man to Cumbria. Bulletin of Geological Survey, **64**, 43pp.

Pearson, G.W., Pilcher, J.R., Baillie, M.G.L., Corbett, D.M. and Qua, F. 1986. High precision ^{14}C measurement of Irish Oaks to show the natural ^{14}C variations from AD 1840 - 5210 BC. Radiocarbon, **28(2B)**, 911-934.

Pearson, G.W. and Stuiver, M. 1986. High-Precision Calibration of the Radiocarbon Timescale, 500-2500 BC. Radiocarbon, **28(2B)**, 839-862.

Peng, T.-H., Broecker, W.S., Freyer, H.D. and Trumbore, S. 1983. A deconvolution of the tree-ring based ^{13}C record. Journal of Geophysical Research, **88**, 3609-3620.

Pentreath, R.J. 1984. The accumulation of long-lived radionuclides by marine organisms: problems past, present and future. In: *International symposium on the behaviour of long-lived radionuclides in the marine environment*, Eds. A.Cigna and C.Myttenaere, 257-268, CEC Report EUR 9214.

Pierson, D.H. 1988. Artificial radioactivity in Cumbria: summary of an assessment by measurement and modelling. Journal of Environmental Radioactivity, **6**, 61-75.

Pietig, F. and Scharpenseel, H.W. 1966. Determination of age by liquid scintillation spectrometry: a new catalyst for the synthesis of benzene. Atompraxis, **12**, 95-97.

Plunkett, M.A. and Rakestraw, N.W. 1955. Dissolved organic matter in the sea. Deep Sea Research, **3 (suppl.)**, 12-14.

Prandle, D. 1984. A modelling study of the mixing of ^{137}Cs in the seas of the European continental shelf. Philosophical Transactions of the Royal Society of London A, **310**, 407-436.

Prentice, K.C. and Fung, I.Y. 1990. The sensitivity of terrestrial carbon storage to climate change. Nature, **346**, 48-51.

Quay, P.D. and Stuiver, M. 1980. Vertical advection-diffusion rates in the oceanic thermocline determined from ^{14}C distributions. Radiocarbon, **22**, 607-625.

Quay, P.D., Stuiver, M. and Broecker, W.S. 1983. Upwelling rates for the equatorial Pacific Ocean derived from the bomb ^{14}C distribution. Journal of Marine Research, **41**, 769-792.

Rafter, T.A. 1968. Carbon-14 measurements in the South Pacific and Antarctic Oceans. New Zealand Journal of Science, **11**, 551-589.

Raiswell, R.W., Brimblecombe, P., Dent, D.L. and Liss, P.S. 1991. *Environmental Chemistry: The Earth-Air-Water Factory*, Resource and Environmental Science Series. Arnold, London.

Redfield, A.C. 1934. On the proportions of organic derivatives in sea water and their relation to the composition of plankton. In: *James Johnstone Memorial Volume*, 177-192, Liverpool University Press.

Redfield, A.C. 1938. The biological control of chemical factors in the environment. American Journal of Science, **46**, 205-221.

Revelle, R. and Suess, H. 1957. Carbon dioxide exchange between atmosphere and ocean and the question of an increase of atmospheric CO_2 during the past decades. Tellus, **9**, 18-27.

Richey, J.E., Brock, J.T., Naiman, R.J., Wissmar, R.C. and Stallard, R.F. 1980. Organic carbon: Oxidation and transport by the Amazon river. Science, **207**, 1348-1351.

Ross, H., Noakes, J.E. and Spalding, J.D. 1991. *Liquid scintillation counting and organic scintillators*. Lewis, Michigan.

Rotty, R.M. and Masters, C.D. 1985. Carbon dioxide from fossil fuel combustion: trends, resources and technological implications. In: *Atmospheric Carbon Dioxide and the Global Carbon Cycle*, Ed. J.R.Trabalka, 63-80, US Department of Energy Report DOE/ER-0239, NTIS, Springfield, Virginia.

Scheele, R.D. and Burger, L.L. 1976. Carbon-14 production in fusion reactors. Battelle Pacific Northwest Laboratories, Richland, Washington, BNWL-2105.

Schlesinger, W.H. 1990. Evidence from chronosequence studies for a low carbon-storage potential of soils. Nature, **348**, 232-234.

Schlesinger, W.H. and Melack, J.M. 1981. Transport of organic carbon in the world's rivers. Tellus, **33**, 172-187.

Segl, M., Levin, I., Schoch-Fischer, H., Munnich, M., Kromer, B., Tschiersch, J. and Munnich, K.O. 1983. Anthropogenic ^{14}C variations. Proceedings of the 11th International Radiocarbon Conference. Radiocarbon, **25**, 583-592.

Sharp, J.H. 1973. Total organic carbon in seawater - comparison of measurements using persulphate oxidation and high temperature combustion. Marine Chemistry, **1**, 211-229.

Shepherd, J.G. 1976. A simple model for the dispersion of radioactive wastes dumped in the deep-seabed. MAFF, Directorate of Fisheries Research Technical Report No. 29.

Siegenthaler, U. 1983. Uptake of excess CO_2 by an outcrop-diffusion model of the ocean. Journal of Geophysical Research, **88**, 3599-3608.

Siegenthaler, U. 1989. Carbon-14 in the Oceans. In: *Handbook of Environmental Isotope Geochemistry Vol 3: The Marine Environment, A*, Eds. P.Fritz and J.Ch.Fontes, 75-137, Elsevier.

Siegenthaler, U. 1990. El Nino and atmospheric CO_2. Nature, **345**, 295-296.

Siegenthaler, U., Heimann, M. and Oeschger, H. 1980. ^{14}C variations caused by changes in the global carbon cycle. Radiocarbon, **22**, 177-191.

Siegenthaler, U. and Oeschger, H. 1978. Predicting future atmospheric carbon dioxide levels. Science, **199**, 388-395.

Sills, G.C. and Edge, M.J. 1989. Sediment behaviour in the Irish Sea. DOE Report No. DOE/RW/079.

Skopintsev, B.A., Timofeyeva, S.N. and Vershinina, O.A. 1966. Organic carbon in the near equatorial and Southern Atlantic and in the Mediterranean. Oceanology, **6**, 201-210.

Skopintsev, B.A., Romenskaya, N.N. and Sokolova, M.V. 1968. Organic carbon in the waters of the Norwegian Sea and the Northeast Atlantic. Oceanology, **8**, 178-186.

Smith, K.L., Williams, P.M. and Druffel, E.R.M. 1989. Upward fluxes of particulate organic matter in the deep North Pacific. Nature, **337**, 724-726.

Solomon, A.M., Trabalka, J.R., Reichle, D.E. and Voorhees, L.D. 1985. The global carbon cycle. In: *Atmospheric Carbon Dioxide and the Global Carbon Cycle*, Ed. J.R.Trabalka, 1-14, US Department of Energy Report DOE/ER-0239. NTIS, Springfield, Virginia.

Starik, I.Y., Arslanov, K.A. and Zharkov, A.P. 1961. Scintillation technique for counting natural radiocarbon and its use for the determination of absolute age. Radiokhimiya, **2**, 825-827.

Starikova, N.D. and Yablokova, O.G. 1974. Organic matter in Northwestern Pacific ocean water (Tsugaru Strait-Wake Island section). Oceanology, **14**, 833-837.

Stenhouse, M.J. and Baxter, M.S. 1977. Bomb-^{14}C as a biological tracer. Nature, **267**, 828-832.

Sternberg, A. and Olsson, I.U. 1967. Uppsala radiocarbon measurements VII. Radiocarbon, **9**, 471-476.

Stommel, H. 1958. The abyssal circulation. Deep Sea Research, **5**, 80-82.

Stuermer, D.H. and Harvey, G.R. 1977. The isolation of humic substances and alcohol-soluble organic matter from seawater. Deep Sea Research, **24**, 303-309.

Stuiver, M. 1961. Variations in radiocarbon concentration and sunspot activity. Journal of Geophysical Research, **66**, 273.

Stuiver, M. 1970. Long term ^{14}C variations. In: *Radiocarbon Variations and Absolute Chronology, Proceedings of the 12th Nobel Symposium*, Uppsala, Sweden, 11-15 August 1969, Ed. I.U.Olson, 197-213, Wiley, New York.

Stuiver, M. 1980. ^{14}C distribution in the Atlantic Ocean. Journal of Geophysical Research, **85**,2711-2718.

Stuiver, M. 1982. A high-precision calibration of the AD radiocarbon timescale. Radiocarbon, **24**, 1-26.

Stuiver, M. and Becker, B. 1986. High-precision decadal calibration of the radiocarbon timescale, AD 1950 - 2500 BC. Radiocarbon, **28(2B)**, 863-910.

Stuiver, M., Kromer, B., Becker, B. and Ferguson, C.W. 1986b. Radiocarbon age calibration back to 13,300 Years BP and the ^{14}C age matching of the German Oak and US Bristlecone Pine chronologies. Radiocarbon, **28(2B)**, 969-979.

Stuiver, M. and Ostlund, H.G. 1980. GEOSECS Atlantic Radiocarbon. Radiocarbon, **22**, 1-24.

Stuiver, M., Ostlund, H.G. and McConnaughey, T.A. 1981. GEOSECS Atlantic and Pacific ^{14}C distribution. In: *Carbon Cycle Modelling, SCOPE 16*, Ed. B.Bolin, 201-221, Wiley, New York.

Stuiver, M. and Pearson, G.W. 1986. High-precision calibration of the radiocarbon timescale, AD 1950-500 BC. Radiocarbon, **28(2B)**, 805-838.

Stuiver, M., Pearson, G.W. and Braziunas, T.F. 1986a. Radiocarbon age calibration of marine samples back to 9000 Cal Yr BP. Radiocarbon, **28(2B)**, 980-1021.

Stuiver, M. and Polach, H.A. 1977. Discussion: Reporting of ^{14}C data. Radiocarbon, **19**, 355-363.

Stuiver, M. and Quay, P.D. 1981. Atmospheric ^{14}C changes resulting from fossil fuel CO_2 release and cosmic ray variability. Earth and Planetary Science Letters, **53**, 349-362.

Stuiver, M., Quay, P.D. and Ostlund, H.G. 1983. Abyssal water carbon-14 distribution and the age of the world ocean. Science, **219**, 849-851.

Suess, E. 1980. Particulate organic carbon flux in the oceans - surface productivity and oxygen utilisation. Nature, **258**, 260-265.

Suess, H.E. 1953. Natural radiocarbon and the rate of exchange of carbon dioxide between the atmosphere and the sea. In: *Nuclear Processes in Geologic Settings*, Ed. W.Aldrich, 52-56, University of Chicago Press, Chicago.

Suess, H.E. 1954. Natural radiocarbon measurements by acetylene counting. Science, **120**, 5-7.

Suess, H.E. 1955. Radiocarbon concentration in modern wood. Science, **122**, 415-417.

Suess, H.E. 1970a. Bristlecone pine calibration of the radiocarbon timescale 5200 BC to the present. In: *Radiocarbon Variations and Absolute Chronology, Proceedings of the 12th Nobel Symposium*, Uppsala, Sweden, 11-15 August 1969, Ed. I.U.Olsson, 303-312, Wiley, New York.

Suess, H.E. 1970b. Three causes of the secular ^{14}C fluctuations, their amplitudes and time constants. In: *Radiocarbon Variations and Absolute Chronology, Proceedings of the 12th Nobel Symposium*, Uppsala, Sweden, 11-15 August 1969, Ed. I.U.Olsson, 595-606, Wiley, New York.

Sugimura, Y. and Suzuki, Y. 1988. A high-temperature catalytic oxidation method for the determination of non-volatile dissolved organic carbon in seawater by direct injection of a liquid sample. Marine Chemistry, **24**, 105-131.

Switsur, R. 1990. A consideration of some basic ideas for quality assurance in radiocarbon dating laboratories. Radiocarbon, **32(3)**, 341-346.

Takahasi, T., Broecker, W.S. and Langer, S. 1985. Redfield ratio based on chemical data from isopycnal surfaces. Journal of Geophysical Research, **90**, 6907-6924.

Tamers, M.A. 1960. Carbon-14 dating with the liquid scintillation counter: total synthesis of the benzene solvent. Science, **132**, 668-669.

Tamers, M.A. 1965. Routine carbon-14 dating using liquid scintillation techniques. In: *Radiocarbon and Tritium Dating, Proceedings of the 6th International Conference*, 53-67, US Atomic Energy Commission Report CONF-650652. NTIS, Springfield, Virginia.

Tanaka, N., Monaghan, M.C. and Rye, D.M. 1986. Contribution of metabolic carbon to mollusc and barnacle shell carbonate. Nature, **320**, 520-523.

Tans, P. 1978. Carbon-13 and carbon-14 in trees and the atmospheric CO_2 increase. PhD Thesis, University of Groningen.

Tans, P. 1981. A compilation of bomb ^{14}C data for use in global carbon model calculations. In: *Carbon Cycle Modelling, SCOPE 16*, Ed. B.Bolin, 131-157, Wiley, New York.

Tauber, H. 1970. The Scandinavian varve chronology and C-14 dating. In: *Radiocarbon Variations and Absolute Chronology, Proceedings of the 12th Nobel Symposium*, Uppsala, Sweden 11-15 August 1969, Ed. I.U.Olson, 173-196, Wiley, New York.

Taylor, D.M., Moroni, J.P., Snihs, J-O. and Richmond, C.R. 1990. The metabolism of ^{3}H and ^{14}C with special reference to radiation protection. Radiation Protection Dosimetry, **30(2)**, 87-93.

Thommeret, J., Thommeret, Y. and Baxter, M.S. 1983. The recent ^{14}C record in the north-west Mediterranean atmosphere. Journal de Recherches Atmospheriques, **177**, 45-51.

Thurman, E.M., Malcolm, R. L. and Aiken, G.R. 1978. Prediction of capacity factors for aqueous organic solutes adsorbed on a porous acrylic resin. Analytical Chemistry, **50(6)**, 775-779.

Toggweiler, J.R. 1992. Catalytic conversions. Nature, **356**, 665-666.

Toggweiler, J.R., Dixon, K. and Bryan, K. 1989a. Simulations of radiocarbon in a coarse-resolution world ocean model: 1. Steady state prebomb distributions. Journal of Geophysical Research, **94(C6)**, 8217-8242.

Toggweiler, J.R., Dixon, K. and Bryan, K. 1989b. Simulations of radiocarbon in a coarse-resolution world ocean model: 2. Distributions of bomb-produced carbon-14. Journal of Geophysical Research, **94(C6)**, 8243-8264.

United Nations 1977. Sources and effects of ionizing radiation. United National Scientific Committee on the Effects of Atomic Radiation 1977 Report to the General Assembly, United Nations, New York.

United Nations 1982. Ionizing radiation: sources and biological effects. United National Scientific Committee on the Effects of Atomic Radiation 1982 Report to the General Assembly, United Nations, New York.

United Nations 1988. Sources, effects and risks of ionizing radiation. United National Scientific Committee on the Effects of Atomic Radiation 1988 Report to the General Assembly, United Nations, New York.

van Cauter, S. 1986. Three dimensional spectrum analysis: a new approach to reduce background of liquid scintillation counters. Packard Instrument Company Application Bulletin No. 006.

Vogel, J.C. 1970. Groningen radiocarbon dates IX. Radiocarbon, **12**, 444-471.

Vogel, J.C., Fulis, A. and Visser, E. 1986. Radiocarbon fluctuations during the third millennium BC. Radiocarbon, **28(2B)**, 935-938.

Vogel, J.C. and Lerman, J.C. 1969. Groningen radiocarbon dates VIII. Radiocarbon, **11**, 351-390.

Vogel, J.C and Marais, M. 1971. Pretoria radiocarbon dates I. Radiocarbon, **13**, 378-394.

Walsh, G.E. and Douglass, J. 1966. Vertical distribution of dissolved carbohydrate in the Sargasso Sea off Bermuda. Limnology Oceanography, **11**, 406-408.

Walton, A., Ergin, M. and Harkness, D.D. 1970. Carbon-14 concentrations in the atmosphere and carbon dioxide exchange rates. Journal of Geophysical Research, **75**, 3089-3098.

Watson, A.J. and Whitfield, M. 1985. Composition of particles in the global ocean. Deep Sea Research, **32**, 1023-1039.

Watson, D.C. and Norton, T.A. 1985. Dietary preferences of the common periwinkle, *Littorina littorea* (L). Journal of Experimental Marine Biology Ecology, **88**, 193.

Weiss, R.F., Ostlund, H.G. and Craig, H. 1979. Geochemical studies in the Weddell Sea. Deep Sea Research, **26**, 1093-1120.

Williams, P.J. 1975. Biological and chemical aspects of dissolved organic material in sea water. In: *Chemical Oceanography Vol. 2*, Eds. J.P.Riley and G.Skirrow, 301-363, Academic Press, London.

Williams, P.J. and Gordon, L.I. 1970. Carbon-13:Carbon-12 ratios in dissolved and particulate organic matter in the sea. Deep Sea Research, **17**, 19-27.

Williams, P.M. and Druffel, E.R.M. 1987. Radiocarbon in dissolved organic matter in the central North Pacific Ocean. Nature, **330**, 246-248.

Williams, P.M. and Druffel, E.R.M. 1988. Dissolved organic matter in the ocean: Comments on a controversy. Oceanography Magazine, **1**, 14-17.

Williams, P.M., Oeschger, H. and Kinney, P. 1969. Natural radiocarbon activity of the dissolved organic carbon in the north-east Pacific ocean. Nature, **224**, 256-258.

Williams, P.M., Stenhouse, M.J., Druffel, E.M. and Koide, M. 1978. Organic ^{14}C activity in abyssal marine sediment. Nature, **276**, 698-701.

Willis, E.H., Tauber, H. and Munnich, K.O. 1960. Variations in the atmospheric radiocarbon concentration over the past 1300 years. American Journal of Science, Radiocarbon Supplement, **2**, 1-4.

Wirth, E. 1982. The applicability of the ^{14}C specific activity model. Health Physics, **43**, 919-922.

Wunsch, C. 1984. An estimate of the upwelling rate in the equatorial Atlantic Ocean based on the distribution of bomb radiocarbon and quasi-geotrophic dynamics. Journal of Geophysical Research, **89**, 7971-7978.

Young, J.R. and Fairhall, A.W. 1968. Radiocarbon from nuclear weapon tests. Journal of Geophysical Research, **73**, 1185-1200.